THE M_W9.0 TŌHOKU EARTHQUAKE AND TSUNAMI OF 11TH MARCH 2011

A FIELD REPORT BY EEFIT

EEFIT

THE M_W9.0 TŌHOKU EARTHQUAKE AND TSUNAMI OF 11TH MARCH 2011

A FIELD REPORT BY EEFIT

Mr. Antonios Pomonis, ***CAR Limited, Global Earthquake Model*** **(Team Leader)**

Dr. Keiko Saito, ***CAR Limited, Willis Research Fellow*** **(Deputy Team Leader)**

Mr. Stuart Fraser, ***Massey University / GNS Science Joint Centre for Disaster Research*** **(Editor)**

Mr. Siau Chen Chian, ***University of Cambridge***

Dr. Katsu Goda, ***University of Bristol***

Mr. Joshua Macabuag, ***Building Design Partnership***

Mr. Mark Offord, ***Sellafield Ltd***

Dr. Alison Raby, ***Plymouth University***

Prof. Peter Sammonds, ***Institute for Risk & Disaster Reduction, University College London***

Report prepared in association with:

Dr. Eri Gavanski, ***Tōhoku University***

Dr. Maki Koyama, ***Kyoto University***

Prof. Hitomi Murakami, ***Yamaguchi University***

Report reviewed by:

Dr. Tiziana Rossetto, ***University College London***

Dr. Damian Grant, ***Arup***

Dr. John E. Alarcon, ***Willis***

Acknowledgements

The EEFIT Japan team would like to express our sincere thanks to the many following organisations and individuals for their support prior, during and following this mission, without whom we would not have been able to carry out the field trip and research so effectively.

- Ms. Berenice Chan, *Institution of Structural Engineers*
- Professor David Cope, Director, *Parliamentary Office of Science and Technology*
- Mr. Tomonori Goto, *PASCO*
- Mr. Ryota Hamamoto, Mr. Yasumasa Matsunaga, *ESRI-J*
- Professor Hideyuki Horii and Dr Riki Honda, *Tokyo University*
- Professor Fumihiko Imamura, Abdul Muhari and Dr. Anawat Suppasri, *Disaster Control Centre, Tōhoku University*
- Mr. Go Ishikawa, *GIS NEXT*
- Dr. Aiming Lin, *Shizuoka University*
- Dr. Lee Manjae, *Sendai National College of Technology*
- Professor Akira Mano, *Japan Society of Civil Engineers and Disaster Control Centre, Tōhoku University*
- Mr. Akihito Morikawa, *Miyagi Prefecture Government official*
- Michaela Musilova, *University College London*
- Dr Alessio Patalano, *Kings College London*
- Dr. Rui Pinho, Dr. Helen Crowley, *Global Earthquake Model*
- Mr. Chris Pook, Mr. Kevin Knappett, Ms. Naomi Takegoshi, *British Embassy Tokyo*
- Mr. John Riding, *Sellafield Ltd.*
- Mr. KenTarō Sakagawa, Mr. Akira Marusaki, Mr. Koichi Sanefuji, Mr. Yushi Matsumoto, Mr. Hisanaga, Okuyama*, Japanese Self Defence Force*
- Mr. Satoshi Sugai, *Japanese Red Cross*
- Professor David Tappin, *British Geological Survey*
- Mr. Shoji Yamada, Tsutomu Kawabata, Mr. Noritoshi Kamagata, Professor Shibayama, *Waseda University*
- Mr. Mamoru Yamada, Kamaishi City, Officials of Natori City, Ōfunato City and Rikuzentakata City
- *Kokusai Kogyo KK*

Thanks are also due to the following organisations for funding the participation of team members:

- EEFIT and the Global Earthquake Model, for funding Antonios Pomonis
- EPSRC for funding Dr. Alison Raby, Dr. Katsu Goda and Siau Chen Chian
- Aon Benfield for funding Stuart Fraser
- Institution of Civil Engineers QUEST Travel Award and Building Design Partnership for funding Joshua Macabuag
- Sasakawa Foundation for funding Professor Peter Sammonds
- Sellafield Ltd. for funding Mark Offord
- Willis Research Network, Cambridge Architectural Research Ltd. and Department of Architecture, University of Cambridge for funding Dr. Keiko Saito

EEFIT would like to acknowledge the ongoing support of its corporate sponsors: AIR Worldwide, Aon Benfield, Arup, British Geological Survey, CREA Consultants, Malishev Wilson Engineers, Risk Management Solutions and Sellafield Ltd

Contents

List of figures

List of tables

1. Introduction

1.1. Preamble

On 11th March 2011, a moment magnitude (M_w) 9.0 earthquake occurred in the Japan Trench off the coast of Tōhoku in north-east Japan (Figure 1.1). Ground shaking was felt as far as western Japan and lasted for almost four minutes (220 seconds), generating tsunami that seriously affected approximately 650 km of the Sanriku, Miyagi, Joban and Kanto coastline along the Pacific Ocean shores of Northern Honshu Island (Figure 1.2). The large, unprecedented tsunami toppled sea defences, inundating more than 500 km^2 of land and destroying entire settlements and towns along the coastline. This M_w9.0 earthquake is the largest event that has been recorded in Japan since the beginning of instrumental seismology circa 1900 and contributes 5% of the global cumulative seismic energy released since 1900 (Witze, 2011). An event of such magnitude had not been foreseen for the Japan Trench where the maximum magnitude was not expected to exceed M_w8.4 (see section 2 for details). On the 24th June 2011, the government of Japan (GoJ, 2011) announced the estimated total direct loss to be around ¥16.9 trillion (US$215 billion), making this the World"s costliest earthquake. Indirect costs related to the nuclear crisis in Fukushima prefecture are expected to push the cost of the earthquake beyond ¥25 trillion (see section 2.4).

Japan is exposed to some of the world"s most extreme natural hazards and is considered to be one of the most prepared countries in terms of earthquake and tsunami defence. An early warning system is in place for both earthquakes and tsunami; sea defences had been erected along the key locations of the coastline; evacuation drills, both for earthquakes and tsunami take place frequently within the local communities and at schools and work places. There are strict building codes in place, the most recent implemented in 1981 and 1997 respectively (see section 4.1). Many lessons have been learnt from large natural hazard events in the recent past, including the Hanshin Awaji (Kobe) earthquake (1995), Niigata Chuetsu earthquake (2004) and Niigata Chuetsu-oki earthquake (2007).

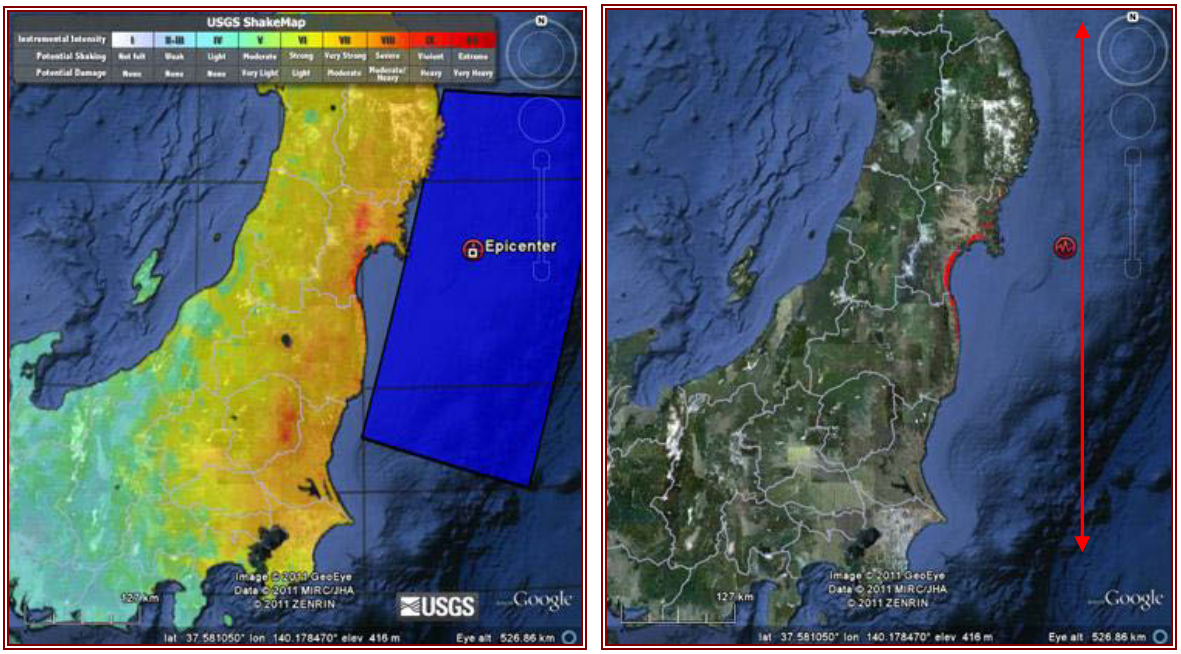

Figure 1.1 (left) USGS Shake map in Google Earth showing the epicentre, fault plane and the Modified Mercalli Intensity (MMI) distribution.

Figure 1.2 (right) Tsunami inundation extent mapped by Asia Air Survey KK (Asia Air Survey, 2011), overlaid on map of Tōhoku region, Japan, in Google earth. An approximately 500 km long coastline (in red) has been affected.

1.2. The EEFIT Tōhoku mission

Considering the historic significance of the event, its magnitude and the effect it has had on the Japanese society and the built environment, EEFIT deployed a field mission to the Tōhoku region to collect data on the effect of the earthquake and tsunami, as well as to learn lessons from the response and early recovery activities and the effectiveness of the preparedness measures in place. The team consisted of the 9 members with wide-ranging backgrounds and research interests reflecting the complex nature of the March 11, 2011 event (see Table 1.1).

Table 1.1 EEFIT Tōhoku team members (in alphabetical order).

Name	Initials	Affiliations	Research interests
Mr. Siau Chen Chian	DC	PhD student, University of Cambridge	Earthquake Geotechnical Engineering
Mr. Stuart Fraser	SF	PhD student, Massey University / GNS Science Joint Centre for Disaster Research	Tsunami warning and evacuation; Performance of RC buildings
Dr. Katsu Goda	KG	Lecturer in Civil Engineering, University of Bristol	Earthquake risk assessment & Engineering seismology
Mr. Joshua Macabuag	JM	Structural Engineer, BDP, London	Seismic Structural Engineering & Disaster Relief
Mr. Mark Offord	MO	Structural Engineer, Sellafield Ltd.	Nuclear Facilities & Building performance
Mr. Antonios Pomonis *(Team Leader)*	AP	Structural Engineer and Director, Cambridge Architectural Research, Ltd., Global Earthquake Model"s Principal Investigator for Global Earthquake Consequences Database	Earthquake risk assessment & mitigation; Tsunami resilience
Dr. Alison Raby	AR	Reader in Marine Science and Coastal Engineering, University of Plymouth	Coastal Engineering: Extreme wave impacts and overtopping
Dr. Keiko Saito *(Deputy Team Leader)*	KS	Remote sensing and GIS specialist, and Director, Cambridge Architectural Research Ltd; Willis Research Fellow; Senior Research Associate, Department of Architecture, University of Cambridge	Application of RS & GIS to disaster management, post disaster needs assessment and long term recovery
Professor Peter Sammonds	PS	Professor of Geophysics; Director, Institute for Risk & Disaster Reduction, University College London	Earthquake mechanics & Seismology

The main objectives of the mission were as follows:

1. Investigate the effectiveness of the coastal defences in the affected regions, and to compare run-up heights to sea wall defences heights;

2. Investigate the extent of the damage to buildings inland (around 100-150 people lost lives in areas inland that was not affected by the tsunami due to building collapses and land failures);

3. Carry out sampled damage surveys in area nearby strong motion recording stations to investigate correlation of ground motion to damage in inland areas;
4. Study the performance of tall buildings in Sendai downtown and other cities that experienced very strong shaking;
5. Investigate performance of transportation infrastructure and other lifelines in relation to ground motion severity and geotechnical hazards;
6. Investigate landslide and liquefaction effects in the region affected by ground shaking;
7. Investigate performance of industrial facilities to severe ground shaking and tsunami. Visit large industrial areas on the coast of Miyagi and Iwate prefectures;
8. Understand how efficient the warnings were and why people were caught by the waves in relation to the tsunami arrival times. Collect data on run-up heights and inundation distance inland;
9. Assess performance of vertical evacuation structures during the tsunami;
10. Collect information on the effectiveness of the immediate response activities by governmental organisations as well as NGOs, as well as long term recovery;
11. Establish contact and exchange information with Japanese organisations, governmental organisations (national and prefecture level) and NGOs, involved in the response and recovery activities;
12. Establish contacts and exchange information with the Japanese academic community involved in the post-event activities.

The mission was carried out between 27 May and 4 June 2011. Following JSCE"s advisory to foreign field teams, EEFIT waited for the Tōhoku Shinkansen railway line to reopen before launching its mission. The team hired three cars and separated into two to three teams, depending on the itinerary for the day. The team returned to Sendai every day, apart from day 2-3 when some members stayed in the north. The itinerary is shown in Table 1.2 and the main locations visited are marked in Figure 1.3.

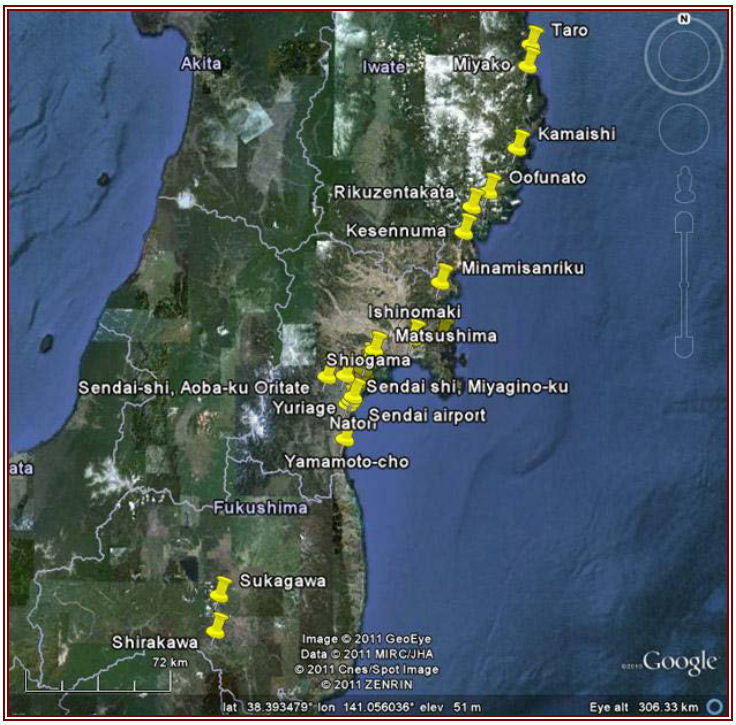

Figure 1.3 Locations visited by the EEFIT team during the 5-day mission, spread over three prefectures (350 km stretch) of the Tōhoku region.

Table 1.2 Locations visited by EEFIT.

Date	Locations visited	EEFIT Team	Accompanied by
Day 1 (Sunday, 29 May) team 1	Sendai city, i.e. Miyagino-ku, Wakabayashi-ku (Oroshi-machi), Sendai Port, Arahama,	All except SF	Dr. Eri Gavanski, Professor Manjae Lee
Day 1 (Sunday, 29 May) team 2	Sendai Airport, Yuriage, Arahama, Sendai Port	SF	JST-JICA and RISTEK Indonesia field trip, organised by Tōhoku University
Day 2 (Monday, 30 May) team 1	Ōfunato tsunami building damage survey and meeting with Mr. Sasaki of the Ōfunato municipality	AP, AR, SF, DC, PS, JM	Professor Hitomi Murakami, Dr. Maki Koyama
Day 2 (Monday, 30 May) team 2	Meeting with JSCE-Professor Mano. Sendai Oritate (ground failure), Minami-Gamou Sewage plant, Tagajyo, Shiogama, Shichigahama, Matsushima	KS, KG, MO	Dr. Eri Gavanski,
Day 3 (Tuesday, 31 May) team 1	Kamaishi tsunami damage survey and meeting with officials of the Kamaishi municipality	PS, AR, SF, JM	
Day 3 (Tuesday, 31 May) team 2	Miyako, Tarō sea defences damage survey	PS, AR	
Day 3 (Tuesday, 31 May) team 3	Rikuzentakata tsunami building damage survey and meeting with Mr. Kikuchi of the Rikuzentakata municipality	AP, DC	Professor Hitomi Murakami, Dr. Maki Koyama
Day 3 (Tuesday, 31 May) team 4	Kesennuma, Matsuzaki Maehama, Shiogama, Ishinomaki. Tsunami damage to buildings and industrial facilities.	KS, KG, MO	

Day 4 (Wednesday, 1 June) team 1	Yuriage, Natori, Watari, Yamamoto-cho. Tsunami building damage survey, sea defences damage survey, geotechnical investigations and meeting with Mr. Yoshida of the Natori municipality.	AP, SF, DC, KG, AR	Professor Hitomi Murakami, Professor Manjae Lee
Day 4 (Wednesday, 1 June) team 2	Meeting with MoD in Sendai, Matsushima	PS, KS, JM, MO	
Day 5 (Thursday, 2 June) team 1	Minamisanriku, Onagawa, Ishinomaki. Tsunami building damage and sea defence damage surveys.	AP, SF, AR, JM, MO	Officials of Miyagi prefecture Civil Engineering Division (Mr. Morikawa and Mr. Osanai)
Day 5 (Thursday, 2 June) team 2	Shirakawa, Sukagawa. Building damage surveys near ground motion recording stations and landslide, liquefaction investigations	KG, KS, DC, PS	
Day 6 (Friday, 3 June) team 1	(Tokyo) Japanese Red Cross meeting, MoD meeting	JM, KS, MO	
Day 6 (Friday, 3 June) team 2	Arahama, Natori	KG, DC, PS, SF	British Geological Survey
Day 6 afternoon	British Embassy Tokyo	All except SF	Chris Pook, Kevin Knappett, Naomi Takegishi (British Embassy) Professor Horii (Tokyo U), Mr. Matsumoto and Mr. Marusaki (MoD)

1.3. Japanese collaboration

Whilst in Tohoku, the EEFIT team received assistance from numerous Japanese organisations and individuals which include: Japanese Society of Civil Engineering (JSCE), in particular Professor Akira Mano (Chairman, Joint Academic Research Group for the Great East Japan earthquake, JSCE and Tōhoku University, Disaster Control Research Centre); Dr. Eri Gavanski (Department of Architecture, Tōhoku University); Professor Manjae Lee (Sendai National College of Technology); Professor Hitomi Murakami (Department of Engineering, Yamaguchi University); Dr. Maki Koyama (Department of Engineering, Kyoto University).

We are also grateful to Mr. Morikawa and Mr. Osanai (Miyagi Prefecture, Civil Engineering Division) for showing us around in Ishinomaki, Onagawa and Minamisanriku; to Mr. Kikuchi of the Rikuzentakata municipality; Mr. Sasaki of the Ōfunato municipality; Mr. Yoshida of the Natori municipality and Mr Yamada of Kamaishi municipality, for receiving us in their offices and giving us details of the effects in their cities. We were also fortunate to have meetings with the following organisations: in Sendai, Ministry of Defence (Colonel Sanefuji and Mr. Marusaki); in Tokyo, we had the pleasure of meeting Mr. Sugai (Japanese Red Cross), Mr. Okuyama, Mr. Matsumoto and Mr. Sakagawa (Ministry of Defence) to hear about the response activities following the earthquake and tsunami. On the last day, the British Embassy kindly hosted the EEFIT team and guests where a summary of the trip was provided and future collaboration opportunities were discussed.

A full acknowledgements list is presented at the beginning of this report.

Figure 1.4 EEFIT team (DC, AP, KG, PS, MO, KS, JM) and Professor Murakami (2nd from left) and Dr. Koyama (middle).

Figure 1.5 EEFIT team (AR, DC, PS, JM, KS, MO, KG – see table 1-1 for initials) with Dr. Eri Gavanski (4th from left) and Professor Lee (far right).

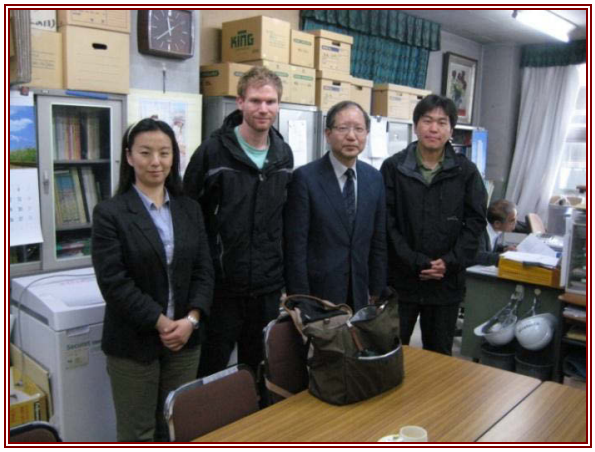

Figure 1.6 (left) EEFIT team (KS, MO, KG) with Professor Mano (Tōhoku University, Disaster Control Research Centre and JSCE).

Figure 1.7 (right) EEFIT team (JM, AP, MO, AR, SF - see table 1-1 for initials) with Mr. Osanai from Miyagi Prefecture, Civil Engineering Division office.

Figure 1.8 (left) EEFIT team talking to Miyagi Prefecture officials (left). From right, SF, JM and AP.

Figure 1.9 (right) EEFIT team at the British Embassy in Tokyo. Mr. Matsumoto-Prouten (far right) and Ms. Takegoshi (second from right) from the British Embassy, Professor Horikawa Tokyo University (front row, third from right) Mr. Marusaki (behind Professor Horikawa) and Mr. Matsumoto (behind AP) from the Ministry of Defence.

1.4. References

Asia Air Survey, 2011. Inundation vector map. Available at: <http://113.37.94.100/gdms/downloads/index.php?id=file_4db17403eb93a> [Accessed 22 July 2011].

Government of Japan, 2011. March quake-tsunami estimated to cost Japan 16.9 trillion yen. Available at: <http://mdn.mainichi.jp/mdnnews/business/archive/news/2011/06/24/20110624p2g00m0bu067000c.html> [Accessed 21 July 2011].

Witze, A., 2011. Seismologists rumble over quake clusters. *Science News* 179(10) 7 May 2011.

2. The earthquake of 11th March 2011

2.1. Rupture zone and tectonics of the Japan Trench

The 2011 moment magnitude (M_W) 9.0 Tōhoku earthquake occurred on the 11th March at 14:46 local time (05:46 GMT), 130 km off the coast of Japan in the Pacific Ocean at the Japan Trench. The earthquake was on the megathrust where the Pacific Plate subducts at a rate of 80 to 85 mm/yr (Demets et al., 2010) beneath northern-eastern Honshu (Tōhoku region, Figure 2.1) (Simons et al., 2011). This is part of the Okhotsk Plate, but was formerly considered to be the North American Plate (Seno and Sakurai, 1996). The rupture of the lithosphere was nearly 500 km long and 200 km wide, down-dip, from the subduction trench to the coast of Honshu. This is mapped out by the aftershock distribution in Fig. 2.2. The event triggered a tsunami along the Tōhoku coast with onshore inundation depth of over 15 m in places. It is the largest instrumentally recorded earthquake to have occurred in and around Japan.

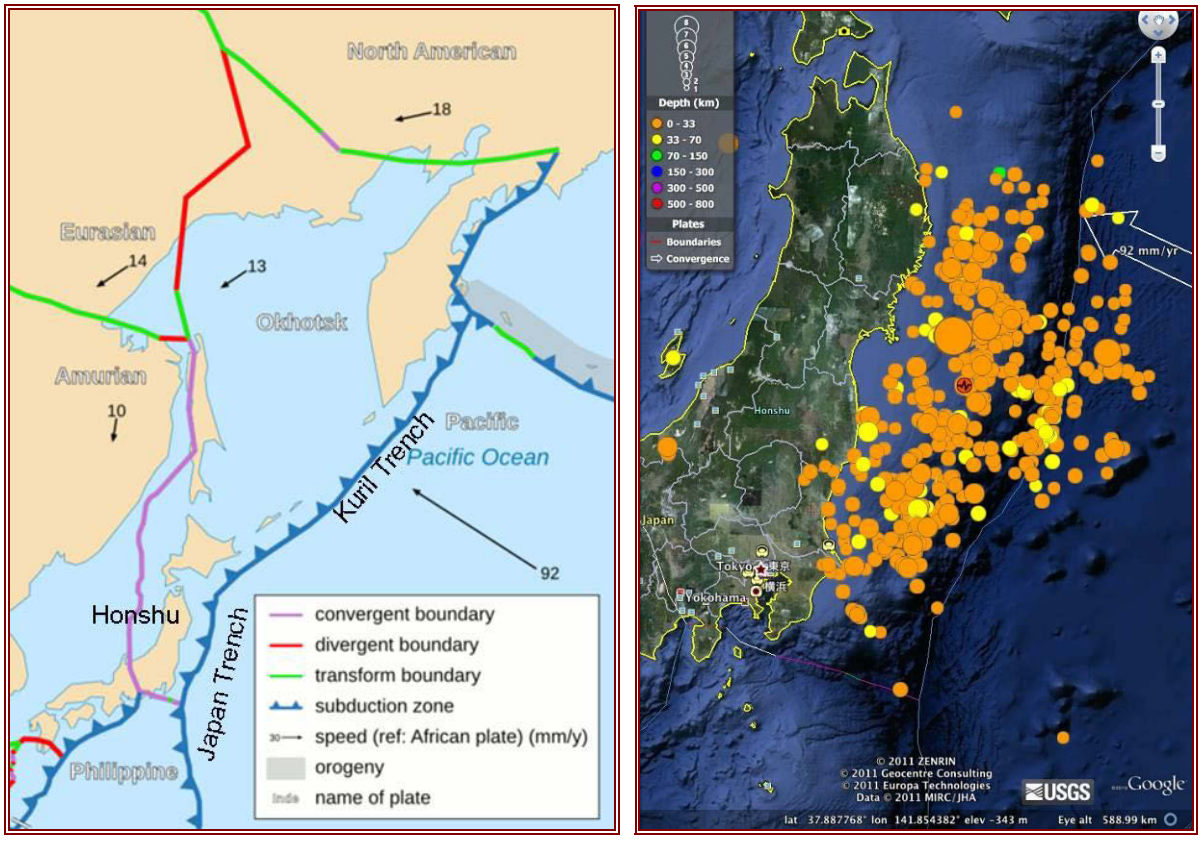

Figure 2.1 (left) The Okhotsk Plate showing the subduction zone where the 2011 Great East Japan Earthquake occurred (adapted from E. Gaba, Wikimedia Commons user: Sting; original data from Bird (2003). Plate motions are shown in mm/yr.

Figure 2.2 (right) Aftershocks in the 7 days following the 2011 Great East Japan Earthquake. (Courtesy of the U.S. Geological Survey. Google Earth image).

The lithosphere off north-east Japan is relatively old (about 130 Ma), while the speed of convergence of the Pacific Plate and the Okhotsk Plate at about 90 mm/yr is within the highest of the world (Ruff and Kanamori, 1980). Lithospheric ages at subduction zones range from roughly 20 to 150 Ma and convergence velocities from roughly 20 to 110 mm/yr. Ruff and Kanamori (1980) proposed that the largest earthquakes (magnitude 8.5 and above), which have the potential to generate giant tsunami, occur only when young lithosphere subducts rapidly. Underpinning this relationship is the concept that subduction zones with young, rapidly subducting lithosphere would be strongly coupled mechanically, resulting in the largest earthquakes. On this basis the magnitude (M_W 9.0) of the 2011 Great East Japan Earthquake and tsunami would not have been predicted. In 2007, following the 2004 Boxing

Day Sumatran Earthquake (M_W 9.3) and Indian Ocean tsunami, Stein and Okal (2007) revisited this question. They concluded that although the correlation of magnitude with lithospheric age and convergence velocities appeared plausible with the data then available in the 1980s (correlation coefficient, r = 0.8), much of the correlation vanished (r = 0.4) using new data and that there is no clear effect of lithospheric age. This has important implications for seismic hazard assessment at subduction zones worldwide, since previous hazard assessments may need to be re-evaluated.

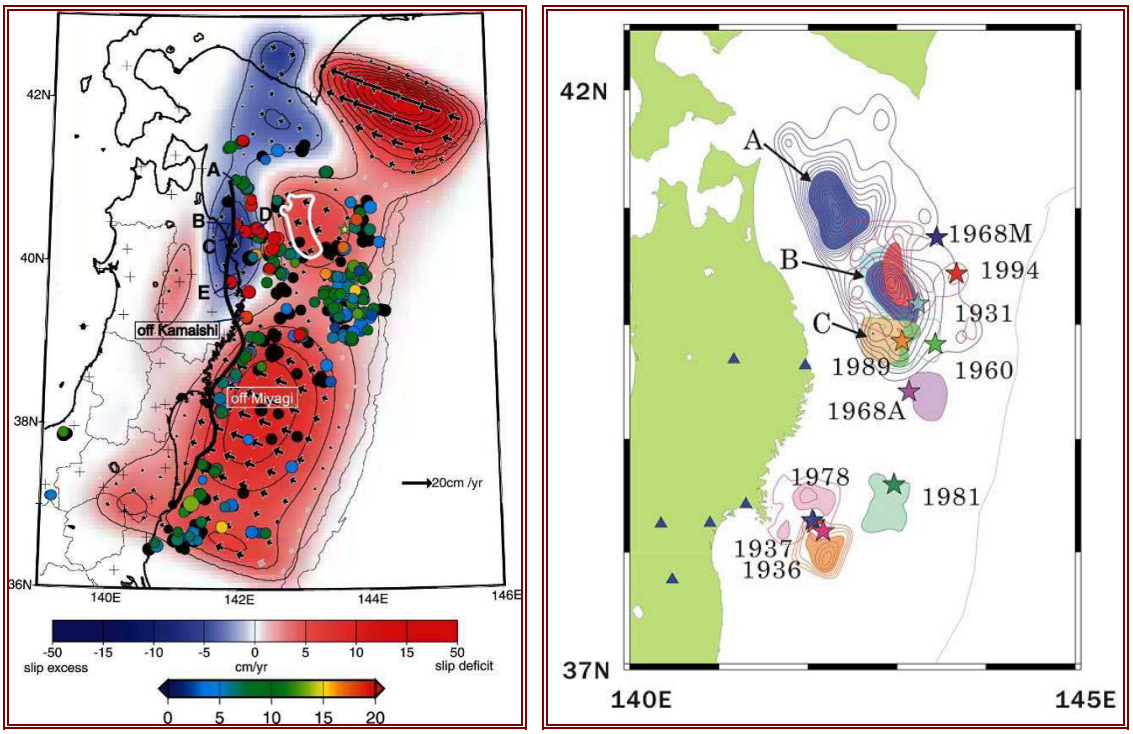

Figure 2.3 (left) Slip deficit modelled from GPS and repeating earthquake data (Igarashi et al., 2003). Contours are at intervals of 20 mm/yr. Arrows indicate the amount of slip. Solid coloured circles show the locations of repeating earthquake clusters and their colours show average slip rate.

Figure 2.4 (right) Asperity map along the subduction zone in north-eastern Japan (Yamanaka and Kikuchi, 2004). Stars show the main shock epicentres and contour lines the moment release distribution.

Japan has one of the best GPS networks in the world for measuring crustal strain. Figure 2.3 shows a comparison of slip rate distributions on the plate boundary estimated from GPS data for the period from April 1996 to March 1999 and from repeating earthquake data, produced by Igarashi et al. in 2003. Red indicates a slip deficit area and blue is a slip excess (i.e., the slip rate is larger than the interplate convergence rate) area. The striking correspondence of the measured slip deficit area off the Honshu coast with the subsequent fault slip area, mapped out by aftershocks, suggests this may be interpreted as a predictor of likely rupture size and hence magnitude of the forthcoming 11th March 2011 earthquake (G. Roberts, Personal Communications, 2011). The slip deficit off the coast of Hokkaido corresponds with the 2003 Hokkaido Tokachi-oki earthquake (M_W8.3) which had not yet occurred when the Igarashi paper was published, c.f. Miyazaki et al. (2004).

2.2. Historical seismicity and tsunami in the Japan Trench

There have been frequent major earthquakes and tsunami on the Japan Trench and southern part of the Kuril Trench (Figure 2.1) which are listed (not exhaustively) in Table 2.1.

The hazard assessment and map of earthquakes on major faults around Japan is based on historical seismicity. Figure 2.5 shows the Headquarters for Earthquake Research Promotion - HERP (2009) hazard map. The segmentation of faults shown is based on recent major earthquakes noted in the figure. Earthquakes expected offshore Tōhoku were of magnitude 7.4 to 8.2, based on the segmentation of the Japan Trench into 6 fault segments (Okumura, 2011). The 11th March 2011 earthquake ruptured all 6 segments in a single megathrust earthquake.

Table 2.1 Notable earthquakes on the Japan Trench and southern most Kuril Trench in chronological order (data is compiled from various sources).

Earthquake	Date	Magnitude	Comment
Fukushima	11 April 2011	6.6	aftershock
Miyagi	7 April 2011	7.1	aftershock
Tōhoku	11 March 2001	7.9	aftershock
Tōhoku	11 March 2011	7.7	aftershock
East Japan	**11 March 2011**	**9.0**	**megathrust**
Tōhoku	9 March 2011	7.2	foreshock
Miyagi	16 August 2005	7.2	
Tokachi-oki	25 September 2003	8.3	
Sanriku-oki	28 December 1994	7.7	
Miyagi	2 November 1989	7.5	
Miyagi	19 January 1981	7.0	
Miyagi	12 June 1978	7.7	tsunami
Nemuro-oki	1972	7.4	tsunami
Miyagi	12 June 1968	7.4	
Aomori	16 May 1968	8.2	tsunami
Miyagi	21 March 1960	7.5	
Tokachi-oki	4 March 1952	8.2	tsunami
Ibaraki	1938	7.9	tsunami
Miyagi	27 July 1937	7.1	
Iwate	3 November 1936	7.5	
Showa Sanriku	**2 March 1933**	**8.4**	**tsunami**
Miyagi	9 March 1931	7.2	
Meiji Sanriku	**15 June 1896**	**8.3**	**tsunami**
Nemuro-oki	1893	7.9	tsunami
Tokachi-oki	1843	8.0	tsunami
Keicho Sanriku	**1611**	**8.6**	**tsunami**
Kanei Sanriku	1793		tsunami
Boso hanto	1703	8.2	tsunami
Jogan Sanriku	**13 June 869**	**8.4**	**tsunami**

Seismicity offshore Tōhoku has been analysed in terms of the asperity model for large earthquakes, proposed in the 1980s, which underpins ideas of fault segmentation. Lay and Kanamori (1981) examined the asperity size of the circum-Pacific subduction zones and found that the size is characteristic of its region, which then Ruff and Kanamori (1983) suggested is the principal control on the eventual earthquake size. Yamanaka and Kikuchi (2004) identified large asperities for eight earthquakes offshore of Tōhoku (Figure 2.4) and concluded that the typical size of individual asperities corresponds to magnitude 7 earthquakes but a magnitude 8 earthquake can be caused when the rupture of several asperities are synchronised. They found a recurrence interval of about 30 years for earthquakes of magnitude 7. They divided the region into three: (i) The north (40°N to 41.3°N) where the mechanical coupling between the over-riding and subducting plates is strong and earthquake magnitude is high; (ii) the central part (39°N to 40°N), where little seismic moment had been released by large earthquakes and the asperity size is small; (iii) the south (37.8°N to 39°N) where the mechanical coupling is of intermediate strength. The fact that the 11th March 2011 earthquake ruptured 500 km of lithosphere incorporating the strongly coupled, weakly coupled and

intermediately coupled areas shows that an assessment of asperities and their coupling can only be used as a part of hazard assessment on subduction zones.

Not all Tōhoku earthquakes are associated with subduction zone asperities. The 1933 magnitude 8.3 Showa Sanriku earthquake and tsunami was due to normal faulting on the outer rise on the east of the Japan Trench for instance.

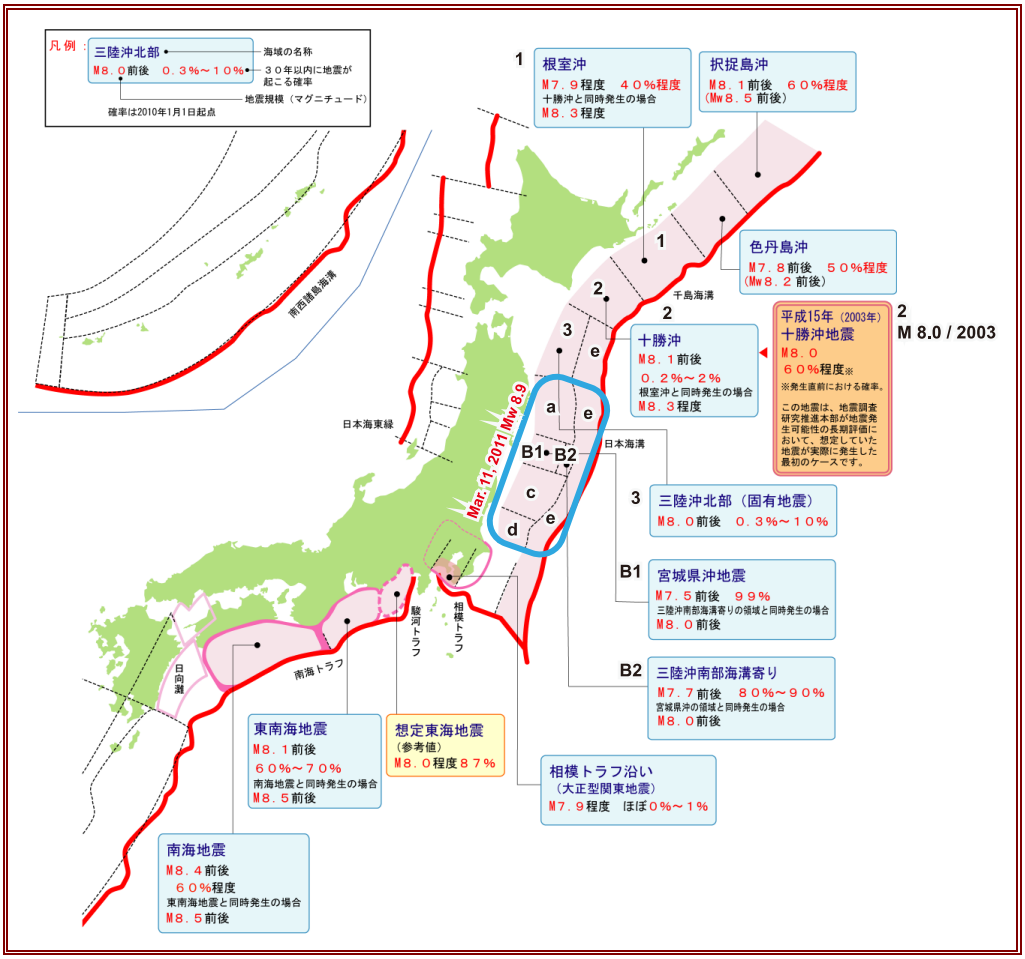

Figure 2.5 HERP: Headquarters for Earthquake Research Promotion (2009) map of fault segments along the Japan subduction zones with the 11th March Tōhoku earthquake marked by blue boundary encompassing fault segments 3 a to e. (Courtesy of HERP).

2.3. Earthquake rupture mechanism and tsunami generation

The 11th March 2011 earthquake occurred on the megathrust at the Japan Trench where old lithosphere of the Pacific Plate subducts rapidly under the Okhotsk Plate. The rupture sequence consisted of a small deep rupture lasting 40 s, followed by extensive shallow rupture after a minute and then continuing deep rupture lasting over 100 s (Ide at al., 2011). The rupture of the lithosphere was nearly 500 km long and 200 km wide, down dip, although the majority of the slip was contained in a region 300 km long by 150 km wide (Ammon et al., 2011). The mechanism of the earthquake was a reverse fault with low angle dip, located along the interface between the subducting and overlying plates (Lay et al., 2011). A combination of a shallow dipping fault and a compliant hanging wall would have enabled the large shallow slip near the trench. Analysis of GPS network data, shows the earthquake caused significant quasi-permanent displacements due to the main-shock, which occurred over the entire northern half of Honshu (Simons et al., 2011), Figure 2.6.

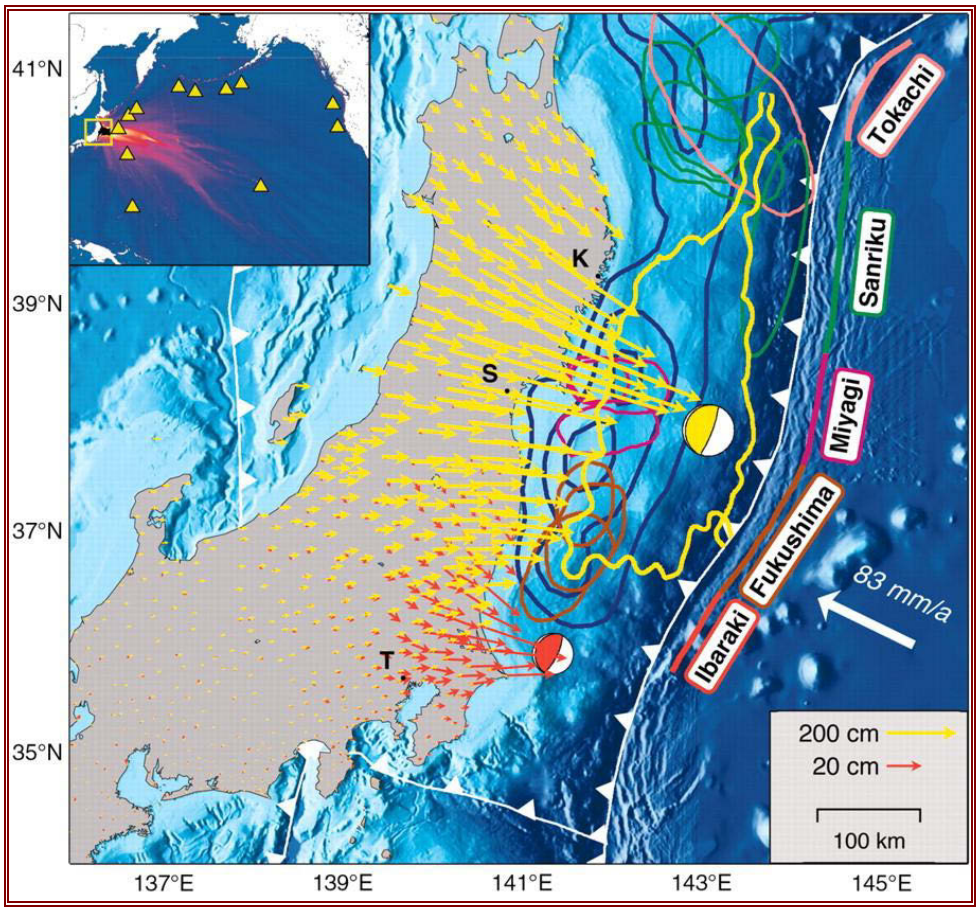

Figure 2.6 Map of central and northern Honshu, Japan. Vectors indicate the horizontal component of the GPS displacements for the mainshock (yellow) and the M_W7.9 aftershock (orange). The closed yellow curve indicates the outline of the M_W9.0 mainshock (8 m slip contour). The region of inferred slip deficit or high plate coupling is indicated by dark blue nested contour lines for 35%, 70%, and 100% coupling. From Simons et al. (2011) reprinted with permission from AAAS.

The earthquake triggered a tsunami over 15 m high in places along the Sanriku, Miyagi, Joban and Kanto coasts. The most likely mechanism for triggering the tsunami is rebound of the overlying plate, although Vita-Finzi (2011) argues that superficial faults on the sea floor may have made a bigger contribution than the megathrust itself. Within 10 minutes of the earthquake the first tsunami reached the coast as minor backwash, probably caused by coastal subsidence; 30 to 40 minutes after the earthquake huge run-ups inundated the coastal lowlands (Okumura, 2011). The short time interval between the earthquake and the arrival of the first tsunami wave indicates the fault reached close to the coast and induced minor subsidence above the western part of the fault plane. InSAR data indicates that most coastal areas seem to have been subsided by around 50 cm (Figure 2.7).

The induced seismicity on Honshu shows normal faulting with a T-axis orientated in a roughly E-W direction (Kato et al., 2011). Comparison of the focal mechanisms recorded before and after the 11th March earthquake suggests that the stress field abruptly changed from one of E-W horizontal compression to E-W extension in the northern part of Ibaraki Prefecture. This is confirmed by field measurements of slip made in the field by the EEFIT team, although compression was also measured on an active shallow reverse fault.

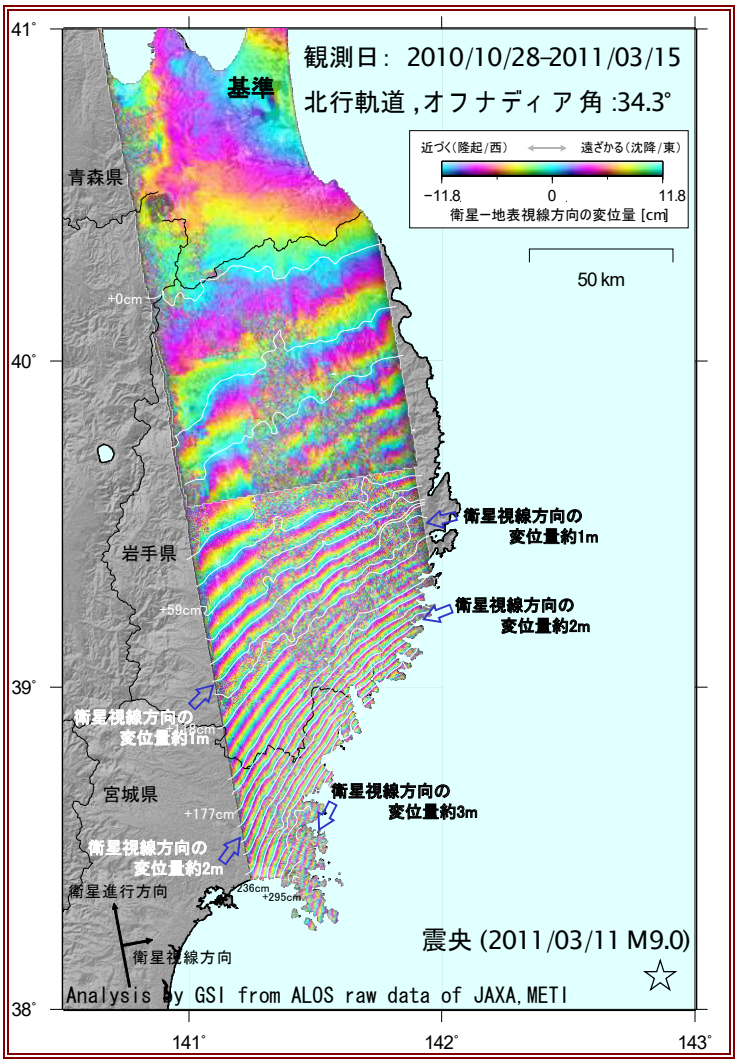

基準+約1m

Figure 2.7 Co-seismic interferogram from ALOS PALSAR (ascending path 401 spanning 2010/10/28-2011/03/15). Each interferogram represents the relative displacement in the line-of-sight direction from the imaging SAR sensor due to the 11th March earthquake. One colour cycle represents 11.8 cm of range change. (Courtesy of METI/JAXA. Analysed by GEO Grid, AIST, Japan).

Kato et al. (2011) state that the rate of shallow seismicity during the eight years before the 11th March earthquake had been extremely low. The rate of seismicity abruptly increased after the megathrust earthquake, and several large magnitude events as high as M 7.9 occurred and Vallianatos and Sammonds (2011) point to evidence of an apparent rise of the rate of strong earthquakes.

The 2011 Tōhoku earthquake, at M_W9.0, was of far higher magnitude than had been proposed in the HERP hazard map based on historical seismicity or had been expected from the subduction zone segmentation earthquake models. Proposed magnitudes for earthquakes in the Tōhoku region had been M 7.4 to M 8.2, rupturing one or two fault segments of the Japan Trench. However, the 2004 Boxing Day Sumatran earthquake (M_w 9.3) and tsunami, was much larger than expected (Stein and Okal, 2007), and should have meant a re-evaluation of the tsunami hazard assessment for Japan. The 11th March earthquake and tsunami should similarly call for the re-evaluation of subduction zone earthquake hazard globally.

2.4. Economic loss due to the earthquake and tsunami

Since 1995 Japan has suffered tremendous economic losses due to earthquakes. The 17th January 1995 Hanshin-Awaji earthquake in Kobe was (until 11th March 2011) the costliest earthquake event ever: ¥11.6 tn has been spent for reconstruction and recovery in the Kobe region (US$147.5 bn using

exchange rate as of July 2011). The 23rd October 2004 Niigata-ken earthquake was the fifth largest earthquake loss globally, with an US$28 bn loss (2004 values) (III, 2011).

The municipalities affected by the Tōhoku earthquake and tsunami contribute just 2.4% of the shipment value and gross value added of the municipalities of Japan along the Pacific Ocean coast (GoJ, 2011) and the 3 worst-affected prefectures (Iwate, Miyagi and Fukushima) contribute only 4% to Japan"s GDP (US$5.46 tn in 2010; Ministry of Internal Affairs and Communications, 2011). Despite this, the 11th March 2011 earthquake, with its tremendous tsunami damage, moderate but widespread ground shaking and geotechnical damage, and effects of the nuclear crisis, has now become the costliest earthquake globally. The economic loss due to this event far exceeds the loss of the 1995 earthquake in Kobe and the 2008 earthquake in Wenchuan (China) after which the Chinese government pledged to spend US$146.5 bn for reconstruction, recovery and development plans.

As early as five days after the earthquake the first economic loss estimates were produced by Japanese economists (Reuters, 2011) ranging from ¥10 tn to ¥16 tn (US$125 bn to US$200 bn). Few days later the World Bank (2011) gave its own assessment for the likely cost of this event at US$122 bn to US$235 bn. The Japanese Cabinet Office gave its first detailed estimate of the cost of the earthquake on 23rd March, saying that the extensive damage to housing, roads, utilities and businesses across 7 Prefectures would result in losses that could range between ¥16 tn and ¥25 tn (US$198 bn to US$309 bn). This value is 3.6% to 5.7% of the country"s GDP, and excludes the effects of the nuclear crisis (GoJ, 2011b).

Uncertainties in loss estimates stemmed from the Fukushima Daiichi nuclear power plant disaster and its effects on energy supply and the population"s health, and were naturally predominant in the first weeks after the earthquake as the crisis was still on-going and the outcome uncertain. “Rolling blackouts” that lasted until 29th March (GoJ, 2011) were another concern in the first two to three weeks after the earthquake. Other uncertainties in the initial weeks occurred due to direct damage and supply-chain effects on Toyota and Nissan motor vehicle manufacturers, as they produce 22% and 38% respectively of their annual vehicle output in Japan.

Insured loss estimates were also produced soon after the event by catastrophe risk modelling companies. On 16th March, EQECAT estimated that the total insured loss from this event would be US$12 bn to US$24 bn, with US$2 bn to US$4 bn of the total insured loss expected to be ceded to the Japan Earthquake Reinsurance Pool, which will reduce the total losses to non-life property insurers in Japan (EQECAT, 2011). On 25th March, AIR Worldwide estimated that the insured loss would be in the range of US$19 bn to US$30.7 bn (their estimate comprised US$11 bn to US$21 bn due to ground shaking and fire following damage, and US$8 bn to US$9.7 bn due to tsunami damage, including pay-outs from the Japan Earthquake Reinsurance Company (AIR, 2011). On 12th April, Risk Management Solutions estimated that the insured loss would be in the range of US$21 bn to US$34 bn, comprising US$3 bn to US$8 bn in losses to the life and health insurance sectors and US$18 bn to US$26 bn in property insurance losses (Reuters, 2011b). The world"s two biggest reinsurance companies, Munich Re and Swiss Re estimated their respective losses at US$2.15 bn and US$1.2 bn on 22nd March and 21st March (Munich Re, 2011 and Swiss Re, 2011).

Two months after the earthquake it was announced that insurance pay-outs had already reached ¥670 bn (US$8.25 bn) (Daily Yomiuri, 2011a). Kyodo News (2011) reported on 21st May, that the insurance pay-outs were expected to reach ¥2.6 tn (US$32 bn) as more categories of loss were added to the ¥970 bn expected to be paid for repair and reconstruction of residential properties damaged by the earthquake and tsunami. Additional categories would include property damage due to fire losses incurred by companies, life insurance claims, and payments of mutual insurance cooperatives to their members such as farmers.

On 27th April, the rating agency Standard and Poor"s projected the reconstruction costs at between ¥20 tn and ¥50 tn (US$245 bn to US$613 bn) in a report that cut the credit outlook of Japan"s sovereign credit rating (Reuters, 2011c). This was followed by a similar warning from the rating agency Fitch, on 27th May. Fitch refrained from making any estimates about the cost of the 11th March earthquake, but said that "there is considerable downside risk for the public finances from the still-unknown cost of cleaning up the Fukushima nuclear plant. Delays in restoring power supplies could lead Fitch to revise down its 2011 growth forecast from 0.5 per cent”, while noting that government spending on rebuilding the quake-ravaged areas could boost the economy in 2011 and 2012 (Reuters, 2011d).

It is clear that great uncertainty continued to prevail 11 weeks after the earthquake as to the effects of the nuclear crisis on the Japanese economy. The Japan Centre for Economic Research estimates that the costs of this crisis could range from US$71 bn to US$250 bn; the estimated cost of the nuclear incident is discussed in more detail in section 9.2.5.

On 24th June, the Japanese government completed its loss assessments announcing that the final estimate of economic loss was ¥16.9 tn (US$210 bn). The estimate was based on hearings from ministries concerned and the 9 affected prefectures: Aomori, Iwate, Miyagi, Fukushima, Tochigi, Ibaraki, Chiba, Niigata and Nagano. This estimate is thus considered more accurate than the previous estimate of 23rd March (GoJ, 2011c). The expected loss includes about ¥10.4 tn (61.5%) to reconstruct buildings such as homes, stores and corporate facilities, ¥2.2 tn (13%) to rebuild social infrastructure such as roads and harbours, ¥1.9 tn (11%) for agriculture and fisheries, ¥1.35 tn (8%) for general infrastructure e.g. water supply, sewage, power grid and ¥1 tn (6%) for other facilities including schools and hospitals. This estimate does not include losses due to the crisis in the Fukushima Daiichi nuclear power plant.

Compared to Kobe, the cost of damage to structures is 1.8 times higher while the cost of damage to agriculture is 20 times higher. On 22nd July, the Japanese government provisionally increased its estimation of the cost of the earthquake by ¥6.1 tn to a new total of ¥23 tn (US$297 bn), foreseeing that this expenditure would be spread across a 10-year period, with 80% being spent in the first 5 years (GoJ, 2011d). The increased estimate was obtained when expenditure was added for demarcating land affected by the 11th March event, relocating people who used to live in devastated areas as well as infrastructure development related to the farming and fisheries industries.

As a result of the disaster the Japanese government approved ¥1 tn (US$12.9 bn) expenditure from its 2010 Fiscal Year budget which ended on 31st March 2011 (World Bank, 2011). Then on 2nd May, an additional ¥4 tn (US$51.7 bn) was approved, intended for restoration work such as clearing massive amounts of rubble and building temporary housing for the thousands of people who lost their homes, rebuilding of roads, airports, hospitals and schools as well as recovery and clean-up of farms and loans to small- and medium-sized businesses (GoJ, 2011e). The reconstruction of the circa 110,000 destroyed buildings and housing will require additional funds.

The May expenditures were followed by an additional ¥2 tn (US$25.9 bn) of funds that include ¥275 bn (US$3.55 bn) for costs related to the nuclear crisis (incl. health checks on people affected) and ¥300 bn (US$3.87 bn) for additional financial support to people whose homes were badly damaged or destroyed (Japan Times, 2011). On 21st October 2011, the Japanese Cabinet approved a third supplementary budget allocating an additional ¥9.24 tn (US$119.4 bn) intended for the reconstruction of the affected areas (Daily Yomiuri, 2011b). This supplementary budget was expected to be approved by the Parliament in mid-November 2011.

Thus the Japanese government has already approved expenditure totalling ¥16.2 tn (US$210 bn) in the first 8 months since the earthquake. So far the budgeted earthquake expenditures in the current fiscal year amount to almost 14.3% of the country"s current fiscal year budget.

Adding the estimate of the Japanese government of 22nd July and the total insured loss estimate of 14th May, a total cost of ¥25 tn (US$323 bn) is obtained, which is equivalent to 5.9% of Japan"s GDP in 2010. This amount does not include the costs of business interruption and other indirect effects on Japan"s production industries, nor is it clear whether commercial and industrial properties would have complete insurance coverage to finance the costs of the direct and indirect damage to their production and trading capacity. It is also not clear whether all the costs stemming from the nuclear crisis had been assessed by 22nd July. On 4th November 2011 the government approved TEPCO's request for ¥1.01 tn (US$13 bn) in financial aid to compensate victims of the crisis at TEPCO's Fukushima Daiichi nuclear power plant (Daily Yomiuri, 2011c). Clearly there are still many uncertainties and it will take more time until the final cost of this earthquake will be assessed more accurately.

2.5. Conclusions on the earthquake of 11th March 2011

The 2011 Tohoku earthquake had a magnitude of 9.0 (M_w). This exceeded considerably the expected magnitude range of 7.4 to 8.2 for the region (HERP, 2009). The magnitude of the 11th March event meant that the generation of a tsunami was highly likely. The 2004 Boxing Day Sumatran earthquake and tsunami should also have meant a re-evaluation of the tsunami hazard assessment for Japan.

The 11th March earthquake and tsunami should similarly call for the re-evaluation of subduction zone earthquake hazard globally.

With tremendous tsunami damage and moderate but widespread ground shaking and geotechnical damages, this event has now become the World"s costliest earthquake. The World Bank"s (2011) assessment for the likely cost of this event is US$122-235 bn, while the rating agency Standard and Poor"s projected the reconstruction costs at between US$245-613 bn, in a report that cut the credit outlook of Japan"s sovereign credit rating. Uncertainties stemming from the Fukushima Daiichi nuclear power plant disaster and its effects on energy supply and the population"s health are still on going.

2.6. References

AIR (2011). AIR Worldwide Updates Estimate of Insured Losses from the M_W9.0 Tōhoku earthquake Based on Detailed Analysis of Ground Motion and Tsunami Footprint. http://www.air-worldwide.com/NewsAndEventsItem.aspx?id=20437 (accessed on July 22, 2011).

Ammon, C.j., T. Lay, H. Kanaore and M. Cleveland (2011) A rupture model of the great 2011 Tohoku earthquake, *Earth Planets Space* **63**, 693-696.

Bird, P. (2003). An updated digital model of plate boundaries, *Geochem. Geophys. Geosyst.* 4 , no. 3, doi 10.1029/2001GC000252.

Daily Yomiuri (2011a). Quake insurance system must give peace of mind. http://www.yomiuri.co.jp/dy/editorial/T110514002500.htm (accessed on July 22, 2011).

Daily Yomiuri (2011b). Cabinet approves 3rd extra budget for FY11. http://www.yomiuri.co.jp/dy/national/T111021005455.htm (accessed on November 11, 2011).

Daily Yomiuri (2011c). Govt certifies financial aid to TEPCO. http://www.yomiuri.co.jp/dy/national/T111104004596.htm (accessed on November 11, 2011).

DeMets, C., Richard G. Gordon and D. F. Argus (2010) Geologically current plate motions, *Geophys. J. Int.* 181, 1-80.

Eqecat (2011). Estimated Total Insured Losses at $12-25 bn USD for M9 Tōhoku Pacific Offshore Event. http://www.eqecat.com/catWatchRev/secureSite/report.cfm?id=313 (accessed on July 22, 2011).

FDMA (2011). Fire and Disaster Management Agency of Japan, Report 133 on the effects of the March 11, 2011 Great Tōhoku earthquake, July 21, 2011. http://www.fdma.go.jp/bn/2011/detail/691.html (accessed on July 22, 2011).

GoJ (2011a). Economic Impact of the Great East Japan Earthquake and Current Status of Recovery. May 16, 2011 Powerpoint presentation of the Government of Japan.

GoJ (2011b). Official: Quake, tsunami could cost Japan $300 bn. http://articles.cnn.com/2011-03-31/world/japan.disaster.budget_1_tsunami-quake-yen?_s=PM:WORLD (accessed on July 22, 2011).

GoJ (2011c). March quake-tsunami estimated to cost Japan 16.9 tn yen. http://mdn.mainichi.jp/mdnnews/business/archive/news/2011/06/24/20110624p2g00m0bu067000c.html (accessed on July 21, 2011).

GoJ (2011d). Reconstruction of quake-hit areas could cost gov't 23 tn yen. http://mdn.mainichi.jp/mdnnews/news/20110722p2g00m0dm023000c.html (accessed on July 22, 2011).

GoJ (2011e). Japan passes 4 tn yen disaster relief budget. http://www.terradaily.com/reports/Japan_passes_4_tn_yen_disaster_relief_budget_999.html (accessed on July 22, 2011).

GoJ (2011f). Japan quake pushes budget spending to 1.1 tn dollar yearly. http://bnn-news.com/japan-quake-pushes-budget-spending-1-1-tn-dollar-yearly-22529 (accessed on July 22, 2011).

HERP: Headquarters for Earthquake Research Promotion (2009) map home.hiroshima-u.ac.jp/kojiok/110311EQ/HERPmapwithnotes1.pdf.

Ide, S., A. Baltay and G. C. Beroza (2011), Shallow dynamic overshoot and energetic deep rupture in the 2011 M_W9.0 Tōhoku-Oki Earthquake, *Science* doi: 10.1126/science.1207020.

Igarashi, T., T. Matsuzawa and A. Hasegawa (2003) Repeating earthquakes and interplate aseismic slip in the northeastern Japan subduction zone, J. Geophys. Res. 108, (B5), 2249, doi:10.1029/2002JB001920.

Japan Times (2011). Cabinet OKs ¥2 tn quake-aid budget. http://search.japantimes.co.jp/cgi-bin/nb20110706a1.html (accessed on July 22, 2011).

Kato, A., S. Sakai and K. Obara (2011) A normal-faulting seismic sequence triggered by the 2011 off the Pacific coast of Tōhoku Earthquake: Wholesale stress regime changes in the upper plate, (sub).

Kyodo News (2011). Insurance payments to quake victims to total 2.6 tn yen. http://www.breitbart.com/print.php?id=D9NBS7GO0&show_article=1 (accessed on July 22, 2011).

Lay, T. and H. Kanamori (1981) An asperity model of large earthquake sequences, in Earthquake Prediction: An International Review, *Maurice Ewing Ser.*, vol. 4, edited by D. W. Simpson and P. G. Richards, pp. 579 – 592, AGU, Washington, D. C.

Lay, T., C.J. Ammon, H. Kanamori, L. Xue and M.J. Kim (2011) Possible large near-trench slip during the great 2011 Tōhoku (M_W9.0) earthquake, *Earth Planets Space*, 63, 1-6).

Ministry of Internal Affairs and Communications, 2011, Statistics Bureau, Director-General for Policy Planning (Statistical Standards) and Statistical Research and Training Institute, Japan Statistical Yearbook [online] <http://www.stat.go.jp/english/data/nenkan/1431-03.htm>. Accessed on 26th July 2011.

Miyazaki, S., P. Segall, J. Fukuda and T. Kato (2004) Space time distribution of afterslip following the 2003 Tokachi-oki earthquake: Implications for variations in fault zone frictional properties, *Geophys. Res. Ltts*., 31, L06623, doi:10.1029/2003GL019410.

Munich Re (2011). Munich Re estimates claims burden from earthquake in Japan at around €1.5bn. http://www.munichre.com/en/media_relations/press_releases/2011/2011_03_22_press_release.aspx (accessed on July 22, 2011).

Okumura, K (2011) Interplate megathrust earthquakes and tsunami along Japan Trench offshore Northeastern Japan, U. Hiroshima, Japan, home.hiroshima-u.ac.jp/kojiok/110311EQ/.

Reuters (2011). March 16, 2011: Economic hit from Japan quake seen up to $200 bn.

Reuters (2011b). RMS estimates Japan insured losses up to $34 bln. http://uk.reuters.com/article/2011/04/12/japan-insurance idUKN1218576520110412 (accessed on July 22, 2011).

Reuters (2011c). S&P Cuts Japan Credit Outlook On Quake Concerns. http://www.huffingtonpost.com/2011/04/27/sp-changes-japan-economic-outlook_n_854255.html (accessed on July 22, 2011).

Reuters (2011d). Fitch cuts Japan credit rating outlook to negative. http://www.reuters.com/article/2011/05/27/us-japan-economy-fitch-idUSTRE74Q1QQ20110527 (accessed on July 22, 2011).

Ruff, L. and H. Kanamori (1983), The rupture process and asperity distribution of three great earthquakes from long-period diffracted P-waves, *Phys. Earth Planet. Inter*. 31, 202–230.

Ruff, L., and H. Kanamori (1980). Seismicity and the subduction process, *Phys. Earth Planet. Interiors* 23, 240–252.

Satake, K., Y. Namegaya and S. Yamaki (2008) Numerical simulation of the AD 869 Jogan tsunami in Ishinomaki and Sendai plains, 活断層・古地震研究報告, No. 8, p. 71-89. (In Japanese.).

Seno T & Sakurai T (1996) Can the Okhotsk plate be discriminated from the North American plate? *J. Geophys. Res.* 101 (B5) 11,305-11,315.

Simons, M. et al. (2011) The 2011 magnitude 9.0 Tōhoku-Oki Earthquake: Mosaicking the megathrust from seconds to centuries, *Science* 332, 1421-1425.

Stein, S and E. A. Okal (2007) Ultralong period seismic study of the December 2004 Indian Ocean Earthquake and implications for regional tectonics and the subduction process, Bull. Seism. Soc. of Am, 97 (1A), S279–S295 doi: 10.1785/0120050617.

Swiss Re (2011). Swiss Re provides estimate of its claims costs from Japan earthquake and tsunami. http://www.swissre.com/media/news_releases/pr_20110321_japan.html (accessed on July 22, 2011).

Vallianatos, F. and P. Sammonds (2011) Evidence of non-extensive thermodynamic lithospheric instability at the approach of the 2004 Sumatran- Andaman and 2011 Honshu mega-earthquakes, *Geophys. J. Int* (sub.).

Vita-Finzi (2011) Misattributed tsunami 2: the Tōhoku Japan (M_W9.0) 2011.3.11 earthquake, (sub).

World Bank (2011). East Asia and Pacific Economic Update 2011, vol. 1, March 21, 2011: The recent earthquake and tsunami in Japan: implications for East Asia.

Yamanaka, Y. and M. Kikuchi (2004) Asperity map along the subduction zone in northeastern Japan inferred from regional seismic data, *J. Geophys. Res.* 109, B07307, doi:10.1029/2003JB002683.

3. Earthquake ground motion report

A catastrophic megathrust interface subduction earthquake occurred on 11th March, 2011. The moment magnitude was M_W9.0, significantly greater than anticipated earthquake scenarios with M_W7.5 to M_W8.0. One of the main causes for this large size event is the coupled co-seismic rupture of several major fault segments along the Japan trench off-shore Iwate, Miyagi, Fukushima, and Ibaraki Prefectures, which were thought to rupture individually. Such simultaneous rupture has not happened since the 869 Jogan earthquake, which caused massive tsunami along the coastal areas of the Tōhoku region (Minoura et al., 2001).

This chapter is focused on overall characteristics of observed ground motions during both the M_W9.0 mainshock and major aftershocks. Detailed investigations of instrumentally recorded ground motions offer valuable insight on structural and non-structural damage to existing building stocks in the Tōhoku region (section 4). In particular, the following aspects will be covered: (i) complex rupture process of a mainshock and observed ground motions at different locations along the coast (e.g. directivity of rupture/wave propagation and frequency content of ground motions); (ii) comparison of the ground motion parameters for the M_W9.0 mainshock with those for major aftershocks and past significant events; and (iii) damage potential evaluation based on Arias intensity (Arias, 1970) and cumulative absolute velocity (CAV; EPRI, 1988), in addition to 5%-damped elastic response spectra - noting that the Arias intensity and CAV are able to capture long duration effects of ground motions on engineering structures.

3.1. Ground motions of the M_W9.0 mainshock and major aftershocks

The entire rupture process involved a large fault plane 400-500 km in length by 100-200 km in width (GSI, 2011; Shao et al., 2011). The fault rupture models estimated by Shao et al. (2011) (hereafter, UCSB model) and by the Geo-Spatial Information Authority of Japan (2011) (hereafter, GSI model) are illustrated in Figure 3.1 (note: many other fault plane models are available). The UCSB model is shown with estimated slip distribution over the fault plane. The GSI model consists of two rupture processes; the rupture of the northern plane preceded that of the southern one. They were derived by focusing on macro features of observed ground deformation and long-period ground motions. Although the overall extent of the estimated fault rupture area is different for the UCSB and GSI models, locations for large slip are broadly similar (i.e. an area around the GSI"s rupture plane 1 in Figure 3.1). The difference is due to different approaches/datasets/assumptions adopted during the teleseismic wave inversion that envelopes the estimation of fault ruptures. A significant amount of permanent ground deformation/slip occurred along the trench line off-shore the Tōhoku region (i.e. eastern boundary of the GSI/UCSB fault planes in Figure 3.1), and this is mainly responsible for the generation of the tsunami.

The macro rupture process based on analyses conducted by various research groups generally indicate that the rupture initiated at the earthquake epicentre and propagated south, rupturing segments off-shore Fukushima and Ibaraki Prefectures (GSI, 2011). Moreover, a closer investigation into strong motion generation areas in the short-period range by Irikura and Kurahashi (2011) suggests that the rupture also propagated towards deeper segments along dip and triggered rupture of several small patches with high stress drop(i.e. asperities). In particular, the source model by Irikura and Kurahashi (2011) includes four small rupture segments (see grey patches shown in Figure 3.1): two segments are placed in the west of the epicentre off-shore Miyagi Prefecture, while the other two segments are located in the west of the GSI"s southern plane off-shore Fukushima and Ibaraki Prefectures. These four segments are closer to the coastal areas of the Tōhoku region and are at deeper locations; generated seismic waves travel through a so-called high Q region (Kanno et al., 2006), experiencing less attenuation of seismic waves over distance, and thus resulting in larger ground motions (similar to inslab events). Moreover, as stress drops associated with these localised ruptures are much higher (about 200-400 bars) than other parts of the fault, short-period energy level is particularly intense.

The rupture and wave propagation process of the Tōhoku mainshock is rather complex, because multiple sub-rupture processes are responsible for different phases of the overall rupture and their effects on generated ground motions differ, depending on the frequency range of interest. Another important consideration in understanding a relationship between a complex rupture process and

observed ground motions is the directivity effect. Generally, observed ground motion time-series data tend to be greater in peak and more concentrated in duration, if the rupture propagation direction coincides with the orientation from the rupture source to the site. On the other hand, they tend to be smaller in peak and stretched over longer duration, if the rupture direction is opposite of the source-to-site orientation.

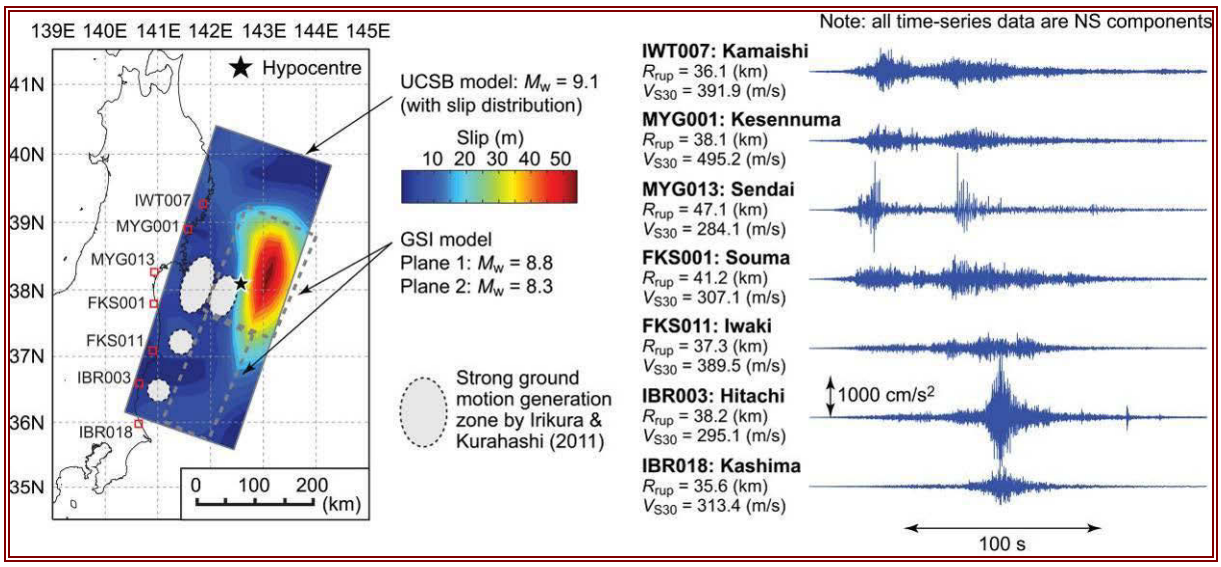

Figure 3.1 Fault plane models of the 2011 Tōhoku mainshock and observed ground motion time-series at seven K-NET stations along the coast.

The complex rupture process described above can be illustrated by inspecting recorded acceleration time-series data at seven K-NET stations along the coast (Figure 3.1). For the seven K-NET stations, the shortest rupture distances to the overall fault plane R_{rup} are similar, whereas local soil conditions, which are represented by average shear-wave velocity in the uppermost 30 m (V_{S30}), vary to some extent. For MYG013 (as well as IWT007, MYG001, and FKS001), two clear phases of seismic wave arrivals can be seen, whereas for IBR003 and IBR013 (as well as FKS011), a single phase of seismic wave arrivals is featured. In particular, for IBR003, a strong motion part of the record is shorter but with greater amplitude than the other stations. This may be due to the combined effects of the complex rupture process with multiple strong motion generation sources and the source-to-site directivity.

Arrivals of the triggered seismic waves at different parts of the fault tend to be more concentrated in time, if a recording station is located towards the direction of the fault rupture process (e.g. IBR003), whereas they become more spread out (or arrive with multiple phases), if a recording station is in the opposite of the rupture propagation direction (e.g. MYG001). It is also noted that the observed values of peak ground acceleration (PGA) at these K-NET stations are relatively large; for instance, for MYG013 and IBR003, PGA has exceeded 1000 cm/s^2. Large observed PGAs at several stations in Miyagi, Fukushima, and Ibaraki Prefectures may be partly due to proximity to localised strong motion generation areas along the coastline, which are indicated by grey patches in Figure 3.1 (Irikura and Kurahashi, 2011).

The tremendously large mainshock has induced numerous large aftershocks; the enhanced seismic activities in the affected region pose significant risk to evacuees and residents, because some buildings and infrastructure have been damaged from the mainshock and thus are more vulnerable to aftershocks. Figure 3.2a shows the locations of major aftershocks with magnitudes greater than 5.0 over the period of 90 days after the mainshock (note: the raw data are based on the Japan Metrological Agency (JMA) catalogue). The aftershock activity is enhanced in off-the-Fukushima-Ibaraki region and outside of the mainshock fault plane, dotted rectangle in Figure 3.2a (i.e. outer-rise events). Several major aftershocks occurred, which aggravated seismic damage to buildings and infrastructure (e.g. M_W7.1 inslab event on 7th April). The number of aftershocks with magnitude greater than 7.0 and 6.0 during the three-month period after the mainshock is 5 and 84, respectively (note: these numbers are not necessarily complete, because of the disruption of JMA recording stations

immediately after the mainshock). The increased seismicity tends to decay with the elapsed time (e.g. modified Omori"s law). However, the current seismicity is still much greater than the background/normal seismicity and therefore, vigilance must be maintained at high level for an extended period (up to a few years).

To show the magnitude-frequency relationship as well as temporal decay characteristics of the Tōhoku aftershock sequence, empirical Gutenberg-Richter and modified Omori"s relationships are developed (Gutenberg and Richter, 1954; Utsu et al., 1995; Shcherbakov et al., 2005) and shown in Figure 3.2b and Figure 3.2c, respectively. The Gutenberg-Richter relationship describes the correlation of aftershock magnitudes and their frequency (i.e. larger aftershocks occur less frequently). Note that the Gutenberg-Richter relationship is often used for mainshocks in the context of seismic hazard analysis, whereas it is also applicable to aftershock sequences. The modified Omori"s law characterises the occurrence rate of major aftershocks as a function of elapsed time since the mainshock (i.e. aftershock occurrence rate decays with time). The fitting of the aftershock data to the Gutenberg-Richter relationship is reasonable (Figure 3.2b); the estimated slope parameter (i.e. *b*-value) is typical for previous events (Guo and Ogata, 1997). However, the number of aftershocks with magnitudes less than 5.5 appears to be deficient (i.e. the *b*-value is less than 1.0). This may be due to missing events immediately after the mainshock and future events that have not occurred yet (a period of 90 days is not long enough to show the full aftershock sequence of a M_W9.0 megathrust event). Figure 3.2c shows that the modified Omori"s law fits reasonably well with the aftershock data (note: two equations in the figure are based on different fitting methods). The above results generally support the applicability of well-established empirical relationships for characterising aftershock data, which is very useful for preparing for future subduction events (e.g. other parts of Japan, Mexico, Cascadia, Peru, and Chile).

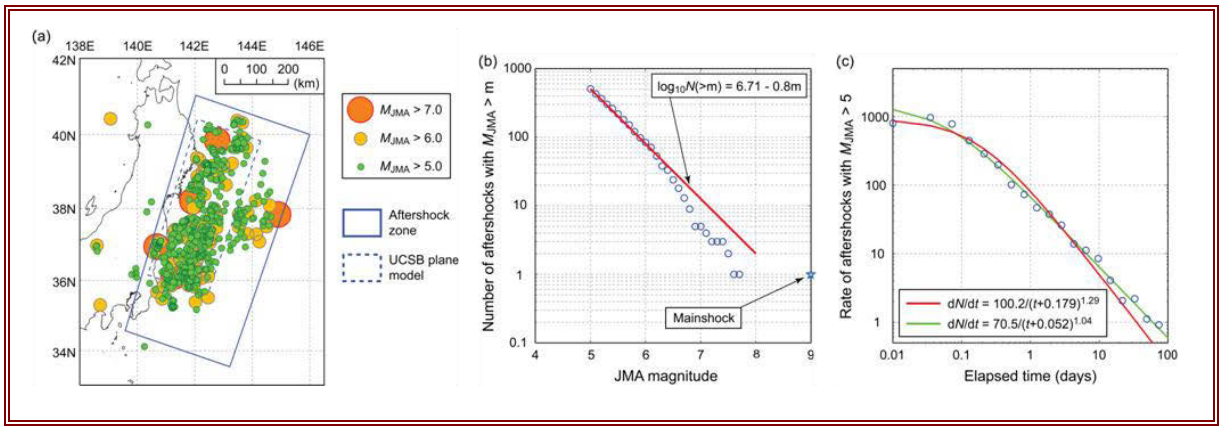

Figure 3.2 Spatial distribution of the major aftershocks (a) and aftershock statistics (Gutenberg-Richter relationship (b) and modified Omori"s law (c)).

3.2. Ground motion characteristics

Detailed investigations of observed ground motions at different recording stations offer quantitative information on the extent of ground motions and thus are valuable for damage assessment of buildings and infrastructure. For such purposes, recorded accelerograms of the 2011 Tōhoku mainshock and two major aftershocks (M_W7.9 event on 11th March, about 30 minutes after the mainshock, and M_W7.1 event on 7th April, which caused additional damage to structures) were assembled from K-NET and KiK-NET records (Aoi et al., 2004). In addition, ground motion records for three significant events in the Tōhoku region (2003 M_W7.0 Miyagi-Oki earthquake, 2005 M_W7.2 Miyagi-Oki earthquake, and 2008 M_W6.9 Iwate-Miyagi Nairiku earthquake) were gathered to conduct comparative studies (the results are presented in section 3.3). For these events, various seismic intensity measures, such as spectral accelerations (SAs) at different vibration periods, were calculated (note: prior to the calculation of seismic intensity parameters, time-series data were base-corrected and band-pass-filtered; see Goda and Atkinson, 2009).

A summary of the considered events is presented in Table 3.1. Note that the selection of the three significant events is motivated to facilitate the direct comparison of observed ground motion intensities

at the same geographical locations (thus no need to adjust site conditions). Similar comparisons were conducted for other major events, such as the 2003 Tokachi-Oki earthquake and 2004 Mid-Niigata earthquake; the results are beyond the scope of this report.

It is noteworthy that the three past events differ in earthquake type (i.e. interface, inslab, and intraplate) and are of expected magnitude in the region (i.e. M_W7.0 class). The consideration of both interface and inslab earthquakes is of particular importance in light of the detailed earthquake source rupture investigation carried out by Irikura and Kurahshi (2011), which indicates that several patches of fault rupture with high stress drop happened at deeper segments of the fault plane (see Figure 3.1).

Table 3.1 Summary of the Tōhoku mainshock / aftershocks and three other significant events considered in this report.

Event	M_W[(1)]	Earthquake type	Focal depth (km)	Number of records[(2)]	Fault plane model[(3)]
2011 Tōhoku mainshock	9.0	Interface	24	1199	UCSB model (Shao et al., 2011)
2011 Tōhoku aftershock (11th March)	7.9	Interface	29	745	Harvard CMT and Strasser et al. (2010)[(4)]
2011 Tōhoku aftershock (7th April)	7.1	Inslab	53	918	Harvard CMT and Yamanaka (2011)[(5)]
2003 Miyagi-Oki	7.0	Inslab	71	794	GSI model
2005 Miyagi-Oki	7.2	Interface	42	847	GSI model
2008 Iwate-Miyagi Nairiku	6.9	Intraplate	8	655	GSI model

[(1)]The estimate is based on the Harvard CMT catalog; [(2)]The number of records is the sum of available K-NET and KiK-NET strong motion data at ground surface; [(3)]The fault plane model is used to calculate the shortest distance to rupture plane; [(4)]The information on moment magnitude and strike/dip is obtained from the Harvard CMT catalog, whereas empirical fault length/width-magnitude relationships by Strasser et al. *(2010) are applied to determine the size of the fault rupture; the epicentre is considered to be located in the middle of the fault plane; [(5)]The information on moment magnitude and strike/dip was obtained from the Harvard CMT catalog, whereas the fault rupture dimension is adopted from Yamanaka (2011).*

3.2.1. Specific cases

Firstly, ground motion characteristics in terms of 5%-damped elastic response spectra are studied for the seven K-NET stations shown in Figure 3.1. The response spectra at the seven stations vary significantly over the vibration period range, despite the similarity of the rupture distance from the fault plane and local site condition. The observed variability is attributed to the complex rupture process and source-to-site directivity (i.e. source and path effects). This variability is particularly large at closer rupture distances (see Figure 3.3). Comparison of the response spectra for different locations indicates that the response spectrum for IBR003 is larger at short vibration periods than other records, while that for MYG013 is remarkably larger than others at an intermediate vibration period range (between 0.5 s and 1.5 s) – this may be a main reason for relatively extensive damage to mid-/high-rise buildings in Sendai (section 4.3.2). It is also noteworthy that the shape of the response spectra (i.e. relative amplitude of spectral acceleration (SA) ordinates of the response spectrum at different vibration periods) varies significantly among the seven K-NET stations (e.g. FKS011 versus IBR003), suggesting the importance of capturing local features of the rupture propagation process for improved prediction of ground motion parameters due to a large earthquake.

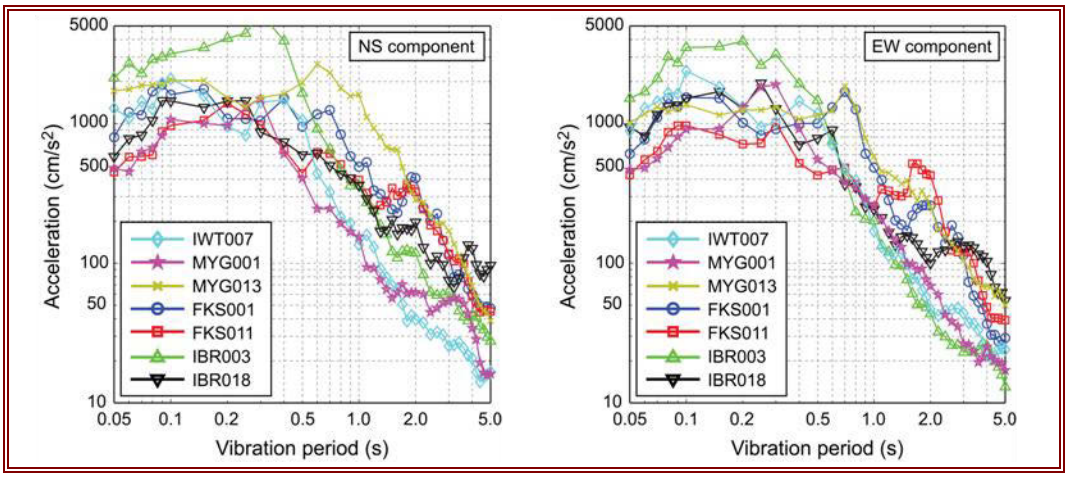

Figure 3.3 Comparison of elastic response spectra of the recorded mainshock ground motions at the seven K-NET stations: North-South component and East-West component.

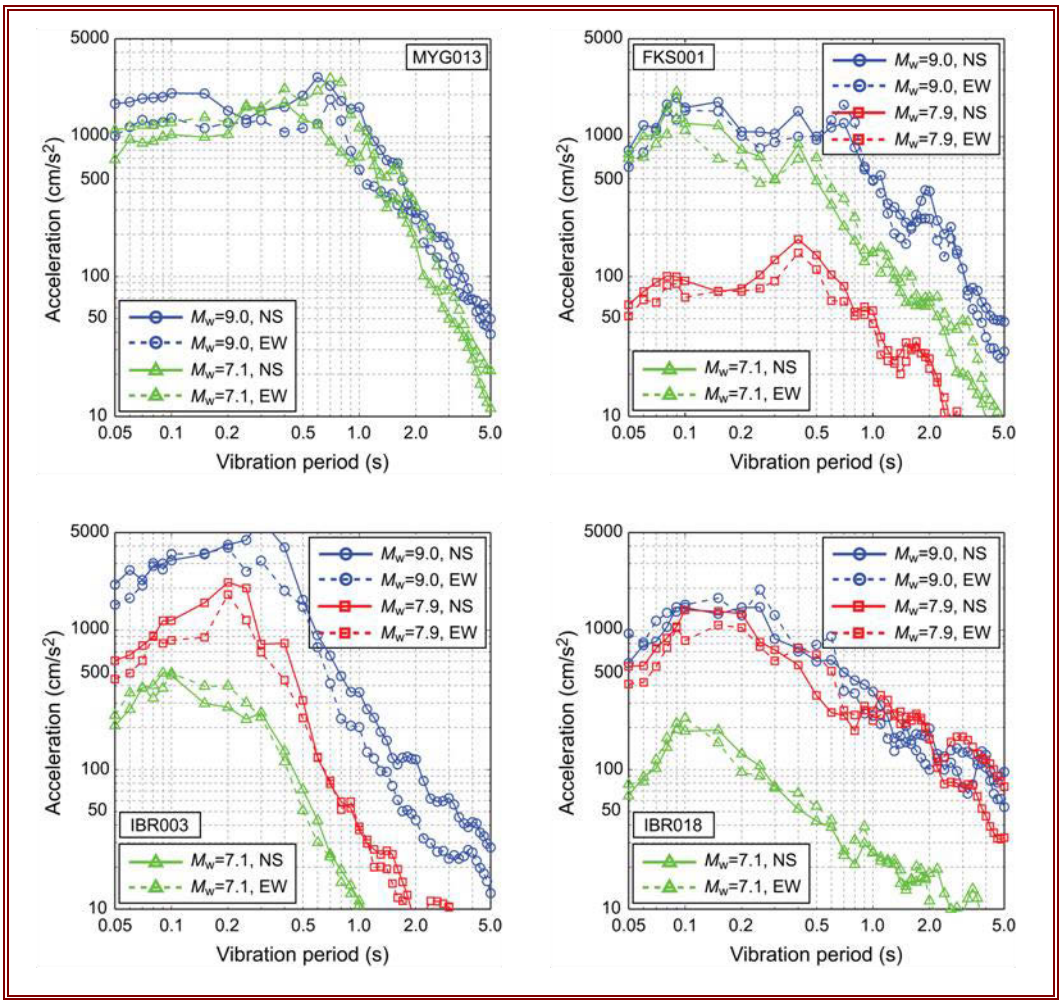

Figure 3.4 Comparison of elastic response spectra due to the M_W9.0 mainshock and M_W7.9 and M_W7.1 aftershocks for the four K-NET stations (MYG013, FKS001, IBR003, and IBR018).

To further investigate the elastic seismic demand due to different earthquakes, response spectra for the mainshock and two major aftershocks, M_W7.9 event on 11th March and M_W7.1 event on 7th April (see Table 3.1), are compared for the four K-NET stations, MYG013, FKS001, IBR003, and IBR018 (note: ground motion records for the M_W7.9 aftershock are not available for MYG013). The results are

shown in Figure 3.4. As the event types of the three earthquakes are different (interface versus inslab events), spectral content of the recorded ground motions is expected to be different (e.g. generally speaking, inslab ground motions tend to have rich spectral content in the short period range, while interface ground motions tend to have rich spectral content in the long vibration period).For MYG013 and IBR018, response spectra for the mainshock and one of the aftershocks (M_W7.1 event for MYG013 and M_W7.9 event for IBR018) are similar, although moment magnitudes differ significantly (note: response spectra at long vibration periods for the mainshock, which tend to be more influenced by the earthquake size, are greater than those for the M_W7.1 aftershock). For FKS001, which is about 30 km south of MYG013 (thus, being away from the rupture source of the M_W7.1 event), the difference between the M_W9.0 mainshock and M_W7.1 aftershock is increased, particularly at longer vibration periods. For IBR003, response spectra for the three events differ significantly, because of different wave propagation paths between source and site (distance as well as directivity). In general, response spectra shapes for different earthquakes at the same sites are similar, indicating strong influence of site effects at individual locations.

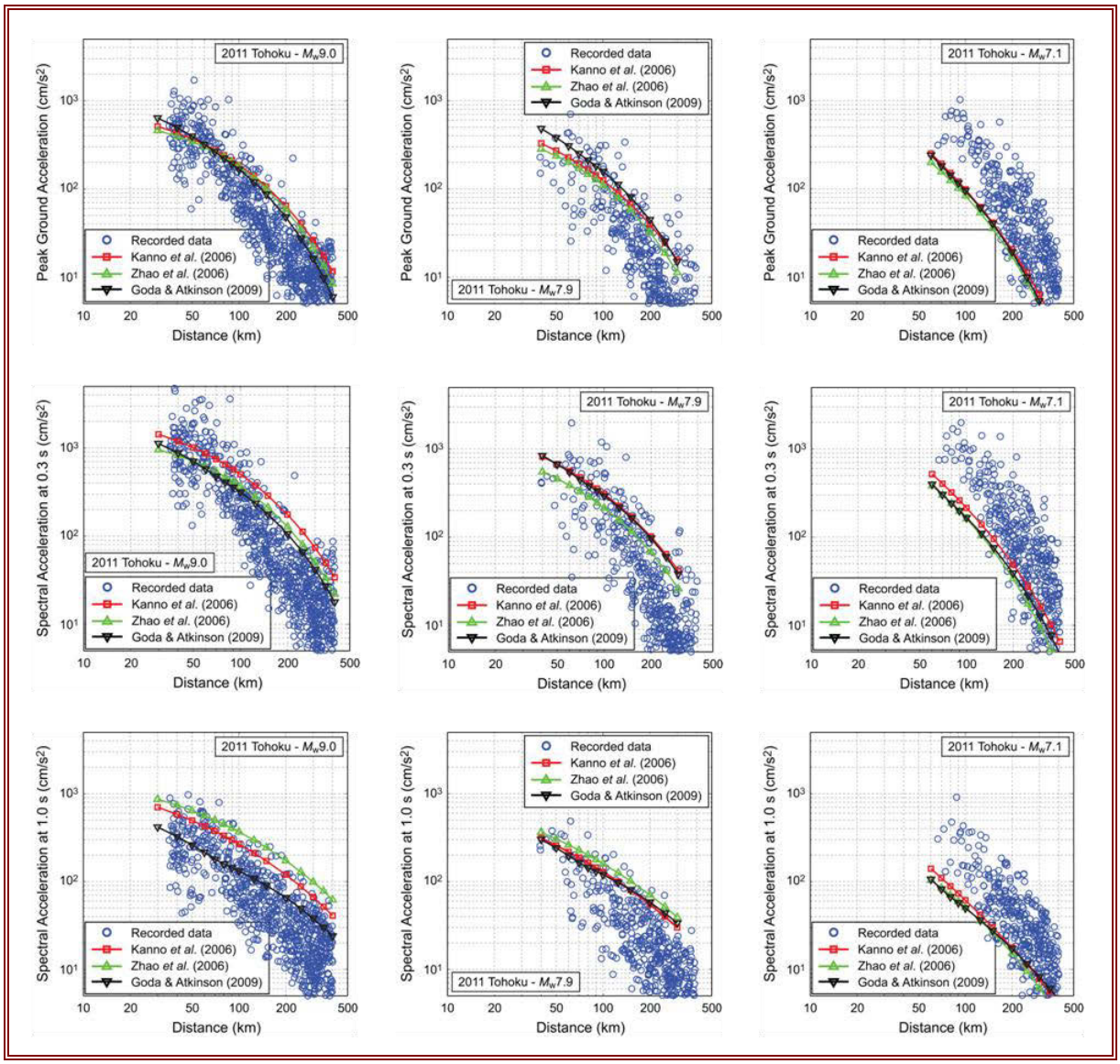

Figure 3.5 Distance attenuation characteristics of PGA and SAs at 0.3 s and 1.0 s for the M_W9.0 mainshock and M_W7.9 and M_W7.1 aftershocks.

3.2.2. General cases

Next, general characteristics of observed ground motions during the M_W9.0 mainshock and M_W7.9/7.1 aftershocks are investigated by inspecting plots of PGA and SAs at 0.3 and 1.0 s with respect to rupture distance. The results are shown in Figure 3.5; the presented data are the geometric mean of two horizontal components, recorded on soft/firm soils, where the average shear-wave velocity in the top 30 m is between 180 m/s and 760 m/s (i.e. NEHRP site class C or D). To view the observed data from an empirical perspective, three recent ground motion prediction equations for Japanese earthquakes by Kanno et al. (2006) relation, Zhao et al. (2006) relation, and Goda and Atkinson (2009) relation, are included in the figures. Generally speaking, the three recent attenuation models predict similar ground motion levels for the three scenarios. It is noted that when the prediction equations are applied for the M_W9.0 mainshock, the input magnitude value is capped at 8.5 for the relations in Kanno et al. and Zhao et al., whereas the cap value of 8.0 is considered for Goda and Atkinson (2009) relation; this is to avoid unwarranted extrapolation of the applicable magnitude range of the existing models. In other words, if these equations are applied with M_W = 9.0, the predicted ground motions tend to be greater than the observed motions during the 2011 Tōhoku mainshock. It is noteworthy that the magnitude scaling of ground motions, that was derived based on M_W6.0-8.0 earthquakes, may not be directly applicable because the spatial extent of M_W9.0 earthquakes is much greater than M_W6.0-8.0 earthquakes. For such large events, seismic waves generated from various segments of the entire fault may not constructively contribute to observed ground motions at specific sites (as evidenced in Figure 3.1). The rupture process, locations of asperities and directivity between site and source have a significant impact.

The comparison of the recorded data with three prediction equations indicates:

1. For the M_W9.0 mainshock, the observed data are generally in agreement with prediction equations in terms of amplitude, although the equations tend to overestimate the data (note: the magnitude value is capped at values lower than 9.0; unless the difference would be greater). The Tōhoku mainshock produced less severe ground motions than anticipated. This may be the reason that ground shaking damage was not as severe as it was thought to be for the magnitude 9.0 class event. Moreover, the long-period content of ground motions is significantly lower than the expected level, resulting in less damage to mid-/high-rise buildings that are more susceptible to long-period excitations. The attenuation of observed ground motions in terms of rupture distance at short vibration periods is steeper than that of the prediction equations. An important observation to be noticed for the M_W9.0 mainshock data is the greater variability at rupture distances less than 50 km (i.e. locations along the coastline) – this is due to the complex rupture process of the mainshock and the seismic wave propagation directivity.
2. For the M_W7.9 aftershock, ground motions are lower than the expected ground motion levels based on the prediction equations. Similar observations, as mentioned above for the M_W9.0 mainshock, are applicable to this event (e.g. more gradual attenuation and deficient spectral content in the long-period range). It is noted that seismic intensities for the M_W7.9 aftershock are smaller than those for M_W9.0 mainshock (as expected).
3. For the M_W7.1 aftershock, observed ground motion data are comparable to those for the M_W9.0 mainshock, despite much smaller magnitude, and are significantly higher than the three prediction equations. In other words, ground shaking due to the 7th April aftershock was exceptional in light of past events and caused additional structural damage and disruption of infrastructure (e.g. electricity and water supply). It is noted that the attenuation slope of the data and the prediction equations are similar.

Next, spatial variability of observed ground motions for the M_W9.0 mainshock and M_W7.9/7.1 aftershocks is investigated by developing contour maps for PGA and SAs at 0.3 s and 1.0 s. The results are shown in Figure 3.6; in each sub-figure, the fault plane model is indicated as a blue rectangle (see also Table 3.1). Visual assessment of the contour maps for different events clearly shows that: (i) spatial extent of the ground shaking (red/yellow-coloured areas) for the mainshock is much larger than the two aftershocks, affecting a larger population and building stock, and (ii) several hot spots can be identified from the mainshock contour maps, whereas a single, or at most a few, hot spot exists for the two aftershocks.

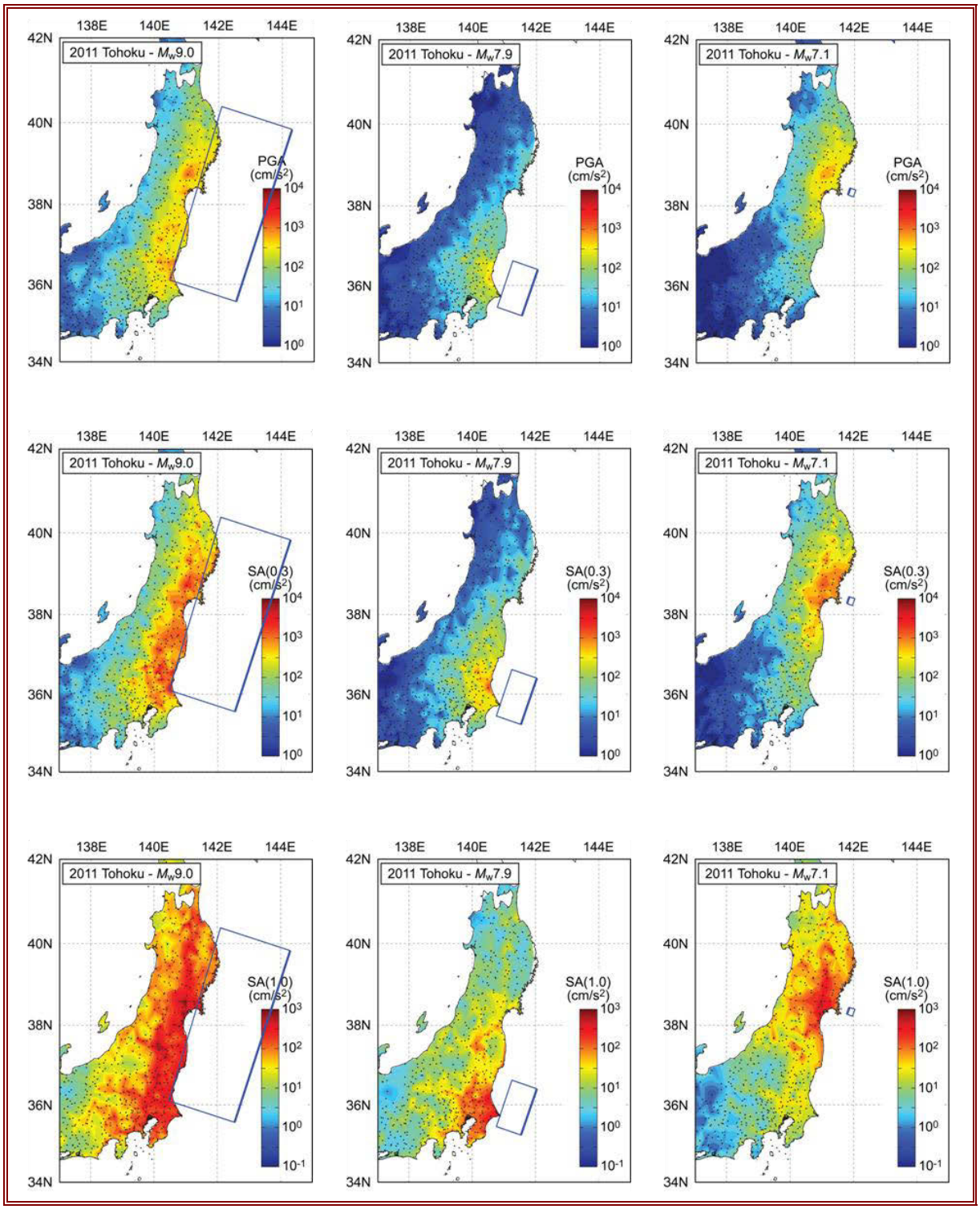

Figure 3.6 Contour maps of PGA and SAs at 0.3 s and 1.0 s for the M_W9.0 mainshock and M_W7.9 and M_W7.1 aftershocks (blue rectangles are the fault plane models).

The former observation is of utmost importance from a regional/national earthquake risk management viewpoint, because seismic damage and disruption of lifelines and essential services can happen simultaneously in widespread areas. In such cases, an original emergency plan may not work effectively in comparison with a situation where a similar level of seismic damage/disruption is caused on a smaller geographic scale (e.g. support from municipalities in the vicinity may not be available).

The latter observation above reflects the complex rupture process of the mainshock and indicates the existence of local rupture segments within the fault plane (Irikura and Kurahashi, 2011).

3.3. Comparison of ground motions with past significant events

To further gain insight into seismic effects of the 2011 Tōhoku mainshock, recorded ground motions due to other significant events in the Tōhoku region, such as 2003 and 2005 Miyagi-Oki earthquakes, are considered. The contour maps of PGA and SAs at 0.3 s and 1.0 s are presented in Figure 3.7. Note that the colour intensity scales in Figure 3.7 are the same for each parameter as those in Figure 3.6; thus a direct visual comparison is facilitated.

The comparison of Figure 3.6 and Figure 3.7 suggests that: (i) overall, the 2011 Tōhoku mainshock did not produce abnormally large ground motions; and (ii) (as expected) the Tōhoku mainshock affected much greater areas with significant ground shaking than these previous events. The observed features (i.e. significant but not abnormal ground shaking in widespread areas) may be explained by noting that peak ground motions are strongly affected by local features, such as smaller patches of strong motion generation areas (e.g. grey patches in Figure 3.1), and seismic waves generated over a vast rupture area attenuate while travelling through the crust of the Earth (i.e. effects due to distant rupture sources are obscured). Therefore, a large earthquake size and released energy do not necessarily have significant influence on peak ground motions. These facts are usually reflected in the saturation of magnitude scaling for megathrust earthquakes. The above results may imply that for megathrust subduction events, the magnitude scaling effects on peak ground motion parameters are not especially strong. These aspects of the seismic risk due to large subduction events must be taken into account, when emergency planning and risk management decisions are made.

It is also insightful to examine time-series data and response spectra of the Tōhoku mainshock records having very large PGA values, as well as several past significant records (e.g. 1995 Kobe earthquake, which caused significant damage to structures). For this purpose, ground motion records for IBR003 (Hitachi in Fukushima Prefecture), MYG004 (Tsukidate in Miyagi Prefecture), and MYG013 (Sendai in Miyagi Prefecture) are chosen, and their time-series data and response spectra are compared in Figure 3.8 with those for two records for NIG019 (Ojiya in Niigata Prefecture) and NIG028 (Nagaoka in Niigata Prefecture) from the 2004 Mid-Niigata earthquake, and for one record (Takatori in Hyogo Prefecture) from the 1995 Kobe earthquake. The response spectra shown in Figure 3.8b are the geometric mean of response spectra for two horizontal components (to show overall trends). It is noted that the acceleration data for MYG004 have registered the largest PGA value in the entire K-NET and KiK-NET databases, exceeding 2500 cm/s^2. Inspection of Figure 3.8a suggests that the Tōhoku motions have larger PGA values and significantly longer duration in comparison with those from the Mid-Niigata and Kobe earthquakes, which is expected from the difference of magnitudes for these three earthquakes.

Figure 3.8b shows that at short vibration periods, the Tōhoku mainshock motions have greater SA values, while at long vibration periods, the Mid-Niigata and Kobe motions have significantly larger SA values (e.g. the response spectrum for the Takatori record exceeds 1000 cm/s^2 at 1.0 s). The latter phenomenon is typically known as near-fault motions (Mavroeidis and Papageorgiou, 2003), where very large velocity pulses with long vibration periods are generated due to the coincidence of source-to-site wave propagation direction and rupture propagation direction (i.e. forward directivity). The near-fault motions during the Mi-Niigata and Kobe earthquakes caused very devastating damage to structures. This final comparison partially explains the reason why the Tōhoku motions with very large accelerations did not cause so much damage/disruption to buildings and infrastructure in the Tōhoku region, in comparison with the Mid-Niigata and Kobe ground motions.

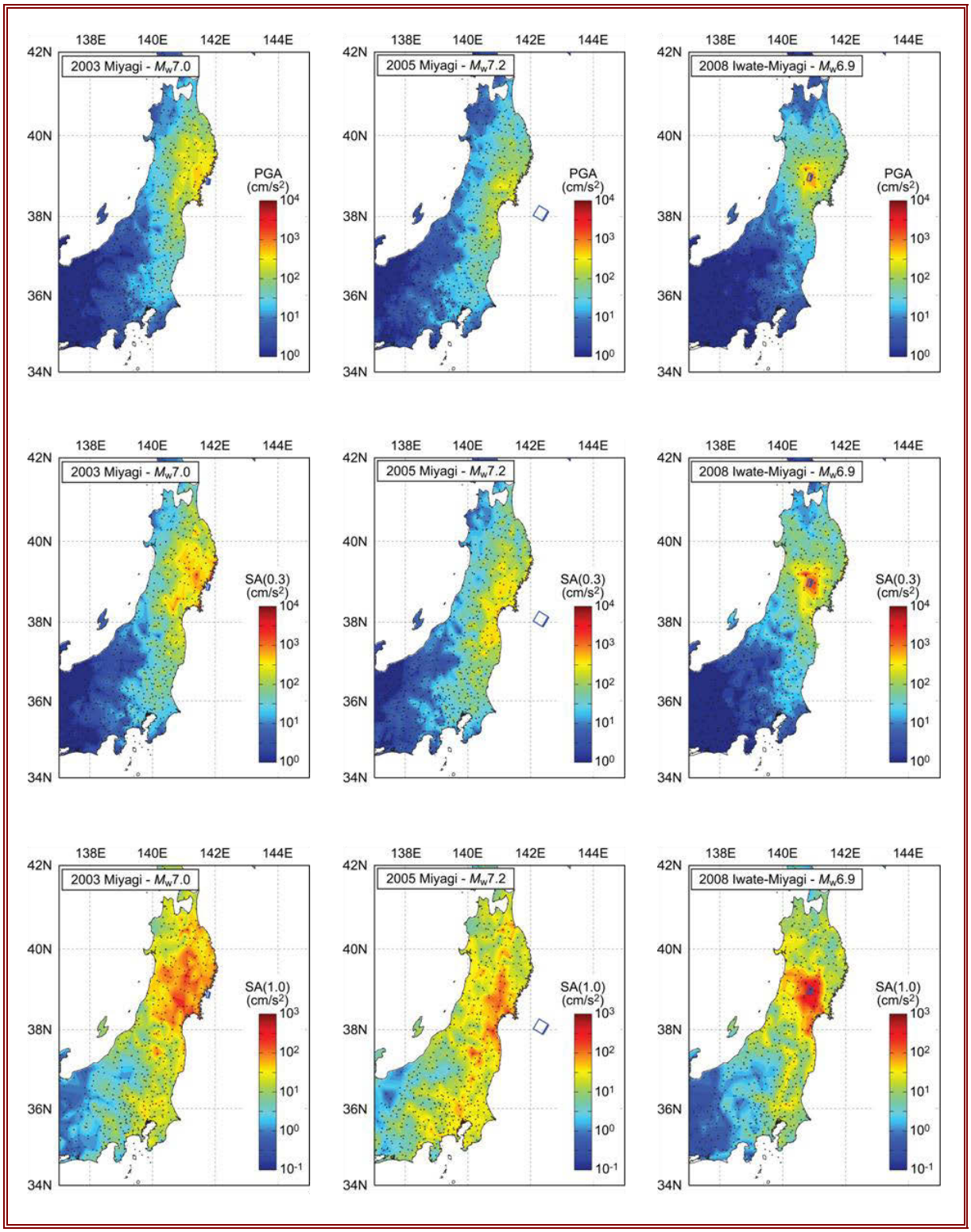

Figure 3.7 Contour maps of PGA and SAs at 0.3 and 1.0 s for the 2003 Miyagi earthquake, 2005 Miyagi earthquake, and 2008 Iwate-Miyagi Nairiku earthquake (blue rectangles are the fault plane models).

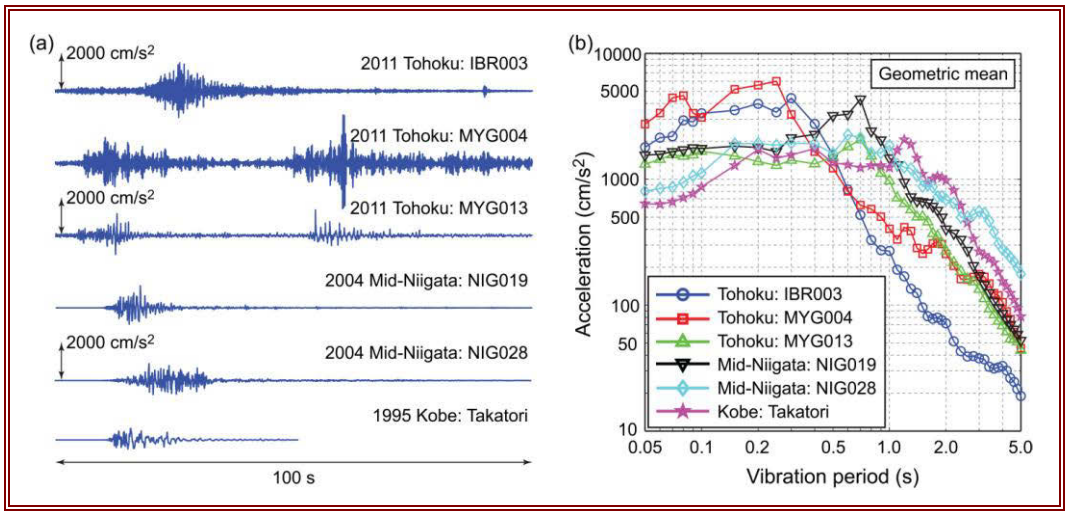

Figure 3.8 Time-series data and their response spectra of three Tōhoku mainshock records and three significant records from the 1995 Kobe earthquake and the 2004 Mid-Niigata earthquake.

3.4. Damage potential of long duration ground motions

PGA and SAs are popular measures for "peak" elastic seismic demand, and are particularly relevant in modern seismic design codes (i.e. design spectra for structures are specified in terms of PGA and SAs). However, such peak-related parameters fail to capture the long duration effects of strong ground motions (i.e. repeated load reversals with significant amplitudes).

By contrast, Arias intensity and CAV can take long duration effects into account; they are used in geotechnical applications (e.g. liquefaction potential evaluation) and in the nuclear industry (EPRI, 1988). Similar investigations, as carried out in sections 3.2 and 3.3, focusing on Arias intensity and CAV will provide valuable information on damage potential of the Tōhoku mainshock, because of its rather long duration (200-300 seconds). For instance, there are many liquefaction-related failures reported after the 2011 Tōhoku mainshock – wide areas surrounding the Tokyo Bay (e.g. Urayasu, Chiba) suffered from extensive liquefaction-related ground settlement and the amount of ejected soil was massive.

Specifically, Arias intensity is given by:

$$AI = \frac{\pi}{2g}\int_{t_1}^{t_2}[a(t)]^2\,\mathrm{d}t$$

Equation 3.1

where g is the gravitational acceleration (e.g. g = 981 cm/s^2); $a(t)$ is the ground acceleration time-series; and t_1 and t_2 are the start and end of the significant ground excitations.

CAV is defined as:

$$CAV = \int_0^{t_{max}} |\,a(t)\,|\,\mathrm{d}t = \sum_{i=1}^{N}|\Delta v_i|$$

Equation 3.2

where $|a(t)|$ is the absolute value of ground acceleration time-series; t_{max} is the total duration of a record; and $|\Delta v_i|$ is the i-th incremental value of an area enclosed by the acceleration time-series data and zero acceleration over a short period. In short, CAV is the sum of such enclosed areas having a unit of velocity over the entire duration.

To assess duration-related damage potential of the Tōhoku mainshock, in comparison with other major events, values of Arias intensity and CAV were evaluated for the six events listed in Table 3.1, and contour maps for Arias intensity and CAV are presented in Figure 3.9 and Figure 3.10, respectively. Inspection of Figure 3.9 and Figure 3.10 indicates that:

- Arias intensity for the Tōhoku mainshock (in actual values) tends to be greater than other events. This is due to the long duration of seismic waves, and is particularly noticeable for sites at short distances, where values of Arias intensity reach 2000-4000 cm/s. The magnitude scaling of Arias intensity is more significant than PGA and SAs, and this should be reflected in future ground motion prediction equations for Arias intensity
- Generally, the above observations for Arias intensity are applicable to CAV. Note that CAV for the Tōhoku mainshock reaches 10-15 *g*-s (and several records are close to this level); this seismic intensity level has not been attained in any other events that are considered in this report

Practical implications of these observations/findings are that depending on structures (e.g. foundation subject to liquefaction and lateral spreading risks and structures with degradation/deterioration characteristics), a megathrust subduction earthquake with long duration can be far more destructive than smaller earthquakes. These new features must be incorporated into seismic hazard/risk assessment in the future.

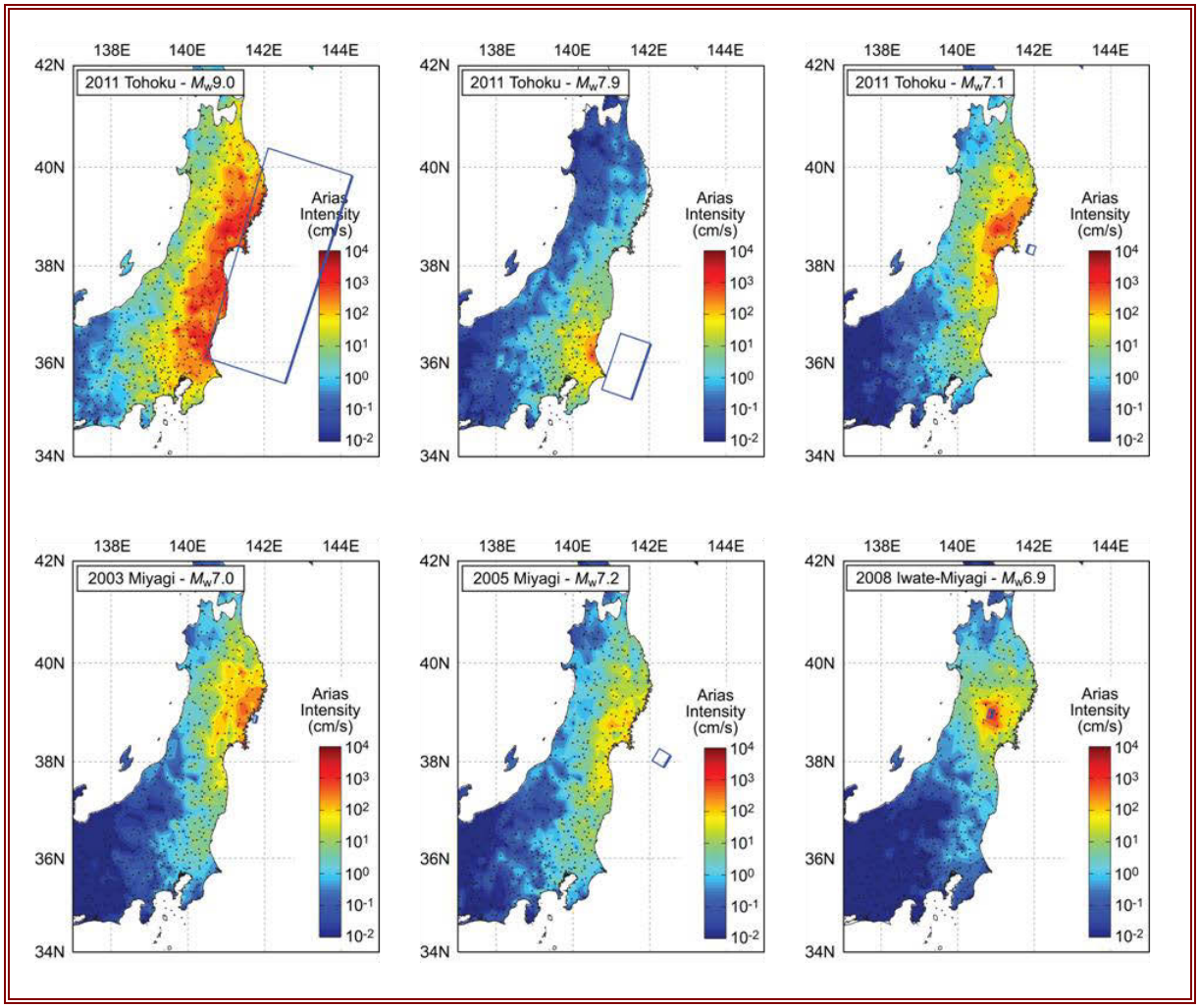

Figure 3.9 Contour maps of Arias intensity for the 2011 Tōhoku earthquakes (mainshock and two aftershocks), the 2003 Miyagi earthquake, 2005 Miyagi earthquake, and 2008 Iwate-Miyagi Nairiku earthquake.

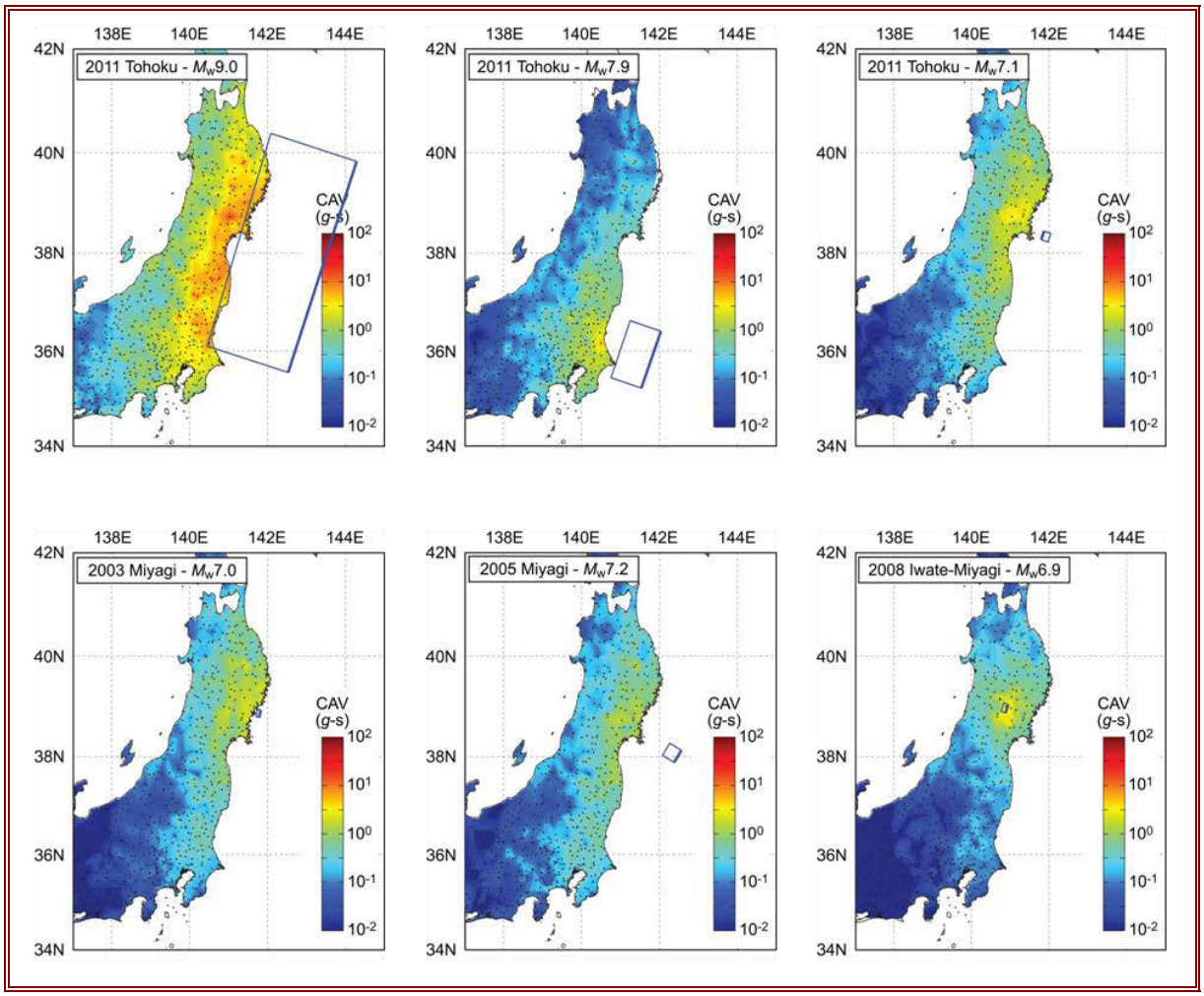

Figure 3.10 Contour maps of CAV for the 2011 Tōhoku earthquakes (mainshock and two aftershocks), the 2003 Miyagi earthquake, 2005 Miyagi earthquake, and 2008 Iwate-Miyagi Nairiku earthquake.

3.5. Conclusions on ground motion

The coupled co-seismic rupture of fault segments along the Japan Trench has resulted in a megathrust earthquake of M_w9.0 with a rupture area spanning 500 km in length and 200 km in width. The recorded ground motions at various locations have unique features, in comparison with ground motions from other significant earthquakes:

(i) very large peak ground accelerations at several locations (e.g. Tsukidate in Miyagi Prefecture and Hitachi in Ibaraki Prefecture),
(ii) high spectral content in short vibration period range (at distances less than 100 km),
(iii) very long duration of significant part of ground motions, and
(iv) strong effects due to directivity and local asperities.

The strong short-period content but moderate intermediate-to-long period content of observed ground motions might be the primary reason for moderate ground shaking-related damage that occurred to buildings and infrastructure in the Tōhoku region (see Chapter 4). On the other hand, long-duration ground motions with moderate ground accelerations have caused significant liquefaction-related damage to reclaimed lands around the Tokyo Bay area.

Regarding (iv), significant variability of ground motion parameters was observed at locations along the coast line, where distances to the fault rupture plane are similar and thus from a conventional perspective of ground motion prediction, ground shaking was thought to be similar. In general, the

northern part of the Tōhoku region (Iwate Prefecture) experienced less severe ground shaking (but unfortunately massive tsunami), whereas the southern part of the Tōhoku region (Miyagi Prefecture and Fukushima Prefecture) experienced ground motions with large peak acceleration. Furthermore, detailed comparison of ground motions observed during the 11th March Tōhoku mainshock with two major aftershocks and three significant recent events (in 2003, 2005, and 2008) in the Tōhoku region indicates that peak-based ground motion parameters (e.g. spectral accelerations) do not show a significant scaling trend with respect to moment magnitude. By contrast, the results indicate that duration-based ground motion parameters (e.g. Arias intensity and cumulative absolute velocity) increase significantly with moment magnitude (or more precisely, duration of significant ground motions). These observations render valuable empirical evidence on ground motion characteristics of megathrust subduction earthquakes (which were missing prior to the Tōhoku earthquake), and provide with important insight on future developments of ground motion models.

3.6. References

Aoi, S. Kunugi, T. and Fujiwara, H., 2004. Strong-motion Seismograph network operated by NIED: K-NET and KiK-net. *Journal of Japan Association for Earthquake Engineering*, 4(3), pp. 65–74.

Arias, A., 1970. A measure of earthquake intensity. In: *Seismic Design for Nuclear Power Plants*. Cambridge: MIT Press, pp. 438–483.

Geo-Spatial Information Authority of Japan (GSI), 2011. *Crustal deformation and fault model obtained from GEONET data analysis*. [online] Available at <http://www.gsi.go.jp/cais/topic110313-index-e.html> [Accessed 30 June 2011].

Electrical Power Research Institute (EPRI), 1988. *A criterion for determining exceedance of the operating basis earthquake* (*EPRI NP-5930*). Palo Alto, CA: Electrical Power Research Institute.

Global Centroid Moment Tensor (CMT) catalog, 2011, *Global CMT catalog search*. Cambridge, MA: Harvard University [online] Available at <http://www.globalcmt.org/CMTsearch.html> [Accessed 30 June 2011].

Goda, K. and Atkinson, G.M., (2009). Probabilistic characterization of spatially-correlated response spectra for earthquakes in Japan. *Bulletin of the Seismological Society of America*, 99(5), pp. 3003–3020.

Gutenberg, B. and Richter, C.F., 1954. *Seismicity of the Earth and associated phenomena*. Princeton, MA: Princeton University Press.

Irikura, K. and Kurahashi, S., 2011. Source model for generating strong ground motions during the 11th March 2011 off Tōhoku, Japan earthquake. In: *Proceedings of the Japan Geoscience Union International Symposium 2011*, Makuhari, Chiba, Japan, 22-27 May 2011.

Kanno, T. Narita, A. Morikawa, N. Fujiwara, H. and Fukushima, Y., 2006. A new attenuation relation for strong ground motion in Japan based on recorded data. *Bulletin of the Seismological Society of America*, 96(3), pp. 879–897.

Mavroeidis, G.P. and Papageorgiou, A.S., 2003. A mathematical representation of near-fault ground motions. *Bulletin of the Seismological Society of America*, 93(3), pp. 1099–1131.

Minoura, K. Imamura, F. Sugawara, D. Kono, Y. and Iwashita T., 2001. The 869 Jogan tsunami deposit and recurrence interval of large-scale tsunami on the Pacific coast of northeast Japan. *Journal of Natural Disaster Science* 23(2), pp. 83–88.

Shao, G. Li, X., Ji, C. and Maeda, T., 2011. *Preliminary results of the March 11, 2011 M_W9.1 Honshu earthquake*. Santa Barbara, CA: University of California [online] Available at <http://www.geol.ucsb.edu/faculty/ji/big_earthquakes/2011/03/0311/Honshu_main.html> [Assessed 30 June 2011].

Strasser, F.O. Arango, M.C. and Bommer, J.J., 2010. Scaling of the source dimensions of interface and intraslab subduction-zone earthquakes with moment magnitude. *Seismological Research Letters*, 81(6), pp. 941–950.

Yamanaka, Y., 2011. *Real-time seismological note*. Nagoya: Nagoya University [online] Available at <http://www.seis.nagoya-u.ac.jp/sanchu/Seismo_Note/> [Accessed 30 June 2011].

Zhao, J.X. Zhang, J. Asano, A. Ohno, Y. Oouchi, T. Takahashi, T. Ogawa, H. Irikura, K. Thio, H.K. Somerville, P.G. Fukushima, Y. and Fukushima, Y., 2006. Attenuation relations of strong ground motion in Japan using site classification based on predominant period. *Bulletin of the Seismological Society of America*, 96(3), pp. 898–913.

Utsu, T. Ogata, Y. and Matsu'ura, R.S., 1995. The centenary of the Omori formula for a decay law of aftershock activity. *Journal of Physics of the Earth*, 43(1), pp. 1–33.

Guo, Z. and Ogata, Y., 1997. Statistical relations between the parameters of aftershocks in time, space, and magnitude. *Journal of Geophysical Research*, 102(B2), pp. 2857–2873.

Shcherbakov, R. Turcotte, D.L. and Rundle, J.B., 2005. Aftershock statistics. *Pure & Applied Geophysics*, 162(6-7), pp. 1051–1076.

4. Field observations on ground shaking damage

4.1. Building regulations in Japan

A brief history of building regulations in Japan is presented in Table 4.1:

Table 4.1 Brief history of building regulations in Japan.

Year	Summary of regulations
1895	The first, (non-compulsory) building requirements introduced following the 1891 Nobi earthquake.
1919 and 1920	*City Planning Act* and *Urban Building Standards Act* introduced in response to urban expansion: specific regulations dictating and regulating building in 6 major urban centres in Japan, including a height limit of 100 feet; structural design for timber, masonry, brick, RC and steel constructions; Allowable stress design; quality of materials; dead and live loads. No seismic requirement included.
1924	*Urban Design Law of Japan* introduced base shear force equivalent to 0.10g as a requirement for 6 major urban centres in Japan.
1950	Ultimate strength design introduced in the *Building Standard Law*. Base shear increased to 0.20g and made compulsory nationwide.
1971	Amendment introduced after the 1968 Offshore Tokachi earthquake, to improve ductility of RC columns by reducing the required tie hoop space
1981	Incorporating experience from the 1978 Miyagi-Oki earthquake, a 2-level approach (serviceability limit state and ultimate limit state) was introduced and building permission procedures simplified for seismic isolation and active/passive vibration control (Okazaki, 2008). All buildings >31 m high must be analysed for storey drift, stiffness, lateral and torsional eccentricity, while those >60 m must be designed using dynamic analysis. Allowable storey drift was limited to 0.5% of the storey height, although this could be increased to 0.8% if guarantees of no severe damage to non-structural elements could be provided. Although seen as the most advanced code in the world at the time, criticisms included: incentive to omit shear walls / bracing to satisfy shape factor requirements; incentive to use unnecessarily large columns; structural coefficient for ultimate limit state is required for each storey rather than the whole structure; crude seismic zonation of the country; lack of provisions for sub-structure and non-structural damage; importance factor not applied (Ishiyama, 1989). For a more detailed review of the 1981 building code see EEFIT (1997).
2000	Amendment of the *Building Standard Law* to include performance-based regulation. The revised code precisely defines seismic performance requirements and verification based on earthquake response spectra at engineering bedrock and additional surface-soil-layer amplification factors. This approach retains the use of life safety and damage limitation limit states introduced previously, with design ground motion damage limitation limit state reduced to 1/5 of that for life safety, which is based on an earthquake with return period of c. 1 in 500 years (Kuramoto, 2006)

4.2. Composition of building stock

Single-family houses in Japan are traditionally timber-frame construction, while multi-family residential buildings range from small mid-rise to very large high-rise structures which are predominantly steel frame or reinforced concrete (RC) construction. Pre-fabricated timber-frame single-family dwellings (typically one or two storeys) are also increasingly popular.

The dwelling stock in the areas visited by EEFIT comprises 74% detached housing (80% of which is 2 or more storeys) and 24% apartment blocks (85% of which are 2 to 5 storeys). The remaining residential stock is in tenement blocks. The dwelling stock by construction type is distributed as follows: non fire-proofed timber (35%), fire-proofed timber (44%), steel (4%), reinforced concrete (14%), non-timber (3%). The distribution is variable in each city (-shi, -ku in Japanese) / town (-cho, -machi); RC and steel frame construction are not differentiated for the towns, which accounts for the „non-timber" construction category (Figure 4.1).

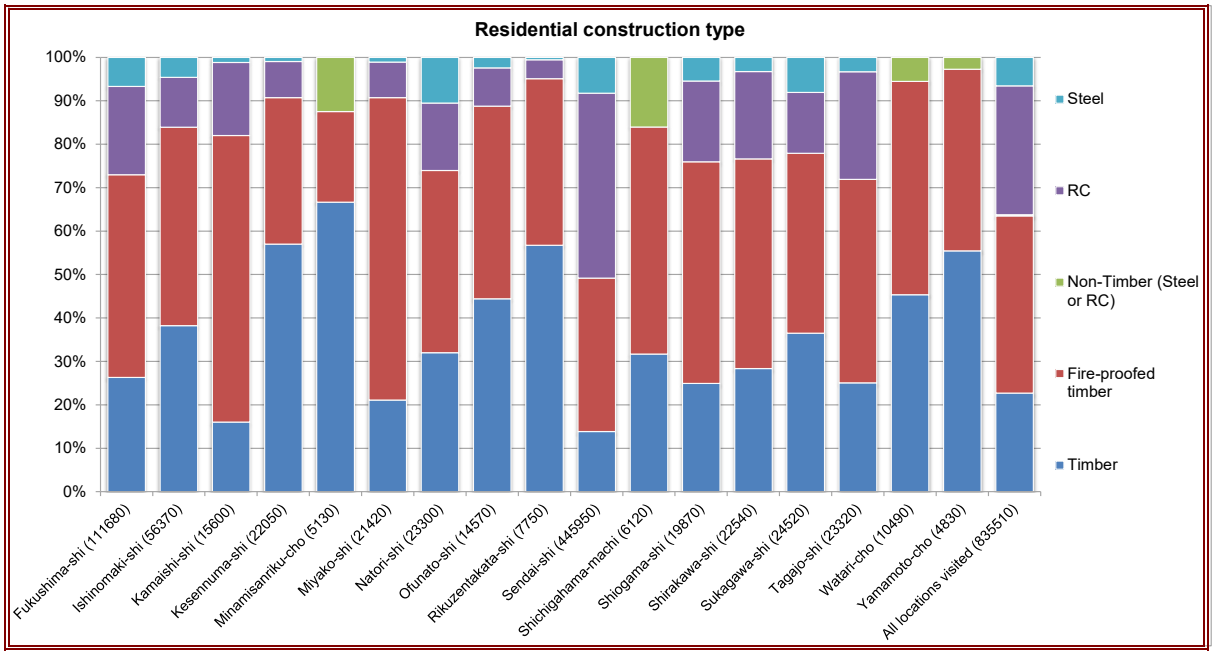

Figure 4.1 Distribution of the dwelling stock by construction type (in terms of per cent of the existing dwelling units) for the towns and cities visited by EEFIT, with the total number of dwelling units for each city / town shown in parenthesis. The weighted distribution for all places visited is shown furthest on right (Source: Statistics Bureau of Japan, 2008 Housing and Land Survey, http://www.stat.go.jp/english/data/jyutaku/results.htm).

Commercial structures are most commonly steel frame or one of several variations of composite steel and RC (SRC) construction, while industrial buildings are mostly steel frame or RC. Given the history of building codes and seismic design in Japan, older structures are less seismically resistant than modern structures.

More details about the structural attributes of the Japanese dwelling stock are given below including discussion on the typologies of wooden dwellings. In addition the various types of residential and non-residential reinforced concrete and steel buildings in Japan are briefly described.

Low-rise timber frame housing

Traditional shinkabe / okabe (light wood post and beam construction) structures were observed by EEFIT. These structures are described by Scawthorn et al. (1981) as comprising a post and lintel vertical load carrying system and a lateral load resisting system of mud-infilled bamboo lattice walls (shinkabe) or braced timber lath-stucco system (okabe). Heavy tile roofing (due to frequent typhoon winds) and large interior wall openings decrease seismic resistance. Most of these dwellings are in the non-fire proofed timber category.

More modern residential construction (light wood stud walls) tends to result in a larger amount of internal wall area (veneer plank boards have replaced sliding paper doors and modern living favours smaller rooms over an open living space layout) and a lower mass (mud- infilled bamboo lattice walls replaced by concrete veneer walls). Pre-fabricated timber frame housing has gradually gained popularity since the 1970s (around 30% of 1990s dwellings were prefabricated) and is considered to be more seismically resistant, in part due to their plan symmetry. The sill plate of the timber frame is bolted to a shallow concrete foundation. Most of these dwellings are in the fire proofed timber category.

Two to three storey timber frame structures with hollow concrete block masonry infill walls were commonly observed in small commercial and mixed residential/commercial premises.

Unreinforced Masonry

Following the 1891 Nobi earthquake, this type of construction was made illegal in many areas and is uncommon for residential use in Japan. Two examples of cut stone unreinforced masonry were observed by EEFIT in Kamaishi and Yuriage (an old bathhouse) – both structures survived the earthquake and tsunami, although shaking damage in the vicinity of these two buildings was negligible. This dwelling construction type is not included in Figure 4.1, because the number of dwellings in unreinforced masonry is negligible in Japan and in the areas visited by EEFIT.

RC frame without shear walls

Pre-1950 RC frame structures were built on the basis of the 1924 Urban Design Law with seismic engineering standards of the time. As such, they usually lack shear walls, while those that do have shear walls, these would cover a small part of the plan area. There were very few such buildings in the areas visited by EEFIT.

Moment resisting RC frame with shear walls

This construction is preferred for 4 to 10-storey buildings in Japan and is designed with a base shear coefficient of at least 0.20g. Following implementation of the 1981 code amendments, seismic performance of this type of building was further enhanced in a construction type already characterised by high quality design, construction and code implementation. Many modern schools in Japan are of this type of construction.

Precast RC

The most common element of precast RC construction in Japan is hollow slabs, covered with a 5 cm layer of cast-in-situ concrete reinforced with a steel mesh. However precast RC buildings are also commonly used in industrial buildings incl. in the area visited by EEFIT.

Steel frame

This type of construction is preferred in high-rise office or other commercial and warehouse structures but is also widely used for industrial buildings and increasingly for residential buildings. The type of bracing varies, but concentric bracing was seen more often in the areas visited by EEFIT. Industrial steel frame structures typically have steel panel walls, while most residential steel structures have exterior walls of concrete fibre panelling.

Steel RC composite (SRC)

SRC (where steel rolled sections are embedded in RC columns and beams) is the most commonly used system for building between 8 and 20 storeys. Many buildings over 7 storeys are SRC in the lower 5 to 7 floors and RC in floors above; the SRC construction providing increased strength and ductility while retaining the large open plan floors available with RC construction. RC construction is retained for the upper floors as it is lighter than SRC construction.

4.3. Field Observations

Damage due to ground shaking is one of the major causes of casualties and economic loss in earthquakes. The understanding of correlation between ground motion intensity and damage severity, from past and current events, is essential to assess the damage potential of future earthquakes. Field observations of earthquake damage provide first-hand and raw data to develop such a correlation and serve as an empirical benchmark.

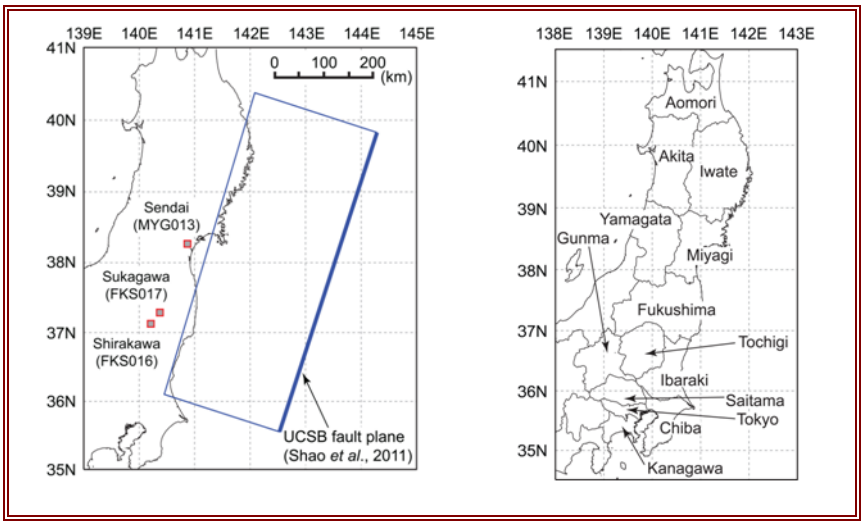

Figure 4.2 Locations of Sendai, Shirakawa, and Sukagawa, and Prefectural boundaries.

During the EEFIT mission, building damage surveys were conducted in Sendai (Miyagi Prefecture), Shirakawa and Sukagawa (both Fukushima Prefecture). The extent of the surveys varies depending on locations, and they were done quickly because of time and resource constraints and due to a wide spatial area to be covered. A comprehensive and systematic damage survey by inspecting all buildings in a designated area was not feasible. Rather, EEFIT teams visited specific places by following local information provided by collaborators. The locations of the three cities are shown in Figure 4.2. The selection of the survey locations was guided by technical reports produced by researchers/engineers in Japan (AIJ Tōhoku, 2011; NILIM and BRI, 2011).

For the three cities, instrumentally recorded ground motions are available from the K-NET (Aoi et al., 2004): MYG013 for Sendai, FKS016 for Shirakawa, and FKS017 for Sukagawa. Rupture distances and soil conditions are broadly similar at the three locations. Ground motion parameters observed in Sendai, Shirakawa, and Sukagawa are summarised in Table 4.2. All three locations experienced ground shaking of JMA intensity of 6+, which is the second severest intensity level in the JMA scale. The JMA intensity scale is a scalar measure between 0 and 7, and describes the intensity of ground shaking and its effects on structures by taking into account not only the amplitude of ground acceleration but also its frequency content and duration. At this ground shaking level, the JMA scale predicts that weak structures may be severely damaged, resulting in tilt or falling of major building parts, while strong structures may suffer from major cracks in columns/beams/walls. Therefore, based on the observed JMA intensity, major damage/disruption to buildings and infrastructure in the three cities was anticipated.

Table 4.2 Summary of the ground motion parameters at Sendai, Shirakawa, and Sukagawa.

Parameter	Sendai (MYG013) [NS, EW, UD]	Shirakawa (FKS016) [NS, EW, UD]	Sukagawa (FKS017) [NS, EW, UD]
Distance (km)	47.1	63.3	56.2
V_{S30} (m/s)	284.1	308.0	265.8
JMA intensity	6+	6+	6+
Arias intensity (cm/s)	[1701, 1128, 375]	[4094, 2697, 494]	[1052, 1025, 203]
CAV (g-s)	[7.887, 7.733, 4.653]	[12.049, 10.517, 4.155]	[7.273, 7.041, 3.225]
PGA (cm/s^2)	[1329.8, 799.9, 283.7]	[1269.2, 838.9, 403.8]	[658.2, 490.0, 264.8]
SA at 0.3 s (cm/s^2)	[1528.8, 1312.3, 795.2]	[3851.4, 2398.2, 538.3]	[1330.4, 1253.7, 444.9]
SA at 1.0 s (cm/s^2)	[1619.5, 581.4, 173.8]	[528.2, 288.8, 236.1]	[548.5, 644.6, 213.3]
SA at 3.0 s (cm/s^2)	[170.5, 104.9, 31.9]	[77.6, 54.7, 34.2]	[84.5, 138.6, 66.6]

In section 4.3.1, overall damage statistics for structures are summarised. Then, field observations from the earthquake damage surveys at Sendai (MYG013), Shirakawa (FKS016), and Sukagawa (FKS017) are presented in sections 4.3.2, 4.3.3, and 4.3.4, respectively. Damage severity and characteristics are discussed for each location in relation to recorded ground motion data and their characteristics (e.g. spectral amplitude and frequency content). It is noted that ground motions at the surveyed building sites can be significantly different from those recorded at the K-NET stations (which are about 0.5 to 3 km apart).

4.3.1. Overall damage statistics

The Tōhoku mainshock and aftershocks (in particular, M_W7.1 event on 7th April) caused tremendous seismic damage to buildings and infrastructure, including ports, bridges, railways, roads, Sendai airport, electricity grids, power generation plants, water supply and treatment facilities, and etc. To provide an overview of the damage to buildings/roads/bridges, damage statistics collected by the National Police Agency (NPA) as of 8th November 2011, are summarised in Table 4.3 (see Figure 4.2 for the locations of the prefectures). The statistics indicate that the building damage is concentrated at Miyagi, Iwate, Fukushima and Ibaraki Prefectures, which were severely affected by the tsunami (see sections 5, 6 and 7). A high number of road damage incidents in Chiba Prefecture are related to wide-spread liquefaction damage in the Tokyo Bay area (Bhattacharya et al., 2011).

Table 4.3 Damage statistics as of 8th November 2011 (NPA, 2011). Includes shaking-affected and tsunami-affected buildings.

Prefecture	Total collapse	Half collapse	Partial damage	Non-residential damage	Road	Bridge
Iwate	20,182	4,539	7,212	4,148	30	4
Miyagi	77,021	93,378	178,121	27,677	390	29
Fukushima	18,364	55,786	131,276	1,052	19	3
Ibaraki	3,196	22,739	161,243	12,341	307	41
Tochigi	264	2,030	65,371	295	257	0
Gunma	0	7	16,154	195	7	0
Saitama	0	5	1,800	33	160	0
Chiba	783	9,175	32,656	660	2,343	0
Tokyo	0	11	257	20	13	0
Kanagawa	0	38	405	24	0	0
Others	347	935	138	1,683	33	0
Total	120,157	188,643	594,633	48,128	3,559	77

The damage assessment and rapid structural inspection of buildings and infrastructure are urgent and important. Immediately after the mainshock, aftershocks are very active and strong aftershocks might occur at any moment; thus safety against potential seismic risk due to aftershocks must be assessed quickly and decision-making regarding reoccupation of buildings needs to be done promptly. Table 4.4 summarises the results of the rapid structural inspection at municipality level in the Tōhoku and Kanto regions as of 27th June 2011 (MLIT, 2011; data for municipalities with the number of red-tagged buildings less than 200 are not shown individually and categorised as „others"). In Table 4.4, the majority of tsunami-affected buildings are not included (thus the total number of inspected buildings in Table 4.4 and the total number of damaged buildings in Table 4.3 differs). Inspection results are presented in terms of three damage levels: red-tag (unsafe), yellow-tag (limited entry), and green-tag (inspected), and represent the outcome of evaluation by a qualified engineer or architect (JBDPA, 2011). It is noteworthy that the evaluation is primarily concerned with safety of occupants; for instance, a building without significant damage to structural components (columns, beams, and load-resisting walls), but with significant cladding damage may be red-tagged if a hazard due to falling objects is judged as unsafe. Therefore, red-tagged buildings do not necessarily mean that they are in

immediate danger of structural collapse. This system is consistent with that used in other countries to assess structures following an earthquake.

Table 4.4 Rapid inspection of damaged buildings as of 27th June, 2011 (MLIT, 2011).

Prefecture	City	Red-tag: Unsafe	Yellow-tag: Limited entry	Green-tag: Inspected	Total
Iwate	*Subtotal*	*168*	*445*	*459*	*1,072*
Miyagi	Sendai	1,543	2,711	4,653	8,907
	Ishinomaki	221	104	9,074	9,399
	Shiroishi	247	460	1,862	2,569
	Iwanuma	204	261	1,383	1,848
	Tomeshi	334	150	434	918
	Kurihara	221	308	587	1,116
	Ohsaki	338	396	1,876	2,610
	Watari	572	377	1,450	2,399
	Yamamoto	250	563	1,562	2,375
	Onagawa	243	412	789	1,444
	Others	915	1,769	14,298	16,982
	Subtotal	*5,088*	*7,511*	*37,968*	*50,567*
Fukushima	Koriyama	722	913	1,722	3,357
	Iwaki	351	2,247	299	2,897
	Shirakawa	259	486	275	1,020
	Sukagawa	321	375	588	1,284
	Kagamiishi	207	416	730	1,353
	Yabuki	248	261	88	597
	Others	1,206	2,020	2,073	5,299
	Subtotal	*3,314*	*6,718*	*5,775*	*15,807*
Ibaraki	Takahagi	208	337	654	1,199
	Others	1,353	4,347	8,964	14,664
	Subtotal	*1,561*	*4,684*	*9,618*	*15,863*
Tochigi	Ustunomiya	270	932	1,681	2,883
	Others	406	913	977	2,296
	Subtotal	*676*	*1,845*	*2,658*	*5,179*
Gunma	*Subtotal*	*30*	*61*	*19*	*110*
Saitama	*Subtotal*	*0*	*42*	*83*	*125*
Chiba	Asahi	248	535	1,577	2,360
	Katori	357	725	616	1,698
	Others	72	365	1,020	1,457
	Subtotal	*677*	*1,625*	*3,213*	*5,515*
Tokyo	*Subtotal*	*59*	*137*	*252*	*448*
Kanagawa	*Subtotal*	*14*	*81*	*446*	*541*
Total		11,587	23,149	60,491	95,227

4.3.2. Damage survey in Sendai, Miyagi Prefecture

General observations in Sendai

A damage survey was conducted in the Miyagino district of Sendai. The focused areas include Yamato, Oroshi, and Takasago (Figure 4.3). In Yamato, there are many mid- to high-rise residential RC (RC) buildings (up to about 15 storeys), whereas in Oroshi there are many commercial low- to mid-rise buildings and warehouses (RC and steel buildings). In Takasago, there are mixture of high-rise buildings and low-rise wooden houses.

Figure 4.3 Locations of the MYG013 station and areas surveyed in Sendai (38° 16' 04" N, 140° 55' 46" E).

Generally speaking, shaking damage to buildings was found at various locations (e.g. diagonal cracks on wall; scaffolding to high-rise buildings; roof damage; falling of cladding materials for wooden houses). In Oroshi, shear failures of RC columns were seen, resulting in building collapse due to soft-storey mechanism (Figure 4.5c). Moreover, in Yamato, ground settlement due to liquefaction was observed at many sites (see section 8).

Observed ground motions in Sendai

The damage survey was carried out in the vicinity of K-NET MYG013 station. The recorded ground motion time-series data, local soil profile and geophysical data (*N* value and shear-wave velocity), and response spectra for MYG013 are shown in Figure 4.4. It is noteworthy that the ground motion time-series data for MYG013 have two distinct wave arrivals: one is before 75 s, while the other is after 75 s; these two episodes are related to local ruptures and energy releases within the entire fault plane at different times and segments (Irikura and Kurahashi, 2011) and directivity of wave propagation. Such two-phase wave arrivals were not observed in FKS016 and FKS017 (see Figure 4.7 and Figure 4.10).

The response spectra for MYG013 (Figure 4.4c), which are calculated using the entire acceleration time-series data, have two peaks: one for short vibration periods (less than 0.2 s) and another for intermediate vibration periods (around 0.5 s to 0.9 s). A detailed investigation of the response spectra indicates that the local peak of the response spectra at intermediate vibration periods corresponds to the first seismic wave episode, whereas the peak values at short and long vibration periods were mainly contributed by the second seismic wave episode.

The soil condition for MYG013 has rather low *N* value (or shear-wave velocity) at depths less than 6 m. These soil layers may be susceptible to liquefaction-induced ground settlement (the layer with low *N* values corresponds to silt, which may or may not be liquefiable). Note that sand boil was observed around the MYG013 station.

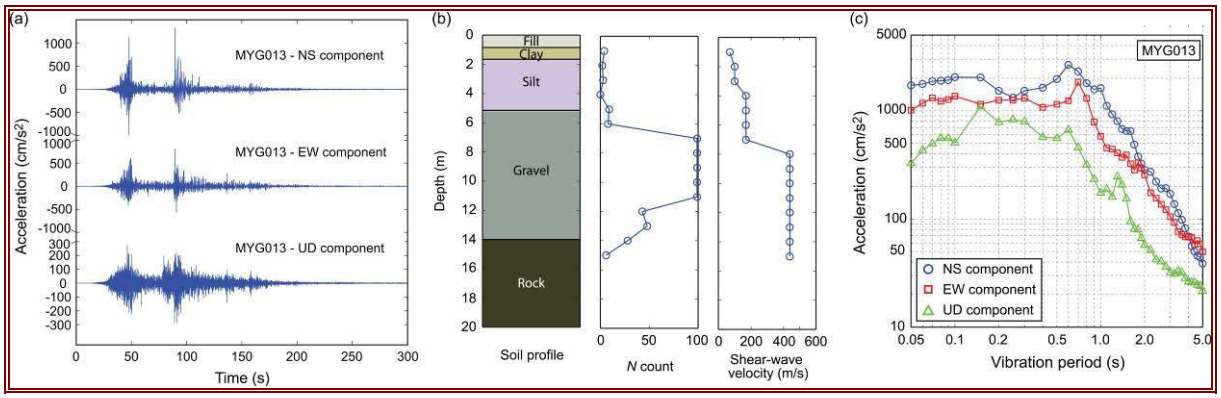

Figure 4.4 Summary of observed ground motions in Sendai (MYG013): (a) time-series data; (b) soil profile, *N* value, and shear-wave velocity; and (c) response spectra.

Case studies in Sendai

Three case studies of damaged buildings in Yamato, Oroshi, and Takasago are discussed below. They are selected because the EEFIT team inspected the building damage in detail.

The residential apartment building in Yamato was a 12-storey RC building that suffered significant damage to walls and columns (Figure 4.5a and Figure 4.5b). The building is about 2200 m south of the MYG013 station. It was constructed in 1975, prior to 1981 when major improvements in seismic provisions were incorporated (Nakashima and Chusilp, 2003). Many shear cracks on non-structural walls were observed at various storey levels. Obvious defects of this RC building include the use of smooth reinforcement bars, insufficient hook length, and 90° hook angles. It is noted that in nearby areas, ground settlement was observed (about 10-20 cm settlement; see section 8.1).

The second case study is a 2-storey RC office building in Oroshi (Figure 4.5c and Figure 4.5d), which was constructed in 1969. This building is about 1500 m south of the MYG013 station. It completely collapsed due to a soft storey mechanism (Figure 4.5c), and at the 1st storey level, shear failures of columns and fracture of lateral reinforcement stirrups were observed (Figure 4.5d).

The third case study is a 14-storey residential apartment building (Figure 4.5e-f), which is about 3000 m east of the MYG013 station. This building consists of two structures, which are connected by expansion joints, and forms an L-shape in plan as a whole. It was constructed in 1975, and suffered from damage during the 1978 Miyagi-Oki earthquake (cracks on non-structural walls in the lower part of the building); repairs were done by replacing damaged RC walls with new ones of increased thickness (NILIM and BRI, 2011). During the Tōhoku earthquake, many shear cracks occurred in non-structural-walls (Figure 4.5e) and several major cracks occurred in columns and beams. Furthermore, one of the two structures was tilted by about 2 degrees due to ground settlement (Figure 4.5f and Figure 4.5g). This building will be demolished; the decision was reached by the consensus of the residents/owners.

(a) Yamato apartment

(b) Column-floor joint failure

(c) Oroshi office building

(d) Shear failure of column (1st storey level)

(e) Takasago apartment

(f) Gap between two buildings

(g) Ground settlement

Figure 4.5 Photographs of damaged buildings in Sendai.

4.3.3. Damage survey in Shirakawa, Fukushima Prefecture

General observations in Shirakawa

The damage survey conducted in Shirakawa, Fukushima Prefecture, focused on Shirakawa City Office, Komine Castle, Shin-Shirakawa train station (close to the K-NET FKS016 station), and Hanokidaira (Figure 4.6). According to the rapid inspection conducted by the City (NILIM and BRI,

2011), 155 buildings were re-tagged (unsafe). In particular, many damage incidents due to failure of retaining walls were reported in the newly-developed residential areas (e.g. Midorigaoka). Despite the registration of the JMA intensity of 6+, major structural damage and collapse were not observed in downtown Shirakawa during the field survey (noting that our investigation was brief). Another feature of the shaking damage in Shirakawa is the occurrence of landslides at several locations around the city and the collapse of stone walls of the Komine Castle.

Figure 4.6 Locations of the FKS016 station and areas surveyed in Shirakawa (37° 07' 24" N, 140° 11' 30" E).

Observed ground motions in Shirakawa

The recorded ground motion time-series data, local soil profile and geophysical data (*N* value and shear-wave velocity), and response spectra for FKS016 are shown in Figure 4.7. One major seismic wave arrival was observed at FKS016. The response spectra of the FKS016 data indicate very strong energy concentration at vibration periods between 0.1 s and 0.3 s (reaching 3000-4000 cm/s^2); this might have affected stiff and low-rise structures and acceleration-sensitive structural/non-structural components/contents significantly. It is noted that the long-period spectral content of the FKS016 ground motion data is not as intense as that for MYG013. This might be the reason why not so many mid- to high-rise buildings in Shirakawa were damaged due to ground shaking, compared to Sendai. From the soil data, the potential for massive liquefaction is low, because of rather high *N* values and the presence of a thick gravel layer from 3 m and below.

Case studies in Shirakawa

No major structural damage was observed during the on-foot survey around the Shirakawa City Office and the Shin-Shirakawa train station close to the FKS016 station (note: a few buildings that suffered from severe damage were observed while driving through the city). Collapsed walls of a traditional warehouse were observed (Figure 4.8a), and several houses had sustained roof damage. Generally speaking, damage in downtown Shirakawa was minor.

At the Komine Castle, stone walls had collapsed due to a combination of ground shaking and landslide (Figure 4.8b). This is related to large ground accelerations observed in Shirakawa. In total, the collapse occurred at eight locations (North and South sides of the Castle, noting that ground shaking in the North-South direction was greater than that in the East-West direction; see Figure 4.7a and Figure 4.7c).

At Hanokidaira, there was a landslide (Figure 4.8c) which killed ten people and destroyed several houses at the foot of the slope (Figure 4.8d). Landslides at the Komine Castle and Hanokidaira are discussed further in section 8.2

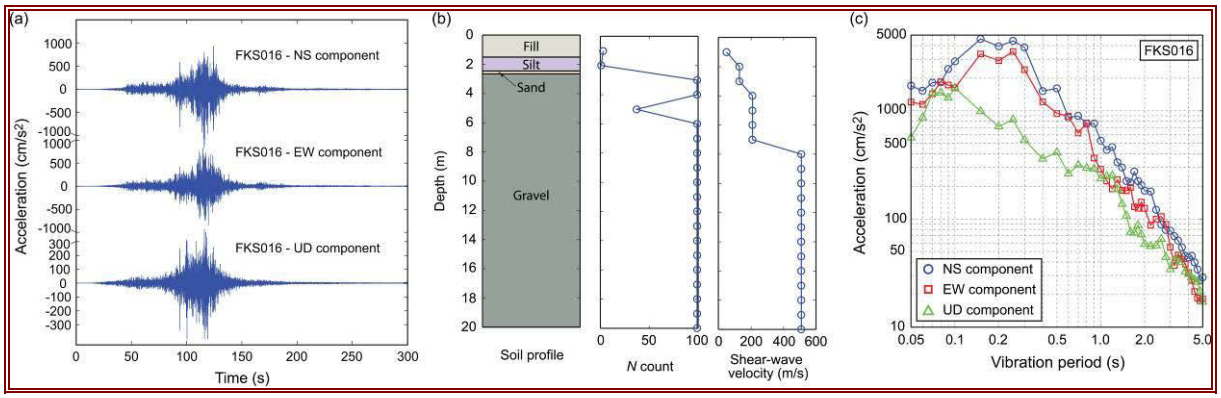

Figure 4.7 Summary of observed ground motions in Shirakawa (FKS016): (a) time-series data; (b) soil profile, *N* value, and shear-wave velocity; and (c) response spectra.

(a) Damage to traditional warehouse

(b) Collapse of stone wall

(c) Hanokidaira landslide

(d) Foundations of destroyed houses

Figure 4.8 Photographs of ground shaking and landslide damage in Shirakawa.

4.3.4. Damage survey in Sukagawa, Fukushima Prefecture

General observations in Sukagawa

A damage survey was conducted in Sukagawa, Fukushima Prefecture. The survey area was around the Sukagawa City Office (Figure 4.9). Generally speaking, relatively significant damage was observed in Sukagawa, particularly in comparison with Shirakawa (despite JMA intensity 6+ being registered at both locations). The damage was concentrated in areas close to the City Office and the

City Office itself was severely damaged (Figure 4.12a to Figure 4.12c). The concentration of damage in these areas may be partly attributed to soft soil conditions (the buildings are constructed on fill material, where the Sukagawa Castle moat had previously existed). Moreover, several sand boils were observed in these areas (NILIM and BRI, 2011).

Overall, major ground shaking damage was observed and damage to roofing, cladding, and traditional warehouses was seen in many places while driving through the city. To provide a summary of structural damage in Sukagawa, results of the rapid building inspection in Sukagawa are shown in Table 4.5 (NILIM and BRI, 2011). The damage statistics shown in Table 4.5 indicate that damage occurred to various kinds of structures, wooden, RC, and steel, and that about 25% of the inspected buildings were red-tagged (note: the number of red-tagged buildings in Sukagawa is about twice as large as that in Shirakawa). This is in agreement with our impression after visiting both Shirakawa and Sukagawa.

Figure 4.9 Locations of FKS017 station and surveyed areas in Sukagawa (37° 17' 02" N, 140° 22' 06" E).

Table 4.5 Results of rapid inspection of damaged buildings in Sukagawa as of 24th March 2011 (NILIM and BRI, 2011).

Structural type	Red-tag: Unsafe	Yellow-tag: Limited entry	Green-tag: Inspected	Total
Timber	245	315	463	1,023
Steel	51	44	93	188
RC	25	16	32	73
Total	321 (25.0%)	375 (29.2%)	588 (45.8%)	1,284 (100.0%)

Observed ground motions in Sukagawa

The recorded acceleration data for FKS017 (Figure 4.10) were less intense than those for MYG013 and FKS016. In particular, comparison with FKS016 is relevant because of the geographical proximity and different observed damage severities at the two locations. Although PGAs and SAs at short vibration periods for Sukagawa were much smaller than those for Shirakawa, SAs at intermediate and longer vibration periods were greater for Sukagawa. Therefore, seismic demand to mid-/high-rise structures in Sukagawa were more intense than that in Sukagawa. It is noted that the soil profile for FKS017 is different from that for FKS016, containing sand and volcanic ash layers with low *N* values; they may be subjected to liquefaction-induced ground settlement given intense ground shaking.

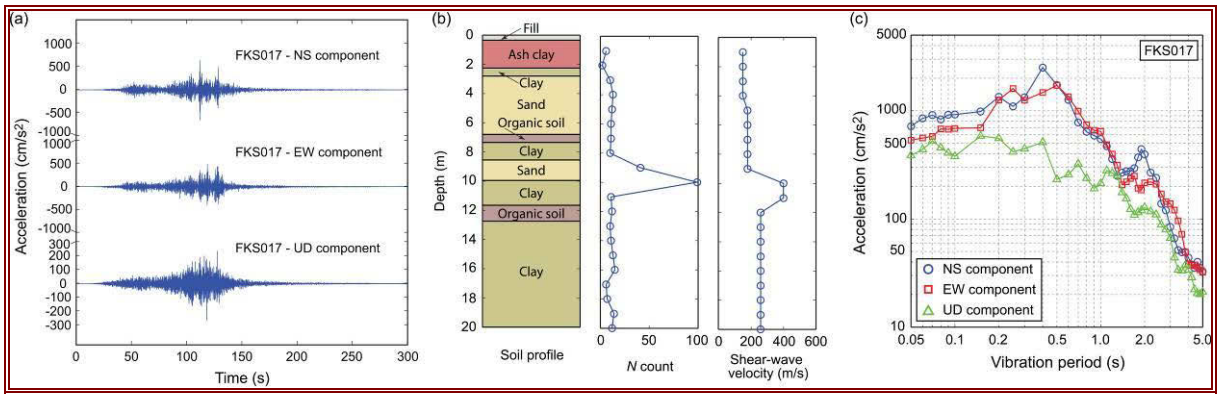

Figure 4.10 Summary of observed ground motions in Sukagawa (FKS017): (a) time-series data; (b) soil profile, *N* value, and shear-wave velocity; and (c) response spectra.

Case studies in Sukagawa

In Sukagawa, a small survey was conducted around the City Office by inspecting individual buildings, recording damage features, and assigning damage grades based on the EMS-98 scale (ESC Working Group on Macroseismic Scales, 1998). A summary of the damage survey results is shown in Figure 4.11; the number shown inside the box corresponds to the assigned EMS-98 grade (e.g. grade 0 corresponds to no damage, while grade 5 corresponds to collapse). Several observations and results from the survey are summarised below.

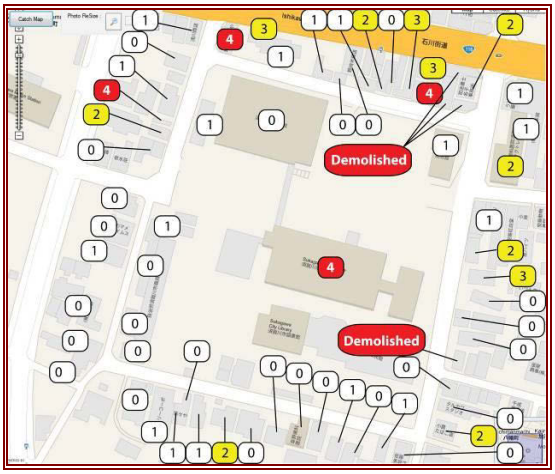

Figure 4.11 Summary of the damage survey conducted in the surrounding of the Sukagawa City Office (37° 17' 12" N, 140° 22' 22" E). The number indicated in the figure corresponds to the assigned EMS-98 grade.

The City Office, a 4-storey RC building constructed in 1970 (Figure 4.12a), was severely damaged due to ground shaking. No seismic upgrading was conducted. Many large diagonal cracks on non-structural walls and shear failures of structural walls/columns were observed (Figure 4.12b and Figure 4.12c). The locations of shear failure in columns correspond to a change in the amount of reinforcement (NILIM and BRI, 2011): more reinforcement was placed at joints but less reinforcement was placed in the middle of the columns. Shear failures of columns due to the change of steel reinforcement were also observed in the 1995 Kobe earthquake. Because of the severe damage, the building was not occupied at the time of the survey; all departments of the City Office were operating from at the gymnasium beside the City Office, which had no apparent damage.

Out of 63 surveyed buildings (Figure 4.11), 4 buildings were demolished, 4 buildings were severely damaged (grade 4), 11 buildings were partially damaged (grade 2 or 3), and 17 buildings were with minor damage (grade 1). In general, the survey results are in agreement with the damage statistics shown in Table 4.5. Three photographs for two damaged buildings with grade 4 are shown in Figure 4.12d to Figure 4.12f. For the damaged liquor store, a 3-storey RC building, (Figure 4.12e and Figure 4.12f), many cracks on non-structural walls and falling of concrete covers were observed.

(a) Sukagawa City Office

(b) Large diagonal cracks on wall

(c) Shear failure of a column

(d) Damaged house at the ground floor level

(e) Damaged liquor store

(f) Falling of concrete cover

Figure 4.12 Photos of damaged buildings in Sukagawa.

4.4. Conclusions on ground shaking damage

The 11th March, 2011 Tōhoku mainshock and its major aftershocks have caused significant damage and disruption to structures and infrastructure, including buildings, building foundations and geotechnical structures (pile and retaining wall), highways and railway bridges, road networks, and lifelines (electricity, water, and gas supply). In addition, ground failures (liquefaction and landslides) were widespread and extensive, while damage due to induced hazards (tsunami, fire following earthquake) was catastrophic. Such devastation resulted in tremendous casualties and economic loss. To mitigate seismic risk in the future, lessons must be learned from what happened to existing

buildings and infrastructure, and they must be incorporated into current seismic design codes/practices to improve our capability in managing catastrophic earthquake risk.

In order to gain useful lessons/experiences from this tragic event, ground shaking-related damage surveys were conducted during the EEFIT mission. For this purpose, three locations, Sendai, Shirakawa, and Sukagawa, were focused upon. They were selected, because:

(i) JMA intensity of 6+ was reported there (hence, based on the observed JMA intensity, severe damage to old/weak buildings was expected); and.

(ii) Instrumentally recorded ground motion data from the K-NET were readily available (thus various ground motion parameters, as discussed in section 3, can be computed and compared for different locations; moreover, rupture distances and soil conditions are broadly similar at the three locations).

The field building damage surveys and analysis of observed ground motion data indicate that:

(i) Many of the damaged/collapsed buildings in Sendai were reinforced concrete structures, constructed prior to 1981 when a major revision to the Japanese seismic design code was implemented;

(ii) Damage to buildings in Sendai and Sukagawa was more severe than that in Shirakawa;

(iii) Occurrence of landslides and damage to geotechnical structures (retaining walls and filled ground) in Shirakawa might be caused by intense ground shaking with rich short-period spectral content; and

(iv) Relatively major damage in Sukagawa near the City Office may be due to soft soil conditions.

Importantly, the observation related to (ii) can be linked with different observed response spectra values at intermediate-to-long vibration periods at the three locations (i.e. richer intermediate-to-long spectral content for Sendai and Sukagawa, in comparison with Shirakawa).

4.5. References

Aoi, S. Kunugi, T. and Fujiwara, H., 2004. Strong-motion Seismograph network operated by NIED: K-NET and KiK-net. *Journal of Japan Association for Earthquake Engineering*, 4(3), pp. 65–74.

Architectural Institute of Japan Tōhoku Chapter (AIJ-Tōhoku), 2011. *Reconnaissance report of the 2011 off the Pacific coast of Tōhoku earthquake*. [online] Available at <http://news-sv.aij.or.jp/Tōhoku/englishportal.html> [Accessed 30 June 2011].

Bhattacharya, S. Hyodo, M. Goda, K., Tazoh, T. and Taylor, C.A., 2011. Liquefaction of soil in the Tokyo Bay area from the 2011 Tōhoku (Japan) earthquake. *Soil Dynamics and Earthquake Engineering*, 31(11), pp. 1618–1628.

EEFIT, 1997. The Hyogo-Ken Nanbu (Kobe) Earthquake of 17 January 1995: a field report by EEFIT. [online] Available at <http://www.istructe.org/knowledge/EEFIT/Pages/reports.aspx> [Accessed 30 June 2011].

European Seismological Commission (ESC) Working Group on Macroseismic Scales, 1998. *European Macroseismic Scale 1998*. Luxembourg.

Ishiyama, Y., 1989. Japanese seismic design method and its history. In: *Proceedings of the Third U.S.-Japan Workshop on the Improvement of Building Design and Construction Practices*, Tokyo, Japan, pp. 55–64.

Japan Building Disaster Prevention Association (JBDPA), 2011. *Post-earthquake quick inspection of damaged buildings*. [online] Available at<http://www.kenchiku-bosai.or.jp/jimukyoku/Oukyu/data/epanf/epanfall.PDF> [Accessed 30 June 2011].

Kuramoto, H., 2006, Seismic design codes for buildings in Japan. *Journal of Disaster Research*, 1(3), pp. 341-356.

Ministry of Land, Infrastructure, Transport, and Tourism (MLIT), 2011. Great East Japan earthquake. [online] Available at <http://www.mlit.go.jp/common/000139083.pdf> [Accessed 30 June 2011] (in Japanese).

Nakashima, M. and Chusilp, P., 2003. A partial view of Japanese post-Kobe seismic design and construction practices. *Earthquake Engineering and Engineering Seismology*, 4(1), pp. 3–13.

National Institute for Land and Infrastructure Management (NILIM) and Building Research Institute (BRI), 2011. *Quick report of the field survey and research on the 2011 off the Pacific coast of Tōhoku earthquake (the Great East Japan earthquake)*. [online] Available at <http://www.kenken.go.jp/japanese/contents/topics/20110311/0311quickreport.html> [Accessed 30 June 2011] (in Japanese).

NPA, 2011. *Damage Situation and Police Countermeasure, 8 November 2011* [online]. Available at: <http://www.npa.go.jp/archive/keibi/biki/higaijokyo_e.pdf> [Accessed 9 November 2011].

Scawthorn, C. Iemura, H. and Yamada, Y., 1981. Seismic damage estimation for low- and mid-rise buildings in Japan. *Earthquake Engineering and Structural Dynamics*, 9(2), pp. 93–115.

Statistics Bureau of Japan, 2008. *2008 Housing and Land Survey*, [online] Available at < http://www.stat.go.jp/english/data/jyutaku/results.htm > [Accessed 7 October 2011].

Umemura, J., 2011. Landslide and failure of slopes. In: *The First Symposium for the Great East Japan earthquake*. Sendai, Miyagi, Japan. 28 April 2011 (in Japanese).

5. The 11th March 2011 tsunami and its impact

Historically there have been a number of disastrous tsunami along the Tōhoku region. Okumura (2011) has summarised tsunami along the Sanriku coast of Honshu (Figure 5.1), which has suffered repeated damage, particularly from the 1896 Meiji-Sanriku (22,000 deaths; PWRI, 2008), 1933 Showa Sanriku (3,064 deaths; Takata, 2009) and the distal (remote) 1960 Chilean (142 deaths; Takata, 2009) earthquakes. In the Sanriku area of Iwate Prefecture tsunami heights (see section 5.1 for definition of tsunami height) exceeded 10 m during these events. Further south in Miyagi Prefecture, tsunami heights have been mostly less than 5 m and further south still around Sendai and down the Joban coast, mostly less than 2 m. So in Miyagi and Fukushima Prefectures, previous recent tsunami did not result in the 4-7 m (and greater) heights experienced on 11th March 2011.

However, historic tsunami are believed to have occurred with tsunami heights similar to those experienced on 11th March 2011. In the 1611 Keicho earthquake, a 6-8 m high tsunami devastated the Sendai Plain. Satake et al. (2008) have also modelled the 869 Jogan earthquake and tsunami with estimates of tsunami inundation extent 1.0 km to 3.0 km inland from the coastline of the Sendai and Ishinomaki Plains. Further south in Fukushima Prefecture, the modelled 869 tsunami reached 1.5 to 2.0 km inland. These are comparable to, or exceed the inundation of the 2011 tsunami. It is possible that the 869 earthquake had a similar location and magnitude to the 11th March earthquake (Simon et al., 2011).

Figure 5.1 The Sanriku, Miyagi and Joban coast of Honshu (Okumura, 2011).

5.1. Tsunami terminology

The word “tsunami” comes from “tsu” meaning anchorage or harbour and “nami” meaning waves. The expression had been used in Japan during the Edo period (1603-1867) but it gained international acceptance following the 1896 Sanriku tsunami (Horikawa, 2000).

Tsunami waves, when offshore, are described by their height and speed (which will influence the time of arrival at a coastline). When the wave (or waves, as is most often the case) reach the shore and inundate land, there are a number of further parameters that may be used to describe their severity. It is important to clearly identify these parameters as they are often used interchangeably, and sometimes incorrectly. Definitions are as follows (PARI, 2011a) and are illustrated in Figure 5.2.

- Run-up height: vertical measure of the highest extent of wave with respect to the tidal level at the time of the event
- Inundation depth: vertical measure of the wave profile at a particular location with respect to the local ground elevation
- Inundation height: vertical measure of the wave profile at a particular location with respect to the tide level at the time of the event
- Distance from shoreline: horizontal measurement of the observation with respect to the shoreline
- Inundation extent: horizontal distance to further inland point of tsunami flow with respect to the shoreline

The run-up and inundation depth are measured against a structure (e.g. tall building) or a sharp change in topography (cliff face).

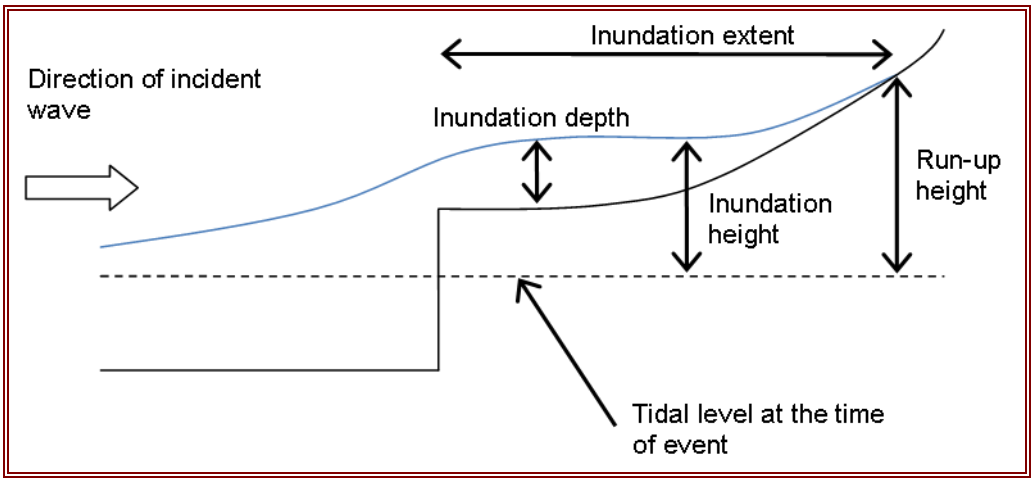

Figure 5.2 Definition sketch of tsunami variables (after PARI, 2011a).

Additionally, tsunami height can be measured either at a shoreline tide measurement station or at sea by GPS system. It is measured as the difference in height between the crest of the wave and the tidal level wherever the station is located.

5.2. Coastal morphology and bathymetry in the affected region

The east coast of the Tōhoku region comprises two very different forms: rias and plains (Figure 5.3). The rias are drowned river valleys which are open to the sea and lie to the north of Sendai. They are characterised by a jagged-shaped coastline. Neighbouring rias are separated by ridges that extend inland. In sharp contrast are the coastal plains to the south which are vast areas of fairly flat land, often used for agriculture. The different topography has a markedly different effect on a tsunami.

In rias the shape of the valley constrains the movement of the incoming wave, amplifying its height and leading to much greater run-up. In contrast, coastal plains offer little resistance to flow so the run-up of the tsunami is not nearly so great. It was found that the rias coastline experienced the greatest run-up levels in this event, though the wave did not reach very far inland from the shoreline (except where the tsunami propagated up a river channel). In contrast, those regions in the Sendai basin with its coastal plains experienced limited run-up but the tsunami travelled up to 7 km inland (GSI, 2011).

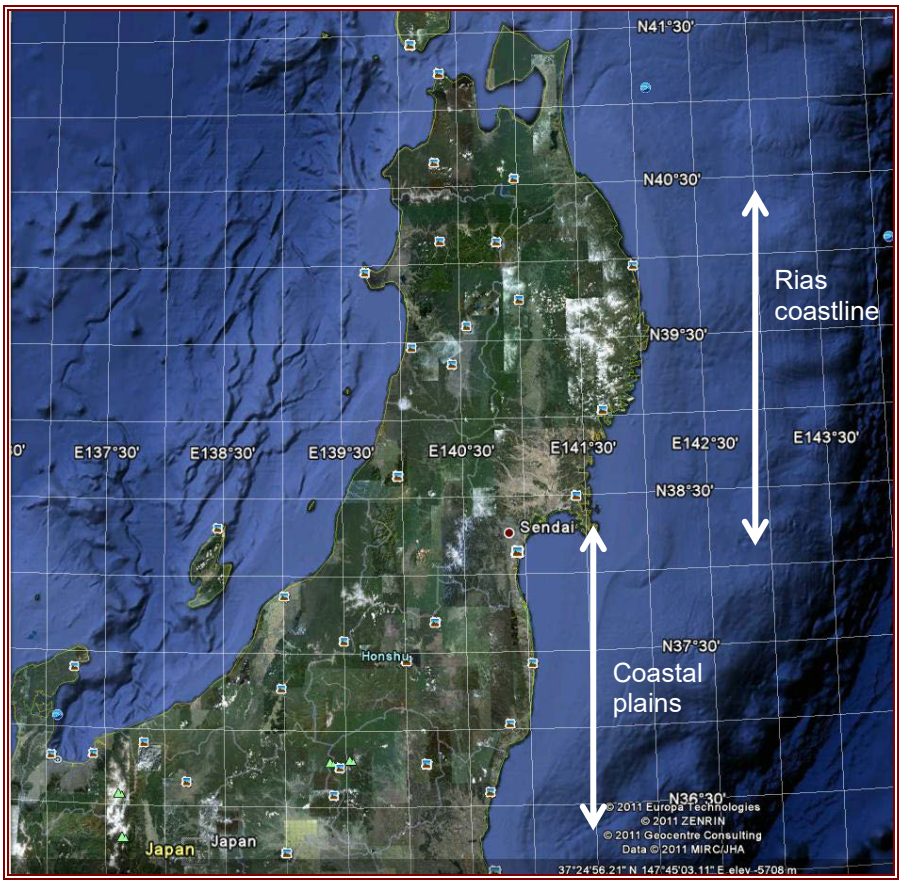

Figure 5.3 Coastline types of the Tōhoku region (image from Google Earth).

5.3. Coastal defences in Japan

With a very high proportion of coastline to unit area of land (92 m/km^2 c.f. about 50 m/km^2 in the UK) and with a large proportion (71%) of the land being described as mountainous or hilly, the Japanese population is concentrated along coastlines (Horikawa, 2000). Japan has 75% of its assets and 50% of its population of 130 mn people in the 10% of the total land area that is flat coastal plain (Kokusai Kogyo Group, 2011).

Within the survey region of the EEFIT team, Miyako, Kamaishi, Ōfunato and Ishinomaki are classified as major ports, and Sendai-Shiogama one of only 23 'specially designated major ports' (meaning that it serves international marine networks). The ports act as centres of import/export, passenger transport hubs, business activities, production bases, housing and recreation. As a result of these activities tsunami damage has a knock-on effect beyond its geographical location. An example of a previous disaster affecting a large port was the Great Hanshin-Awaji Earthquake of 17th January 1995 which affected the port of Kobe particularly badly, effectively paralysing it due to large-scale damage of the quay walls and loading sites. The cost to reconstruct the port amounted to some ¥570 bn and led to a new policy: “Basic Policy on Construction and Reinforcement of Facilities to Cope with Large-Scale Earthquakes in Ports and Harbors”. Technological Standards exist for port facilities and they aim to guarantee safety and functionality. These have been revised according to international standards e.g. ISO (MLIT, 2006). The Port and Harbor Law was revised in 2000 to increase the government"s contribution to infrastructure development in major ports but conversely to reduce its contribution to small port and harbour facilities (MLIT, 2006). This presumably has implications for the protection of communities situated close to these smaller facilities.

Added to the importance of coastal land and facilities, the frequent occurrence of natural disasters in the form of typhoons, storm surges and tsunami, means it is easy to understand why Japanese coastal defences are amongst the most extensive in the world. In addition to the historic tsunami

discussed at the beginning of this section there have also been significant storm surges that led to significant loss of life during Typhoon No. 13 in 1953, and Typhoon No. 15 in 1959 (Horikawa, 2000).

Typical coastal structures of jetties, groynes, breakwaters (both detached and submerged) may be seen along the coastline. There have also been significant land reclamation projects including the building of artificial islands. The importance of sediment transport along the coastline is recognised following difficulties of erosion near river mouths due to construction of dams for water supply, flood control etc. Harbour construction has also led to an increased understanding of the effect of coastal structures (harbour walls) on the local sediment budget. Technical committees comprising civil engineers, oceanographers, geomorphologists and others exist to understand the cause of coastal erosion at various locations (Horikawa, 2000).

Tsunami breakwaters and tsunami walls have been built along vulnerable coastlines, often at those locations badly affected by previous events such as Tarō, Kamaishi and Ōfunato which will be described in detail in section 6. Table 5.1 shows coastal defences that have been constructed as a result of previous tsunami damage. An international delegation, formed of officials from the countries worst-affected by the 2004 Indian Ocean tsunami, visited Japan in 2008 under the auspices of UNESCO (ICHARM) and reported that they were “amazed to see gigantic structures, such as tsunami breakwaters and sea walls” (PWRI, 2008).

Many of these coastal protection structures used design conditions based upon the Meiji Sanriku tsunami which was considerably smaller than the one that occurred in 2011. As a result they were not effective in stopping the waves from overtopping, and in many situations suffered catastrophic failure. These will be reported in section 6. PARI (2011b) suggest that, rather than building even bigger structures, coastal defences should remain of moderate size, but with special attention given to their stability in order that they survive even a huge tsunami despite being overtopped. The rationale for this is that a defence that survives will be partially effective even if it is overtopped.

Table 5.1 Coastal protection measures following previous damaging tsunami waves (MLIT, 2006).

Coast name	Facilities	Past tsunami damage
Port of Kiritappu (Hokkaido)	Tsunami protection station	1960 Chile earthquake tsunami, etc.
Port of Kuji (Iwate)	Tsunami protection breakwater	1896 Meiji Sanriku Earthquake tsunami, etc.
Port of Kamaishi (Iwate)	Tsunami protection breakwater	1896 Meiji Sanriku Earthquake tsunami, etc.
Port of Ōfunato (Iwate)	Tsunami protection station	1896 Meiji Sanriku Earthquake tsunami, etc.
Port of Shimizu (Shizuoka)	Tsunami protection station	1944 Tonankai Earthquake tsunami
Port of Sagara (Shizuoka)	Tsunami protection station	1944 Tonankai Earthquake tsunami
Port of Susaki (Kochi)	Tsunami protection breakwater	1946 Nankai Earthquake tsunami, etc.

Japan has historically worked in isolation from the international community and as a result has sought innovative solutions to issues of coastal defence and tsunami mitigation. Dual cylindrical caisson breakwaters have been built at the end of the conventional breakwater in Sakai Port, Osaka Prefecture (Sankarbabu, 2008). Japanese strategies for tsunami vertical evacuation are the most developed in the world and purpose-built / adapted refuges exist in many locations around the country, including the Nishiki Tower, Mie Prefecture and the refuge at Shirahama Beach Resort, Tokushima Prefecture (FEMA, 2008). Vertical evacuation refuges observed during this EEFIT mission are discussed in section 10.3. Since the 1950s Japanese coastal engineers have contributed to international research conferences but it must still be recognised that only a small part of Japanese research is published in the English language. This will remain a barrier for the exchange of ideas / good practice in coastal structure design.

It should be noted that the role that natural beaches and defences play in shoreline protection from wind waves has been extensively investigated and many schemes implemented. The conservation of sandy beaches by, for example, detached offshore breakwaters also has a beneficial effect on recreational utilisation, habitat conservation etc. (Horikawa, 2000). As a consequence of beach erosion, the Ministry of Transport (now Ministry of Land, Infrastructure and Transport, MLIT) has been actively pursuing an Integrated Shore Protection System since the 1980s (Herbich, 2000). In this approach, the single hard-edged structures are replaced by sandy beaches, tree planting and low-crested step-type revetments as can be seen at Tsuda Port, Kagawa Prefecture, and at Arahama, Miyagi Prefecture. MLIT (2006) also state that they intend constructing tsunami and storm surge protection stations, using integrated monitoring and control of facilities such as sluice gates to allow normal river flow. Ōfunato is one such example where monitoring and control of flood gates is in place, although this pre-dates the MLIT report in 2006 (section 10.3.2).

5.4. Tsunami severity

5.4.1. GPS measurements

The effects of this tsunami were first detected by GPS tsunami monitoring buoys installed by the Port and Harbour Bureau of the MLIT, located at strategic locations around the Japanese coast. Some typical tsunami heights detected by these buoys were: 6.7 m at 15:12, (18 km off Kamaishi) and 5.6 m at 15:14 (off the coast of Rikuzentakata). Allowing for the effects of shoaling once the wave enters shallow water this suggested that the tsunami might be as much as 10 m high once it reached the shoreline. The earlier tsunami warning that was issued by the Japan Meteorological Agency (JMA) at 14:49 was amended to more than 10 m on the basis of these GPS measurements (PARI, 2011b).

PARI (2011c) published maximum heights measured at the buoys off the Sanriku coast, shown in Figure 5.4. Table 5.2 shows the names of the offshore stations with their water depth and distance from shore. Time histories of the tsunami detected at these buoys have also been published (PARI, 2011d). Figure 5.5 shows the time history at Kamaishi station number 4, 18 km offshore. The y-axis shows the sea level in metres and the x-axis shows the time (14:00 to 22:00). The graph shows up to 7 large waves over a period of about 6 hours, roughly equally spaced in time. However, each wave comprised a number of local maxima so to an observer it may have seemed that there were even more individual waves, and with shorter periods. Note that the buoy shows a rise in sea level of 55 cm once it stabilised at the end of the day (Kazama, 2011).

Table 5.2 Location details of GPS buoys off the Sanriku coast (PARI, 2011c cited in Kazama, 2011).

Buoy location	Water depth (m)	Distance from shoreline (km)
1 - Hachinohe	87	18
2 - Kuji	125	17
3 - Miyako	200	13
4 - Kamaishi	204	11
5 - Hirota-wan	160	18
6 - Kinkazan	144	10
7 - Onahama	137	19

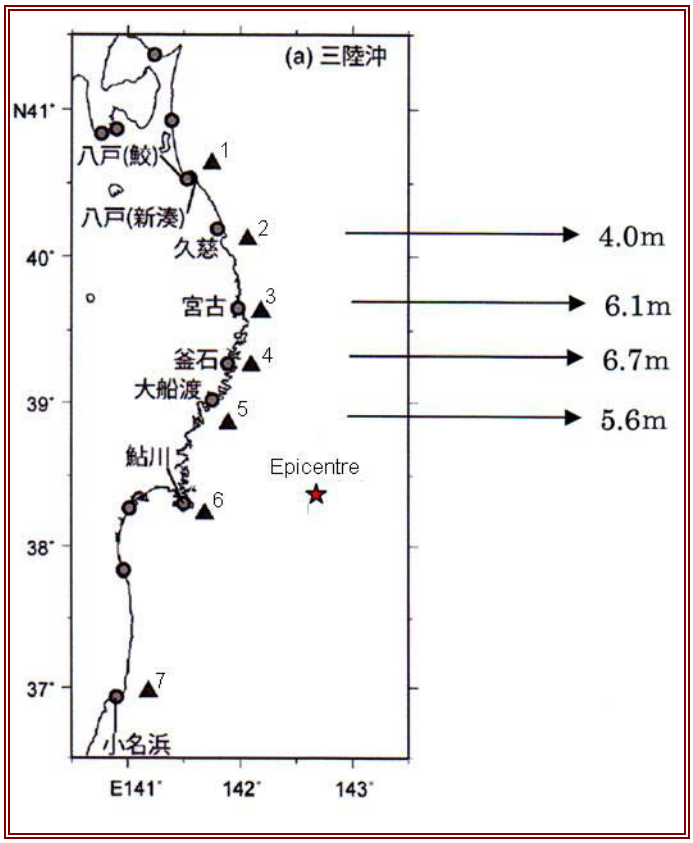

Figure 5.4 Maximum tsunami heights recorded at GPS buoys off the Sanriku coast (PARI (2011c) cited in Kazama (2011)). Black triangles denote the position of buoys; Buoy number relates to location in Table 5.2.

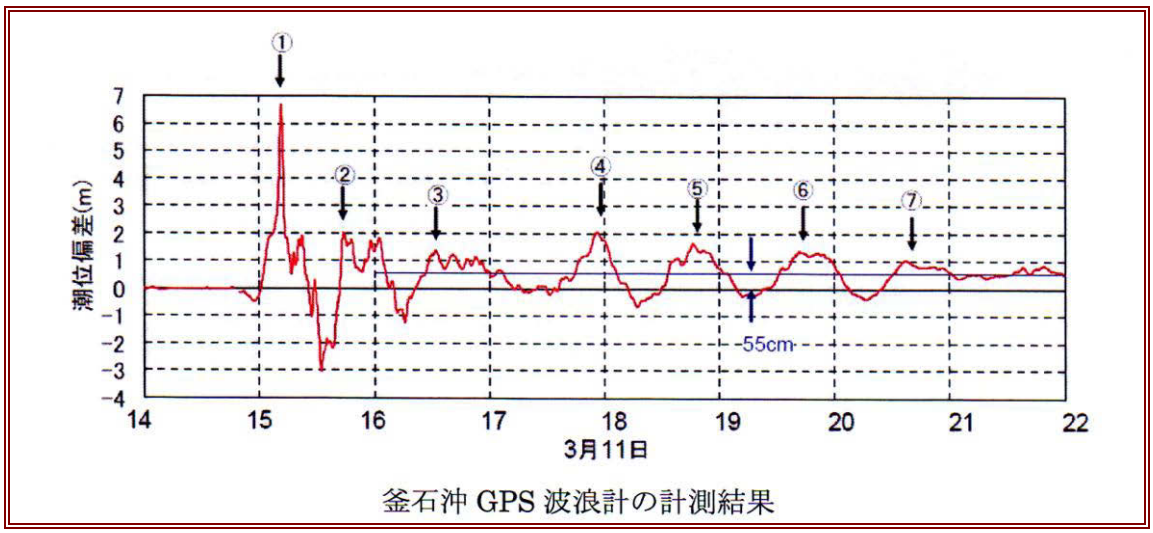

Figure 5.5 Sea surface elevation time history of the tsunami in metres, plotted against time (hours shown) on 11th March, 2011. Measured at buoy number 4, 18 km off the coast of Kamaishi (PARI, 2011c).

5.4.2. Initial estimates of arrival times and tsunami heights

As introduced in section 5.4.1, JMA issued warnings that included the expected size of tsunami. As gauge recordings and observations became available the predictions of the size of the tsunami were adjusted and re-issued. The maximum expected tsunami heights for Iwate, Miyagi and Fukushima Prefectures in the first 3 warning bulletins are given in Table 5.3, showing that in the 47 minutes following the earthquake, significant revisions were made to the tsunami height estimates. These revisions are based on observations at GPS monitoring systems (see section 5.4 for observed wave height and arrival times in this event). Post-tsunami investigations have shown the estimates from the warning at 15:14 as relatively in line with observations of maximum tsunami height in coastal areas of Miyagi.

Table 5.3 Predicted tsunami heights at shore immediately following the earthquake, for the three worst-affected Prefectures. As published in JMA warnings on 11th March 2011 (JMA, 2011b).

Time	Time after earthquake (minutes)	Estimated height - Iwate (m)	Estimated height - Miyagi (m)	Estimated height - Fukushima (m)
14:49	3	3	6	3
15:14	28	6 (+100%)	10 (+67%)	6 (+100%)
15:33	47	10 (+67%)	10 (0%)	10 (+67%)

Revisions in tsunami height after initial estimates are common due to the initial analysis of tsunami height being reliant on preliminary earthquake data in order to provide a warning as early as possible. This preliminary data comprises magnitude and hypocentral location derived from seismograph data, often within seconds of the earthquake and from only a few monitoring stations. Moment magnitude is only calculated once the fault geometry and amount of slip have been constrained; this can then be used to provide a more accurate estimate of tsunami height. Parameter uncertainty occurs in rapid assessment of all earthquake events and revision of magnitude is common. In this event the initial estimated JMA magnitude was 7.9 (this was the one used for initial tsunami height estimations) and was revised to moment magnitude 9.0 three days later as fault parameters were constrained and tsunami estimations refined – this is reflected in the adjustments shown in Table 5.3. The JMA warning system and evolution of warnings on 11th March are discussed further in section 10.2.

Table 5.4 Tsunami wave height and arrival time recorded by tide gauges (Shaw et al., 2011).

City	Wave height (m)	Arrival time relative to earthquake
Ryori	10.48	0:37
Kesennuma	10.48	0:53
Kamaishi	6.99	0:33
Ishinomaki	6.28	1:03
Ryoishi	5.58	0:37
Aratame	4.88	0:50
Yamada	4.88	0:50
Rikuzen-Takata	4.88	1:03
Ōfunato	4.88	1:03
Arahama	4.88	1:12
Tarō	4.18	0:42
Fudai	4.18	0:44
Sendai	4.18	1:39
Miyako	3.49	0:44
Otsuchi	3.49	0:50

5.4.3. *Observed arrival times, tsunami heights and inundation*

Okumura (2011) reports that within 10 minutes of the earthquake the first small waves, only tens of centimetres in height, had reached 3 tide gauges between Chosi and Miyako on the Sanriku coast. However, the more significant waves of more than 3 m in height reached the low-lying coastal plains about 30-40 minutes after the earthquake (Okumura, 2011). Table 5.4 contains wave heights and arrival times for locations visited by EEFIT for the three worst-affected Prefectures, many of which were visited during the EEFIT mission. This information was extracted from tide gauges, some of which was not available until several days after the tsunami due to operational difficulties. This data should be considered together with that in Table 5.5, which shows tsunami run-up and inundation depth on land from various sources, rather than the offshore / nearshore wave height.

Table 5.5 Wave arrival and onshore tsunami height survey data in areas investigated by EEFIT, listed from North to South.

Location (North to South)	[A] Arrival time of 1st wave (mins after EQ)	[B] Time to max. inundation extent / height (mins after [A])	[C] Max. tsunami height (metres) - corrected for tide	[D] Number of data points	[E] Mean tsunami height (m)	[D] Standard deviation of tsunami height (m)
Fudai	n/a	n/a	24.16	36	14.44	4.92
Tarō	n/a	n/a	37.49	76	21.47	7.90
Miyako	29	11	40.45	310	15.98	8.42
Kamaishi	28	9	30.40	140	14.31	5.08
Ōfunato	25	6	31.99	252	13.13	3.95
Rikuzentakata	37	n/a	21.63	155	14.24	2.60
Kesennuma	n/a	n/a	23.00	97	10.50	5.04
Minamisanriku	n/a	n/a	20.54	59	12.63	5.14
Onagawa	n/a	n/a	34.74	60	15.55	4.95
Ishinomaki	23	16	25.84	120	6.51	5.63
Shiogama	n/a	n/a	4.89	13	3.28	1.12
Shichigahama	n/a	n/a	9.21	17	5.09	2.15
Miyagino-ku	n/a	n/a	16.65	13	6.63	4.17
Sendai Port	n/a	n/a	5.23	16	2.62	1.41
Wakabayashi-ku	n/a	n/a	19.55	28	5.90	5.99
Natori	63	n/a	12.96	54	4.36	3.56
Iwanuma	64	n/a	8.75	6	5.38	3.30
Watari-cho	65	n/a	7.71	26	2.88	2.22
Yamamoto-cho	65	n/a	12.78	20	5.88	3.22

Notes: [A,B] Arrival times: Kamaishi - Fujita (2011); Rikuzentakata - @disaster_i (2011); Miyako, Ōfunato, Ishinomaki - tide gauge records; additional - JMA (2011b). [C,D,E] Inundation depth / run-up from tsunami watermarks on buildings, in-situ debris, eye witness accounts - The 2011 Tōhoku Earthquake Tsunami Joint Survey Group (2011).

The Ōfunato tide gauge record from 11th March is shown in Figure 5.6. The dashed line shows real-time data, while the solid line portion of the graph shows recovered data obtained several days later.

The UN Office for the Coordination of Humanitarian Affairs state in a situation report that the JMA reports that the highest tsunami wave on the day of the quake was 15 meters high in Mekawa, Miyagi

(UNOCHA, 2011). These measured heights may be compared with those predicted from a simple shoaling formula based upon offshore heights and depth:

Equation 5.1

$$\eta = \left(h_G \eta_G{}^4\right)^{0.2}$$

where η is the estimated tsunami height at the shoreline and h_G and η_G are respectively the water depth and tsunami height at the GPS station location. These theoretical values are 12.6 m at Miyako, 13.3 m at Kamaishi and 11.1 m at Rikuzentakata (PARI, 2011b).

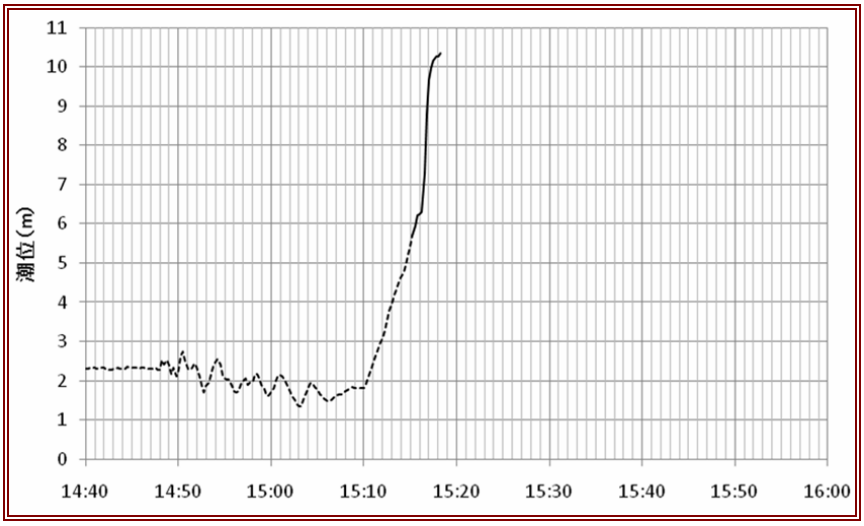

Figure 5.6 Tide gauge data from Ōfunato showing the sea level (y-axis) against time (x-axis), with dashed line indicating real-time data and the solid line showing recovered data obtained several days later. The time history is with respect to a local datum level which is referenced to Mean Sea Level at Tokyo Bay (JMA, 2011d as cited by UNESCO, 2011a).

Run-up and inundation heights

In the weeks following the event, tsunami run-up and inundation measurements shown in Figure 5.7 were issued (JSCE, 2011), corrected for tide from 3,410 locations. Data has now been collected from a total of 5,400 locations from Hokkaido to Okinawa Prefecture (Daily Yomiuri, 2011).

The plots indicate the location of the greatest run-up and inundation height, around the Miyako district in Iwate. The maximum observed value of tsunami run-up is 40.545 m at Omoe Aneyoshi in Miyako district. This exceeds the previous highest ever observed run-up of 38.2 m at Ryori Bay, Iwate Prefecture in 1896 (USGS, 2011). Other values of run-up greater than 30 m were recorded to the north of Tarō, in Miyako City. It is interesting to note the gap in the data around the Fukushima nuclear power plant presumably due to the exclusion zone affecting access for survey teams.

Inundation heights greater than 10 m were recorded between Miyako to the north and Soma to the south (PARI, 2011d). In Kamaishi there were 6.9 m, 8.1 m and 9.0 m inundation heights in the inner port area (PARI, 2011a). Because of the relatively large depth of water in the port the tsunami did not break (due to depth-limited breaking) so the unbroken wave overtopped the quay walls and seawalls in Kamaishi and travelled through the town with a speed velocity of between 2.8 and 8.3 m/s (10 and 30 km/h). In Ōfunato 9.5 m inundation height was measured in the inner port area: run-up of 11.0 m (directly facing Pacific Ocean) and 23.6 m (measured just to the east of Ryori; here the seabed slope is 1:100 at a depth of 10 m and steepens to 1:10 on land). In Onagawa, inundation height of 14.8 m was measured in the port area and an 18.31 m inundation height was measured immediately to the west of the port (PARI, 2011e). In Ishinomaki, 4.1 m to 5 m inundation height was measured in port area in Sendai Port 7.3 m to 8.0 m and Arahama Beach 9.7 m. At Sendai Airport 5.7 m inundation height was recorded on the airport building and 12.2 m inundation height on the beach in front of the building with significant scour causing its collapse (PARI, 2011a). At Sendai airport the tsunami broke close to the shore and overtopped a 5-10 m high sand dune before flowing several kilometres inland through paddy fields. The slope of the seabed at this location is 1:200 to 1:500 between depths of 10 m and 100 m.

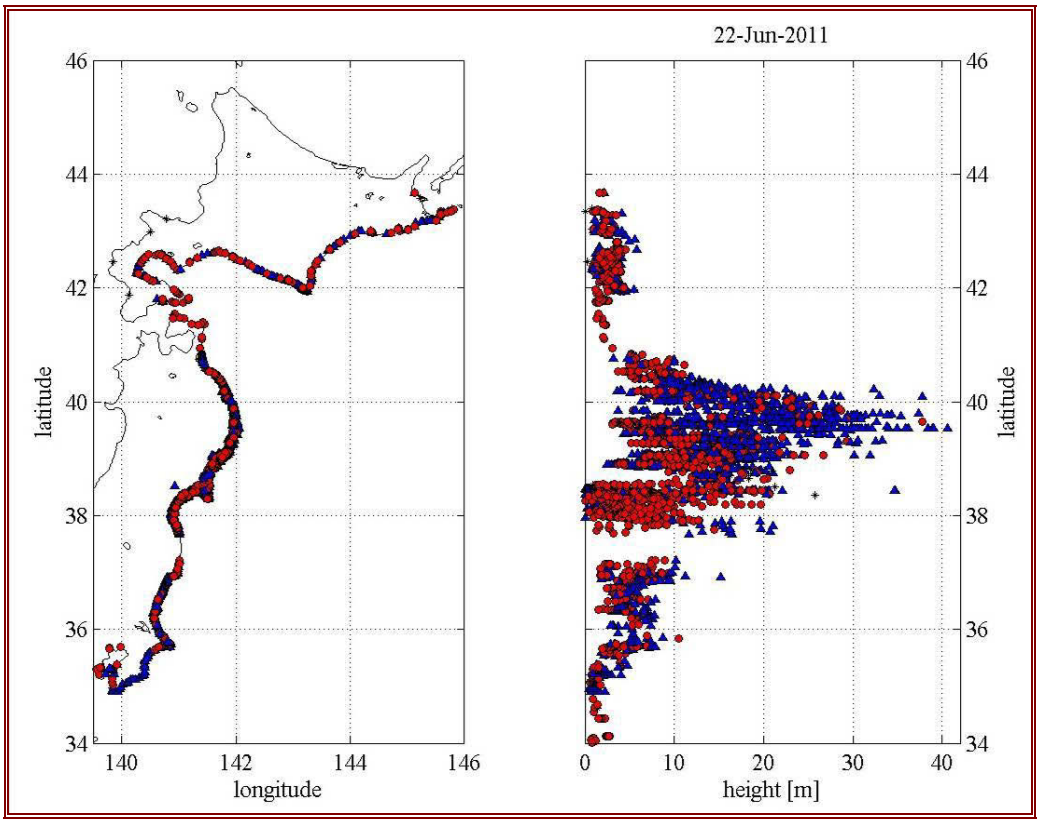

Figure 5.7 Run-up and tsunami heights for the northern part of Japan; blue triangles indicate run-up and red circles are inundation heights (JSCE, 2011).

Extent of inundation

The tsunami is reported to have caused damage along 600 km of coastline (CEDMHA, 2011) and up to 7 km inland in places (GSI, 2011). In terms of the area of land inundated CEDMHA (2011) report that the United Nations and the Geospatial Information Authority (GSI) estimate around 400 km^2, a slightly lower figure than the 500 km^2 estimated by Pasco (a geospatial company based in Tokyo). Pasco report that 300 km^2 alone is inundated in Miyagi Prefecture. CEDMHA (2011) also report that a NHK (2011a) broadcast that 70% of inundated areas in Miyagi were still under water two weeks after the tsunami. Within built-up areas of towns there was also widespread inundation. For example, GSI estimate that half of Otsuchi was inundated and 46% in both Ishinomaki and Yamamoto. With that extent of inundation there will be obvious difficulties in the reconstruction of shelters and infrastructure (NHK (2011b), cited by CEDMHA, 2011).

Figure 5.8 shows a sample of sediment deposited during the tsunami on the Sendai Plains. The upper 100 mm is the tsunami sediment consisting of layers of sands and muds. The sands are normally graded with an approximate grain size near the base of 1 mm. Below 100 mm are muds from rice fields, as this is a cultivated area.

As might be expected, due to little resistance, the tsunami flowed along and overflowed from, river channels (PARI, 2011b). In fact the tsunami flowed over 40 km inland along some rivers. Water levels rose by 11 cm, 49 km along the Kitakami River, 3 hours after the earthquake (NHK (2011b), cited by CEDMHA, 2011). If the sluice gates had all been open the situation would have been much worse.

Figure 5.8 Sediment deposited by the 11th March 2011 tsunami approximately 1 km from the coast at Arahama Beach in the Sendai Plains (38° 14' 14.55" N, 140° 59' 02.25").

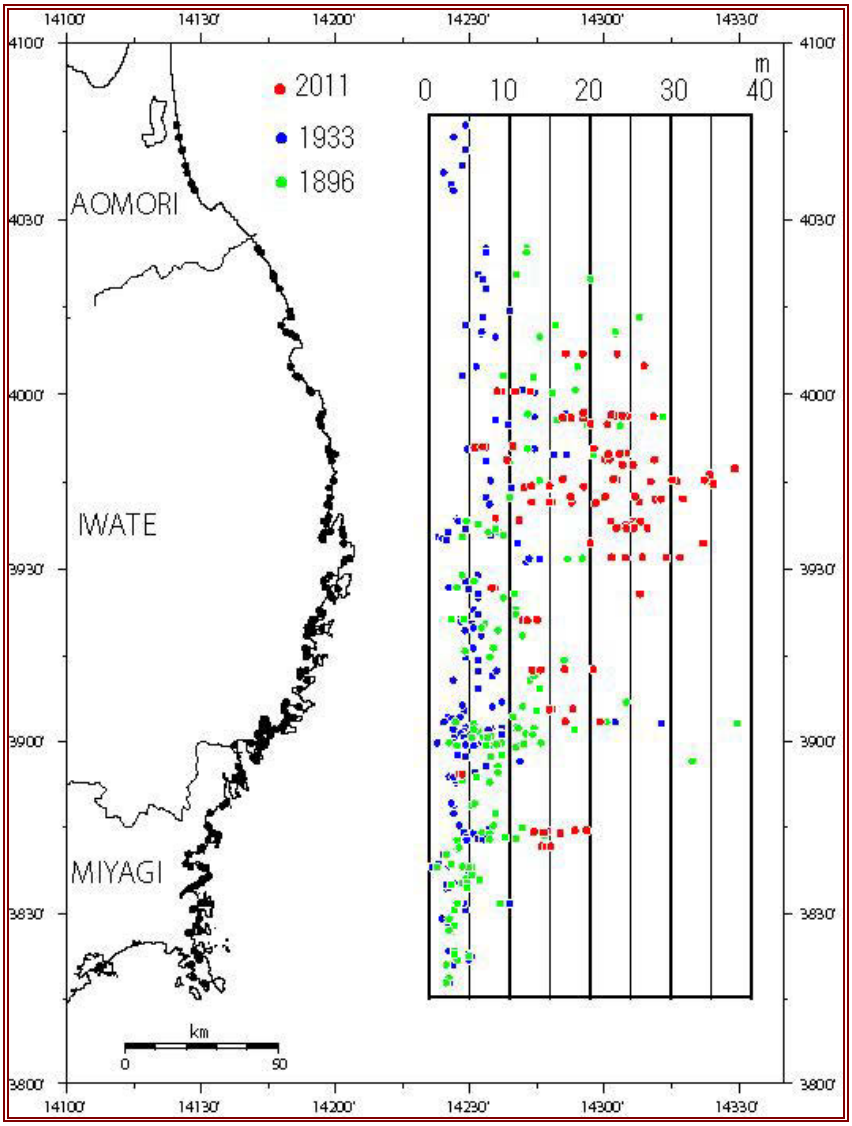

Figure 5.9 Comparisons of tsunami run-up for the 1896, 1933 and 2011 tsunami events (ERI, 2011).

Comparison with previous significant events

The tsunami events of 1896 and 1933 have already been mentioned as being much less significant in terms of size and devastation; however, Figure 5.9 attempts to quantify these events by comparing their run-up measurements at different locations along the coast of Sanriku (ERI, 2011). It can be seen that the 1896 event was fairly comparable with the 2011 event but the 1933 tsunami was clearly much smaller in the part of the coast shown (i.e. the rias coastline). Takata (2009) provides slightly different data for the maximum heights: 1896 – 38.2 m; 1933 – 29 m; 1960 – 6 m.

Global effects

The 11th March earthquake produced a tsunami that propagated across the Pacific Ocean, detected by DART buoys and tide gauges. The NOAA/NWS West Coast/Alaska Tsunami Warning Centre produced predictions of travel time and maximum amplitude for the Pacific region, as are shown in Figure 5.10 and Figure 5.11.

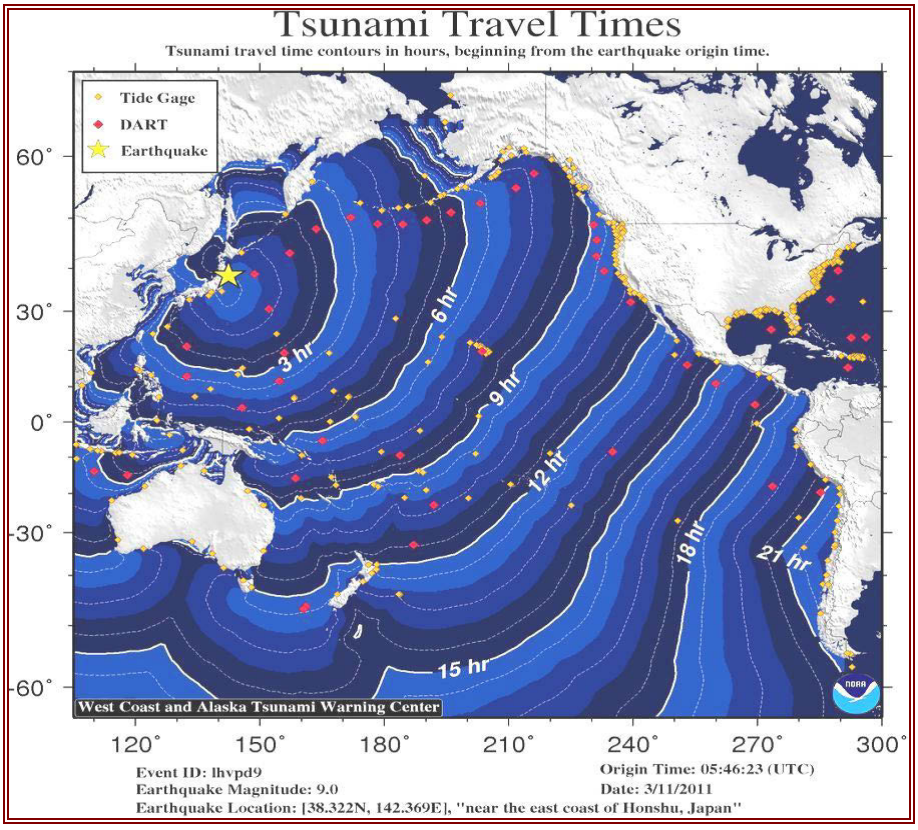

Figure 5.10 Travel time map (NOAA, 2011a, with acknowledgement to NOAA / PMEL / Center for Tsunami Research).

Significant tsunami waves of height greater than 2 m affected regions around the Pacific Ocean: Chile, Ecuador, Russia, California and Oregon (NOAA, 2011a). In Papua New Guinea the wave inundated a major referral hospital during the night, but as all patients had been evacuated following warnings by the Pacific Tsunami Warning Center and Northwest Pacific Tsunami Advisory Center there were no casualties (UNESCO, 2011b).

Additional tsunami

In addition to the 11th March earthquake there have been two other earthquakes that have caused small tsunami: On March 9th a 0.5 m tsunami at Ōfunato (NOAA, 2011b) and on April 7th (NOAA, 2011c) at the same location. It is not known whether the small tsunami of 9th March affected the attitude towards the evacuation 2 days later. The US Army (2011) also reports a tsunami advisory following an earthquake on 28th March for the Miyagi Prefecture which was later lifted.

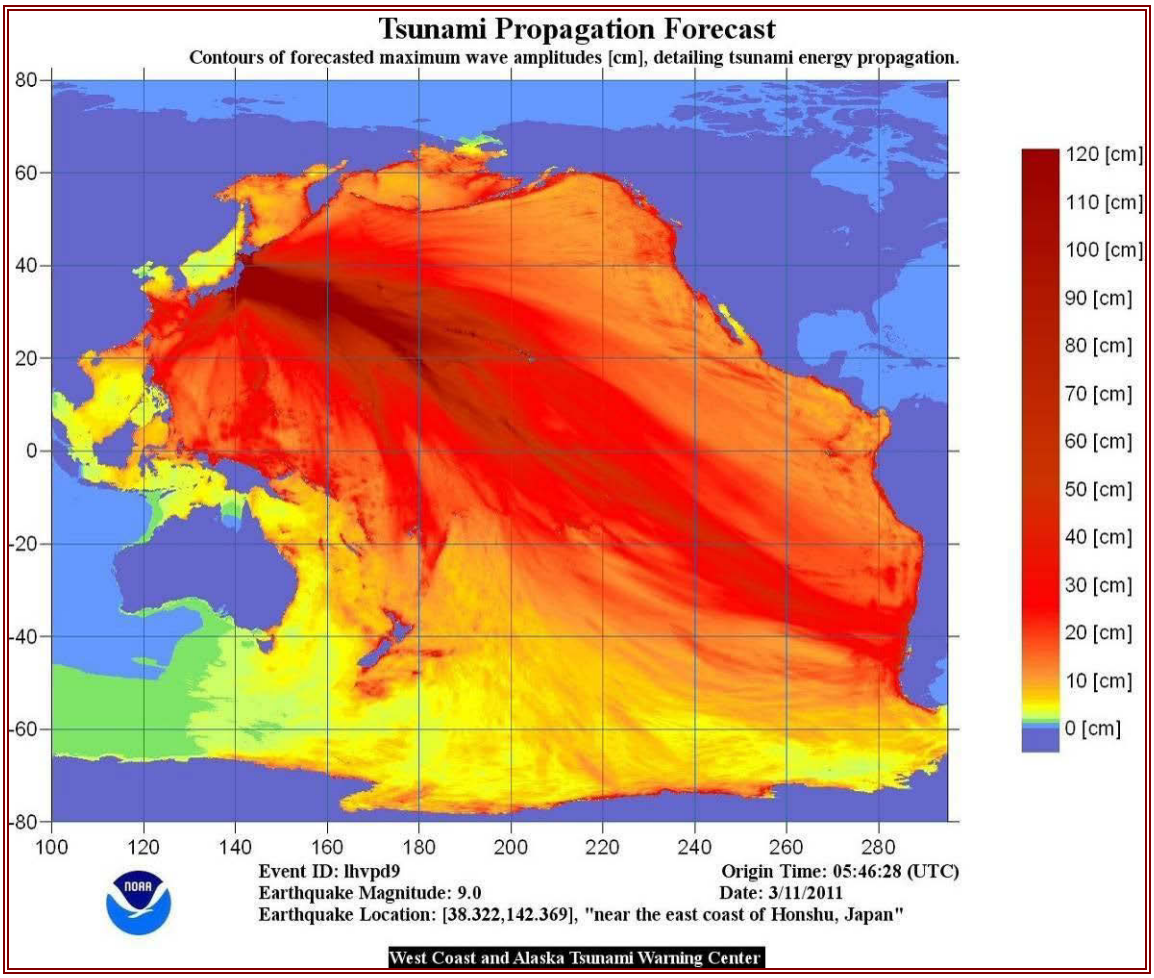

Figure 5.11 Maximum tsunami amplitude graph (NOAA, 2011a, with acknowledgement to NOAA / PMEL / Center for Tsunami Research).

5.5. Overview of tsunami impacts

5.5.1. Damage to buildings

Damage surveys carried out by the Fire and Disaster Management Agency give the following damage figures in its report of July 21st (FDMA, 2011a): 109,862 buildings destroyed; 127,100 buildings partially destroyed and 482,273 buildings damaged; in total 719,235 affected buildings. Damage surveys have not yet been completed as enormous numbers of buildings were affected. Moreover, buildings in worst affected areas were often completely washed away making accurate assessments quite difficult. Damage surveys in the 30 km exclusion zone around the Fukushima Daiichi nuclear power station are also not complete.

In terms of critical infrastructure, 53 hospitals in the worst-affected areas were closed or running at limited capacity in the weeks after the disaster, while 80% of the hospitals in the three worst affected Prefectures (Iwate, Miyagi and Fukushima) were completely or partially destroyed.

The Joint Research Centre (European Commission) identified 88 cities, towns and villages affected by the tsunami (Shaw et al., 2011). Table 5.6 shows a breakdown of the damage sustained by 54 towns and cities in the 4 worst-affected prefectures.

Table 5.6 Number of towns / cities affected by the tsunami (Shaw et al., 2011).

Prefecture	Number of cities in prefecture	Number of cities affected
Iwate	35	14
Miyagi	36	17
Fukushima	58	12
Ibaraki	45	11
Total	174	54

Detailed building damage data as of 8th November 2011 is given in Table 5.7, obtained from the Emergency Disaster Countermeasures Headquarters of the National Police Agency (NPA, 2011). It is shown that by far the majority of collapsed houses are in Miyagi Prefecture.

Table 5.7 Breakdown of building damage by damage type and prefecture at 8th October 2011 (after NPA, 2011).

Damage type / level	Iwate	Miyagi	Fukushima	Ibaraki
Total collapse	20,182	77,031	18,401	3,196
Partial collapse	4,539	93,533	56,153	22,739
Completely burnt	15	135	77	31
Partially burnt			3	
Inundation above ground floor level	1,761	7,053	62	1,607
Inundation below ground floor level	323	11,009	339	724
Partially damaged	7,212	179,423	131,551	161,243
Damaged non-residential	4,148	27,777	1,052	12,341
Total	38,180	395,961	207,638	201,881

5.5.2. Transport infrastructure

Transport and infrastructure was heavily impacted: Sendai Airport was closed for 6 weeks due to extensive damage, while many ports including those in Sendai, Ishinomaki and Kesennuma were severely affected by the tsunami. Aside from damage to ports, local ferries to islands off the mainland were also affected. An example of this is Oshima Island located off Kesennuma – all of the ferries were damaged by earthquake, tsunami or fire. As a result a small boat designed to carry 12 people was being used as the only source of transport for the population of 3,200 people who wanted to reach the mainland. For several days following 11th March there was no assistance due to the extent of the devastation on the mainland. A passenger ship capable of carrying 90 people was subsequently arranged for the island (Asahi, 2011).

Affected roads and railways were reported as: 1 expressway, 18 national highways (under MLIT's management), 31 national highways (under management of local government) and 232 Prefectural and Municipal roads were closed in the initial weeks, while at least 2,126 roads, 56 bridges and 26 railway lines have been destroyed. Japan Railways East reported that 23 railway stations and 60 km of railway track were washed away, 101 rail bridges were damaged and tracks were bent in 210 separate locations (JR East, 2011). Nikken Construction report that power pillars at 540 sites along the Shinkansen railway suffered damage (Kazama (2011).

5.5.3. Debris

Due to the extent of the devastation and proportion of collapsed buildings there is an overwhelming amount of debris deposited inland and also being washed onto shore from the sea. It is reported that the total amount of waste to be disposed is equivalent to more than twenty times the average annual waste for Miyagi Prefecture (Kazama, 2011). This debris is salt-laden, hence difficult to dispose of in

the conventional manner of incineration. There is also the problem of contaminated soil, particularly in the coastal plains which were primarily used for agricultural purposes. Section 11.1.2 outlines debris clearance activities in place as part of the recovery process.

5.5.4. Coastal subsidence

Co-seismic subsidence on 11th March 2011 has resulted in an elevated risk of tidal flooding in many parts of the coast. Significant work has been carried out to mitigate this risk, through reconstruction of coastal defences and increasing the elevation of wharfs and roads. However, in Onagawa Town, where co-seismic subsidence of 1.2 m occurred, the sites of buildings up to 50 m inland are subject to significant flooding, as is the railway line between Ishinomaki and Onagawa. More details on coastal subsidence are presented in section 8.4.

5.5.5. Impact on industry

Nearly 2,350 fishing boats were damaged or destroyed and 20,000 hectares of agricultural land in Iwate, Miyagi and Fukushima Prefectures has been contaminated by the tsunami. In addition, 64 sewage treatment facilities and 74 sewage pumps were damaged. More details on impact to industry are provided in section 9.

5.5.6. Casualty figures

At 11th October 2011, the death toll had reached 15,881 with 3,804 registered as missing (FDMA, 2011a). The worst-affected Prefectures were Iwate, Miyagi and Fukushima, with the highest number of casualties in Ishinomaki. Figure 5.12 shows the distribution of fatality rates along the coastline within the inundation zones; the highest rate of 12.18% was recorded in Onagawa Town in Miyagi Prefecture, though this had a relatively small population of 10,051 in the inundation zone. Fatality rate is obtained by dividing the number of people dead and missing with the number estimated by the GSI to be living in the tsunami inundation zone. Data for the graph has been taken from FDMA (2011a).

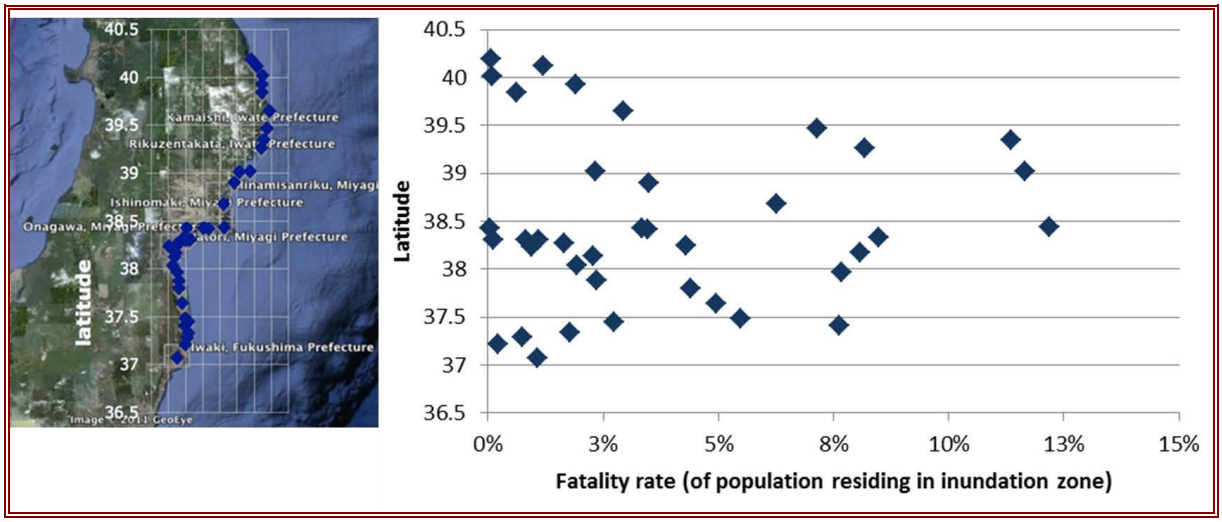

Figure 5.12 Position of towns along the inundated coastline and distribution of fatality rates (at 11th October 2011) by latitude (FDMA, 2011a).

One of the factors contributing to variable fatality rates was the number of elderly people in a location. The rias coastline has a higher percentage of elderly residents (Statistics Bureau, 2005): for population data that exists from Kuji (Iwate Prefecture) south to Onagawa (Miyagi Prefecture) the over-65s comprise 28.4% of the population. This is compared with the coastal plains (Tagajo, Miyagi Prefecture to Yamamoto, Miyagi Prefecture further south) where the over-65s make up only 18.25% of the population (MIAC, 2011a). This can be compared with the mean fatality rates (using data from the same towns) of 6.92% in the rias coastline and 3.51% in the coastal plains (FDMA, 2011b; MIAC, 2011b).

Table 5.8 shows a breakdown of the causes of death (Japan Times, 2011) as reported on 21st April when the number of confirmed deaths was 13,135. In the three worst-affected Prefectures, the percentages of those that died from drowning were a little varied: the highest was 95.7% in Miyagi-ken, 87.3% in Iwate-ken and 87.0% in Fukushima-ken (The Japan Times, 2011).

Table 5.8 Causes of death from the M_w9.0 Tōhoku earthquake and tsunami (The Japan Times, 2011).

Cause of death	Number of victims	% of victims
Drowning	12,143	92.5%
Burns	148	1.1%
Crushed/died of injuries	578	4.4%
Unknown	266	2.0%
Total	13,135	100%

Whilst there are other factors to take into account such as arrival time of the tsunami, inundation height and velocity, and distance of population centres from the coast, age clearly played a role in the fatalities in this event. Age distribution of 11,080 identified victims is shown in Figure 5.13 (The Japan Times, 2011 and Jiji, 2011). Of the 11,080 victims, 65.2% are aged 60 or older, indicating the disproportionately large number of elderly victims, with an increased proportion of each group with increasing age. This distribution may be partially due to the time of the event: had this event occurred when younger people were not at school (which tend to be multi-storey concrete buildings) or when families were at home and able to help elderly relatives evacuate, a more equal fatality distribution might have emerged. As of 11th April 5,971 of the 13,135 had been identified as male and 7,036 female. Due to injuries sustained it was not possible to identify the gender of 128 victims.

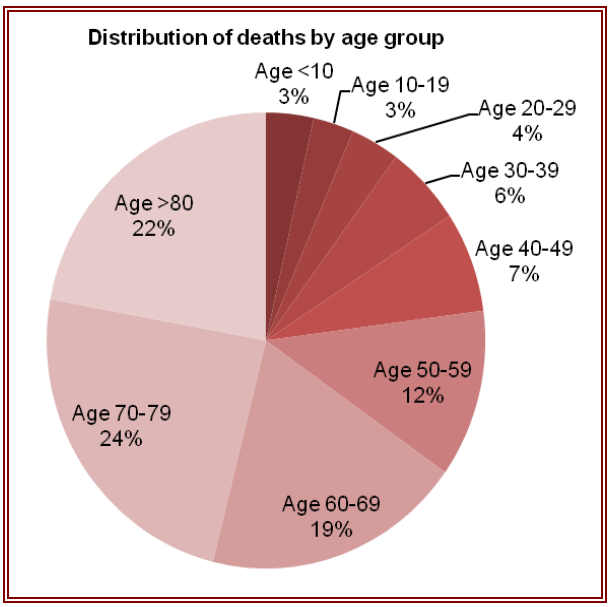

Figure 5.13 Distribution of victims" ages, where this could be identified (The Japan Times, 2011 and Jiji, 2011).

As reported by Yomiuri Online (2011), since the earthquake and tsunami a further 282 people have died whilst living in the emergency shelters. Deaths are possibly linked to trauma following the event, the stress of living in the shelters and the cold weather. Causes of death include respiratory disease and suicide.

5.6. Conclusions on the 11th March 2011 tsunami and its impact

Japan has a long history of deadly tsunami waves: in recent history the 1896 Meiji-Sanriku tsunami killed 22,000 and the 1933 Showa Sanriku tsunami killed 3,064. The 1896 tsunami, in particular,

informed the design of coastal defences and the evacuation plans which were intended to guide people to safe locations.

Data from GPS buoys situated off the coastline at a number of locations were the first indication that the initial predictions of a 3 m to 6 m tsunami were inadequate. In these offshore locations the wave had already registered a magnitude of the order of 5-6 m even before the amplifying effect of the coastline. Warnings of higher waves were then given, but not until the tsunami was reaching the Sanriku coastline. The GPS buoys showed a total of seven waves over a period of six hours. Tide gauges along the shoreline were mostly destroyed and only a few remained operational, but failed at the highest point of the wave, registering waves of the order of 8 m or more above the current tide level.

The maximum inundation height of 40.545 m recorded at Omoe Aneyoshi in Miyako district broke the previous highest inundation height recorded at Ryori Bay, Iwate prefecture due to the 1896 event. Overall, the run-up heights were considerably higher than the last two major tsunami events of 1933 and 1896.

More than 500 km^2 of land was inundated and at places the waves travelled up to 7 km inland. Many areas were left under water for weeks. The effects of the tsunami were felt around the Pacific Ocean as far away as Russia, the west coast of the US and Chile as waves of more than 2 m hit coastlines.

The areas of Japan most badly hit were Iwate, Miyagi, Fukushima and Ibaraki Prefectures. Damage statistics at 8th November 2011 (NPA, 2011) state that in these 4 prefectures, over 118,000 houses suffered total collapse. Over 176,000 houses were seriously damaged and a further 480,000 partially damaged by the tsunami waves. At least 45,000 non-residential buildings were damaged (overwhelmingly by the tsunami). Permanent coastal subsidence in some regions now results in flooding during high tides.

As of 11th October 2011, 19,685 people are known to have died or are still missing (FDMA, 2011). The highest death rate among the estimated population in the inundation zone reached 13.5% in Otsuchi, Iwate prefecture. The elderly (over 65) made up the largest proportion of fatalities. They also made up the largest proportion of the population in the rias coastline (28% vs. the national rate of 20%) where the death rate was higher than in the coastal plains where the tsunami arrived 30 to 60 minutes later (6.3% vs. 3.0% death rate). The vast majority (92.5%) of the people that died were drowned, and the numbers of female casualties outnumbered the males.

It is worth noting that when compared to the 1896 tsunami, though the numbers of casualties are similar, the wave that struck the north-east of Japan on March 11th 2011 was of far greater size and therefore had the potential to be far more deadly. It is a testament to the coastal defence measures, the evacuation procedures and the preparedness of the Japanese population that so many in fact survived.

5.7. References

@disaster_i, 2011. 牛山素行, 9 May, [image online] Available at: <http://twitpic.com/4veg66> [Accessed 5 July 2011].

Asahi, 2011. Islanders cut off from mainland due to tsunami The Asahi Shimbun [online] 29 March 2011. Available at: http://www.asahi.com/english/TKY201103280148.html [Accessed 29 July 2011].

CEDMHA, 2011. *Japan Earthquake and Tsunami Update Wednesday, March 30, 2011*, Centre for **Excellence in** Disaster Management & Humanitarian Assistance [online]. Available at: <http://www.coe-dmha.org/Research/ResearchInfoMgmt/Japan/Japan03302011.pdf > [Accessed 27th July 2011].

Daily Yomiuri, 2011. *Tsunami reached record 40.4 meters in Miyako* Daily Yomiuri [online]. Available at: <http://www.yomiuri.co.jp/dy/national/T110717002475.htm> [Accessed 27 July 2011].

ERI, 2011. *Tsunami survey*, Earthquake Research Institute, The University of Tokyo [image online]. Available at: <http://outreach.eri.u-tokyo.ac.jp/eqvolc/201103_Tōhoku/eng/> [Accessed 27 July 2011].

FDMA, 2011a. *FDMA Report 140*, Fire and Disaster Management Agency of Japan. October 11, 2011 Fire and Disaster Management Agency (in Japanese).

FDMA, 2011b. *FDMA Report 132 on the effects of the March 11, 2011 Great Tōhoku earthquake*, Fire and Disaster Management Agency of Japan. July 14, 2011. Available at: <http://www.fdma.go.jp/bn/2011/detail/691.html> [Accessed on 15 July 2011].

FEMA, 2008. *Guidelines For Design Of Structures For Vertical Evacuation From Tsunamis,* FEMA P646 [online] Available at: <http://www.fema.gov/library/viewRecord.do?id=3808> [Accessed 27 July 2011].

Fujita T., 2011. *Tsunami impacting Eastern Japan and Preparedness for Extraordinary Disaster*. (Presentation, 25 May) Available at: <http://www.pari.go.jp/en/files/items/3733/File/2011052327IAPH.pdf> [Accessed 28 July 2011].

GSI, 2011. *Inundation extent maps*, Geospatial Information Authority of Japan (in Japanese) [online]. Available at: <http://www.gsi.go.jp/kikaku/kikaku60003.html> [Accessed 27 July 2011].

Herbich, J.B., 2000. *Handbook of Coastal Engineering*, McGraw-Hill.

Horikawa, K., 2000. History of Coastal Engineering in Japan. In: P. L.-F. Liu, ed. *Advances in Coastal and Ocean Engineering - Vol. 6*. World Scientific. Ch. 1. Available through: <http://ebooks.worldscinet.com/ISBN/9789812797537/9789812797537.html> [Accessed 27 July 2011].

Jiji, 2011. 犠牲者、６０歳以上が６５％＝津波で逃げ遅れ、水死９割－東日本大震災の３県分析 (in Japanese) [online]. Available at: <http://www.jiji.com/jc/zc?k=201104/2011041900708> [Accessed 27 July 2011].

JMA, 2011a. *The 2011 off the Pacific coast of Tōhoku Earthquake -Portal-* [online] Available at: <http://www.jma.go.jp/jma/en/2011_Earthquake.html> [Accessed 27 July 2011].

JMA, 2011b. *JMA monthly report for earthquakes and volcanoes, 2011* (in Japanese) [online]. Available at: <http://www.seisvol.kishou.go.jp/eq/gaikyo/monthly201103/20110311_Tōhoku_1.pdf> [Accessed 27 July 2011].

JMA, 2011c. *The 2011 off the Pacific coast of Tōhoku Earthquake Observed Tsunami* [online]. Available at: <http://www.jma.go.jp/jma/en/2011_Earthquake/2011_Earthquake_Tsunami.pdf> [Accessed 27 July 2011].

JMA, 2011d. 「宮古」，「大船渡」の津波観測点の観測値について (in Japanese) [image online]. Available at: <http://www.jma.go.jp/jma/press/1103/23b/stn03231400.pdf> [Accessed 27 July 2011].

JMA, 2011e. *Higher Risks of Tide Inundations during Summer to Fall 21 June 2011* [online]. Available at: <http://www.jma.go.jp/jma/en/News/Tide_Calendar.html> [Accessed 27 July 2011].

JSCE, 2011. *Tōhoku Earthquake Tsunami Information: The 2011 Tōhoku Earthquake Tsunami Joint Survey Group,* Coastal Engineering Committee of the Japan Society of Civil Engineers [image online] Available at: <http://www.coastal.jp/ttjt/index.php?%E7%8F%BE%E5%9C%B0%E8%AA%BF%E6%9F%BB%E7%B5%90%E6%9E%9C> [Accessed 27 July 2011].

Kazama, M., 2011. *The 2011 off the Pacific Coast of Tōhoku Earthquake – After two months.* In: 14th Asian Regional Conference on Soil Mechanics and Geotechnical Engineering [online]. Available at: <http://www.jiban.or.jp/file/file/kazama520e2.pdf> [Accessed 27 July 2011].

Kokusai Kogyo Group, 2011. Characteristics of Japan"s DRR: A perspective from the spatial information sector, In: UN ISDR, *Third session of the Global Platform for disaster risk reduction* Geneva, May 2011.

MIAC, 2011a. Ministry of Internal Affairs and Communications – Statistics Bureau, Director-General for Policy Planning (Statistical Standards) & Statistical Research and Training Institute. Information on the Great East Japan Earthquake. Basic Complete Tabulation on Population and Households of Iwate, Miyagi and Fukushima prefectures. Available at:<http://www.e-stat.go.jp/SG1/estat/NewListE.do?tid=000001039448> [Accessed on: 15 June 2011].

MIAC, 2011b. Ministry of Internal Affairs and Communications – Statistics Bureau, Director-General for Policy Planning (Statistical Standards) & Statistical Research and Training Institute. Information on the Great East Japan Earthquake. Population of the inundation area analyzed and estimated based on the information provided by the GSI on 18 April, 2011. Available at: <http://www.stat.go.jp/info/shinsai/zuhyou/sinsui.xls> [Accessed on 15 June 2011].

MLIT, 2011. *Ports and Harbours in Japan* [online]. Available at: <http://www.mlit.go.jp/english/2006/k_port_and_harbors_bureau/17_p_and_h/index.html> [Accessed 27 July 2011].

NHK, 2011a. Nippon Hōsō Kyōkai (Japan Broadcasting Corporation) March 26 2011 [online]. Available at: <http://www.nhk.or.jp/> [Accessed 27 July 2011].

NHK, 2011b. Nippon Hōsō Kyōkai (Japan Broadcasting Corporation) March 29 2011 [online]. Available at: <http://www.nhk.or.jp/> [Accessed 27 July 2011].

NOAA, 2011a. *West Coast/Alaska Tsunami Warning Center, NOAA/NWS TSUNAMI of 11 March, 2011 (Honshu, Japan)* [online]. Available at: <http://wcatwc.arh.noaa.gov/previous.events/03-11-11_Honshu/03-11-11.htm> [Accessed 27 July 2011].

NOAA, 2011b. *West Coast/Alaska Tsunami Warning Center, NOAA/NWS TSUNAMI of 9 March, 2011 (Honshu, Japan)* [online]. Available at: <http://wcatwc.arh.noaa.gov/previous.events/03-09-11/03-09-11.htm> [Accessed 27 July 2011].

NOAA, 2011c. West Coast/Alaska Tsunami Warning Center, *NOAA/NWS TSUNAMI of 7 April, 2011 (Near East Coast of Honshu, Japan)* [online]. Available at: <http://wcatwc.arh.noaa.gov/previous.events/04-07-2011/04-07-11.html> [Accessed 27 July 2011].

NPA, 2011. *Damage Situation and Police Countermeasure, 8 November 2011* [online]. Available at: <http://www.npa.go.jp/archive/keibi/biki/higaijokyo_e.pdf> [Accessed 9 November 2011].

Okumura, K., 2011. *Interplate megathrust earthquakes and tsunamis along Japan Trench offshore Northeast Japan*, Hiroshima University, Japan [online]. Available at: <http://www.homeofgeography.org/uk/news_2011/jogan_e.pdf> [Accessed 27 July 2011].

PARI, 2011a. *Executive Summary of Urgent Field Survey of Earthquake and Tsunami Disasters March 25, 2011* [online]. Available at: <http://www.pari.go.jp/en/eq2011/20110325.html> [Accessed 27 July 2011].

PARI, 2011b. *An English Abstract of the Technical Note of Port and Air Port Research Institute, No. 1231, April 28, 2011. Urgent Survey for 2011 Great East Japan Earthquake and Tsunami Disaster in Ports and Coasts – Part I (Tsunami)* [online]. Available at: <http://www.pari.go.jp/en/files/3653/460607839.pdf> [Accessed 27 July 2011].

PARI, 2011c. 津波は三陸沿岸で7波襲来-釜石沖GPS波浪計のデータ回収・分析結果- (in Japanese) [image online]. Available at: <http://www.pari.go.jp/info/Tōhoku-eq/20110328mlit.html> [Accessed 27 July 2011].

PARI, 2011d. *Tsunami Impacting Eastern Japan and Preparedness for Extraordinary Natural Disaster, May 25, 2011* [online]. Available at: <http://www.pari.go.jp/files/items/3459/File/2011052327IAPH.pdf> [Accessed 27 July 2011].

PARI, 2011e. *Technical Note of Port and Air Port Research Institute, No. 1231, April 28, 2011. Urgent Survey for 2011 Great East Japan Earthquake and Tsunami Disaster in Ports and Coasts* (in Japanese) [online]. Available at: <http://www.pari.go.jp/files/3642/1049951767.pdf> [Accessed 27 July 2011].

PWRI, 2008. *Comprehensive Tsunami Disaster Prevention Training Course*, November 2008 ISSN 0386-5878 Technical Memorandum of PWRI No.4114 [online]. Available at: <http://www.preventionweb.net/files/9285_isdrtsunamieng.pdf> [Accessed 27 July 2011].

Sankarbabu, K. Sannasiraj, S.A. and Sundar, V., 2008. *Hydrodynamic performance of a dual cylindrical caisson breakwater*. Coastal Engineering 55: 431–446.

Shaw, R. Parashar, S. Uy, N. Nguyen, H. Fernandez, G. Mulyasari, F. and Joerin, J., 2011. *Mega disaster in a resilient society: The Great East Japan (Tōhoku Kanto) Earthquake and Tsunami of 11th March 2011*, International Environment and Disaster Management Graduate School of Global Environmental Studies, Kyoto University [online]. Available at: <http://www.iedm.ges.kyoto-u.ac.jp/report/2011/IEDM%202%20Week%20Report%20Japan%20EQT.pdf> [Accessed 27 July 2011].

Statistics Bureau, 2005. *Population Census* (in Japanese) [online]. Available at: <http://www.stat.go.jp/> [Accessed 27 July 2011].

Takata, N., 2009. *Tsunami disaster reduction in Japanese ports and harbors*. Proc 6th Intl. Workshop on Coastal Disaster Prevention, Bangkok, Thailand, December 2009 page 93.

The Japan Times, 2011. 90% of disaster casualties drowned *The Japan Times* [online] April 21 2011. Available at: <http://search.japantimes.co.jp/cgi-bin/nn20110421a5.html> [Accessed 27 July 2011].

The 2011 Tōhoku Earthquake Tsunami Joint Survey Group, 2011. *Survey Results – Uniform Survey Data* (data online] (ttjt_survey_15-Jul-2011_tidecorrected.csv). Available at: <http://www.coastal.jp/ttjt/index.php?%E7%8F%BE%E5%9C%B0%E8%AA%BF%E6%9F%BB%E7%B5%90%E6%9E%9C> [Accessed 28 June 2011] (in Japanese).

UNESCO, 2011a. *IOC/UNESCO Bulletin No. 8, 23 March 2011* [online]. Available at: <http://www.eqclearinghouse.org/2011-03-11-sendai/files/2011/03/No.-8-IOC-UNESCO-Bulletin-23-Mar.pdf> [Accessed 27 July 2011].

UNESCO, 2011b. *IOC/UNESCO Bulletin No. 6, 21 March 2011* [online]. Available at: <http://www.eqclearinghouse.org/2011-03-11-sendai/files/2011/03/No.-6-IOC-UNESCO-Bulletin.pdf> [Accessed 27 July 2011].

UNOCHA, 2011. *Japan Earthquake & Tsunami Situation Report No. 6, 17 March 2011* [online]. Available at: <http://reliefweb.int/sites/reliefweb.int/files/resources/8353B696BD3AF80CC12578560045B420-Full_Report.pdf> [Accessed 27 July 2011].

US Army, 2011. *Monday 28th March 2011 REPORT #SOR-014-11* [online] Japan Asian Studies Centre of Excellence. Available at: <https://community.apan.org/hadr/japan_earthquake/b/updates/archive/2011/03/28/asd-japan-earthquake-tsunami-update-report-sor-014-11.aspx> [Accessed 27 July 2011].

USGS, 2011. *Pre-tsunami Japan: 2010 Ryori, Iwate Prefecture* [online]. Available at: <http://walrus.wr.usgs.gov/tsunami/japan/ryori.html> [Accessed 27 July 2011].

Yomiuri Online, 2011. 避難所の不衛生、寒さ…震災関連死疑い２８２人 (in Japanese) [online]. Available at: <http://www.yomiuri.co.jp/national/news/20110411-OYT1T00610.htm> [Accessed 27 July 2011].

6. Field observations on tsunami damage to coastal defence structures

6.1. Introduction

Following the 11th March tsunami, a total of 14 major ports were affected by the earthquake and an estimated length of 8,500 m of breakwaters protecting ports and harbours collapsed (PIANC, 2011). The design forces used were inadequate for this size of tsunami, often derived using the assumption of 5 m waves (Aydan, 2011). Quay walls, designed as earthquake resistant structures faired a little better than breakwaters though some suffered settlement or inclination, sometimes due to liquefaction (PIANC, 2011). Further evidence of the destructive power of the tsunami waves is that scour holes of greater than 10 m depth have been observed at some breakwaters on the mouths of bays (PARI, 2011b).

The general failure mechanisms of the coastal defences fall into four categories: (i) scour due to strong current (most typical failure mechanism) (ii) hydrostatic force due to pressure differential between back and front walls (iii) impulsive breaking wave force, and (iv) hydrodynamic (drag) force on armour stones/blocks (PARI, 2011b).

Members of the EEFIT team visited a number of sites to assess coastal structures, as shown in Figure 6.1. The town of Fudai beyond the northern reach of the EEFIT survey area is also included in this chapter as the findings from this location are very important.

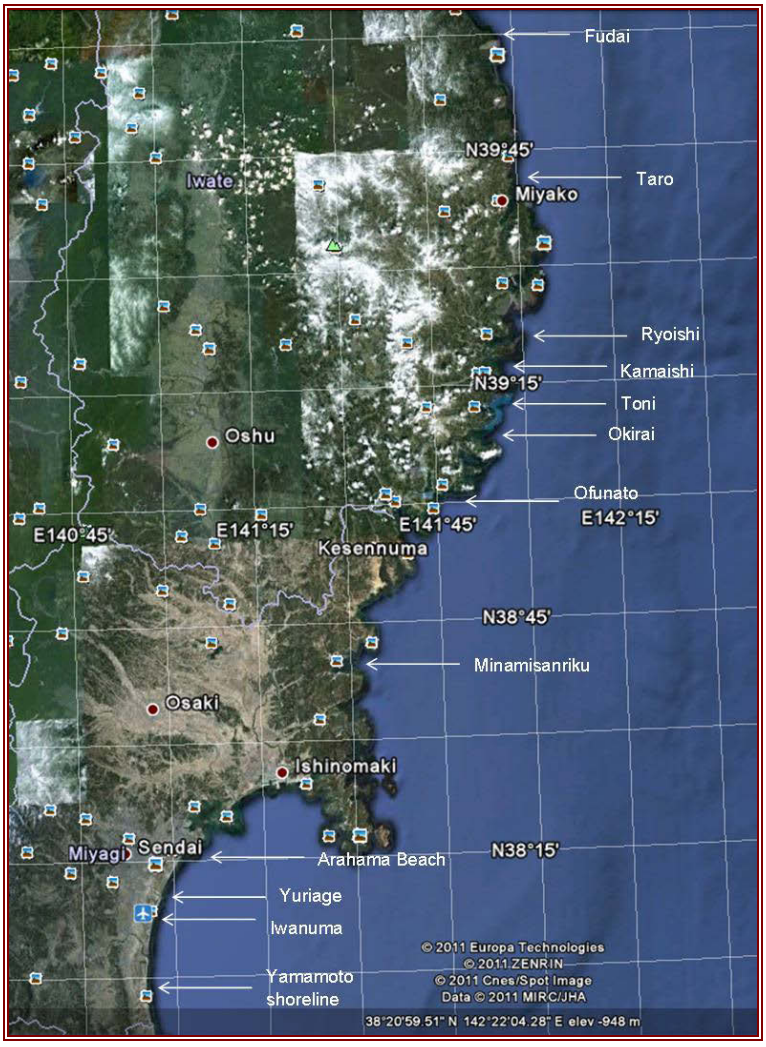

Figure 6.1 Locations with significant coastal structures (image source: Google Earth).

6.2. Offshore breakwaters

Kamaishi

The port of Kamaishi, Iwate Prefecture was home to the deepest breakwater in the world. Construction was finished in 2009 and it entered the Guinness Book of Records in 2010 and the History Book of PIANC (PIANC, 2011). Its deepest stone foundation was at a depth of 63 m. The freeboard of the breakwater was 6 m and there was a north section of 990 m length and a south section of 670 m in length, with an opening of 300 m (Figure 6.2).

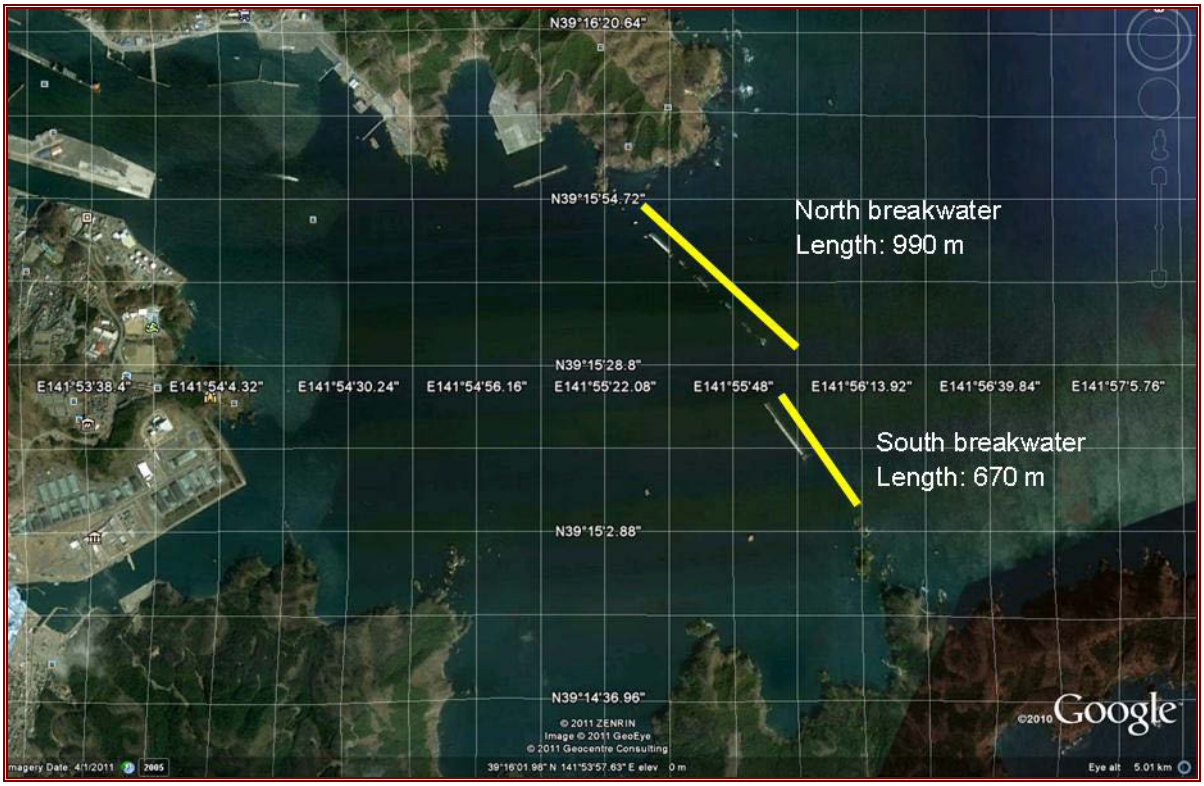

Figure 6.2 Location of the Kamaishi Bay breakwaters. The positions of breakwaters are indicated by yellow lines, which have been offset slightly to the east in order to show the post-tsunami state of the structures.

The breakwater was designed to protect against tsunami waves typical of the 1896 Meiji-Sanriku tsunami (i.e. 5 m to 6 m), and also for protection against storm waves. The tsunami of 11th March, being of a much greater magnitude, overturned the north section of the breakwater and though the south section survived mostly intact it was left inclined.

Consideration has been given to the failure mechanism of the breakwater. The Port and Harbor Research Institute (PARI) have run numerical simulations and have predicted that the tsunami height was 8-10 m on its offshore face but only 2-6 m on the lee side. This difference in water depth created a large difference in pressure on the two faces with a resulting large hydrostatic force. Added to this was the scour caused by flow between the roughly 30 cm gaps between the blocks of the breakwater leading to catastrophic collapse or slump (Kazama, 2011).

However, despite the fact that the breakwaters were severely damaged it has been argued that their role was extremely important in reducing damage due to the tsunami. Video records suggest that the breakwater was intact until the peak of the first wave. Based upon GPS records from the closest location, 18 km off the coast, PARI (2011b) ran simulations which showed that the breakwater reflected energy of its offshore face before being destroyed, and estimate that it a) reduced the height of the tsunami from 13.7 m to 8 m (a 40% reduction); and b) delayed by 6 minutes the arrival time of the 4 m wave height, allowing more time for evacuation. Also, PARI (2011c) estimate that the run-up level was reduced from a potential 20.2 m to 10 m. Despite this, Kamaishi municipality (comprising Kamaishi City, Ryoishi, Kariyado, Heida, Kojirahama, Kerobe and other coastal settlements) suffered

the fourth worst fatality rate among all the tsunami affected municipalities (8.2% of the population estimated to have been living in the tsunami inundation zone was either killed or missing, based on the FDMA report no. 140 issued on 11th October 2011). We currently do not have the spatial distribution of fatalities within Kamaishi municipality, but a false sense of security provided by the tsunami breakwaters could potentially have been a factor for a number of deaths in Kamaishi City.

Ōfunato

The port of Ōfunato, Iwate Prefecture was very badly damaged by the 1960 Chilean tsunami and as a result tsunami breakwaters were built at the entrance to the bay (Murata et al., 2010). Unfortunately the entire combined 540 m length of breakwaters has collapsed (PIANC, 2011). The breakwater caissons were observed to have shifted before the peak of the tsunami (PARI, 2011b) and were left scattered in the bay after the event. Furthermore, 1 m deep settlement of the quay walls occurred (PIANC, 2011). The low freeboard on the quay walls can be seen in Figure 6.3.

Figure 6.3 Quayside at Ōfunato City, showing limited freeboard of the quay walls

6.3. Concrete seawalls

Tarō

Tarō, Iwate Prefecture, is a coastal fishing village (population: approximately 5,000) of social and engineering significance, famous for its tsunami defences, and nicknamed Tsunami-Tarō (Honda, 2011). According to the UN/ISDR team that visited in 2008, the municipal slogan of the town is “The Town of Tsunami Disaster Prevention” (PWRI, 2008). As a result of two large tsunami of the Meiji (1896) and Showa (1933) periods that destroyed the town, residents made strong representations to the Ministry of Land and the Ministry of Fisheries for tsunami defences. These were rejected and instead the town was asked to move to higher ground. However, the residents refused and instead borrowed money and started construction of the defences themselves. Other villages in the Sanriku area had no defences. After some years, the ministries and the Iwate Prefectural government agreed to assist and supported the construction. The wall is 1,350 m in length and built to 10.7 m above mean water level (Smits, 2011). As a result, Tarō had a seawall of sufficient strength, nicknamed "The Great Wall" (Figure 6.8), completed in 1958 and effective against the 1960 Chilean earthquake tsunami, while elsewhere on the Sanriku coast the 1960 tsunami reached up to 3 m above high tide, killing 142 people.

There exists a second layer of tsunami defence in this town, built when development started outside of the Great Wall. There were two periods of construction: from 1962 to 1967 a 582 m length of wall and from 1972 to 1978 a 501 m long section. A remote-controlled gate was also built during this second period (Smits, 2011).The concrete sections were apparently without reinforcement or interlocking blocks and had sand infill (Figure 6.4). As a result, despite their enormous size (approx. 10 m height) they were almost all toppled from their positions. The only part of the newer wall left standing were some buttress supports (Figure 6.5) and the sections around the gates (Figure 6.6 and Figure 6.7).

Outside the Great Wall there was utter devastation (Figure 6.8). The waves in fact overtopped the Great Wall but the extra defence provided some reduction in overtopping and certainly reduced the level of damage. Substantial resources were being devoted to the clear-up operation when we visited, which may be indicative of the strong links the village has with local government.

In Tarō the offshore breakwater also showed signs of severe damage as shown in Figure 6.9 and Figure 6.10.

Figure 6.4 Unreinforced concrete interlocking blocks and sand infill of the sea wall at Tarō.

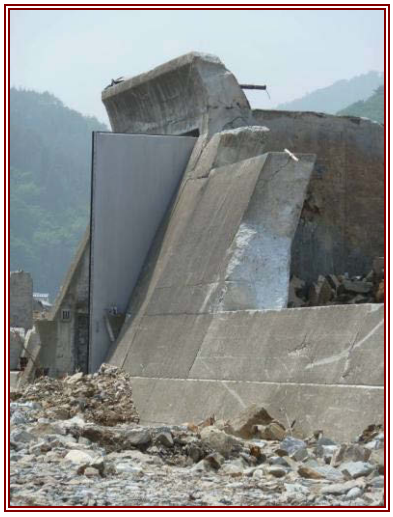

Figure 6.5 (left) Remaining buttress supports around a tsunami gate in the sea wall at Tarō.

Figure 6.6 (right) Tsunami gate that remained intact in the seawall at Tarō.

Figure 6.7 (left) A surviving gate structure and buttresses in Tarō. The seawall has been destroyed either side of this gate.

Figure 6.8 (right) Devastation seaward of the „Great Wall" in Tarō.

Figure 6.9 (left) Offshore breakwater in Tarō, visible from the shore.

Figure 6.10 (right) Parts of the breakwater lying in the bay at Tarō.

Minamisanriku

The coastal structures of Minamisanriku, Miyagi Prefecture suffered extensive damage. The main defences for the town appear to have consisted of a wall and a tsunami gate across each of the three rivers; north to south, these are the Niida River, Hachiman River and Mizushiri River. The collapsed wall is shown in Figure 6.11a to Figure 6.11d. Again, there was evidence of inadequate interlocking of adjacent blocks, relying instead on self-weight for stability. This may have been effective had the tsunami been of a similar size to the 1960 tsunami, but not for this latest event.

Ryoishi

Close to the centre of this town, whole sections of a large concrete wall were displaced as shown in Figure 6.12. This photograph was taken from a vehicle and it was not possible to get a closer look at the concrete units.

(a) (b)

(c) (d)

Figure 6.11 Failure of the Minamisanriku seawall (a) failure of end section (b) end block close-up (c) view along crest of wall (d) submerged blocks.

Figure 6.12 Toppled concrete blocks from the seawall in Ryoishi.

6.4. Concrete block revetment

Yamamoto-cho

The shoreline of Yamamoto-cho, Miyagi Prefecture comprised a gentle sloped beach, some large periodically placed groynes and a concrete block revetment behind which were pine trees. Both sides of the revetment comprised a concrete lattice, block infill and a sand core with a concrete pathway on top (Figure 6.13).

At several locations along the wall there were breaks in the lattice and most of the concrete blocks had „popped out". It was surmised that a pressure wave may have passed through the sand infill leading to the blocks being ejected. Breaks in the lattice are shown in Figure 6.14. Reinforcement bars were evident in the lattice: four per connecting member. There was significant wash-out of the sand core as can be seen in Figure 6.14d. This image also shows how the original leeward side might have looked with stone infilling the concrete blocks and vegetation growing in the cracks. The scouring on the leeside is one of the main causes of embankment failures (Kazama, 2011). Just a few metres north the seawall had failed catastrophically, as shown in Figure 6.15.

A gently-sloping beach and a groyne are located seaward of the revetment. These are shown in Figure 6.16. The groyne appeared largely intact and was constructed of slim concrete armour units aligned with the slope and with protective concrete armour units.

Further north along the beach, where the seawall had disappeared there were extensive „debris fields" comprising large blocks of seawall and wave dissipating units (Figure 6.17). The photographs show pine forest to the left and sea to the right; the water in the left of both shots lies in land that is lower than the beach level. The effect of the tsunami on the morphology of this beach is not known.

(a) (b)

Figure 6.13 Concrete block revetment at Yamamoto-cho: (a) leeward side showing vegetation and blocks (b) view along the crest.

(a) (b)

(c) (d)

Figure 6.14 Inland side of concrete block revetment at Yamamoto-cho. (a) to (c): Breaks in the lattice revetment. (d): Sand in-fill wash-out.

(a) (b)

Figure 6.15 Catastrophic failure of the concrete block revetment at Yamamoto-cho.

Arahama

Slightly further north up the coast was Arahama beach which had defences similar to those on the Yamamoto shoreline though the concrete blocks were of a different form (Figure 6.18). The revetment had again failed in places; the concrete blocks were thrown larger distances from the wall – up to 100

m into the coastal forest. The failure mechanism also looked very similar, with the sand infill being washed out (Figure 6.19).

(a) (b)

Figure 6.16 Groyne structure at Yamamoto-cho, (a) with beach in foreground (b) close-up of armour units.

(a) (b)

Figure 6.17 Coastal structure debris on beach at Yamamoto-cho (sea to the right of both shots) (a) along the length of the beach (b) close-up showing concrete sections.

Figure 6.18 (left) Seaward side of concrete block revetment at Arahama Beach.

Figure 6.19 (right) Collapse of revetment at Arahama Beach due to sand fill being washed out.

The mitigating impact of the revetment can be seen in aerial photographs where the coastal forest located behind the defence has suffered less damage than the portion with no defence in front (Figure 6.20). Where the sea wall is present on the beach, the coastal forest at and inland of the channel appears to have suffered less damage from the tsunami flow with some areas of vegetation surviving post-tsunami.

Figure 6.20 Apparent mitigating influence of the sea wall at Arahama Beach.

6.5. Tsunami sluice gates

There are a number of locations where very large gates have been built on rivers. The structures have movable sluice gates to allow normal river flow but can be closed in the event of a storm surge or tsunami. In a number of locations we found undamaged gates, evidently fit for purpose, though some were not quite so successful.

Fudai

One of the great success stories of the Tōhoku Earthquake was the effectiveness of the tsunami gates in the town of Fudai (Figure 6.21). Following the disastrous tsunami waves of 1896 and 1933 when 439 people died a 15.5 m high seawall was built, with the idea for the construction driven forward by the late mayor, Kotaku Wamura. This seawall was to shield homes of the fishing port. Construction was completed in 1967. However, the mayor regarded the defences as unfinished, insisting that floodgates of the same height should be built on the Fudai River. The cost of the scheme and the necessary enforced land purchase made it an unpopular decision, but nevertheless it went ahead in 1972 and was completed in 1984, 3 years before the end of the mayor"s 40 years in office. The gates span 2005 m and cost a total of ¥3.56 bn which was borne by the local and national governments.

When the earthquake struck on 11th March the four main gates were closed remotely, though the smaller side gates needed to be closed by hand as they had jammed. The run-up level of the tsunami was measured at 20 m on the floodgate towers. The town suffered a little damage, though compared with the devastation around similar coves, it was fairly insignificant. Unfortunately, the exposed port on which many livelihoods depend was badly affected.

Figure 6.21 Tsunami sluice gates at Fudai. Notice the man walking along the top of the wall for scale (Komo News, 2011).

Miyako Bay

At the southern end of Miyako Bay there were completely undamaged gates on the Tsugaruishi River as shown in Figure 6.22.

(a) (b)

Figure 6.22 Tsunami gates on the Tsugaruishi River in Miyako Bay.

Ryoishi

Undamaged tsunami gates were observed in the southern part of Ryoishi Bay (Figure 6.23).

Minamisanriku

This location has been previously mentioned for its damaged seawall (see Figure 6.11), but its two tsunami gates also suffered damage as can be seen in Figure 6.24 and Figure 6.25.

Tarō

In addition to Tarō's famous seawalls (see Figure 6.4 to Figure 6.8) are tsunami sluice gates, shown in Figure 6.26. These appeared undamaged from the location where this photograph was taken.

Figure 6.23 (left) Tsunami gates to the south of Ryoishi.

Figure 6.24 (right) Damaged tsunami gates at the mouth of the Hachiman River, Minamisanriku.

Figure 6.25 Damaged tsunami gates on the Mizushiri River in Minamisanriku.

Figure 6.26 Tsunami sluice gate and collapsed wharf at Tarō.

6.6. Natural vegetation

Natural vegetation is one of the „soft engineering" approaches that may be taken in coastal protection. The planting of pine forests as a method of tsunami protection has been undertaken in Japan for at least 15 years (Dengler, 2011). Their efficacy was tested in this tsunami.

Yamamoto-cho

As already mentioned in the concrete revetment section the Yamamoto-cho shoreline has pine forests on the leeward side of the revetments. It was necessary to walk through the small forest of trees to approach the revetment at a location where reconstruction was not taking place. It was clear to see that the pine trees were largely destroyed by the tsunami: they had bent over and snapped very close to their base (Figure 6.27). The coastal forest, where destroyed, provides substantial amounts of debris which was seen to cause structural damage to a steel frame building almost 1 km inland where a whole pine tree trunk had impacted on the steel columns (section 7.2.11).

(a) (b)

Figure 6.27 Pine trees of the coastal forest at Yamamoto-cho, flattened by onshore tsunami flow.

Vegetation was also evidently part of the structure of the revetment (see Figure 6.14 and Figure 6.18), with small trees growing in the cracks, but it is likely that a roughness layer of this magnitude would be completely ineffective at reducing energy, and is more likely planted for aesthetics and to bind the infill material of the defence.

Rikuzentakata

PARI (2011b) reported that the tsunami had the effect of removing the coastal forests and the sandy beaches themselves in this location.

6.7. River protection

Iwanuma

Iwanuma is situated south of Natori, on the Abukama River. Images taken during the inundation of this area show the wave moving across the low-lying land and crossing the river with the channel providing little resistance, though the embankments disrupt the flow a little. There are no sluice gates at the entrance of this river, but the river meanders quite dramatically and it is probably not the case that a gate would make any difference in this coastal plain situation as the wave would merely pass around it.

Yuriage

Along the Natori River in Yuriage there was evidence of damage from the tsunami overtopping river defences, as seen in Figure 6.28.

(a) (b)

(c)

Figure 6.28 Damage to river defences on the south side of the Natori River in Yuriage.

6.8. Coastal Subsidence

Onagawa

There was extensive damage in this bay, but there were no obvious coastal defences in the harbour and only a low harbour wall at the mouth of the bay. Figure 6.29 shows the bay viewed from the raised hospital car park during the tsunami inundation. The EEFIT survey photograph (Figure 6.30) is taken from a slightly different location on 2nd June 2011 (behind the red-brick building) but it is striking how much of the buildings in centre frame of the lower picture were engulfed in the wave as shown by the top picture. The inundation depth of more than 18 m was measured in Onagawa (PARI, 2011a).

The coastal area around Onagawa also suffered from approximately 1.2 m of subsidence. As a result of this the shoreline is now subject to flooding at high tide. Figure 6.31 shows the incoming tide engulfing the quay road.

Figure 6.29 Onagawa Bay during the tsunami. Photograph courtesy of Koji Shudo (Eastern Miyagi Prefecture Civil Engineering office) and Akihito Morikawa (Miyagi Prefecture Civil Engineering office).

Figure 6.30 (left) Onagawa bay on 2nd June 2011. Photograph taken from hospital car park on raised 16 m platform.

Figure 6.31 (right) Inundation of the quay in Onagawa at high tide, as a result of 1.2 m co-seismic subsidence.

6.9. Conclusions on tsunami damage to coastal defence structures

Damage on an almost unimaginable scale has been caused to the coastal defence structures along the north-east coast of Japan: in total 8,500 m of breakwaters collapsed. These included the Kamaishi tsunami breakwater, finished in just 2009 and the world"s deepest breakwater designed to withstand a tsunami, but not of the size that occurred on 11th March 2011. However, it is reported that tsunami breakwaters delayed the tsunami arrival, giving valuable extra time for evacuation. Also they reduced the height of the wave, even where the structures ultimately collapsed.

The famous „Town of Tsunami Disaster Prevention", Tarō, saw the catastrophic loss of one of its tsunami seawalls though the inner wall, the so-called „Great Wall" survived and gave partial protection to most of the town.

In several locations it was evident that blocks forming seawalls did not have any lateral connections, the absence of which inevitably contributed to failure. Failures of concrete revetments along the coastal plains were also observed; here, due to the effect of scour on the leeside.

Many tsunami gates, designed to reduce tsunami inundation along rivers, were observed, and most had survived intact, though it was evident that the largest waves had overtopped the barriers. Where the barriers had been built to a considerable height, e.g. 15.5 m in the village of Fudai, there was more success in reducing the overtopping.

There was evidence, in some places, of the positive effects of planted pine trees in reducing damage inland, though there were also many examples of trees that were snapped off at the base of the trunk and transformed into missiles, puncturing the sides of buildings.

There is understandably considerable reflection on the part of Japanese coastal engineers after the events of 11th March 2011. Japan was seen as a world leader in tsunami defence solutions and in some situations they performed successfully. More often than not however, the defences were not adequate to withstand a wave of this magnitude.

Some initial thoughts that are being expressed are that standards and stability performance should be investigated further for worst case scenarios (PARI, 2011b). In addition to revision of standards, coastal engineers are suggesting changes to behaviour i.e. depopulating hazardous regions Shibayama (2011).

The last word should go to the Tsunami Protection Committee who recognised in 2005 the work that needed to be done and had insight into the type of problem that might exist:

"Tsunami protection measures in the past relied mainly on structural measures such as seawalls designed to guard against a tsunami of an expected magnitude, and there was even no policy for dealing with a tsunami of a greater magnitude. In view of the current state and problems, the basic proposition in the coming years is to enhance the level of safety as soon as possible despite the limitations in the amount of investment and the response time requirements and strategically promote activities for minimizing damage even in the event of a beyond-design-basis tsunami" (Tsunami Protection Committee, 2005).

6.10. References

Aydan, O., 2011. *An overview of the M9.0 earthquake off the Pacific Coast of Tōhoku region of Japan on March 11, 2011 and its lessons*, Tokai University, Shizuoka, Japan [online]. Available at: <http://www.jsce.or.jp/committee/eec2/eq_report/201103Tōhoku/Aydan1.pdf> [Accessed 27th July 2011].

Dengler, L., 2011. *Japan Reconnaissance – Wrap Up*, May 25 2011, Redwood Coast Tsunami Work Group, Humbolt State University, US [online]. Available at: <http://www.humboldt.edu/rctwg/blog> [Accessed 27th July 2011].

Honda, R., 2011. Tokyo University. [email] (Personal Communication, 8 June 2011).

Institute for Fire Safety & Disaster Preparedness, 2011【消防庁長官賞】津波防災のまちづくり（「災害の町」から「防災の町」へ）[image online]. Available at: <http://www.bousaihaku.com/cgi-bin/hp/index2.cgi?ac1=B742&ac2=&ac3=1574&Page=hpd2_view> [Accessed 27th July 2011].

Kazama, M., 2011. *The 2011 off the Pacific Coast of Tōhoku Earthquake – After two months.* In: 14th Asian Regional Conference on Soil Mechanics and Geotechnical Engineering [online]. Available at: <http://www.jiban.or.jp/file/file/kazama520e2.pdf> [Accessed 27 July 2011].

Komo News, 2011. *How one Japanese village defied the tsunami*, May 13 2011 [image online]. Available at: <http://www.komonews.com/news/national/121775754.html> [Accessed 27th July 2011].

Murata, S., Imamura, F., Kato, K., Kawata, Y., Takahashi, S. and Takayama, T., 2010. *Tsunami: To survive from Tsunami*, Advanced Series on Ocean Engineering – Vol 32, World Scientific.

PARI, 2011a. *Technical Note of Port and Air Port Research Institute, No. 1231, April 28, 2011. Urgent Survey for 2011 Great East Japan Earthquake and Tsunami Disaster in Ports and Coasts* (in Japanese) [online]. Available at: <http://www.pari.go.jp/files/3642/1049951767.pdf> [Accessed 27 July 2011].

PARI, 2011b. *An English Abstract of the Technical Note of Port and Air Port Research Institute, No. 1231, April 28, 2011. Urgent Survey for 2011 Great East Japan Earthquake and Tsunami Disaster in Ports and Coasts – Part I (Tsunami)* [online]. Available at: <http://www.pari.go.jp/en/files/3653/460607839.pdf> [Accessed 27 July 2011].

PARI, 2011c. *Tsunami Impacting Eastern Japan and Preparedness for Extraordinary Natural Disaster, May 25, 2011* [online]. Available at: <http://www.pari.go.jp/files/items/3459/File/2011052327IAPH.pdf> [Accessed 27 July 2011].

PIANC, 2011. *Message from Tadahiko Yagyu, Secretary General of PIANC Japan* [online]. Available at: <http://www.pianc.org/downloads/sailingahead/Sailing%20Ahead%20April%202011/Japan%20Earthquake.pdf> [Accessed 27th July 2011].

PWRI, 2008. *Comprehensive Tsunami Disaster Prevention Training Course*, November 2008 ISSN 0386-5878 Technical Memorandum of PWRI No.4114 [online]. Available at: <http://www.preventionweb.net/files/9285_isdrtsunamieng.pdf> [Accessed 27 July 2011].

Reuters, 2011. *Scenic Japan road is now Tsunami Highway*, March 28 2011 [online]. Available at: <http://uk.reuters.com/article/2011/03/28/us-quake-japan-road-idUKTRE72R0HM20110328> [Accessed 27th July 2011].

Seattle Times, 2011. *How one Japanese village defied the tsunami*, May 13 2011 [online]. Available at:

<http://seattletimes.nwsource.com/html/nationworld/2015041260_apasjapanvillagethatsurvived.html> [Accessed 27th July 2011].

Shibayama, T., 2011. *Survey of the Tsunami Disaster and the Need for Recasting Disaster Prevention Plans Coastal Structures Are Not Enough for Protection*, commenting on ASCE Reconnaissance Survey [online]. Available at: <http://www.researchsea.com/html/article.php/aid/6138/cid/5> [Accessed 27th July 2011].

Smits, G., 2011. *Danger in the Lowground: Historical Context for the March 11, 2011 Tōhoku Earthquake and Tsunami* [online]. Available at: <http://forum.gloresis.com/2011/05/16/historical-context-for-the-march-11-2011-Tōhoku-ea/> [Accessed 27th July 2011].

Takata, N., 2009. *Tsunami disaster reduction in Japanese ports and harbors*. Proc 6th Intl. Workshop on Coastal Disaster Prevention, Bangkok, Thailand, December 2009 page 93.

Tsunami Protection Committee, 2005. *Recommendations of the Tsunami Protection Committee (2005)* [online]. Available at: <http://www.mlit.go.jp/river/trash_box/paper/pdf_english/e_140.pdf> [Accessed 27th July 2011].

7. Field observations on tsunami damage to buildings

As shown in the overview of tsunami damage in section 5.5, the damage to buildings from tsunami flow and associated debris impact was extensive. This section presents observations on building damage from the EEFIT mission presented by location, ordered from north to south.

7.1. Tsunami damage scale

Detailed damage surveys were carried out by EEFIT in Kamaishi City and Kesennuma City. Damage level is assigned to buildings using the EEFIT tsunami damage scale developed following the 26th December 2004 Indian Ocean earthquake and tsunami by EEFIT (2005), Table 7.1.

Table 7.1 EEFIT tsunami damage scale for structural damage for low (Category D) and mid-rise (Category E) RC infill frames (EEFIT, 2005).

Damage Level	Description
No Damage (D0)	No visible structural damage to the structure observed during the survey. Immediate occupancy.
Light Damage (D1)	Flood damage to contents. Some non-structural (fittings, windows) damage. Damage is minor and repairable. Suitable for immediate occupancy.
Moderate Damage (D2)	Out-of-plane failure or collapse of parts of or whole sections of infill walls and windows at ground storey. Repairable damage from debris impact to structural members. No structural member failure. Scouring at corners of the structures leaving foundations partly exposed but repairable by backfilling. Unsuitable for immediate occupancy but suitable after light repair.
Heavy Damage (D3)	The structure stands but is severely damaged. Infill panels above the first storey have been damaged or have failed. Structural and non-structural members have been damaged. Failure of a few structural members which are not critical to structure stability. Roofs are damaged and have to be totally replaced or repaired. Structure requires extensive repair and hence is unsuitable for immediate occupancy.
Collapse (D4)	Partial or total collapse of the building. Collapse of large sections of foundations and structures due to heavy scouring. Excessive foundation settlement and tilting beyond repair. Damage to the structure cannot be repaired after the tsunami and must be demolished.

7.2. Field observations

Key observations are presented from locations visited during the EEFIT mission, including data from detailed damage surveys carried out in Kamaishi City and Kesennuma City. A summary of the location and damage statistics are provided for each location to provide some context; this data is tabulated in Table 11.1. The detailed damage surveys aim to establish a relationship between structural damage and tsunami inundation parameters using inundation depth from field observations and flow velocity derived from video evidence (of which there is much from this event) and numerical modelling. The area that can be covered during a field investigation by a small group of investigators is limited and with practical access issues in a disaster zone this inhibits the amount of data that can be collected. A more spatially-complete method is proposed by Koshimura et al. (2009), using post-disaster satellite imagery to include a large sample of structures in calculations of collapse probability, and to present this against field observations or numerical modelling output of tsunami parameters. Despite limitations on the amount of data collected, it remains possible to assess the observed relationship between tsunami inundation depth and structural damage, and to draw useful conclusions from the detailed surveys.

Hatori (1984) and Shuto (1993) present tsunami damage scales from historic tsunami that affected Japan. Shuto suggests a wash-away threshold for timber houses at 2 m inundation depth, derived using data from damaging tsunami worldwide in 1883 (Krakatoa), 1896 (Sanriku), 1908 (Messina

Straits), 1933 (Sanriku), 1946 (Nankai), 1960 (Chile) and 1983 (Japan Sea). Using observations from the 1983 Nihonkai-chubu tsunami, Hatori (1984) suggests that this threshold is applicable to destruction of wooden houses, but that complete wash-away is rare at 2.0 m. Data from the 1933 Showa Sanriku and 1960 Chile tsunami (Hatori, 1984) shows that 10-20% of wooden houses were damaged when subjected to inundation height of 3 m above mean sea level, while at 4 m inundation height this value increases to 50% - this suggests a more appropriate threshold for significant levels of damage to wooden houses is 3.0-4.0 m. Hatori concludes that these thresholds should rise further in the future as there was at that time (1984) an increasing trend of bolting the timber frame of residential houses to their foundations. With regards to masonry houses and RC buildings, Shuto (1993) estimates the minimum inundation height causing destruction to be 7 m and greater than 16 m, respectively.

MLIT (2011) survey data of building damage on 11th March 2011 shows that 12% of buildings were washed away at 1.5-2.0 m inundation height; this value increases gradually with increasing inundation height to 56% at 3.5-4.0 m. When considering heavily damaged buildings as well (those that remain standing but cannot be repaired), the data shows a much clearer threshold at 2.0 m: at 1.0-1.5 m inundation height, only 9% of buildings are washed away or rendered unrepairable while at 1.5-2.0 m, this value is 31% and at 2.0-2.5 m this is 66% of buildings. The survey does not specify the types of buildings surveyed, however, despite to potential inclusion of steel and RC building, the MLIT values suggest a slightly lower threshold for significant damage than Hatori (1984) – 2.0-2.5 m rather than 3.5-4.0 m. The MLIT findings also dismiss Hatori"s expectation that the levels of damage would reduce at comparable inundation heights due to increased bolting of timber frames to foundations.

Observations from Kamaishi City, Kesennuma City and Onagawa Town return to these thresholds in light of observations from the detailed damage surveys.

7.2.1. Tarō Town, Iwate Prefecture

Tarō Town is situated in an east-facing bay 600 m wide at the open ocean, with urban development concentrated in a flat plain at the confluence of two rivers: the Nagauchi River and Tashiro River. A post-tsunami aerial image of the village is shown in Figure 7.1 with the tsunami defences (discussed in section 6.3) marked in red. With reference to the defence indicated: the south-west quadrant was primarily agricultural land while the north-west and north-east quadrants were largely urban development.

In the north-east quadrant, (between the very large defence completed in 1940 and the more modern wall completed 1978) there was almost total destruction of buildings by the tsunami and only two buildings remained standing at the time of our survey. A 7-storey steel-frame hotel building (Figure 7.2) remained standing with significant cladding damage to the lowest 2 storeys, and visible damage up to the 4th floor; from analysis of aerial photography this appears to have been the only building in this quadrant prior to the tsunami that was more than 3-storey in height. In the north-west quadrant behind the wall constructed in 1940, most timber structures had been washed off their foundations but many remained intact, while many steel frame and RC structures also survived with damage to lower-storey cladding. Figure 7.1 shows significant amounts of debris had been washed into this area and trapped behind the defence.

In front of the tsunami defences along the quay, two further buildings survived the 12 m deep tsunami flow: an RC frame building with significant tsunami damage to its lower 4 floors and a steel frame building (Figure 7.2 and Figure 7.3) whose structure appeared to be intact despite removal of non-structural components.

Figure 7.1 Post-tsunami aerial photograph of Tarō Town with coastal defences indicated in red.

Figure 7.2 (right) Steel-frame hotel in Tarō Town showing heavy damage to the third floor and minor damage at the 4th floor.

Figure 7.3 (right) Steel frame building on the quayside (in front of tsunami defences). The structure remains standing despite heavy damage and removal of non-structural elements.

7.2.2. Kamaishi City, Iwate Prefecture - detailed damage survey

Kamaishi City is situated in an east-facing bay, with urban development concentrated along the Kasshi River valley, which is 1.1 km wide at the harbour front and is bounded by steep hills to the north and south. The death toll in Kamaishi as of 11th October 2011 stands at 884 dead and 194 missing (FDMA, 2011). This is 2.72% of the city"s population and 8.19% of the population estimated by the Geospatial Information Authority of Japan (GSI) to be living in the inundated zone. Approximately 33% of Kamaishi"s population resided in the inundation zone prior to the tsunami (MIAC, 2011).

EEFIT carried out a damage survey on 31st May 2011, designed to investigate possible sheltering by the Nippon Steel Factory building and impacts of the tsunami overbank-flow from the Kasshi River channel, which is lined with concrete for flood-control purposes. We surveyed buildings along 1 km of a road comprising 2 to 3-storey mixed-use commercial and residential buildings and a few commercial buildings of over 5-storeys. The eastern end of the survey is 140 m from the harbour front, the western end is 1100 m from the same point. Land-use seaward of the survey route is characterised by industrial buildings of the Nippon Steel Factory (Figure 7.5). Predominant flow direction was from

the south-west, with the possibility of some overbank flow from the Kasshi River. Approximate inundation depth (as defined in section 5.1) was recorded using observable flow features (debris strike, deposited debris, watermarks) on buildings. Estimated inundation depth was 8 m at the eastern end, 5-7 m for the next 400 m along the survey, 4 m consistently between 400 m and 900 m, with an abrupt decrease to 2.5 m at the western end, where the survey terminates at the river. The survey route was consistently around 5 m above mean sea level prior to the earthquake (0.66 m of subsidence was recorded at Kamaishi – see Table 8.1). There is a more substantial rise in ground elevation at the western end of the transect, which appears responsible for the abrupt reduction in inundation depth (see Figure 10.11 for contours).

EEFIT surveyed 154 buildings, the composition of which is shown in Figure 7.4. Failure modes observed during this survey include:

- Soft-storey style failure of several timber structures – it is unclear whether this is ground shaking induced, or the result of tsunami loading / debris strike
- Out-of-plane failure of infill walls and panel walls in all construction types but particularly steel frame structures
- Debris impact damage (from minor damage of exterior cladding to major damage of non-structural components of steel frames)
- Extensive glazing damage at ground floor level, some damage to first second storey glazing

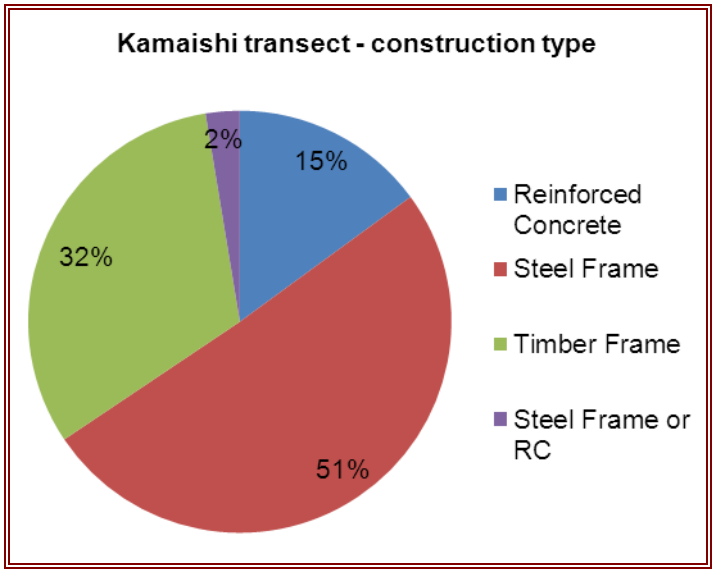

Figure 7.4 Composition of building surveyed in Kamaishi.

Little damage above “heavy damage” was observed in reinforced concrete (RC) and steel structures during this survey. Examples of observed damage and the corresponding damage level are shown in Figure 7.6. Over 50% of surveyed timber building experienced damage level D4 – partial or complete collapse (Figure 7.7). Significantly, no steel frame or RC structures suffered this level of damage in our survey, although few (15% and 4% respectively) did suffer heavy damage (D3). Most steel frame (77%) and RC (83%) buildings suffered heavy non-structural damage but the structural frames were often only lightly damaged (D1 to D2).

The survey indicates a general reduction in damage towards the western end of the survey with distance from the port and variable degrees of sheltering. At the eastern end of the survey most timber buildings suffered complete collapse and several had been washed away or cleared away, while steel frame buildings suffered damage level D1 to D3, and RC buildings D1 to D2.

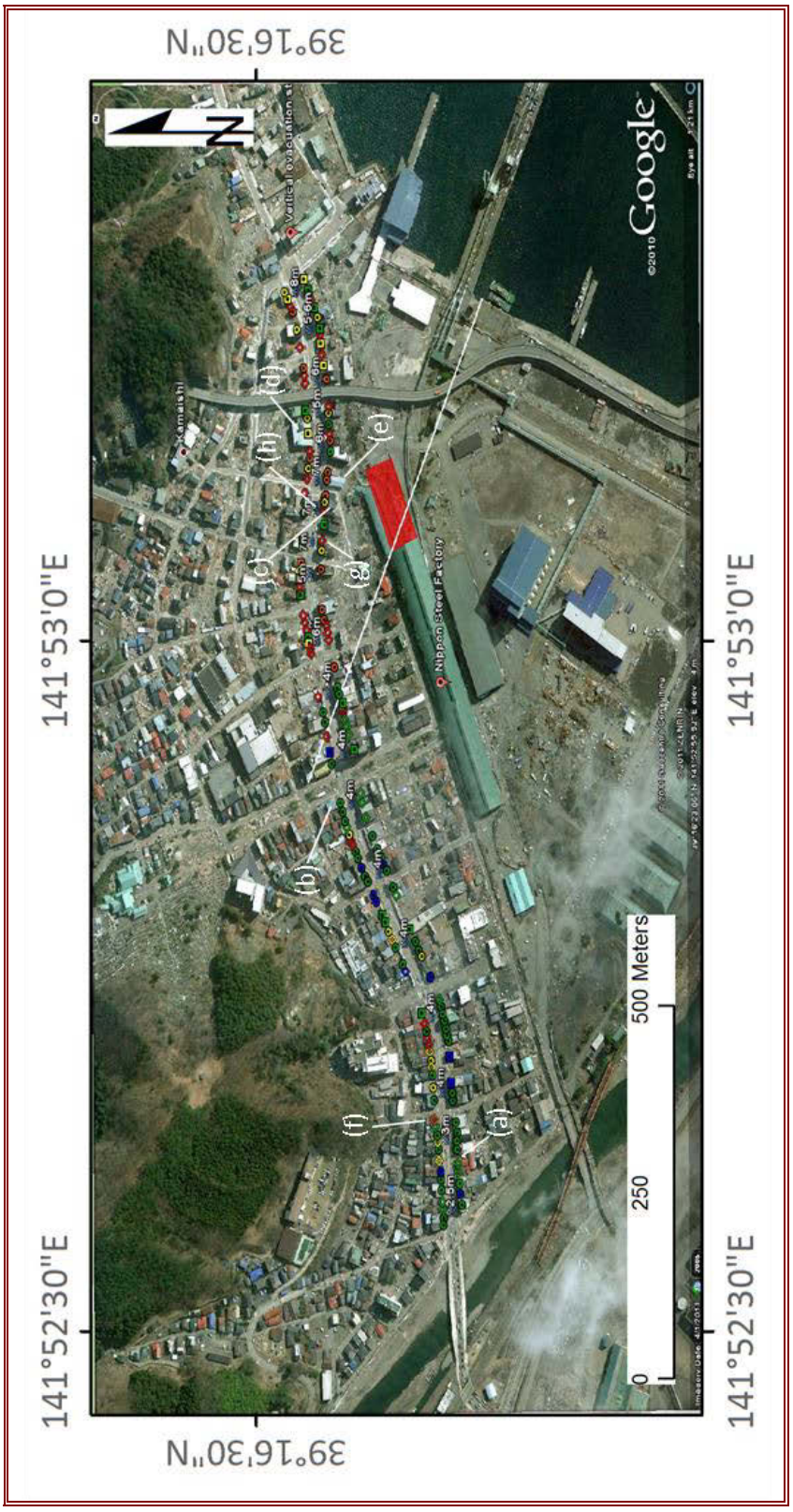

Figure 7.5 Damage survey in Kamaishi City. Construction type indicated by shape – Diamonds: timber frame construction; Squares: RC; Circles: steel frame. Damage level indicated by colour – Blue: D0, Green: D1, Yellow: D2, Orange: D3, Red: D4. Inundation depths and the collapsed section of Nippon Steel Factory building (red polygon) are also shown. Locations of the example buildings listed in Figure 7.6 are marked.

(a) Timber frame structure, damage D1, 3 m inundation.

(b) Steel frame, D1, 4 m inundation.

(c) Steel frame, D2, 7 m inundation.

(d) RC shear wall, D2, 5 m inundation.

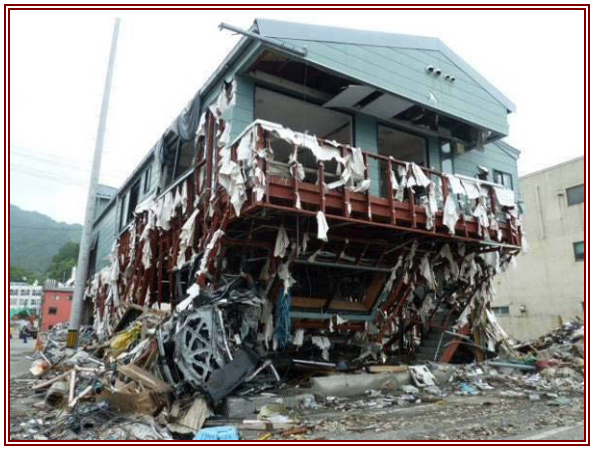

(e) Steel frame, D3, 6 m inundation.

(f) Timber frame, D3, 3 m inundation.

(g) Timber frame, D4, 7 m inundation. (h) Timber frame, D4, 7 m inundation.

Figure 7.6 Example structure types observed in Kamaishi, with damage level and inundation depth. The location of each building is labelled in Figure 7.5.

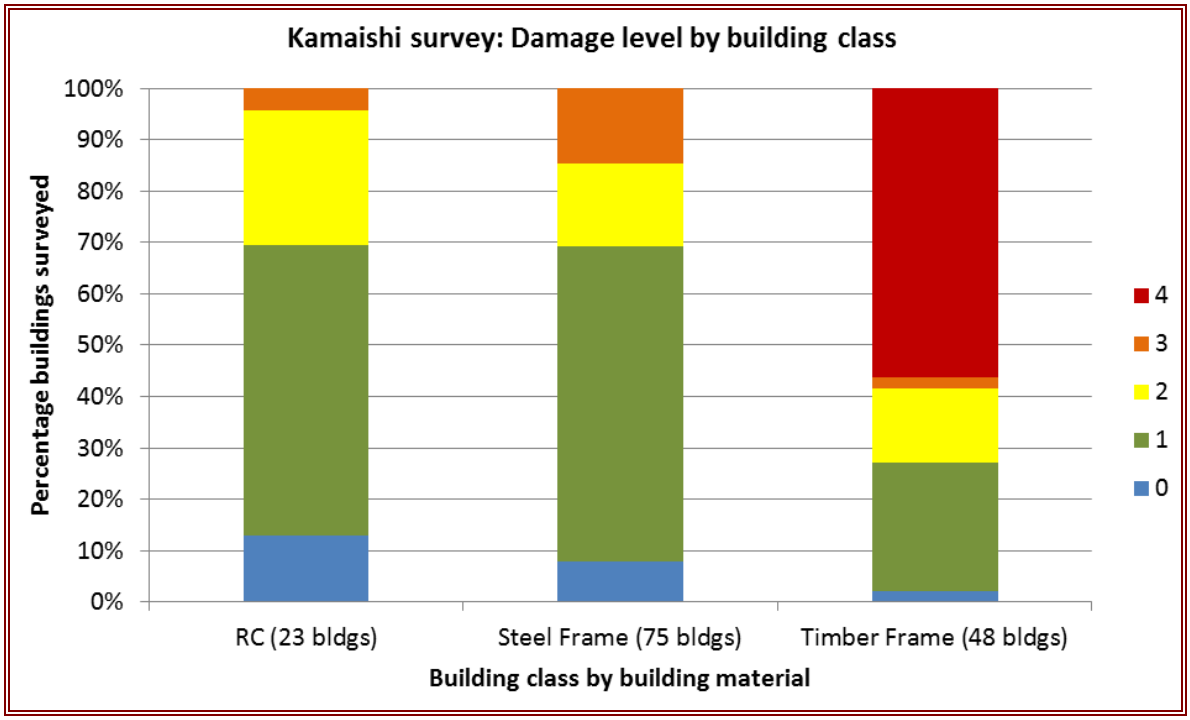

Figure 7.7 Proportion of damage level observed for each general construction type.

There appears to be a boundary (indicated with a white line on Figure 7.5) where heavy damage ceases to occur – this is roughly in line with the end of a large trussed steel portal frame construction forming a long narrow shape on plan. Inundation depth also decreases abruptly around this area, from depths of 5-6 m to 4 m. The eastern-most end of this building suffered partial collapse in the tsunami (red shaded area on Figure 7.5). The lack of major horizontal members across the failed joint (Figure 7.8) suggests that the collapsed section of the building was structurally isolated from the remaining structure. The collapsed section of the building was also likely the same portal frame construction, though the failed columns had already been removed at the time of this survey. Failure of the portal frame columns may have been caused by impact from the large machinery originally contained within the building (Figure 7.9).

The decrease in inundation depth and damage close to this theoretical boundary suggests sheltering from the factory building, and although tsunami flow did cause failure of the light steel panel walls (Figure 7.10), the structure undoubtedly reduced flow velocities immediately to the northwest. It is suggested that sheltering observed along the survey route occurred due to a combination of the surviving factory building, the closely-spaced configuration of groups of surviving buildings and distance from the port.

Moving further inland we observed several timber buildings that had experienced soft storey collapses, including some where the upper floors were resting against adjacent steel or RC buildings (Figure 7.12 and Figure 7.13). Short period component ground motions recorded at K-NET station IWT007, 1.5 km west of Kamaishi port, were sufficiently large and of long duration to cause deformation in these structures: 1g to 2g at 0.1 s to 0.5 s for both N-S and E-W components. This indicates that this failure could be due to earthquake ground shaking, although this cannot be confirmed: observations of purely seismic damage elsewhere in Tōhoku generally showed flexible timber framed buildings to have performed well. This suggests that whereas the steel and RC buildings were able to withstand hydrostatic and hydrodynamic forces of the tsunami (and to some extend the associated debris impact) the flexible timber framed buildings could not. Flexible timber framed buildings have less capacity than RC and steel frame buildings to resist the first-order stresses induced by lateral hydrostatic and impact forces.

Figure 7.8 (left) Large trussed portal frame structure of the Nippon Steel Factory, at the eastern end of remaining structure.

Figure 7.9 (right) Collapsed eastern section of Nippon Steel Factory building.

Figure 7.10 (left) Water and some debris were able to pass through the structure limiting the amount of shelter this building was able to provide to the buildings behind.

Figure 7.11 (right) RC frame building with heavy non-structural damage. Structural frame remains undamaged.

At the western end of the transect (inundation depths of 2.5 m to 3 m, and adjacent to the river) damage levels were variable and at the time of the survey several businesses were preparing to reopen. Timber frame structures at this location generally sustained damage D1 to D2, with one instance of D3 to a timber frame structure on an exposed street corner. Plastic shop signs and some glazing remained undamaged despite being submerged, indicating low flow velocity in this area. Referring to the relationship of flow velocity from the City and County of Honolulu Buildings Standards (CCH, 2000), we could assume that velocity in this location was around 3 m/s. The observed level of damage indicates that the tsunami waters here were rather slow rising, suggesting an even lower velocity that would enable timber frame houses to survive the tsunami with light to moderate damage when well anchored to their foundations. As discussed in section 6.2, the substantial breakwaters in the harbour appear to have mitigated inundation depth and further investigation would be beneficial to quantify the impact of these structures had on onshore flow velocity.

While MLIT (2011) survey data from this event shows a 2.0-2.5 m inundation causing heavy damage or wash-away to 66% of buildings, the depth threshold for heavy damage to timber building damage is extremely variable at a local scale and does not account for variations in flow velocity at a consistent depth, for example where high degree of sheltering exists. A threshold of at least 5 m for heavy damage to timber frame buildings appears more appropriate from this survey although it is of limited extent and is highly influenced by local sheltering factors and flow direction, so flow velocity may be unusually low at inundation depths of 2.5-4 m (at which we recorded light or moderate damage to timber buildings).

Immediately south of the western end of the transect survey, damage was similar to that observed at the eastern end of the transect: collapsed timber structures (D4) and light to moderate damage (D1, D2) of steel frames. This suggests the river channel was overtopped, causing heavy localised damage at this point along the river bank.

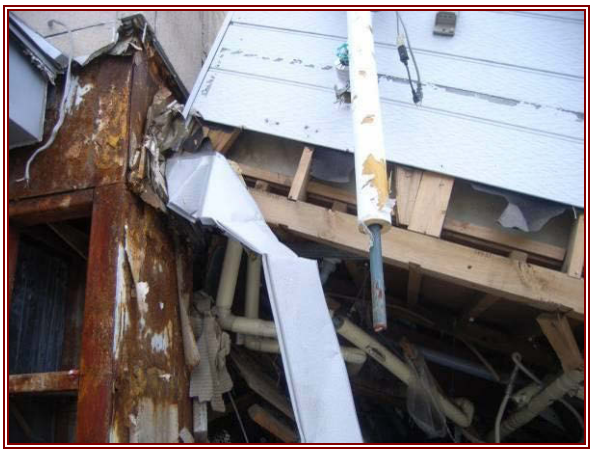

Figure 7.12 (left) Soft story collapse of timber structure. Upper floor intact because of central steel strengthening beam supporting the second storey.

Figure 7.13 (right) Supported from complete collapse because wedged up against adjacent steel frame building.

7.2.3. Ōfunato City, Iwate Prefecture

Ōfunato is situated within a narrow south-facing bay bounded by steep hills on either side. The bay is 5.7 km long from the city to open ocean, and 1.1 km wide at the harbour front. Funnelling of the tsunami wave contributed to a wave height measured at 11.8 m at the coastline.

Approximately 31% of Ōfunato"s population lived in the inundation zone (MIAC, 2011) – most inundation occurred in the industrial / commercial section of the town. The death toll in Ōfunato as of 11th October 2011 stands at 339 dead and 107 missing (FDMA, 2011), which is 2.34% of the population estimated to be live in the inundated area and 1.09% of the total population (MIAC, 2011). Most residential areas of the town are on relatively steep hills on the east and west sides of the Mori River valley. As a result, the fatality rate in Ōfunato is among the lowest in the rias coastline and quite similar to Miyako (0.91% of total population, 2.94% of population living in inundated area, GSI 2011).

Initial tsunami arrival at Ōfunato occurred 25 minutes after the earthquake and according to the tide gauge record at Ōfunato Port, it took a further 6 minutes to reach a height of 8.0 m, at which point the gauge stopped recording. A similar tide gauge record was obtained in Miyako, which showed arrival of the tsunami 29 minutes after the earthquake, taking a further 11 minutes to reach its maximum recorded value of 8.5 m. In both Ōfunato and Miyako, there was a drawdown phase prior to the tsunami arrival (i.e. the sea receded before tsunami wave arrival), and the first tsunami wave was the highest. The city experienced 0.78 m coastal subsidence due to the earthquake and during high tide large parts of its commercial centre could not be entered as they had been partly flooded by more than 10 cm of water. Access to some parts of town was blocked by the authorities.

Despite the majority of residential areas being located on the surrounding hills, housing damage in Ōfunato City was still extensive: 3,600 homes were surveyed by local officials as having heavy or partial damage. Experience from the distal 1960 Chilean tsunami, which reached inundation depths of 5.6 m in Ōfunato (Figure 7.14), led to reconstruction of some residential buildings as 3-storey RC structures, in the belief that these would survive future tsunami. However, on 11th March tsunami height of 11.8 m was recorded at the coastline and many of these buildings were inundated to the roof (Figure 7.15). The vast majority of visible timber structures had collapsed (with some overturned, Figure 7.16) or had been demolished and there was evidence of large debris being washed into the town (Figure 7.17).

The commercial centre of Ōfunato City took the full brunt of the tsunami flow due to its location on the edge of the harbour. Several steel frame and RC buildings remained structurally intact but with heavy damage to non-structural elements such as the removal of cladding (Figure 7.18). This is consistent with observations from Kamaishi and Kesennuma, where inundation depths were also at or below 8 m. Evidence of damage caused during the period or periods when tsunami waters flowed back to the sea (subsequently referred to as „return flow") is seen at an old traditional timber frame warehouse building in the commercial centre that leans seawards (Figure 7.19).

Figure 7.14 (left) Tsunami preparations were based on the 1960 Chilean tsunami which reached a inundation depth of 5.6 m in Ōfunato (sign is located at 39° 3'55.1" N, 141° 43'17.4" E).

Figure 7.15 (right) Three-story residential RC buildings such as this one were thought to be safe due to expected tsunami inundation depths based on the distal 1960 Chile tsunami.

Figure 7.16 (left) An overturned timber building in Ōfunato.

Figure 7.17 (right) Large debris from the port was found in the town (e.g. boat shown).

We inspected a 3-storey RC shear wall building, which had separate entrances for the ground floor (a children"s clinic) on the seaward side and for the top two floors (apartments) on the landward side (Figure 7.20 and Figure 7.21). Inundation reached the top of the third floor and possibly overtopped the building. The structure remains intact as it avoided major debris impacts despite its proximity to the sea and its relatively exposed position. Many windows in this building remained unbroken, however, inside the flooded apartments of the top two floors we could see clear tsunami marks that stopped in line with the top of the window openings (in both front and back rooms), suggesting air void formation. The building did not have egress to the roof. Tsunami watermarks left during the return flow were observed at the rear entrance; during return flow this building had some degree of sheltering from another 3-storey RC shear wall apartment building on its inland side, which exhibited clear debris impact at the second floor balcony on the landward side (Figure 7.21). Adjacent to these 2 RC buildings there was a devastated wooden house that had lost its ground floor despite some sheltering from a structure in front of it, as well as many small debris from wooden houses and building contents.

Figure 7.18 (left) Cladding had been washed away (or subsequently removed) and steel frame appears to have suffered impact damage but the structural steel frame seemed intact.

Figure 7.19 (right) A traditional timber frame warehouse in the commercial centre that was damaged during the tsunami return flow (leaning seawards).

Figure 7.20 (left) RC shear wall building with separate front and rear entrances in the seaward and inland side. Seaward view is shown. The building flooded all the way to the top but its structure remained almost intact.

Figure 7.21 (right) RC shear wall building adjacent to the one seen in Figure 7.20 (this view shows the rear of that building), with clear debris impact damage on the second floor balcony. Landward view is shown.

7.2.4. Rikuzentakata, Iwate Prefecture

Rikuzentakata is situated on the northern shore of the Hirota Bay which is about 3.5 km wide and lies to the southwest of Ōfunato Bay. It was one of the most heavily impacted areas along the rias coast. Prior to the earthquake this city was known in the region as a holiday resort. The city spreads across the northern shore of the Hirota Bay for at least 1.65 km east to west and for around 1 km in the northern (inland) direction, while at its western side it is crossed by the Kesen River. Over this wide zone, the elevation is very low and as the tsunami height exceeded 12 m in this zone (with run-up reaching 19 m), every timber frame house (predominantly two-storey) was totally destroyed. Few RC buildings remain in the inundation zone and the city hall remains standing despite inundation to the third floor. The tsunami waters entered the river and flooded both banks by up to 350 m on either side, for a distance of at least 2.75 km inland.

The death toll in Rikuzentakata as of 11th October stands at 1,554 dead and 385 missing (FDMA, 2011). This is 8.32% relative to the city"s population and 11.65% of the population estimated by the GSI to be living in the inundated zone. Approximately 71% of Rikuzentakata"s population lived in the inundated area, as most of the city was situated on low-lying areas (MIAC, 2011). Only Onagawa Town experienced a higher fatality rate in this earthquake and tsunami (9.75% of total population, 12.18% of population living in inundated area).

We entered the city from the north, viewing the damage along the Kesen River banks; near the inland extent of inundation along the river the railway bridge had been destroyed (Figure 7.22). We inspected a traditional wooden house that lay approximately 200 m from the river"s western bank, near the Mattate Bridge (a road bridge). Direct distance from the mouth of Kesen River to the Mattate Bridge on the National road 343 is about 4.25 km, and distance along the river is about 4.75 km. The house was situated right in front of a very steep hill where the tsunami flooding came to an abrupt stop. Although this beautiful old building is still standing (Figure 7.23), damage to its wooden structure may be too difficult to repair and according to its owner (who we interviewed on May 31st) the house may have to be demolished. Tsunami water marks were visible right near the ceiling level of this single-storey structure. Our measurements showed tsunami inundation at 4.21 m above ground level. The ground elevation at this house was approximately 10 m (based on inspection of the topographical map of Rikuzentakata – GSI, 2003b).

Figure 7.22 (left) The destroyed railway bridge just south of the Mattate Road Bridge in Rikuzentakata at a distance of approximately 2.5 km from the sea shore (May 31st 2011).

Figure 7.23 (right) A traditional single-storey timber frame house approximately 200 m west of the Mattate Road Bridge that was flooded up to its ceiling (4.2 metres above ground) situated approximately 2.75 km from the sea shore (May 31st 2011).

We continued south until reaching the sea front where we inspected the Capital Hotel (Figure 7.24). This is a 7-storey structure over 25 m tall with its first two levels reaching approximately 8 m high. Inundation depth flooded the third level, thus reaching around 10 m. It was too dangerous to enter this building and take accurate measurements but external non-structural damage is shown in Figure 7.25.

Figure 7.24 (left) The Capital Hotel at the seafront of Rikuzentakata (May 31st 2011).

Figure 7.25 (right) Capital Hotel"s sea front side, showing tsunami damage up to the third level (May 31st 2011).

7.2.5. Kesennuma City, Miyagi Prefecture – detailed damage survey

The main developed areas of Kesennuma are situated at the head of a long, 1 km-wide south facing bay, which appears somewhat protected from the open ocean by Ohshima Island and headland to the east. The death toll in Kesennuma as of 11th October 2011 stands at 1,027 dead and 377 missing (FDMA, 2011). This is 1.91% of the city"s population and 3.48% of the population estimated by GSI to be living in the inundated zone (MIAC, 2011).

An extensive area of damage was surveyed in the northern part of Kesennuma (Higashiminato-cho, Nishiminato-cho, Nakaminato-cho and Nishihachiman-cho), from 450 m inland (as close to the port as was accessible due to subsidence and flooding) to 1.1 km inland (where no further damage was observed). Timber frame structures suffered heavy damage to collapse (90% of buildings in this area

surveyed as D4), 60% of steel frame structures registered moderate to heavy damage (D2-D3) and 7 of the 9 surveyed RC structures sustained light damage (D1). A large number of buildings had been washed away or destroyed by fire and often the building footprints were not visible during the survey. Field observations have therefore been augmented with building footprint data (GSI, 2003a) to calculate the total original number of buildings. Steel frame and RC buildings remain standing in even the most fire-affected areas, therefore all buildings identified in GSI data with no corresponding surveyed building are assumed to be timber frame, damage level D4.

The survey does not account for all buildings standing at the time of survey, due to access restrictions (debris, flooding and recovery operations). The number of buildings surveyed and the damage level assigned to those buildings in each construction category is presented in Figure 7.26. Inundation depths of 7-8 m were observed 500 m inland with flow direction from the south.

Figure 7.27 shows a high degree of variability in damage induced by flows of similar depths in this survey area. Although the majority (95%) timber frame structures are in a state of heavy damage or collapse, there are many cases which again indicate the local variability of damage. In the eastern (less fire-damaged) area of the survey, inundation depths of 5-7 m resulted in damage levels from D2 to D4. It is expected that in the western (fire-affected) area, the tsunami-survival (i.e. non-collapse) rate of timber houses is expected to have been higher than apparent in the survey results, and consistent with the eastern side of the survey.

An additional damage survey was carried out in Sakanamachi district of Kesennuma, which highlighted the contrasting damage in two adjacent parts of this town. Sakanamachi is situated within the western development of Kesennuma harbour where, due to steeper relief, there was much less extensive damage than surveyed in the north of the harbour.

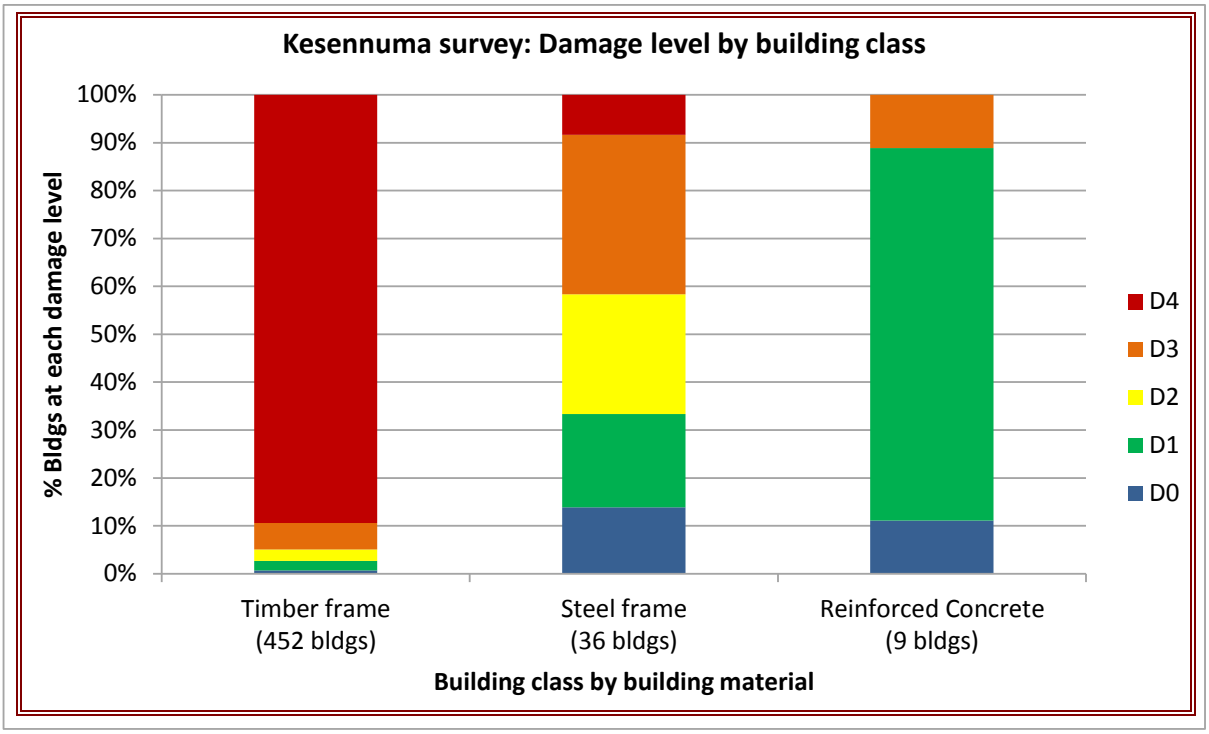

Figure 7.26 Damage level by construction type as surveyed in Kesennuma City.

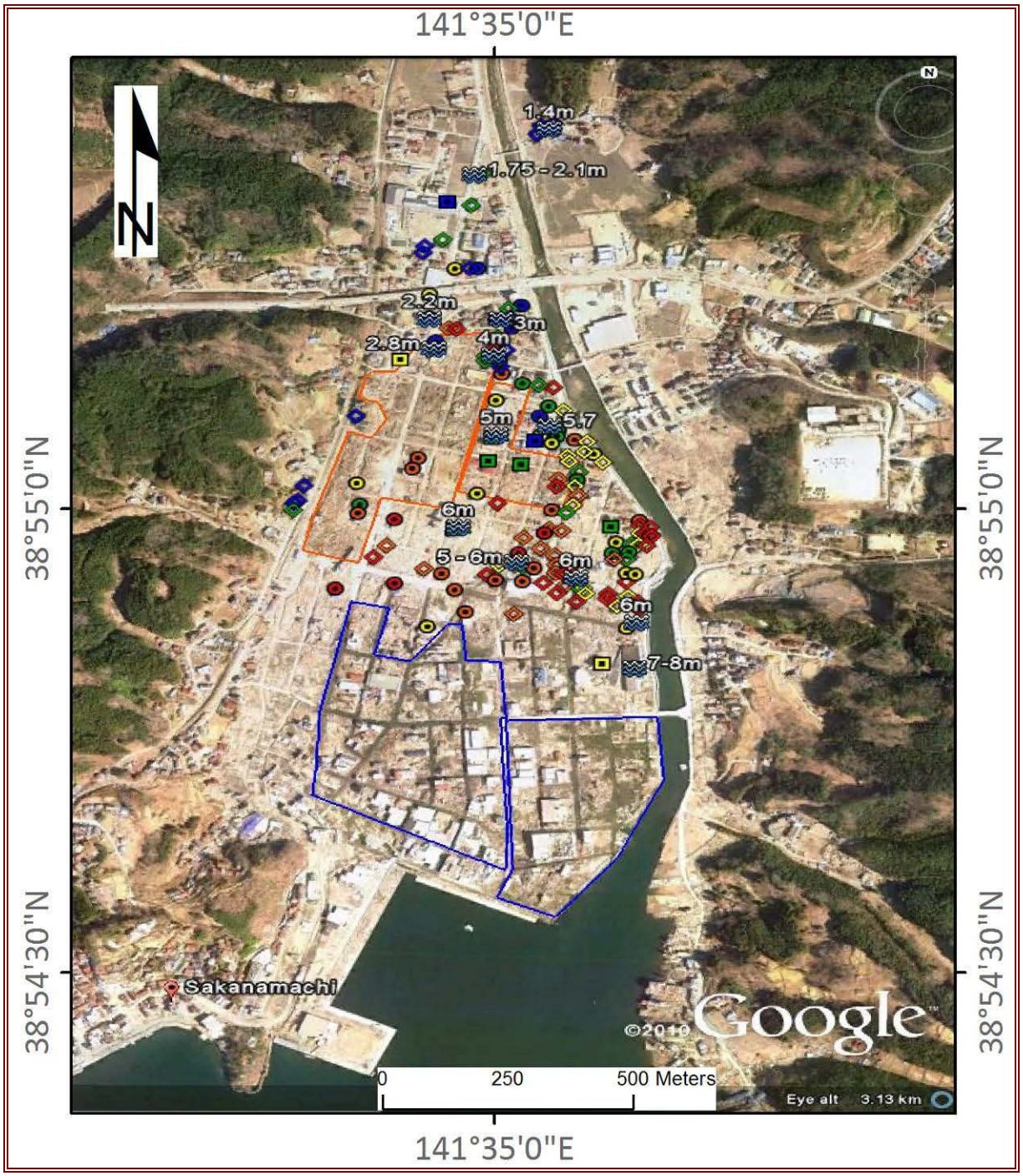

Figure 7.27 Surveyed structures in Kesennuma. Diamonds denote timber frame construction, squares denote RC, circles denote steel frame. Damage level is indicated by colour – Blue: D0, Green: D1, Yellow: D2, Orange: D3, Red: D4. Inundation depths, heavily fire damaged areas (orange outline) and subsided area (blue outline) are also shown. The subsided area was flooded at the time of survey. Many structures that have been washed away are not marked on this map – they are considered to be timber frame, damage level D4.

Raised dwellings

A number of residential dwellings situated on ground floor RC frames or artificially raised land were present in Kesennuma. The impact of raising residential dwellings was variable, with the majority sustaining light to moderate damage, as opposed to suffering heavy damage or collapse like those

built on concrete ring foundation at ground level. Exceptions to this reduced damage occurred where suspected debris impact caused moderate damage to raised structures.

Figure 7.28 (left) Raised concrete foundation; structure built 2 m from ground level, 660 m inland and 100 m from Shikaori River. Inundation depth was approximately 6 m in the area around this building.

Figure 7.29 (right) RC frame providing garage space below the dwelling, which is 3 m from ground level, 780 m inland and 60 m from the Shikaori River. Inundation depth was approximately 6 m in this area.

Infrastructure embankments

Earth embankments provided a large degree of protection to some parts of Kesennuma: the railway running north is situated on an embankment approximately 4 m high, and Highway 4 running west to east across the northern valley is situated on a 6 m high embankment. In both cases, damage to structures behind the embankments was reduced significantly. Damage was not entirely prevented north of Highway 4 embankment, as the tsunami flowed through breaks in the embankment – a road runs north under a bridge at the highway, as does the river. The railway embankment, although overtopped, blocked floating debris and prevented fire spreading to structures west of the railway. Tsunami impact west of the railway was limited to flood-damaged contents in modern residential timber structures. No scour or slope failure was observed at these embankments. Clearly, the impact of embankments is entirely related to their position and height relative to inundation depth; however, these observations provide evidence that in low to moderate inundation depths, placement of infrastructure on embankments limits damage to both the infrastructure and structures in the lee of the embankment.

7.2.6. Shizugawa Old Town, Minamisanriku Town, Miyagi Prefecture

Minamisanriku Town (Shizugawa Old Town) lies in a south-east facing bay at the junction of three river valleys. Inundation depth at the coast was greater than 11 m and resulted in heavy damage to steel frame buildings (Figure 7.30) and collapse of several two to three storey RC buildings (Figure 7.31 and Figure 7.32). Significant scour also contributed to collapse of reinforced buildings within 300 m of the coastline (Figure 7.33). Several RC buildings survived with less damage (Figure 7.34), including vertical evacuation structures, covered further in section 10.3.3. Figure 12.1 shows pre-2011 hazard maps with inundation extent from 1960 Chile tsunami, and the expected Miyagi-Oki event at Shizugawa overlaid with 11th March inundation extent. This shows clearly how much of the town was inundated against expectations.

The death toll in Minamisanriku as of 11th October 2011 is 561 dead and 341 missing (FDMA, 2011). This is 5.17% of the city"s population and 6.27% of the population estimated by the GSI to be living in the inundated zone. 82.5% of Minamisanriku"s population lived in the area inundated (MIAC, 2011).

Figure 7.30 Crisis Management Department of Minamisanriku Town, which shows the building before and after the tsunami (Anon., 2011b).

In the area up to 500 m from the port front, almost all timber frame structures suffered collapse and many steel frame structures sustained damage levels moderate to heavy damage (D2-D3). Many RC structures were observed to have damage at D2-D3, while a few suffered collapse due to extensive scour and / or debris strike.

The 3-storey steel frame Crisis Management Department building (Figure 7.30), 470 m from the harbour front, remains standing with heavy damage after inundation to a height of 10 m. Tsunami warnings were transmitted by an employee from this building via the city's loudspeakers until the last moment before the building was inundated. Thirty of the 130 staff in this building climbed up to the roof of the 3-storey building (c. 9 m high) and 20 of those died. Ten evacuees survived by clinging on to the antenna at the roof top during several minutes of flow at this height.

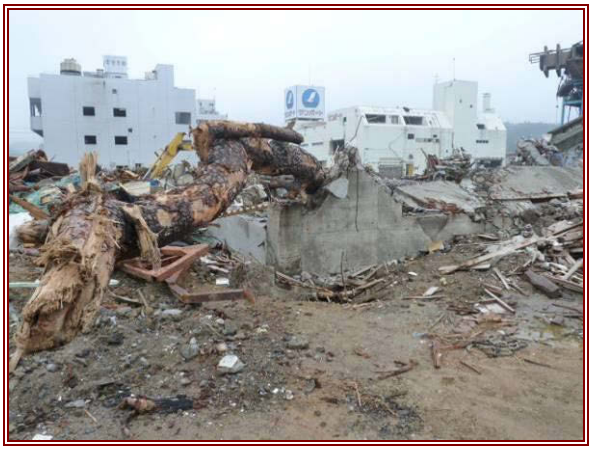

Figure 7.31 (left) Collapse of third storey of a RC building in Shiomi-cho, 100 m from the sea (38° 40' 29.10" N, 141° 26' 44.96" E).

Figure 7.32 (right) Evidence of debris strike at the site of a former gymnasium building in Shiomi-cho, 100 m from the sea. Significant scour and collapse of RC walls was observed.

Figure 7.33 (left) Significant scour in Shiomi-cho, adjacent to the former gymnasium building, 100 m from the sea. Significant scour also occurred at the apartment block (a designated vertical evacuation structure) visible in the background. This structure is discussed further in section 10.3.3.

Figure 7.34 (right) Shizugawa hospital which was inundated to roof level. In the foreground there is a marker showing the tsunami inundation depth from the 1960 Chile event to be 2.8 m. This hospital was used in vertical evacuation and is discussed in further detail in section 10.3.3.

7.2.7. Onagawa Town, Miyagi Prefecture

Onagawa Town is situated in a narrow valley exposed to the coast in the east-facing direction; to the west of the town, there is a lagoon. Maximum inundation depths here exceeded 16 m due to flow from the east. The ground floor of the hospital was inundated despite being located on a 16 m high platform 145 m from the port front (38° 26' 36.17" N, 141° 26' 43.19" E). Inundation above the 16 m platform was sufficient to float cars in the hospital car park, while vehicles were deposited on rooftops of 3-storey buildings in the low-lying main area of town. Prior to the tsunami Onagawa had a small harbour wall at the entrance to the bay (outside of the area shown in Figure 7.35); this was destroyed by the tsunami. General damage levels observed in the area less than 400 m inland were as follows: Timber – almost all D4; Steel frame – most D2 to D3; RC – many D2 and few D4.

The death toll in Onagawa Town as of 11th October 2011 stands at 571 dead and 409 missing (FDMA, 2011). This is 9.75% of the city"s population and 12.18% of the population estimated by the Geospatial Information Authority of Japan (GSI) to be living in the inundated zone. Approximately 80% of the town"s population resided in the inundation zone prior to the tsunami (MIAC, 2011).

Velocity estimates

Large amounts of video footage of inundation in this event have been shared globally via the internet. EEFIT have made preliminary estimates of flow velocity from one such video at Onagawa (Anon., 2011a). The time for a piece of apparently free-flowing debris to flow between 2 or more points of known distance (measured on aerial photographs) is recorded, and estimates of return flow velocity are made at several points (Figure 7.35). It is important to note the location of the recording as local velocity variations occur due to blockage and channelling by topography, structures or dammed debris. It is also important to note that the estimate is only of surface velocity, and sub-surface velocity may vary significantly from this. Unfortunately no suitable footage was available for estimation of inflow velocity. Drawdown velocity recorded between the two buildings of the harbour-front complex was recorded at 7.5 m/s (27 km/hr). This is compared to a recording of 6 m/s (21.6 km/hr) made 80 m further inland.

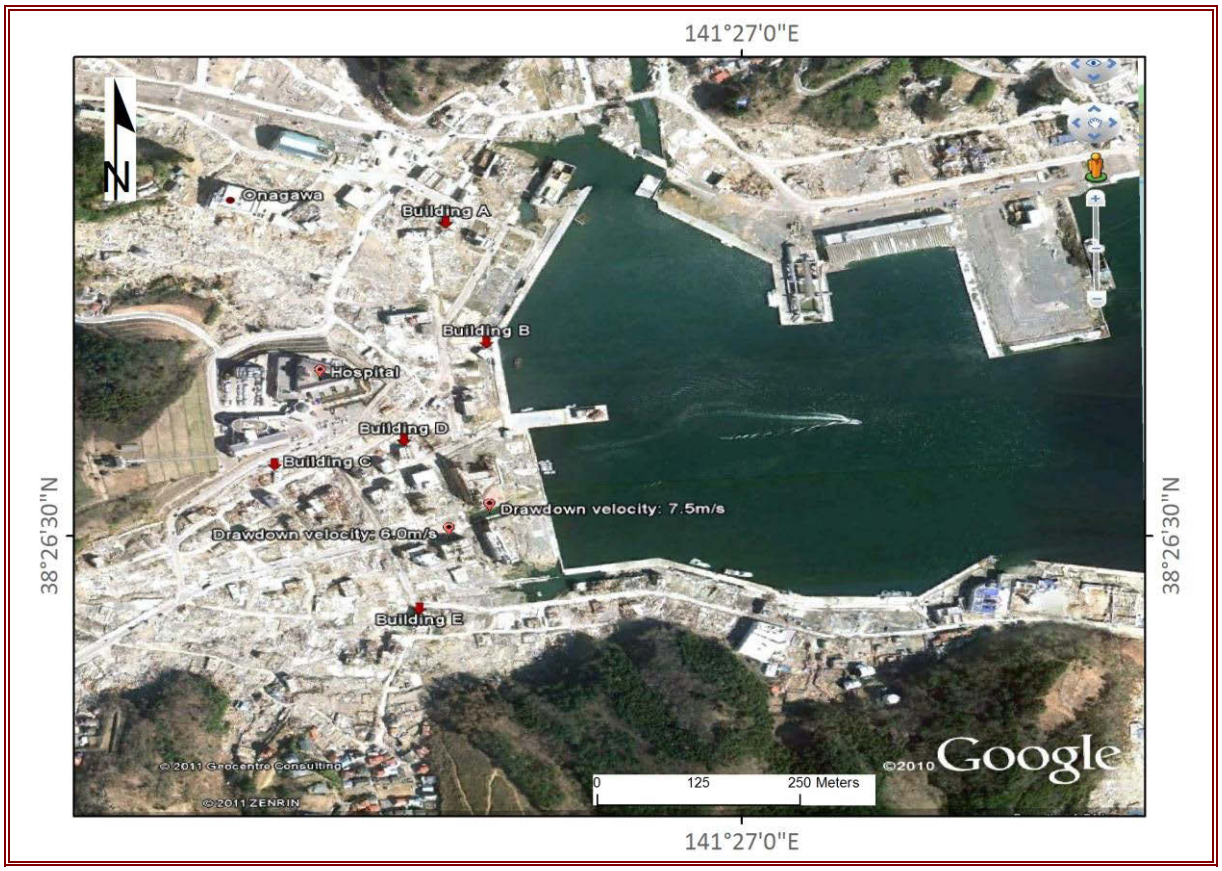

Figure 7.35 The final locations of overturned buildings in Onagawa (red arrows) and locations of EEFIT velocity estimates.

Overturning failure of RC and steel structures

At least 5 RC shear wall and steel frame structures of 2- to 4-storey were overturned in Onagawa. This type of failure had been observed in previous tsunami events for timber structures, but not for RC buildings. The aspect ratio of these buildings may have been higher than other nearby buildings and all had a small building footprint. Some had piled foundations, others were not piled – descriptions of each building are provided below. Witnesses described that the first incoming wave knocked over these buildings (Read, 2011). The failure mechanism of these structures is the subject of much investigation in the tsunami research community, and potential explanations are offered below.

Building A

This 2-storey RC shear wall structure with piled foundations was a police office that was overturned landward during tsunami inflow. The structure has 1 pile at each corner, and 3 closely spaced piles at each of the central pile caps. Refer to Figure 7.35 for the final location of this structure.

The rebar in each pile does not continue very far down the pile and they appear quite lightly reinforced at the top, suggesting they were designed only for shear, rather than also for tension. The failure looks to be due to overturning motion: the uppermost (originally seaward) piles remain connected to the pile cap and are relatively straight, suggesting that they have been pulled out of the ground and then failed in tension (Figure 7.36). In contrast, the bottom (originally landward) piles are sheared off closer to the foundation and are all bent downwards; this suggests the lateral forces imparted by tsunami flow were concentrated on the landward piles, which became the pivot point in the overturning motion. Overturning in this case may have been initiated by debris strike to the top of the structure (Figure 7.37).

Liquefaction is believed to have played a significant role in the overturning failure. During liquefaction, soil shear strength is decreased thereby decreasing resistance between the pile face and the

surrounding soil. This would allow greater lateral movement of the piles while in the ground, and enable the piles to be extracted more easily from the ground when lateral forces are applied to the building. Physical evidence of liquefaction was eradicated in the tsunami, although significant scour was evident at the time of our survey (Figure 7.38).

Another component of the flow apparently contributing to this overturning failure would be uplift forces or buoyancy, or a combination of both, as water flows beneath the foundations. The extent to which uplift or buoyancy contribute are likely determined by the structure type. As these forces are controlled by the rate of water level increase and the inundation depth (>16 m in Onagawa), these forces would be significant at these structures.

Figure 7.36 (left) Foundations of building A showing some piles remain connected to the pile cap.

Figure 7.37 (right) Evidence of a large impact at the top of the building on its seaward side.

Building B

This structure is a 3-storey RC shear wall construction, with a raft foundation (Figure 7.39). Its final location (Figure 7.35) implies the building overturned seaward, however, it is suspected that the initial failure was landward (consistent with other structures) but then the building has been moved to this final position in the tsunami flow. The raft foundation observed at this structure is inadequate for resisting the effects of scour and tsunami flow.

Building C

This structure is a 3-storey hotel of RC shear wall construction, with piled foundation (Figure 7.40). This structure lies approximately 30 m from its original position (Shuto, 2011); refer to Figure 7.35 for its final location.

Building D

This 3-storey steel frame structure has a piled RC foundation with 2 to 3 piles at each of 8 pile caps. The RC pile that remains attached to the foundation beams by only reinforcement bars (right hand side of Figure 7.42). The failure of this building appears consistent with the explanation given for building A, although it is unclear why concrete cover remained on more of the piles in building A than building D. This may be due to a different grade of concrete or level of soil liquefaction at the two sites. Refer to Figure 7.35 for the final location of this structure.

Building E

This 2-storey steel frame structure has a piled RC foundation (Figure 7.43 and Figure 7.44), similar to those in buildings A and D. No piles remain connected to the pile caps in this case, indicating a higher level of shear in the overturning motion than experienced at A and D. Refer to Figure 7.35 for the final location of this structure.

While observations from Onagawa and many other sites in this and previous events shows that RC structures are the most effective in withstanding tsunami loading, it is now clear that there are additional failure modes to consider in their resistance to tsunami loads in extreme flows around 17 m. This has vital implications for the use of RC structures in vertical evacuation strategies. Onagawa Town has planned to leave several of the overturned buildings in place as a memorial to this event (Shuto, 2011).

EEFIT observations in Onagawa appear to support the collapse threshold at >16 m inundation depth for RC structures proposed by Shuto (1993) using limited available historic data on tsunami impact on RC buildings – although it is expected that the data did not previously include overturning failure. Similar overturning failures were observed in Otsuchi (Chock, 2011, Figure 7.45), Rikuzentakata and Miyako.

Figure 7.38 (left) Scour may have contributed to the overturning failures of several RC buildings.

Figure 7.39 (right) Building B with raft foundation.

Figure 7.40 (left) Building C (a hotel) transported 30 m landward from its original location (image from Shuto, 2011).

Figure 7.41 (right) Overturned steel frame structure (building D) viewed from the hospital car park.

Figure 7.42 (left) Foundations of the overturned building D.

Figure 7.43 (right) Foundation view of building E.

Figure 7.44 (left) View of building E showing out-of-plane failure of an infill wall.

Figure 7.45 (right) An overturned RC dormitory building in Otsuchi (Chock, 2011).

Sheltering Effects

Despite extreme hydrodynamic forces in this survey zone, many buildings survived due to dense urban development affording a certain degree of sheltering. A 4-storey harbour-front complex of two buildings provided shelter to landward structures from incoming waves (Figure 7.46 and Figure 7.47). These structures suffered extensive damage to glazing, limited damage to masonry cladding, and the loss of an elevated walkway between the buildings. However, the pattern of surviving smaller buildings in the lee of these substantial structures suggests that sheltering occurred here (Figure 7.35). Of course the harbour-front structures would not have provided shelter in the return flow phase(s), but those buildings surviving the inflow phase would have exerted a sheltering influence during return flow.

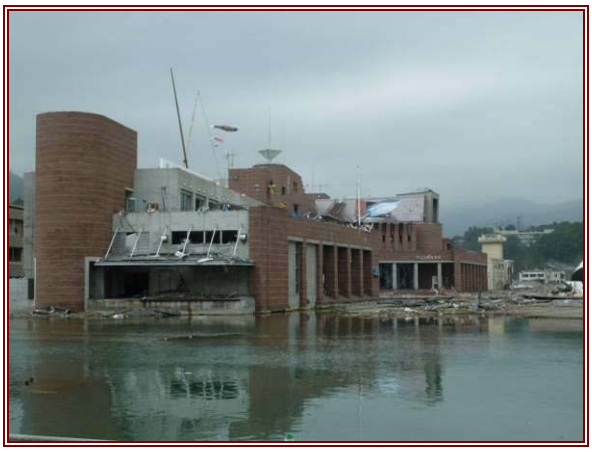

Figure 7.46 (left) Seaward side of the harbour-front buildings.

Figure 7.47 (right) Landward side of the most northern of these buildings. Heavy non-structural damage to the steel frame building is believed to have occurred during tsunami return flow.

7.2.8. Ishinomaki City, Miyagi Prefecture

Ishinomaki City is a port in Miyagi Prefecture with a population of around 163,000 and approximately 10 km of south-facing coastline, much of which is dedicated to industrial activity at the port front. Inland of the port the urban area extends 4.8 km inland at it furthest point; for the first 400 m being commercial and industrial land use, and residential and smaller commercial land use further inland. The city is divided by the Kitakami River running north to south; to both sides east of this river there is high land to an elevation of over 40 m immediately west of the river and 630 m inland, and over 100 m immediately east of the river and 860 m inland.

The inundated area of Ishinomaki was previously home to 69% of the city"s population (MIAC, 2011); as at 11th October 2011, the total number of dead and missing is 3,892 people (3,175 dead, 717 missing; FDMA, 2011). This is a fatality rate of 3.47% within the inundated area. This (along with the fatality rate of neighbouring Higashimatsushima City, 3.35%) is a relatively low fatality rate, when compared to other towns or cities where 70-80% of the population resided in the inundated area (Table 11.1): Otsuchi Town (11.36%), Rikuzentakata (11.65%), Onagawa Town (12.18%).

Inundation maps for Ishinomaki City developed in 2004 (based on an expected Miyagi-oki event of magnitude 8.0, involving rupture of multiple source zones) show the inundation in 1933 and 1960 events occurred along the river and port front only. It was estimated from this modelling that 164 people would be killed in Ishinomaki from the expected event (Miyagi Prefectural Government, 2004). Modelled tsunami height generally reaches a maximum of 3 m (4 m at one location only) along the port front, and maximum of 1 m inland of the port. The modelled inundation extent reaches only 500 m inland to the east of the river and from the southern edge of the port. In contrast, tsunami inundation on 11th March 2011 reached inundation depths of at least 4 m at 470 m and 650 m inland (EEFIT observations of watermarks on buildings) and extended inland until reaching the elevated areas with a run-up of 16 m.

Examination of aerial photographs shows that the majority of structures remain standing in the inundated area of Ishinomaki, although there are some areas of almost entire destruction observed around the mouth of the river. Figure 7.48 shows the area immediately west of the river mouth) where significant subsidence was observed and only RC buildings remain standing. There is evidence of fire in this area, with one school building showing significant fire damage at the inland extent of inundation (see section 10.1.5) where higher land occurs. Subsidence occurred up to 0.78 m (GSI, 2011b) and flooding of land adjacent the river mouth and along the port front occurs at high tide. At the time of the EEFIT investigation new raised gravel roads were being laid and repairs were being made to the coastal defences.

Figure 7.48 Area of destruction west of the Kitakami River mouth in Ishinomaki (left image is dated 25th June 2010; right image is dated 19th March 2011). The burnt school, indicated, is discussed further in section 10.1.5. Land increases in elevation abruptly, initially to around 10 m at the line of trees in the north of this image.

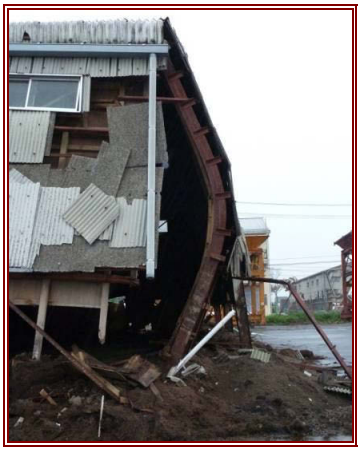

Figure 7.49 (left) Lorry trailer deposited on the first floor roof of house (centre of photo) but otherwise minor damage to the adjacent timber frame structures. Collapsed timber frame structures were also recorded at this observation point.

Figure 7.50 (right) View of the southeast corner of the steel frame warehouse. The structure was leaning landward (to the north), and the frame at the eastern end had buckled outward.

General observations of damage levels were made at points 300-400 m apart, along two transects in the eastern part of the city (6 points in North to South direction, and 17 points East to West at between 400 m and 600 m inland). No counts of structures were made in this survey, only damage levels and inundation depths. The N-S transect located in the far east of the city indicated no structural damage at 850 m (and further) inland, although there was evidence of motor vehicle flotation at this point. Timber frame structures at 400 m inland showed particular variability in damage level in one small area (observed from a single point) – damage varied from light damage (D1) to collapse (D4) – this is typical of observations on both transect surveys. The E-W survey showed significant variability of damage at each observation point: the general range of damage levels across the whole survey is as follows: timber D1-D4, steel frame D1-D3, RC D1-D2.

At 420 m inland (sheltered by a 150 m wide stand of trees that survived the tsunami), a lorry had been deposited on the first-storey roof of a residential building, indicating the extent of floating debris here. Despite the debris, several timber frame houses remain standing close by with damage of D1 (Figure 7.49), suggesting low flow velocity, although heavy damage to a steel frame building, moderate damage to one RC building and collapse of some timber structures complicates the assessment.

Observations of damage at the port front include suspected impact of large debris causing significant bending of the structural columns of a steel frame building (Figure 7.50). It was not clear at the time of our observations, what type of debris had caused the damage to this warehouse.

7.2.9. Wakabayashi, Sendai City, Miyagi Prefecture

EEFIT investigated damage to residential properties approximately 1 km from the coast in Wakabayashi, which suffered severe damage from the tsunami. The death toll in Ōfunato as of 11th October 2011 stands at 375 dead and 28 missing (FDMA, 2011), which is 4.29% of the population estimated to be live in the inundated area and 0.30% of the total population (MIAC, 2011). These figures are in contrast to the neighbouring coastal areas of Tagajo City (1.1% fatality rate in inundation zone) and Shiogama City (0.11%).

The flat terrain of this area contributed to inundation of up to 5 km inland. Many residential properties here were of timber frame construction and suffered complete collapse or were subsequently demolished by the time of our investigation. Based upon our observations, very few residences in the area visited were suitable to be re-occupied. Figure 7.51 and Figure 7.52 shows damage typical of this area and building stock.

Figure 7.51 (left) Many timber houses sustained heavy damage or partial / complete collapse (D4).

Figure 7.52 (right) Typical damage for RC electricity poles in the tsunami inundation zone.

Inundation depth in this area was approximately 7.5 m, recorded at Arahama Elementary School. Significant scour of the sandy soil (old beach deposits) on the seaward side of buildings occurred in this area, causing tilting of several structures and exposure of foundations (Figure 7.53 and Figure 7.54). Scour up to 3 m depth resulted in the collapse of a tsunami warning siren behind the toilet block structure in Figure 7.55. Out-of-plane failure of infill walls of several RC and masonry structures (Figure 7.54) was observed further east at Nakacho, approximately 100 m landward of the concrete sea defences.

Figure 7.53 (left) Tilting due to scour on the seaward side of a residential building in Wakabayashi-ku.

Figure 7.54 (right) Out-of-plane failure of RC residential structure in Wakabayashi-ku.

Figure 7.55 Extreme scour of approximately 86 m^2 around a toilet block constructed on sandy soil with shallow foundations. This building is 40 m landward of sea defences at Wakabayashi-ku.

7.2.10. Natori City, Miyagi Prefecture

The death toll in Natori City as of 11th October 2011 stands at 911 dead and 70 missing (FDMA, 2011). This is 1.34% of the city"s population and 8.07% of the population estimated by the Geospatial Information Authority of Japan (GSI) to be living in the inundated zone. Only 16.6% of the total population of Natori City resided in the inundation zone prior to the tsunami (MIAC, 2011), as the main city is located further inland. Yuriage is the main populated area at the coast in Natori City, and is located immediately south of the Natori River, with a small fishing port and harbour located adjacent to the river mouth. EEFIT investigated damage to the fishing port and residential areas of the Yuriage.

Yuriage fishing port

The hilltop shrine in Yuriage (38° 10' 20.74" N, 140° 57' 13.45" E; Figure 7.56) provides an observation point for the widespread devastation in this area (Figure 7.56 to Figure 7.58). Natori Junior High School, Elementary School and a community centre were used as vertical evacuation sites, and saved many lives. The Junior High School structure is discussed further in section 10.3.5.

Almost all of the timber frame residential building stock in Yuriage sustained complete collapse (D4), while steel and RC structures sustained damage ranging from light (D1) to collapse (D4). Examples of residential construction with open ground floor were observed (Figure 7.59). These buildings, although sustaining minor debris-induced damage on the river-facing side, appear to have avoided significant damage. It was unclear whether scour occurred at the base of the RC columns.

Figure 7.56 Post-tsunami aerial photograph of Yuriage, Natori City.

Figure 7.57 (left) View towards northeast from the hilltop shrine in Yuriage. Prior to the tsunami, this area comprised one and two storey residential buildings.

Figure 7.58 (right) View towards southwest from the hilltop shrine in Yuriage. Debris from collapsed residential and small commercial structures has been cleared from in front of these RC apartment blocks, which were inundated to the second storey.

The port building and wharf sustained partial collapse in this event. Three large scour holes (e.g. Figure 7.60) occurred at the port with footprints measuring approximately 20 m*9 m, 12 m*7 m and 20 m*11 m respectively (and each at least 1.5 m deep). The RC port building remains standing, sustained out-of-plane failure of all hollow block masonry infill walls and the second storey has been removed. The majority of reinforcement of the concrete block infill walls is un-deformed rebar.

Another example showing collapse in RC construction is located immediately inland of the port building (Figure 7.61 and Figure 7.62). The consistent failure direction of columns indicates flow direction from the east (heading of approximately 260°), which indicates that the wave arrived approximately perpendicular to the coastline, directly into the river mouth and crossing Yuriage harbour where there are no significant coastal defences.

Figure 7.59 (left) Residential buildings in Yuriage constructed with an open ground floor.

Figure 7.60 (right) Deep scour of foundations at the front left corner of Yuriage port building.

Figure 7.61 (left) Failure of RC columns showing flow direction adjacent to Yuriage port.

Figure 7.62 (right) Close-up photographs of un-deformed steel reinforcement (Pen for scale: 13 cm).

Scour of apartment blocks, Yuriage

Significant scour was observed at a row of RC apartment buildings in Yuriage. The aerial photograph below shows the location of scour to depths of 2 m around the eastern (seaward) end and northern sides of the buildings, indicated by arrows and polygons in Figure 7.63. Some of the buildings have been undercut to the extent that they have tilted (Figure 7.64 and Figure 7.65). Scour along the edge of block D extended as much as 2.5 m from the edge of the building. The predominance of scouring on the seaward end of the buildings implies this scour is occurred during the return flow of the tsunami (scouring in rivers typically occurs on the downstream-end of pier columns).

Figure 7.63 Aerial photograph of apartments in Natori with significant scour at the seaward end and northern side of each building. Scour is indicated by red polygons along the northern side of buildings, and red arrows (primarily at the south-eastern ends).

Figure 7.64 (left) View along the north side of one apartment block, illustrating scour of the full length of building.

Figure 7.65 (right) Loss of soil providing bearing capacity to support the footings resulted in significant displacement of apartment building – note the displacement of building in foreground compared to building in background.

Sendai airport terminal (38° 8' 17.13" N, 140° 55' 48.88" E)

Sendai airport terminal, 1 km inland, is a 4- storey steel and RC construction with a significant amount of exterior glazing on all floors. Inundation depth at the airport was 5.7 m and caused damage to the ground floor of the terminal – inside the terminal steel frame partition walls had been bent by debris strike, and infill panels were missing from partition walls (Figure 7.66 and Figure 7.67). While the upper floors of the terminal were unaffected by inundation, non-structural earthquake damage (damage to the suspended ceiling) caused these areas to remain closed until at least 29th May 2011. The airport resumed business on 13th April 2011 with a limited number of flights operating and some parts of the terminal still closed.

Airport staff reported that the windows broke only when struck by debris, not due to wave loading alone. No large aircraft were located at the airport when the tsunami occurred (one plane was due to land and was diverted), reducing the potential for more extensive debris damage.

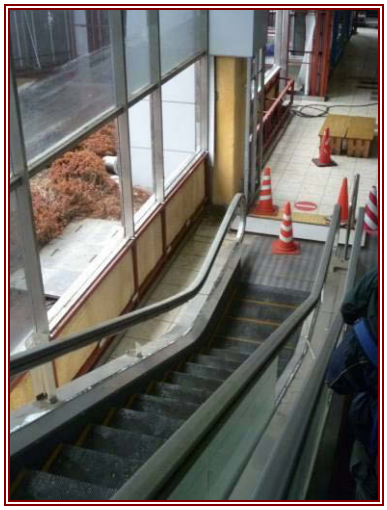

Figure 7.66 (left) View to ground floor showing damaged escalator and glazing, and 3.5 m high watermark on glazing.

Figure 7.67 (right) Damage to ground floor partition walls and clock recording the time of power outage due to tsunami inundation.

7.2.11. Yamamoto-cho and Watari, Miyagi Prefecture

Observations from Yamamoto-cho and Watari provide examples of debris impact on steel structures. One steel frame agricultural building (Figure 7.68 and Figure 7.69) located 1 km inland (37° 57' 26.39" N, 140° 54' 18.44" E) was struck on the front left side by a tree trunk measuring 0.2 m in diameter close to the impact point. The source of this tree appears to be the coastal forest and provides an example of the damage that may be caused by such defensive mechanisms even far inland. The structural columns of this building measure 0.09 m * 0.18 m. We do not have an indication of flow velocity at this location from which to estimate the force of this impact, therefore the load applied by the debris. The front right structural column also appears to be bent to a lesser extent, as a result of the initial impact. The damage to the rest of this building was typical of steel structures observed throughout the mission: steel frame remaining intact with panel walls removed by the tsunami flow.

An example of total collapse of a single storey steel frame (small commercial) building was observed where an apparent debris impact or damming effect has caused bending failure of the structural columns (Figure 7.70 and Figure 7.71). Several of the structural columns show „S-bending" of varying angle with fracturing at the base of the columns. The roof beam is also buckled as a result of the columns bending. There is no evidence of a debris impact from above – with the exception of a small hole (1 m*1 m approximately) in the corrugated roofing, there are no significant damages to the roofing material. We initially considered this to have been caused by an impact from a significantly damaged coach that was situated adjacent to the building. This conclusion was drawn from paint scratches on the coach matching the green paint on this building. However, review of satellite imagery shows no coach at this location in the days immediately after the tsunami, therefore we cannot

confirm its presence against the building. A search of aerial photographs of the immediate area has failed to confirm the final position of the coach during tsunami inundation.

It is postulated that this coach may have struck the building during the course of the tsunami but then have been washed away. As the coach impact cannot be confirmed, an alternative hypothesis is presented: that the debris inside the structure (Figure 7.71) caused a damming effect with major loading on the rear right column, which dragged the rest of the structure towards it.

Figure 7.68 (left) View of the front of steel building, struck by tree trunk on left structural column. Tsunami flow inland was towards this face of the building.

Figure 7.69 (right) View of the left side of steel building. All middle and rear structural columns are intact – only the front columns are bent by the impact of this tree trunk.

Figure 7.70 (left) View of the front left corner of the building, which appears to have been the column struck by debris.

Figure 7.71 (right) The rear of the building. This shows the buckling of one corner column and the roof beam. The structure is full of wooden debris also contains at least 4 classic cars.

7.3. Conclusions on observed tsunami damage to buildings

Tsunami damage can be extremely variable in a local urban area, as shown in the detailed damage surveys carried out in Kamaishi City and Kesennuma City. It is clear that inundation depth, direction of flow, local flow velocity variations, sheltering (during the inflow and/or during the backflow) and debris entrainment must all be considered for a complete assessment of tsunami fragility.

Debris impact is the key structural damage factor for steel frame structures – while tsunami flow alone is shown to cause significant to complete non-structural damage, it is debris impact which most often caused heavy damage or collapse of the structural members.

RC shear wall structures are confirmed once again to withstand tsunami loading. However, more research is required around reduction of scour effects, the level of debris impact they can withstand (see Minamisanriku), and preventing the toppling of piled structures (see Onagawa).

Observations in Onagawa Town support the collapse threshold at above 16 m inundation depth proposed for RC shear wall structures by Shuto (1993) - although from our field observations alone we cannot be certain at what depth the failures and/or toppling occurred as this may in fact have been below the 17 m maximum flow.

Modern construction methods have not been shown to significantly reduce the level of damage in timber frame construction compared to previous events, however, raising timber structures on RC open-structure ground floors has been shown to successfully mitigate damage in inundation depth 6 m and below. This should be a consideration in reconstruction of residential areas as long as potential soft-storey effects during ground shaking are also addressed.

For risk assessment purposes there is also a need to establish a widely accepted tsunami damage and intensity scale related to the various types of building contents in relation to the type of building structure and main tsunami attributes such as inundation depth and velocity.

7.4. References

Anon., 2011a. *New Tsunami Video: Onagawa engulfed by high water – Japan Earthquake 2011* [video online] Available at: <http://japanearthquake.newbfaq.com/2011/07/03/video-recent-tsunami-video-onagawa-engulfed-by-high-water-japan-earthquake-2011-stabilized/> [Accessed 5 July 2011].

Anon., 2011b, 安否不明の町長生還　骨組みだけの庁舎で一夜　宮城・南三陸. *Kahoku Shimpo*, [online] 14 March. Available at: <http://www.kahoku.co.jp/news/2011/03/20110314t13031.htm> [Accessed on 19 March 2011] (in Japanese).

Anu, 2011. "Sea of fire Kesennuma harbor" fire to houses in the city, even explosions. *2011 Japan Tsunami*, [blog] 11 March. Available at: <http://2011japantsunami.blogspot.com/2011/03/sea-of-fire-kesennuma-harbor-fire-to.html> [Accessed 1 July 2011].

CCH, 2000. City and County of Honolulu. Department of Planning and Permitting of Honolulu Hawaii, Chapter 16, City and County of Honolulu Building Code, Chapter 6, Article 11.

Chock, G., 2011. Japan Tsunami Reconnaissance Team – Day 3: More Evidence of Overwhelmed Seawalls, *American Society of Civil Engineers* [online] 13 April, Available at: <http://cms.asce.org/PPLContent.aspx?id=12884906357> [Accessed 30 June 2011].

EEFIT, 2005. The Indian Ocean Tsunami of 26 December 2004: Mission Findings in Sri Lanka and Thailand. Earthquake Engineering Field Investigation Team (EEFIT) Report. The Institution of Structural Engineers, London, UK. Available at: <http://www.istructe.org/knowledge/EEFIT/Documents/Indian_Ocean_Tsunami.pdf> [Accessed 1 June 2011].

FDMA, 2011. Fire and Disaster Management Agency of Japan, Report 140 on the effects of the March 11, 2011 Great Tōhoku earthquake, October 11, 2011. Available at: <http://www.fdma.go.jp/bn/2011/detail/691.html> [Accessed 10 November 2011].

GSI, 2003a. *GSI Web e-Land system (open source version) (Ver.3)*, [online] Available at: <http://portal.cyberjapan.jp/denshi/index3.html> [Accessed 5 July 2011] (in Japanese).

GSI, 2003b. *GSI Web e-Land system (open source version) (Ver.3)*, [online] Available at: <http://portal.cyberjapan.jp/denshi/opencjapan.cgi?x=141.59375&y=39.1875&s=10000> [Accessed 20 July 2011] (in Japanese).

GSI, 2011b. *Year 2011 (2011) due to earthquake subsidence investigation northeastern Pacific Ocean off the coast*, Geospatial Authority of Japan [online] Available at: <http://www.gsi.go.jp/sokuchikijun/sokuchikijun40003.html> [Accessed 20 July 2011] (in Japanese).

Hatori, T., 1984. On the damage to houses from tsunamis. *Bulletin of the Earthquake Research Institute, University of Tokyo*, 59, pp. 433-439.

IEDM, 2011. *Mega Disaster in a Resilient Society, The Great East Japan (Tōhoku Kanto) Earthquake and Tsunami of 11th March 2011, Synthesis and Initial Observations*, International Environment and Disaster Management, Graduate School of Global Environmental Studies, Kyoto University, 25th March 2011.

Koshimura, S., Namegaya, Y. and Yanagiawa, H., 2009. Tsunami Fragility – A New Measure to identify Tsunami Damage. *Journal of Disaster Research,* 4(6), pp.479-488.

MIAC (2011). Estimation of the population in the tsunami inundation zone, by municipality (analysis by the Geographical Information Authority of Japan). Ministry of Internal Affairs and Communications. Available at: <http://www.stat.go.jp/info/shinsai/zuhyou/sinsui.xls> [Accessed on 4 August 2011].

Miyagi Prefectural Government, 2004. *Summary of the third survey in Miyagi Prefecture earthquake damage estimation*, Miyagi Prefectural Government Crisis Control Division [online] (updated 8 June 2004) Available at: <http://www.pref.miyagi.jp/kikitaisaku/jishin_chishiki/3higaishin/index.htm> [Accessed 20 July 2011] (in Japanese).

MLIT, 2011. *Status Survey results affected by the earthquake East (First Report)*. Ministry of Land, Infrastructure, Transport and Tourism Press Release, 4th August 2011. Available at: <http://www.mlit.go.jp/common/000162533.pdf > [Accessed 6 August] (in Japanese).

Nippon Sekai, 2011. *Raw footage released by the Japan Coast Guard of the tsunami and fires in Kesennuma.* [video online] Available at: <https://picasaweb.google.com/lh/photo/cNrrglyXPo5W6-6l4ysuvl6-HV4XK8khGfVE4K2xJdY?feat=embedwebsite> [Accessed 1 July 2011].

Okazaki, K., 2008. *Institutional Mechanism of Building Code Implementation in Japan* [online] Available at: http://www.hyogo.uncrd.or.jp/hesi/pdf/nepal08/training/okazaki2.pdf [Accessed on 4 July 2011].

RCC, 2009. *Building Regulations – Japan*, Inter-Jurisdictional Regulatory Collaboration Committee. [online] (Updated 16 October 2009) Available at: <http://www.irccbuildingregulations.org/pdf/Japan_structure.pdf> [Accessed 4 July 2011].

Read, R., 2011. Japan's 60-foot tsunami overturned four-story concrete building, shattering safety and engineering strategies (Oregonian in Japan). *The Oregonian*, [online] (Last updated 07:59 17 April 2011) Available at: <http://www.oregonlive.com/today/index.ssf/2011/04/surveying_what_survived_the_quake_and_tsunami_--_and_what_didnt_oregonian_in_japan.html> [Accessed on 21 June 2011].

Shuto, N., 1993. Tsunami intensity and disasters. In: Tsunamis in the World, *Fifteenth International Tsunami Symposium,* Vienna, Austria, 15 August 1991. Dordrecht: Kluwer Academic Publishers.

Shuto, N., 2011. „Onagwa Memorial Park", *ITIC Tsunami Bulletin Board*. [online] 12 June 2011, Available at: <http://infolist.nws.noaa.gov> [Accessed 21 June 2011].

8. Field observations on geotechnical effects

Geotechnical failures such as ground settlements, landslides, liquefaction and coastal subsidence were observed in the Tōhoku region. This chapter presents details on these observations. Other geotechnical related failures such as overturning of buildings due to uplift of shallow foundations and shearing of slender pile are presented in section 7. Based on Figure 8.1, liquefaction was reported extensively in the Kanto region in areas of fill material and alluvium (GEER, 2011; Tokimatsu et al., 2011). In contrast, the figure appears to show that there are not many areas of significant soil liquefaction reported in the Tōhoku region. This trend could partly be due to the removal of common evidence of liquefaction by tsunami flow, such as sand boils and lateral spreading in the tsunami affected areas. This is in need of further investigation. Many sites with major geotechnical damage had been repaired or cleared by the time of the EEFIT reconnaissance. Nevertheless, many significant geotechnical failures were still visible, especially after debris was removed at the time of survey.

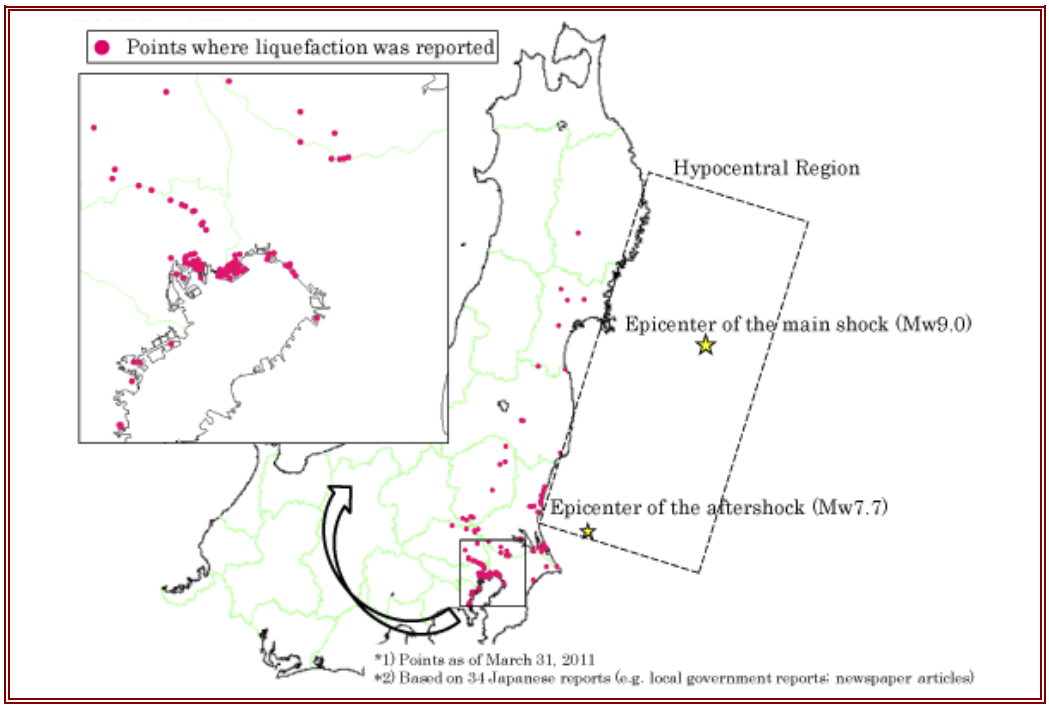

Figure 8.1 Locations of significant liquefaction due to the 11th March 2011 earthquake (Shimizu Corp, 2011).

8.1. Ground settlement

8.1.1. Yamato-machi, Sendai City, Miyagi Prefecture

Several locations in the eastern outskirts of Sendai City (near to the coast) suffered ground settlements. Figure 8.2 shows a 6-storey reinforced concrete (RC) building where the structure has settled relative to the surrounding soil. The adjacent air-conditioner compressor was tilted, indicating weak soil condition. This is substantiated with the borehole data indicating low SPT values at shallow soil depth in Sendai as shown in Figure 8.3. Due to the high water table in combination with the sandy nature of the soil, such effects could also be the result of soil liquefaction. However, there was no other clear indication of liquefaction nearby to confirm the hypothesis. On the contrary, many high-rise buildings in Sendai suffered lower settlement relative to the adjacent soil as shown in Figure 8.4. The difference between the two cases could be due to the difference in pile penetration depth. At further locations, sand boils were observed within the vicinity of the K-NET station near the Oroshi district. The difference between the two cases could be due to the difference in pile penetration depth.

Some damage due to ground settlement was observed on external staircases, parapets and roadways leading to car parks at the ground level as shown in Figure 8.5. Significant settlements measuring as much as 70 mm were observed. However, these generally did not affect the structural integrity of these buildings, which are most likely sited on deep foundations. Some low-rise buildings founded on shallow footings suffered damage that rendered them unsuitable for occupancy. In the case of low-rise wooden structures, the damage was predominantly structural rather than geotechnical as illustrated in Figure 8.6.

Figure 8.2 Settlement of a 6-storey building in Yamoto-machi, Sendai City.

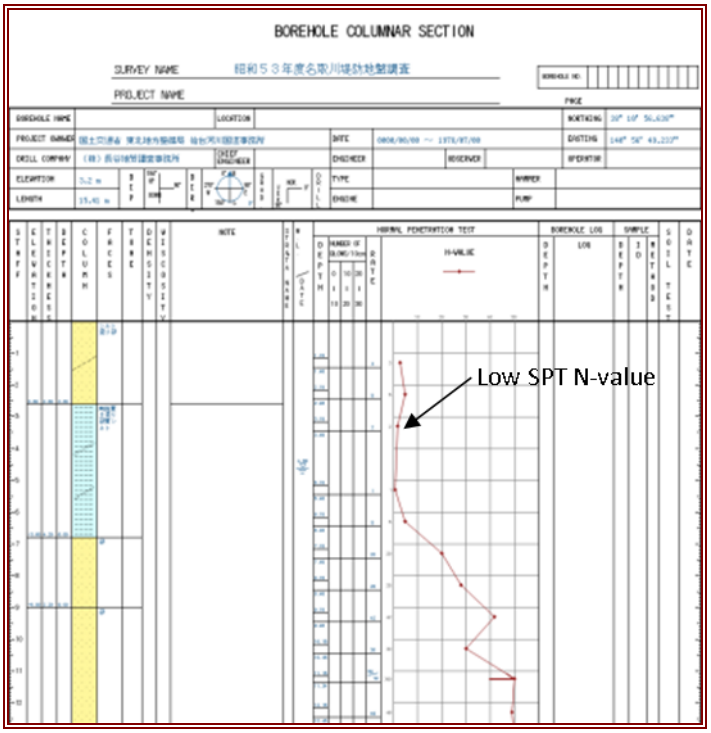

Figure 8.3 Borehole data near areas of suffering from ground settlement (Courtesy of the Ministry of Land, Infrastructure, Transport and Tourism of Japan, MLIT).

Figure 8.4 Lower building settlement relative to surrounding ground, in Yamato-machi, Sendai City.

(a) (b)

Figure 8.5 Settlement-induced damage to (a) car park roadway and (b) external staircase.

Not far from the buildings shown in Figure 8.2 and Figure 8.4 to Figure 8.6, the 14-storey Takasago residential apartment building located about 3 km east of the MYG013 K-NET station suffered significant differential settlement. This building consists of two blocks which are connected by expansion joints. The building, constructed in 1975, suffered damage during the 1978 Miyagi-Oki earthquake with cracking to non-structural walls in the lower part of the building. Repairs were done by replacing damaged RC walls with new ones of increased thickness (NILIM and BRI, 2011). In the 2011 Tōhoku earthquake, differential settlement led to the tilting of one of the building blocks by approximately 2 degrees (see Figure 8.7a). The significant settlement of the building is substantiated in Figure 8.7b. The EEFIT team learned from site interviews that the substantial complex will have to be demolished due to the damage sustained in this earthquake.

Figure 8.6 Earthquake-induced damage on low-rise wooden structures

(a) Left block has tilted due to differential settlement (b) Ground settlement adjacent to building

Figure 8.7 Damage to the Takasago apartment building in Sendai City.

8.2. Slope Failure

8.2.1. Oritate, Sendai City, Miyagi Prefecture

In the mountainous terrain of Sendai, several low-rise residential houses at Oritate suffered damage due to slope failure. These houses are relatively new and are sited on shallow foundations which displaced significantly due to movement of the soil surface layer during ground shaking (Figure 8.8). Tension cracks were also widely observed on the ground. The affected houses had been evacuated and labelled „unsafe" for occupancy. EEFIT was informed by locals that the residential development was built on fill material. Houses sited at boundary areas between cut and fill can also result in significant differential strains, thereby causing more damage. Improvements to either the condition of the ground or to the foundations of these houses and retaining walls may be necessary to prevent similar slope failure in times of heavy rainfall and further strong earthquake shaking. A landslide warning siren was audible at the time of our visit, as it was raining heavily.

(a) (b)

(c) (d)

Figure 8.8 Damage to houses (a, b, d) and tension cracks (c) due to slope instability in Oritate, Sendai City.

8.2.2. Komine Castle, Shirakawa, Fukushima Prefecture

EEFIT investigated several landslide sites in Shirakawa. The Komine Castle was affected by landslides at slopes around the castle embankment as shown in Figure 8.9. These slopes failed due to the increase in active force on the cobble rock walls due to the strong ground shaking. The increased horizontal active force was significantly greater than the weight of the cobble rocks, which led to the toppling of the wall. Based on our observations, the provision of drainage in the form of weep holes was expected to be sufficient between these large cobbles. There were minimal ties between the cobbles to hold the wall in the horizontal direction. The majority of the cobbles near the base of the wall remained intact in these landslides, which further substantiates the above mechanism rather than a slip-circle failure.

(a) (b)

Figure 8.9 Cobble wall failure and landslides around the perimeter of the embankment in the Komine Castle.

8.2.3. Hanokidaira, Shirakawa, Fukushima Prefecture

Another landslide was investigated in the village of Hanokidaira. This is the most significant earthquake-induced landslide reported in this region. The landslide was also reported with aerial photographs in the survey report by PWRI (2011) (Figure 8.10). The landslide killed 13 people and destroyed 10 houses along the path of the runoff. The estimated size of the landslide is 150 m in length and 60 m in width, and the runoff volume was about 10,000 m^3 (Umemura, 2011). The size of the landslide is shown by the presence of an team EEFIT member in Figure 8.11a. Silty sand was observed at the exposed landslide slip surface. Only the foundations of these houses remain as shown in Figure 8.11b. A road adjacent to the debris runoff was also buried, but this had been repaired and the debris moved to the sides of the road at the time of the reconnaissance.

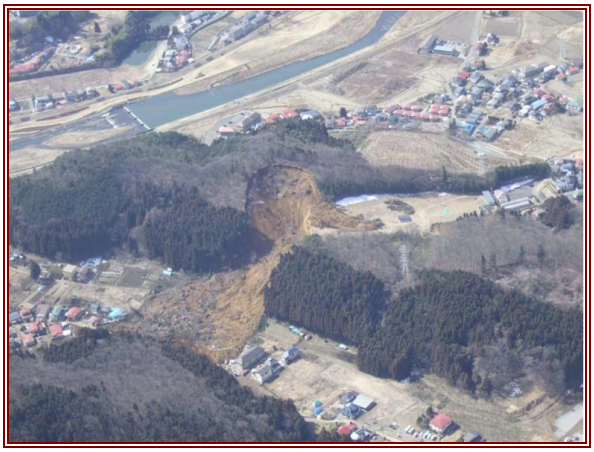

Figure 8.10 Aerial photograph of the landslide at Hanokidaira, Shirakawa (PWRI, 2011).

(a) View of landslide (EEFIT member circled in red) (b) Foundations of destroyed houses remained

Figure 8.11 Landslide viewed from the ground at Hanokidaira, Shirakawa, Fukushima Prefecture.

8.2.4. Akasaka, Shirakawa, Fukushima Prefecture

Another landslide was observed in Akasaka (Figure 8.12a). The road adjacent to the landslide was closed at the time of visit (Figure 8.12b). Based on Figure 8.12c, the landslide consisted of a few loose sections of soil mass displaced from the original slope profile. Tension cracks could also be seen further up the slope as shown in Figure 8.12d, where there is an agriculture plain. With more exposure of the soil to rainfall seepage through tension cracks on the surface of the slope, the loose sections of soil may move further downslope over time. This might be the reason for the apparent delay in road repair at this site.

8.3. Earthquake-induced Liquefaction

8.3.1. Nishishirakawa, Shirakawa, Fukushima Prefecture

Based on other reconnaissance reports (GEER, 2011 and Takahashi, 2011), it was understood that repair work on liquefaction-induced damage to roads and levees has been carried out swiftly. Hence, most evidences of soil liquefaction in the form of sand boils or lateral spreading had been cleared up at the time of the EEFIT reconnaissance. There was, however, some evidence of soil liquefaction observed in the rural areas between Shirakawa and Sukagawa. Manholes have popped above ground level, leading to obstructions to traffic as shown in Figure 8.13a. These manholes generally have a lower submerged unit weight than the surrounding soil. As such, this inherent buoyancy may cause the manholes to float when the surrounding soil liquefies. Lateral spreading was also observed near the raised manholes, as illustrated in Figure 8.13b. The presence of high water table provided by the adjacent agriculture fields could also have encouraged liquefaction to occur at this site.

(a) Landslide at Akasaka (b) Road buried by landslide debris

(c) Loose sections of displaced soil (d) Tension cracks near summit of slope

Figure 8.12 Landslide at Akasaka, Shirakawa, Fukushima Prefecture.

(a) Uplift of manhole (b) Lateral spreading

Figure 8.13 Soil liquefaction induced damage in Nishishirakawa, Shirakawa, Fukushima Prefecture.

8.3.2. *Sendai Port, Miyagino Ward, Sendai, Miyagi Prefecture*

In Sendai Port, lateral spreading led to significant damage to footpaths, street lamps and landscape structures as shown in Figure 8.14. Liquefaction of the sandy beach deposits reduced the shear strength of the soil beneath the concrete pyramid, thereby resulting in its collapse. Tension cracks parallel to the coast resulting from lateral spreading were still visible on the ground which provides evidence of liquefaction. Further inland, uplift (Figure 8.15a) and separation of tarmac from the sub-base of roads (Figure 8.15b) were observed. In these two adjacent locations, the combined effects of tsunami flow action on the tarmac with possible soil liquefaction can be observed. Seepage of fast flowing tsunami water underneath the thin layer of tarmac can cause uplift pressure and deformation of the paved surface. Soil liquefaction leading to excess pore water pressure build-up below the tarmac may also have taken place prior to the tsunami arrival, facilitating the uplift.

(a) Lateral spreading at the port edge (b) Tension cracks on pavement

Figure 8.14 Damage to pavements at Sendai Port due to lateral spreading.

(a) Uplift of tarmac (b) Separation of tarmac from sub-base

Figure 8.15 Damage to roads due to tsunami action and possible liquefaction at Sendai Port.

8.4. Coastal Subsidence

Significant land subsidence has been reported by the Geospatial Information Authority of Japan (GSI, 2011). Ground elevations were measured by GPS on 14th April 2011 and compared against pre-earthquake values. Table 8.1 shows the measured land subsidence of key coastal areas in the Tōhoku region. As a result of the subsidence, the area of land below sea level at the Sendai plain in Miyagi Preference grew five times larger, from 741 acres (3 km^2) to 3,952 acres (16 km^2), according to the Ministry of Land, Infrastructure, Transport and Tourism (NHK, 2011). Figure 8.16 shows the area affected by the subsidence at the Sendai plain. As a result of the subsidence, there has been frequent tidal flooding since 11th March in most locations visited by EEFIT: Ishinomaki City, Onagawa

Town, and Kesennuma City are particularly notable examples. In addition to the threat of rising sea level due to climate change, the heavy summer rains and higher tides in autumn would also exacerbate the problem. The effects of typhoon and associated storm surge would also likely cause more extensive flooding than before.

Table 8.1 Measured land subsidence along the coast of Tōhoku with locations listed north to south (GSI, 2011)

Location	Prefecture	Land Subsidence (m)
Miyako City	Iwate	0.50
Yamada Town	Iwate	0.53
Kamaishi City	Iwate	0.66
Ōfunato City	Iwate	0.73
Rikuzentakata	Iwate	0.84
Kesennuma City	Miyagi	0.74
Minamisanriku Town	Miyagi	0.69
Oshika Peninsula	Miyagi	1.20
Ishinomaki City	Miyagi	0.78
Iwanuma City	Miyagi	0.47
Soma	Fukushima	0.29

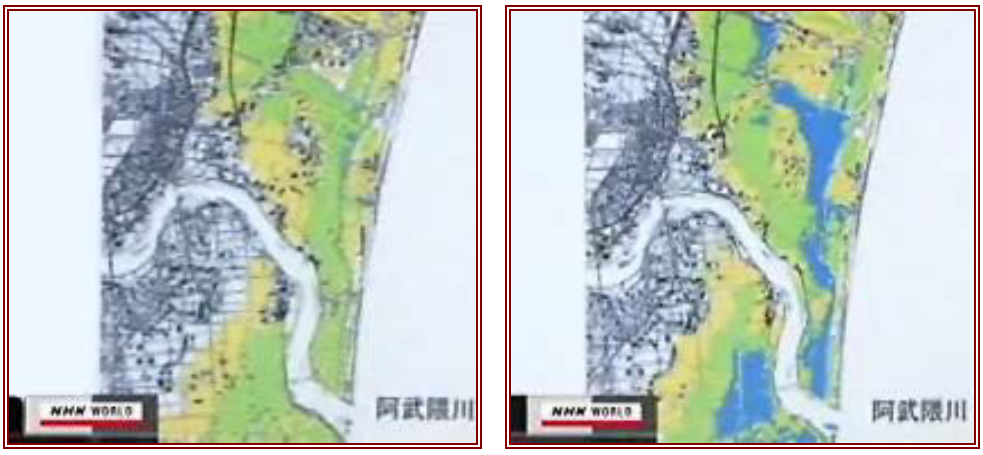

(a) Before earthquake (b) After earthquake

Figure 8.16 Increase in area below sea level due to land subsidence from the earthquake (NHK, 2011).

8.5. Conclusions on geotechnical effects

Based on field observations, it is evident that the earthquake and tsunami had a devastating effect on coastal communities in Tōhoku. Inland, ground settlement has generally not compromised the structural integrity of buildings in in the Tōhoku region. However, slope failures did result in significant displacement of low-rise residential houses sited on shallow foundations in mountainous terrain. Landslides have also led to casualties and property losses. Evidence of soil liquefaction such as lateral spreading and the floatation of manholes were observed. Liquefaction is likely to have occurred near the tsunami affected coastline but much of the evidence would have been washed away by the ensuing tsunami flow. Following these field observations, it may be prudent to construct buildings with sufficiently deep pile foundations to avoid significant settlement, slope stability and liquefaction-related issues. In addition, these failures also indicate the necessity to perform ground improvements to weak backfill deposits.

8.6. References

Geotechnical Extreme Events Reconnaissance Association, GEER (2011).Geotechnical Quick Report on the Kanto Plain Region during the March 11, 2011, Off Pacific Coast of Tōhoku Earthquake, Japan. [Online] <http://www.geerassociation.org/GEER_Post%20EQ%20Reports/Tōhoku_Japan_2011/Cover_Tōhoku_2011.html> [Accessed on 29 Jun 2011].

Geospatial Information Authority of Japan, GSI (2011).The March 11, 2011 Tōhoku Pacific Earthquake Land Subsidence Investigation. [Online] <http://www.gsi.go.jp/sokuchikijun/sokuchikijun40003.html> [Accessed 01 Jul 2011] (In Japanese).

National Institute for Land and Infrastructure Management, NILIM and Building Research Institute, BRI (2011). Quick Report of the Field Survey and Research on the 2011 Tōhoku Earthquake [online] <http://www.kenken.go.jp/japanese/contents/topics/20110311/0311quickreport.html> [Accessed 30 June 2011] (in Japanese).

Nippon Hōsō Kyōkai, NHK (2011). 28 Apr 2011 – Gov't warns of risk from quake-caused subsidence. [Online] <www.nhk.or.jp/daily/english/28_31.html> [Accessed on 01 July 2011].

Public works research institute, PWRI (2011). Landslides Triggered by the 2011 off the Pacific Coast of Tōhoku earthquake (2011 Great East Japan earthquake). [Online] <http://www.pwri.go.jp/team/landslide/topics/topics_Tōhokujishin2011-1.htm> [Accessed on 29 Jun 2011].

Shimizu Corporation (2011). General Perspectives/Report on the Tōhoku Area Pacific Offshore Earthquake. [Online] <http://www.shimz.co.jp/english/theme/earthquake/outline.html> [Accessed on 29 Jun 2011]

Takahashi, A. (2011). Preliminary Report on the 2011 Off the Pacific coast of Tōhoku Earthquake: Liquefaction Induced Damage on Leeves and Embankment. [Online] <http://eqclearinghouse.cuee.titech.ac.jp/groups/Tōhoku2011/wiki/2dfca/Levees_and_Lifelines.html> [Accessed on 29 Jun 2011].

Tokimatsu, K., Tamura, S., Suzuki, H. and Katsumata, K. (2011). Quick Report on Geotechnical Problems in the 2011 Tōhoku Pacific Ocean Earthquake (In Japanese). [Online] <http://eqclearinghouse.cuee.titech.ac.jp/groups/Tōhoku2011/wiki/01411/Geohazard.html> [Accessed on 29 Jun 2011].

Umemura J. (2011). Landslide and failure of slopes. The First Symposium for the Great East Japan earthquake. Sendai, Japan. (in Japanese).

9. Effects of the earthquake and tsunami on the energy sector and other industries

9.1. Effects on nuclear power stations

Several nuclear power facilities were affected by the severe ground motions and multiple large tsunami waves generated during the M_W9.0 Tōhoku earthquake of 11th March 2011. These were (from North to South): Tōhoku/Higashidori, Onagawa, Fukushima Daiichi and Fukushima Daini and Tokai (Figure 9.1).

Eleven reactors (Onagawa Unit 1,2,3; Fukushima Daiichi 1,2,3; Fukushima Daini 1,2,3,4; and Tokai Daini) were automatically shut down at the onset of earthquake shaking. The operational units at these facilities were successfully shutdown by the automatic systems installed as part of the design of the nuclear power plants to protect against earthquakes. However, the subsequent large tsunami waves affected these facilities to varying degrees, with the most serious consequences occurring at the Tokyo Electric Power Company (TEPCO) owned Fukushima Daiichi plant (IAEA, 2011a).

The tsunami caused significant damage to several of the Fukushima Daiichi reactors, leading to a significant nuclear incident rated at International Nuclear Event Scale Level 7 (major release of radioactive material with widespread health and environmental effects requiring implementation of planned and extended countermeasures). Investigations into the incident at Fukushima Daiichi and its causes are underway and this is having significant impact on the nuclear industry and Japanese government. It has been particularly noted that the Nuclear and Industrial Safety Agency (part of the Japanese Nuclear Regulatory Regime) within the Ministry of Economy, Trade and Industry is not sufficiently independent to provide robust regulation (IAEA, 2011a).

9.1.1. Fukushima Daiichi Nuclear Power Station (NPS)

Fukushima Daiichi NPS is located near Okuma Town and Futaba Town, Futaba County, Fukushima Prefecture and consists of six reactors that commenced operation between 1971 and 1979 (IAEA, 2011a). The total power generating capacity of the facilities is 4696 megawatts (MW). A site plan is shown in Figure 9.2.

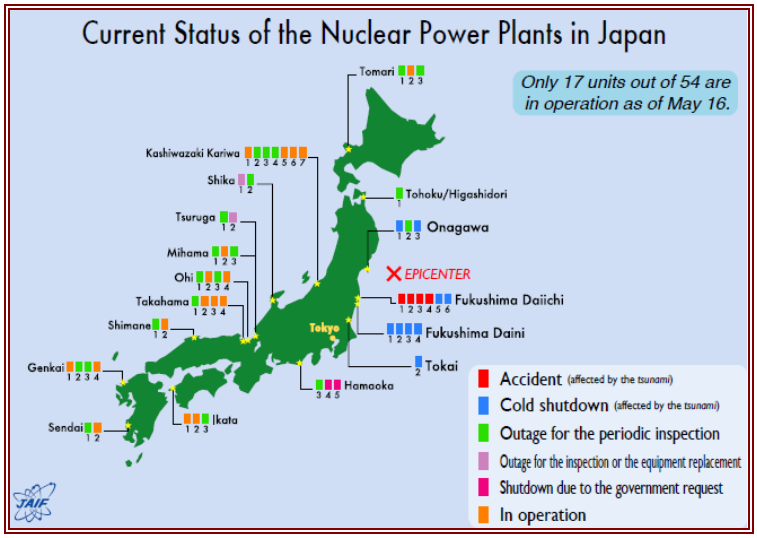

Figure 9.1 (left) Status of Japanese nuclear power stations as May 16th 2011 (JAIF, 2011a).

Figure 9.2 (right) Fukushima Daiichi site plan (TEPCO, 2011a).

At the time of the earthquake, 3 reactors were in operation and the remaining 3 were already shut down for maintenance (TEPCO, 2011b). All units at the site have been out of action since the earthquake (Figure 9.1). It is believed that there has been a fuel meltdown at three of the reactors and spent fuel ponds at the site have also been damaged.

The damage at this power station was mainly caused by the tsunami; however, there was seismic damage to the external grid infrastructure that resulted in the loss of external power supplies. This was critical because, whilst operating, the station uses the electricity it generates to power its essential systems and services. However, once it is shut down it is reliant on the external grid, on-site emergency diesel generators or other reactors at site for AC power (ONR, 2011).

Seismic observations

Table 9.1 shows the maximum response acceleration in three orthogonal directions recorded on 11th March 2011 compared to the standard seismic ground motion (Ss) at the site at the bottom floor of the six reactor buildings. The standard seismic ground motion is the design ground motion caused by a potential plate boundary earthquake off the coast of Fukushima Prefecture, an intraslab earthquake beneath the site, an earthquake by capable fault around the site and possible earthquakes from diffuse seismicity. The design standard seismic response spectra have a probability of exceedance which varies (dependant on period) between 10^{-5} and 10^{-6} per annum (1 in 100,000 and 1 in 1,000,000), IAEA (2011b).

The recorded maximum horizontal acceleration on 11th March 2011 was 550 Gal (0.56g) and maximum vertical acceleration was 302 Gal (0.31g) and it can be seen that observed maximum acceleration is generally less than the design standard seismic ground motion except for the cases shown in bold (Table 9.1).

Table 9.1 Maximum observed and design response acceleration at Fukushima Daiichi NPS. Values in bold indicate observed response greater than response against standard seismic ground motion (TEPCO, 2011b).

Seismometer Location (lowest basement of reactor building)	Observed max. response acceleration on 11th March 2011, in gal			Max. response acceleration against standard seismic ground motion (Ss), in gal		
	Horiz. N-S	Horiz E-W	Vertical	Horiz. N-S	Horiz E-W	Vertical
Unit 1	460	447	258	487	489	412
Unit 2	348	**550**	302	441	438	420
Unit 3	322	**507**	231	449	441	429
Unit 4	281	319	200	447	445	422
Unit 5	311	**548**	256	452	452	427
Unit 6	298	444	244	445	448	415

Tsunami observations

The design tsunami height was 5.4 to 5.7 m (JSCE, 2002) and to include a margin of safety the elevation of the plant was set higher (IAEA, 2011b) – the site elevation of Fukushima Daiichi NPS is 10 m at Units 1 to 4, and 13 m at Units 5 and 6. The tsunami on 11th March 2011 was 14 to 15 m high as it struck the sea defences and overwhelmed the sea protection walls of the plant shown in Figure 9.2 and Figure 9.3 (TEPCO, 2011b).

At the time of construction, the absence of historic large tsunami at this location led to under-estimation of the tsunami hazard in the design of sea wall protection for the plant (Horiuchi, 2011). The potential for large earthquakes and tsunami exceeding those previously experienced at the site was revealed by installation of GPS monitoring offshore of Fukushima Prefecture in 2003. Despite this, no modifications to the plant sea defences were made (Horiuchi, 2011).

Figure 9.4 shows the extent of inundation at Fukushima Daiichi. As the sea water pump facilities for component cooling were at an elevation of between 5.6 to 6 m at Fukushima Daiichi NPS, all units were flooded by the tsunami. Emergency diesel generators and switchboards installed in the

basement floor of the reactor buildings and turbine buildings (elevation: 0 to 5.8 m) were generally flooded and the emergency power source supply was lost. However, in Unit 6, one generator installed on the first floor of the diesel generator building was not flooded and the emergency power supply was available.

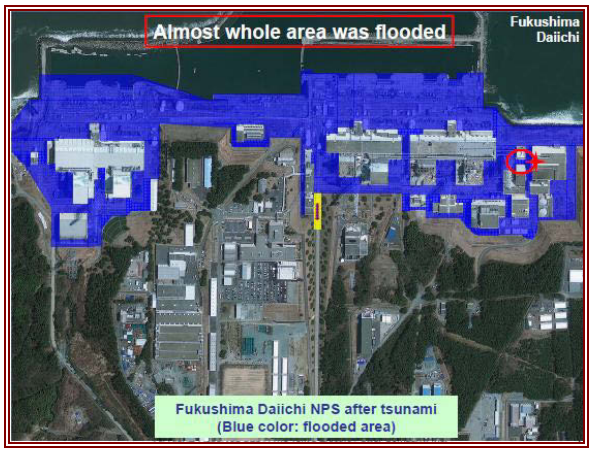

Figure 9.3 (left) Tsunami overtopping sea defences at Fukushima Daiichi (TEPCO, 2011b).

Figure 9.4 (right) Areas of the Fukushima Daiichi NPS inundated by tsunami (TEPCO, 2011b).

9.1.2. Fukushima Daini NPS

Fukushima Daini NPS is located approximately 12 km south of Fukushima Daiichi NPS. Fukushima Daini NPS consists of four reactors that commenced operation between 1982 and 1987. The reactors at the site each have a power output of 1100 MW. All four reactors were in operation at the time of the earthquake (IAEA, 2011b).

Most of the damage at the site was due to the tsunami, with only comparatively minor seismic damage. As shown in Figure 9.1, all four reactors have been left in cold shutdown since the earthquake. As at Fukushima Daiichi, there was seismic damage to the external grid infrastructure which affected power supply to the plant.

Seismic observations

Table 9.2 shows the maximum recorded response acceleration on 11th March 2011 compared to the standard seismic ground motion at the site in three orthogonal directions at the bottom floor of the reactor buildings. Maximum horizontal acceleration was 277 Gal (0.28g) and maximum vertical acceleration was 305 Gal (0.31g). It can be seen that the maximum acceleration of observation records from all units were smaller than maximum response acceleration generated by the standard seismic ground motion.

Tsunami observations

Fukushima Daini NPS consists of a low lying area where seawater pumps are located and a raised area where the reactor buildings are located. The design tsunami height was 5.1 to 5.2 m, again assessed using the method produced by JSCE (2002). The inundation height was 6.5 to 7 m, and approximately 14 to 15 m at the raised area as the tsunami funnelled along a narrow space between the south side of a reactor unit and the slope in the raised area.

Tsunami inundation at Fukushima Daini is shown in Figure 9.5 and was not as significant as at the Fukushima Daiichi site (TEPCO, 2011b). The sea water pump facilities for cooling of all units (elevation: 6 m) were flooded by tsunami and stopped working at all units except Unit 3. The emergency diesel generators installed in the basement of the reactor buildings (elevation: 0 m) continued functioning for Unit 3 and 4, however, these failed for other units due to flooding (IAEA, 2011b).

Table 9.2 Maximum observed and design response acceleration at Fukushima Daini NPS (TEPCO, 2011b).

Seismometer location (lowest basement of reactor building)	Observed max. response acceleration, in gal			Max. response acceleration against standard seismic ground motion (Ss), in gal		
	Horiz. N-S	Horiz E-W	Vertical	Horiz. N-S	Horiz E-W	Vertical
Unit 1	254	230	305	434	434	512
Unit 2	253	196	232	428	429	504
Unit 3	277	216	208	428	430	504
Unit 4	210	205	288	415	415	504

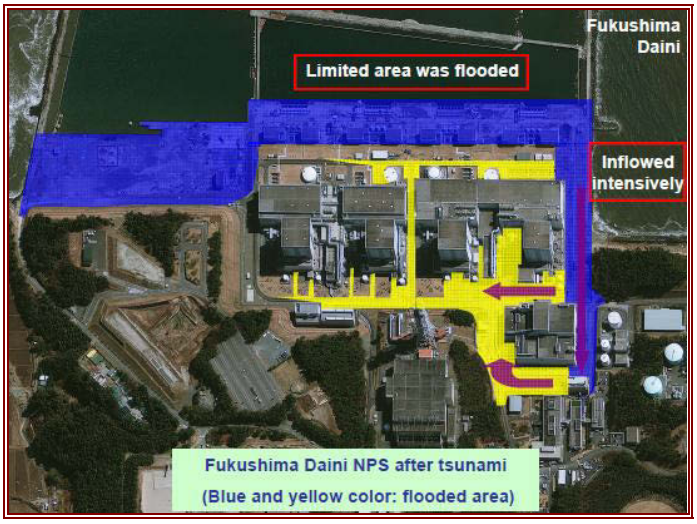

Figure 9.5 Areas inundated by the tsunami at Fukushima Daini NPS (TEPCO, 2011b).

The 500 kV and 66 kV power lines to Units 1 to 4 of Fukushima Daini NPS stopped transmission due to failure of devices on the side of the switchboard, caused by strong ground motion. However, the power supply to Units 1 to 4 was maintained as a separate line was operational (IAEA, 2011b).

9.1.3. Onagawa NPS

The Onagawa Nuclear Power Plant is located south of Onagawa Town in the Oshika District, Miyagi Prefecture. No units at the station have returned to operation since the earthquake and tsunami (Figure 9.1).

Seismic observations

The maximum horizontal acceleration value recorded on 11th March 2011 was 607 Gal (0.62g), and the maximum vertical acceleration value was 439 Gal (0.45g), see Table 9.3. Generally the observed maximum acceleration values are below the maximum response acceleration for the standard seismic ground motion with some exceptions noted in bold (IAEA, 2011b). The earthquake caused damage to the external power supply to the station.

Table 9.3 Maximum observed and design response acceleration at Onagawa NPS. Values in bold indicate observed response greater than response against standard seismic ground motion (after TEPCO, 2011c).

Seismometer location		Observed max. Response acceleration, in gal			Max. response acceleration against standard seismic ground motion (Ss), in gal		
		Horiz. N-S	Horiz. E-W	Vertical	Horiz. N-S	Horiz E-W	Vertical
Unit 1	Roof	2000	1636	**1389**	2202	2200	1388
	5th floor	**1303**	998	**1183**	1281	1443	1061
	1st floor	573	574	510	660	717	527
	Basement	**540**	**587**	439	532	529	451
Unit 2	Roof	1755	1617	**1093**	3023	2634	1091
	3rd floor	**1270**	830	743	1220	1110	968
	1st floor	605	569	330	724	658	768
	Basement	**607**	461	389	594	572	490
Unit 3	Roof	1868	1578	1004	2258	2342	1064
	3rd floor	956	917	888	1201	1200	938
	1st floor	657	692	547	792	872	777
	Basement	**573**	458	321	512	497	476

Tsunami Observations

Co-seismic ground subsidence of about 1 m took place at Onagawa NPS and as a result the elevation of the station at the time of tsunami arrival was around 13.8 m. The observed tsunami height was about 13 m, and therefore this did not exceed the elevation of the site. The design tsunami height was evaluated as 13.6 m (JSCE (2002), therefore the design basis tsunami heights were higher relative to those tsunami height observed above. In contrast to Fukushima Daiichi, the design of sea defences at Onagawa NPS with respect to tsunami was adequate here due to previous experience of significant tsunami at Onagawa in 1896 and 1933 (Horiuchi, 2011).

As the water level rose due to the tsunami, the water level in the underground seawater intake pit also rose. This resulted in seawater overflowing through an opening into a seawater pump room which then infiltrated into the basement floors of the reactor buildings, submerging the heat exchanger room of the component cooling water system in the basement. In addition, a component cooling water pump was submerged, which caused the cooling function of 2 out of 3 emergency diesel generators to fail (IAEA, 2011b).

9.1.4. Tokai Daini NPS

The site is located in Tokai in the Naka District of Ibaraki Prefecture, and is operated by the Japan Atomic Power Company. The reactor at Tokai has not returned to operation since the earthquake and tsunami (Figure 9.1).

Seismic Observations

At reactor building basement level the maximum horizontal acceleration recorded on 11th March 2011 was 214 Gal (0.22g), and maximum vertical acceleration was 189 Gal (0.19g), see Table 9.4. The maximum recorded acceleration of the observed seismic ground motions was generally below the maximum response acceleration for the standard seismic ground motion (IAEA, 2011b). The earthquake caused damage to the external power supply to the station.

Table 9.4 Maximum observed and design response acceleration at Tokai Daini NPS (after The Japan Atomic Power Company, 2011).

Seismometer location		Observed max. Response acceleration, in gal			Max. response acceleration against standard seismic ground motion (Ss), in gal		
		Horiz. N-S	Horiz. E-W	Vertical	Horiz. N-S	Horiz E-W	Vertical
Unit 1	6th floor	492	481	358	799	789	575
	4th floor	301	361	259	658	672	528
	2nd floor	225	306	212	544	546	478
	Basement	214	225	189	393	400	456

Tsunami observations

Elevation of the Tokai NPS is 8.9 m, whilst the design tsunami height for the sea protection structures was 5.8 m (JSCE, 2002). The tsunami on 11th March 2011 was 5.9 to 6.3 m. The tsunami flooded the north emergency seawater pump area in the seawater pump room. Consequently one of three seawater pumps for emergency diesel generators was submerged, and one of three emergency diesel generators stopped. However, other emergency diesel generators were operational, maintaining emergency power supply (IAEA, 2011b).

9.1.5. Effects of nuclear power station shutdown on electricity supply

TEPCO normally supplies electricity to a population of approximately 42 mn people, but lost approximately 40% of its generation capacity following the earthquake and tsunami. This led initially to rolling blackouts (Japan Ministry of Economy, Trade and Industry, 2011). However, following energy saving measures these were stopped on March 29th and it is hoped following increases in generation capacity that they can again be avoided during the peak demand months over the summer (Government of Japan, 2011).

9.2. Fukushima Daiichi NPS crisis

9.2.1. Radioactivity releases from Fukushima Daiichi NPS

At Fukushima Daiichi NPS, the automatic systems successfully inserted the control rods into the operational reactors at the time of the earthquake; this function is designed to halt the fission reaction at the onset of ground shaking to prevent overheating of the reactor. However, the subsequent tsunami damaged emergency power and cooling systems and caused widespread destruction of much of the site infrastructure including roads, pipe work, electrical cabinets and cabling. Having lost the ability to cool the reactor units it was not possible to control their temperature. Despite attempts to cool the reactors and spent fuel, severe damage to the fuel network and a series of hydrogen explosions occurred, releasing radiological contamination into the environment (IAEA, 2011a).

The hydrogen explosions were as a result of venting hydrogen through duct work in the secondary containment to an elevated release point on the refuel floor (at the top of the reactor building). The hydrogen was produced by chemical reaction within the reactor. The hydrogen was vented to control the containment pressure and hydrogen levels, particularly to protect the primary containment from potential failure. Figure 9.6 gives indications of radioactivity levels at the Fukushima Daiichi site in the month after the earthquake and tsunami.

Thirty site workers including 27 TEPCO employees have received a dose of more than 100 millisieverts (mSv). Comparatively, a chest CT scan would typically incur a radiological dose of 6.9 mSv, whilst an average individual annual radiological dose due to background radiation would be 2.4 mSv.

It was inferred that 3 workers from co-operating companies were exposed to radiation of 2000-3000 mSv on their feet and received internal exposure of 200 mSv or less. They received medical treatment at the National Institute of Radiological Sciences in Chiba City. (No health abnormality was found on the medical examination on April 11 2011. (The Federation of Electric Power Companies, 2011).

Two female TEPCO employees had been exposed to radiation exceeding dose limit for a female worker not in pregnancy. They received radiation doses of 17.55 mSv and 7.49 mSv, but doctors subsequently confirmed they had not been adversely affected (The Federation of Electric Power Companies, 2011).

TEPCO has sprayed dust inhibitor agents to reduce spreading of dust containing radioactive materials, and to reduce radioactive contaminated water from running into the sea it has injected coagulants into cracks in concrete walls containing radioactive water and installed rubber plates and jigs to enhance water sealing. Furthermore, as shown in Figure 10.7, large sandbags and silt fences have been installed around the breakwater at the site, to prevent radioactive contamination leaving the site.

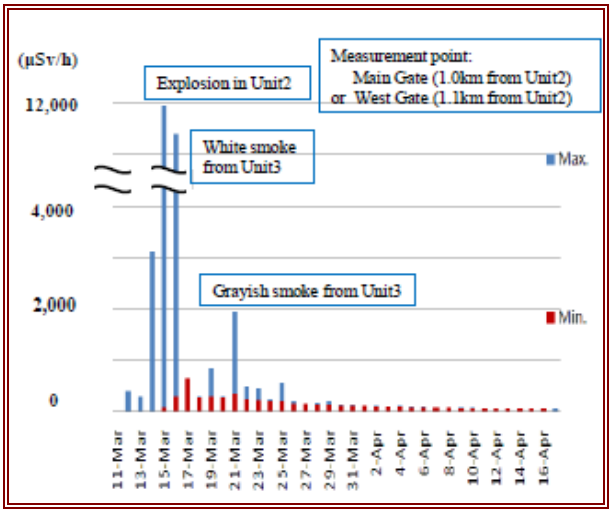

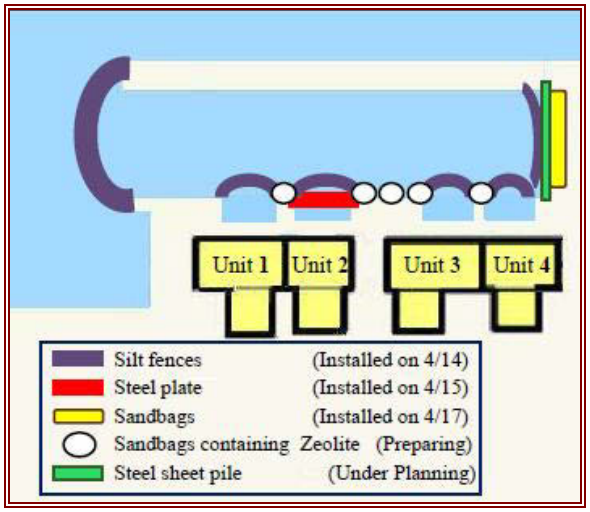

Figure 9.6 (left) Environmental Radioactivity Level at Fukushima Daiichi NPS (Japan Ministry of Economy, Trade and Industry, 2011).

Figure 9.7 (right) Measures to mitigate release of contaminated material from Fukushima Daiichi NPS (Japan Ministry of Economy, Trade and Industry, 2011).

Most of the radioactivity released by the accident has come from Iodine-131 (I-131), which has a half-life of just eight days. It is possible to mitigate the human effects of this by provision of potassium-iodide pills. Furthermore, the released I-131 will have decayed to a small (<0.5%) fraction of its original radioactivity in around two months.

Caesium-137 (Cs-137), which has a half-life of 30 years will present a greater clean-up issue before residents can return home. Some residents of the evacuated areas have been allowed home briefly to collect belongings; however, it may be years before the majority are allowed to return on a permanent basis.

The distribution of these radionuclides on land has been highly uneven with the largest amount in a zone to the northwest of the power plant, near the village of Iitate (Reuters, 2011a).

9.2.2. Management of the Fukushima Daiichi Crisis

Special measures have been implemented in certain areas, while radiation levels in the majority of the 20 kilometre evacuation zone have returned to normal levels.

According to the Act on Special Measures Concerning Nuclear Emergency Preparedness, Articles 10 and 15, local residents living in a 20 km radius of the Fukushima Daiichi NPS were ordered to evacuate (on March 12th) and those living in a 20 to 30 km radius to stay indoors (on March 15th). The

evacuation order was given prior to the release of radioactive material, which limited the exposure of local residents (The Federation of Electric Power Companies, 2011).

On April 21st, a No-Entry Zone (20 km radius) was established. The government issued a notification to prohibit entry to the zone, except those engaged in measures regarding the nuclear accident and those working to recover the bodies of people killed by the tsunami.

On April 22nd, the Government cancelled the order to stay indoors (in the 20 to 30 km radius area) and established Planned Evacuation Zones and Emergency Evacuation Preparation Zones. These zones are defined below:

- Planned Evacuation Zones (20 km radius area) – as there is a concern that within the period of one year following the accident, the cumulative radiation volumes could reach 20 mSv in these zones, the residents living in these zones were requested to evacuate in a planned manner to another location
- Emergency Evacuation Preparation Zones (20 km to 30 km radius area) – given that the status of the power station has not yet been fully stabilised, there remains a possibility that an emergency response may have to be made. Therefore, preparations should be made in these areas so that the residents can take shelter indoors or evacuate by their own means in the event of an emergency (The Federation of Electric Power Companies, 2011).

As of May 14th 2011, the Fukushima Prefecture had carried out radioactive contamination screening (Figure 9.8) on 187,179 residents at refuge sites and health centres. No effects on human health were observed (The Federation of Electric Power Companies, 2011). Radioactive contamination screening is the checking of items or the body for adherence of radioactive material. A level of 1 micro Sieverts per hour (μSv/h) dose rate at 10 cm distance (or 100,000 cpm equivalent) was determined as the appropriate level for decontamination to be undertaken. The results of 102 residents initially exceeded 100,000 counts per minute (cpm) but were reduced to less than 100,000 cpm after they were decontaminated.

Figure 9.8 Contamination screening of residents in Fukushima Prefecture (The Federation of Electric Power Companies, 2011).

9.2.3. Effects of radiation on Agriculture

I-131 and Cs-137 were detected in spinach sampled in Takahagi-city, Ibaraki on March 18th. The I-131 detected value was 15,020 Becquerel per kilogram (Bq/kg) compared to a provisional regulatory limit of 2,000 Bq/kg, whilst the Cs-137 detected value was 524 Bq/kg compared to a provisional regulatory limit of 500 Bq/kg (The Federation of Electric Power Companies, 2011).

The Japanese government issued instructions as of 9th May 2011 not to distribute the following products until the level of radiation recorded in the product returns to less than the regulatory limit. Unless stated, these restrictions apply to Fukushima Prefecture:

- Raw milk

- Non-head and head type leafy vegetables such as spinach and cabbage
- Flowerhead brassicas such cauliflower and broccoli
- Turnip
- Log grown shiitake
- Bamboo shoot
- Ostrich fern
- Baby Japanese sand lance fish
- Spinach from Ibaraki Prefecture and Tochigi Prefecture

Farmers in Fukushima Prefecture plan to demand millions of dollars in damages from TEPCO over radioactive contamination from the Fukushima Daiichi nuclear plant. It is claimed that farmers lost about US$1.8 mn by the end of April because they could not sell vegetables such as spinach due to the contamination (JAIF, 2011b).

Similarly I-131 was detected in raw milk sampled in Date-gun, Fukushima Prefecture on March 17th. The detected value was 1,510 Bq/kg, compared to a provisional regulatory limit of 300 Bq/kg (The Federation of Electric Power Companies, 2011). Dairy farmers estimate that losses from halted shipments of raw milk in March reached about US$3.7 mn (JAIF, 2011b).

9.2.4. Effects of radiation on the fishing industry

Radioactive contamination of the Pacific Ocean following the nuclear incident has raised public concerns about seafood safety. The Japanese regulatory authorities have imposed provisional regulation limits for radionuclides and other restrictions for food whilst the Japanese government is monitoring the presence of I-131, Cs-134 and Cs-137 in local seafood. Regular sampling of seawater takes place at 16 different sites (near-shore, at 3 km, 8 km and 15 km off-shore. Moreover, steps have been taken to prevent further spreading of contaminated water into the sea (such as the installation of steel plates, silt fences, sandbags filled with zeolite etc. at the power plant).

To date, mainly I-131, Cs-134 and Cs-137 have been measured in the marine environment; however no long-term impact is to be expected from I-131. It rapidly decays, (I-131 has a half-life of 8 days) and will soon no longer be detectable. Testing of marine water 30 km from Fukushima Daiichi has shown that the concentrations of radionuclides dropped rapidly to very low levels: Radioactivity measurements of sea water at the port of Sendai on May 18th, 2011 indicated a radiation dosage measured at 0.065 μSv/h, whilst radioactivity measurements of sea water did not detect radioactive Iodine or radioactive Caesium (Miyagi, 2011).

Radioactive pollution of the marine environment has occurred through:

- direct leakage of highly-contaminated water used to cool the damaged reactors
- voluntary discharge of low-contaminated water to increase the on-site storage capacity for highly-contaminated water
- transport of radioactive pollution by rainwater run-offs
- radioactive fallout of the atmospheric plume on the surface of the Pacific up to tens of kilometres from Fukushima Daiichi NPS

The Japanese sand lance is the only fish for which levels of radionuclides exceeding their provisional regulation limits have been measured to date. I-131 and Cs-137 were detected in kounago (sand lance) sampled in Kitaibaraki-city, Ibaraki Prefecture on 1st and 4th April 2011. The detected value of I-131 was 4,080 Bq/kg compared to a provisional limit of 2,000 Bq/kg, while the detected value of Cs-137 was 526 Bq/kg, compared to a provisional limit of 500 Bq/kg (The Federation of Electric Power Companies, 2011). Results of the inspection in fisheries products are published by the Japanese Fisheries Agency (Fisheries Agency, 2011).

A fisheries cooperative in Ibaraki Prefecture has demanded more than US$5 mn in damages from the operator of the Fukushima Daiichi nuclear power plant. Delegates of the fisheries cooperative visited the TEPCO headquarters in Tokyo, and handed its officials documents supporting their claim. They demanded US$5.2 mn which they say equals losses incurred in March 2011 from the nuclear accident. TEPCO's official in charge of Fukushima accident compensation said the company wants to examine the contents of the demand quickly, and make a quick provisional payment (JAIF, 2011b)

9.2.5. Cost of nuclear incident to the energy production sector

TEPCO announced in May that the costs associated with the M_W9.0 Tōhoku earthquake of 11th March 2011 would reach ¥1.25 tn (US$15 bn). This comprises:

- Damage to fossil facilities was put at ¥49.7 bn (US$608 mn)
- Grid infrastructure, ¥83.3 bn (US$1.01 bn)
- Direct cost of emergency measures at the Fukushima Daiichi, ¥426.2 bn (US$5.21 bn)
- Keeping six undamaged reactors at Daiichi and Daini in cold shutdown, ¥211.8 bn (US$2.59 bn)
- Starting to decommission units 1 to 4 in Fukushima Daiichi, ¥207.0 bn (US$2.53 bn)
- Scrapping plans for two more reactors at Fukushima Daiichi ,¥39.3 bn (US$480 mn) (WNN, 2011)

The final cost of compensation to the thousands of evacuees was not determined, however, it is reported that the cost would be met in compliance with law and with support from government (World Nuclear News, 2011). Pursuant to Act of Special Measures concerning Nuclear emergency preparedness, the governments „economic damage response headquarters" decided TEPCO should pay „temporary compensation" of ¥1 mn per household and ¥750,000 per individuals household to the people forced to evacuate due to the accident (TEPCO, 2011d). The U.N. Office for the Coordination of Humanitarian Affairs (OCHA) reports that nearly 84,000 people have evacuated from the 20 km exclusion zone (USAID, 2011).

Further estimates of the total cost from Kazumasa Iwata, president of the Japan Center for Economic Research, suggest the costs of the accident could range from nearly US$71 bn to US$250 bn (JAIF, 2011c). The costs include:

- US$54 bn to buy up all land within 20 km of the plant
- US$8 bn for compensation payments to local residents
- Up to US$188 bn to scrap the Fukushima Daiichi plant's reactors (JAIF, 2011c)

9.3. Effects of the earthquake and tsunami on other industries

9.3.1. Steel production

Sumitomo Metal"s Kashima plant stopped production following the earthquake. The Kashima works produces approximately 7% (6,800 thousand tonnes) of the national steel production. However, the blast furnaces at Kashima operated normally on April 30th, and Sumitomo Metal Industries returned to completely normal operation at Kashima by the end of April 2011 (Government of Japan, 2011).

Some facilities of Nippon Steel"s Kamaishi steelworks were inundated by the tsunami, causing them to cease operations. The plant makes wire rods used mainly in tyres, with a monthly output of 60,000 tonnes. In addition the port facilities were damaged (Nippon Steel Corporation, 2011). Operations were restarted in April 2011.

9.3.2. Automobile industry

Production of more than half a million vehicles was prevented in Japan in the month following the March 11th earthquake and tsunami. Toyota lost production of 260,000 units at its 18 Japanese plants through to April 8th, whilst Honda suspended car and component production in Japan losing production of 58,000 units. Car production at its Suzuka and Sayama factories resumed from April 11th, however parts supply from Japan remained 'unstable' and at around 50 per cent of the original plan (Automark, 2011).

Nissan lost production of 55,000 vehicles. Suzuki lost production of 45,000 units through to March 31st, rising to 59,000 through to April 9th. Mazda lost 43,000 units of output in Japan since the earthquake, while Subaru lost 29,000 units through to April 5th. Mitsubishi Motors has lost 26,000 units through to April 10th (Automark, 2011).

The global automotive industry has also been affected by supply-chain disruption. Nissan was forced to shut down production for three days at its Sunderland plant because of a shortage of vital components. Similarly, reduced production at Honda's Swindon plant will result in 22,500 fewer cars being built. Many electronic components, computerised engine management systems, batteries and petrol-electric hybrid engines are produced and shipped from Japan. However, more recently most of the motor production companies have restarted production. Toyota, Nissan and Honda all resumed production by 18th April (Reuters, 2011)

It must also be said that tsunami destroyed a huge number of vehicles, and it was evident that second hand car prices had increased dramatically following the tsunami, therefore there is likely also to be an increased domestic demand within Japan for new cars, which may well offset any losses from production from the earthquake.

9.3.3. Inspection of industrial facilities

Inspection of Minami Gamou Sewage Treatment Plant (38° 15' 00" N, 141° 00' 21" E)

The construction of Minami Gamou treatment centre was started in 1959 and completed in 1964. The plant was operated initially based on the "deposition" method. Afterwards, the method was improved and "sludge activation" was adopted in 1979. In 2008, the facility had a capacity of 292,485 cubic meters. Untreated waters are gathered at the treatment centre and, after treatment, released to the adjacent sea.

Minami-Gamou centre in Sendai was severely affected by the tsunami, as can be seen in Figure 9.9. The plant is constructed at an elevation of about 1.5 m above the beach level, behind a vertical concrete sea wall of the same height. The plant is located approximately 300 m from the sea. The height of the tsunami was approximately 7 m in this area.

The earthquake and tsunami caused considerable damage to the structures of the site and Figure 9.10 shows plastic yielding of 300 mm thick wall panels at the „Reaction Place" of the Sewage Treatment Plant. The span of the wall was approximately 4 m, and height approximately 6 m. The wall was reinforced in both directions with bars approximately 10 mm in diameter at approximately 250 mm centres. Similarly, across the sewage treatment plant there was considerable damage to pipework, building structures, roads, pumps, and electrical cabinets within the building structures (Figure 9.11).

Inspection of Shichigahama Power Plant (38° 18' 58 "N, 141° 4' 16" E)

The Sendai Thermal Power Plant is located in Yogasakihama, Shichigahama. The plant is owned and operated by TEPCO. The plant was originally constructed as a coal-fired power plant but has since been converted to run on natural gas. The operation of Plant 1 was started in 1959. Plants 1-3 have been abandoned due to aging and only Plant 4 was in operation during the earthquake (TEPCO, 2010).

The site was visited on 30th May 2011, and can be seen in Figure 9.12. The station is approximately 300 m from the coast. The external appearance of the site at the time of inspection seemed to be in good order, however, it was clear from the damaged domestic properties across the street that the

area had been affected by tsunami, and the ground floor was submerged. The height of the tsunami in this area was approximately 12 m. Plant 4 stopped its operation automatically. Plant 4 is not restored as of June 2011 and will not be restored until the summer of 2011 (Anon., 2011).

Figure 9.9 (left) Tsunami at Minami Gamou Sewage Treatment Plant (Sendai City, 2011a).

Figure 9.10 (right) Plastic yielding (due to tsunami flow) of 300 mm thick RC panel at Minami Gamou Sewage Treatment Plant.

Figure 9.11 (left) Damage to Minami Gamou Sewage Treatment Plant (Sendai City, 2011b).

Figure 9.12 (right) Sendai Thermal Power Plant at Shichigahama.

9.4. Conclusions on the impacts of the earthquake and tsunami on the nuclear industry

The Fukushima Daiichi nuclear incident has already had a significant effect on the worldwide nuclear industry, with many countries considering the future of their current, and plans for new nuclear power stations. The industry is also reviewing its emergency plans and vulnerability to beyond design basis environmental events.

To date no adverse health effects have been reported in any person as a result of radiation exposure from the nuclear accident (IAEA, 2011a).

Within Japan, there will be a significant impact on the area around the Fukushima Daiichi plant for many years, and the decommissioning of the damaged reactors will be a long, difficult and expensive process. There is likely to be significant scrutiny regarding the continued operation of the remaining nuclear power plants. This may leave Japan with an energy shortfall over the coming months and years, and place increasing reliance on reducing energy demand and generating energy by means other than nuclear. Unfortunately any restriction on energy is likely to constrain the growth of the wider Japanese economy, and affect living standards, further increasing the negative impact of the incident.

Radiological contamination dispersed following the unfortunate events at the Fukushima Daiichi nuclear power plant is causing anxiety within Japanese society. There is conflicting information and a mistrust of the Japanese Government's handling of this crisis and as a result, a lot of confusion and concern amongst the general public. For instance, there is currently high anxiety about food safety and many people are refusing to buy produce from the Tohoku region. The nuclear crisis will have significant effect on how the recovery will occur in the country as a whole.

9.5. References

Anon., 2011. Electric Power: Public thermal power plant disaster, "unrecoverable until this summer", *Mainichi Shimbun*. [online] (31 March 2011) Available at: <http://megalodon.jp/2011-0414-1930-48/mainichi.jp/select/biz/news/20110401k0000m040100000c.html> [Accessed 8 July 2011].

Automark, 2011. Japan loses half mn units in month since quake. [online] (Updated 16 April 2011) Available at: <http://www.automark.pk/latest-prices/car-prices/item/213-japan-loses-half-mn-units-in-month-since-quake.html> [Accessed 6 June 2011].

Fisheries Agency, 2011. Results of the inspection on radioactivity materials in fisheries products. [online] Available at: <http://www.jfa.maff.go.jp/e/inspection/index.html> [Accessed 14 July 2011].

Government of Japan, 2011. Economic Impact of the Great East Japan Earthquake and Current Status of Recovery, May 16th 2011.

Horiuchi, S., 2011. *The mitigation of earthquake damage by earthquake early warning*, Massey University Seminar Series, Massey University, Wellington, New Zealand, 6 July 2011.

IAEA, 2011a. *Fact Finding Expert Mission of the Nuclear Accident Following the Great East Japan Earthquake and Tsunami Preliminary Summary*. International Atomic Energy Agency International [online] (16 June 2011) Available at: <http://www-pub.iaea.org/MTCD/Meetings/PDFplus/2011/cn200/documentation/cn200_Final-Fukushima-Mission_Report.pdf> [Accessed 14 July 2011].

IAEA, 2011b. *Report of Japanese Government to IAEA Ministerial Conference on Nuclear Safety - Accident at TEPCO's Fukushima Nuclear Power Stations*. International Atomic Energy Agency International. [online] (7 June 2011) Available at: <http://www.iaea.org/newscenter/focus/fukushima/japan-report/> [Accessed 14 July 2011].

JAIF, 2011a. *Information on Status of Nuclear Power Plants in Fukushima*. Japan Atomic Industrial Forum. [online] (16 May 2011.) Available at: <http://www.jaif.or.jp/english/news_images/pdf/ENGNEWS01_1305518757P.pdf> [Accessed 14 July 2011].

JAIF, 2011b. *Earthquake Report No. 85.* Japan Atomic Industrial Forum. [online] (18 May 2011) Available at: <http://www.jaif.or.jp/english/news_images/pdf/ENGNEWS01_1305711249P.pdf> [Accessed 14 July 2011].

JAIF, 2011c. *Earthquake Report No. 99.* Japan Atomic Industrial Forum. [online] (1 June 2011) Available at: <http://www.jaif.or.jp/english/news_images/pdf/ENGNEWS01_1306919449P.pdf> [Accessed 6 June 2011].

Japan Ministry of Economy, Trade and Industry, 2011. *Japan's Challenges, Concerning the Domestic and International Implications of TEPCO Fukushima Daiichi Nuclear Power Station*, April 2011.

JSCE, 2002. *Tsunami Assessment Method for Nuclear Power Plants in Japan (2002)*, Japan Society of Civil Engineers.

Miyagi Prefectural Government, 2011. *Information of Accidents at the Fukushima Daiichi Nuclear Power Plant*. [online] (18 May 2011) Available at: <http://www.pref.miyagi.jp/kokusai/en/accidents_fukushima_nuclear.htm> [Accessed 6 June 2011].

Nippon Steel Corporation, 2011. *Tōhoku Pacific Earthquake*, March 14 2011, [online] Available at <http://www.nsc.co.jp/CGI/news/whatsnew_detail.cgi?section=11&seq=00020921> [Accessed 14 July 2011].

ONR, 2011. *Japanese earthquake and tsunami: Implications for the UK Nuclear Industry Interim Report*. HM Chief Inspector of Nuclear Installations, 18 May 2011.

Reuters, 2011. Japan automakers eye broad restart at half of output plans. *Reuters*. [online] (Last updated 06:25 8 April 2011) Available at: <http://www.reuters.com/article/2011/04/08/japan-autos-idUSL3E7F81GD20110408> [Accessed 6 June 2011].

Reuters, 2011a. High radiation outside Japan exclusion zone: IAEA. *Reuters.* [online] (Last updated 17:33 30 March 2011) Available at: <http://www.reuters.com/article/2011/03/30/us-japan-radiation-idUSTRE72T78120110330> [Accessed at 6th June 2011].

Sendai City, 2011a, *Gamo Damages South purification center*. [online] (25 March 2011) Available at: <http://www.city.sendai.jp/gesui/1197924_2478.html> [Accessed 14 July 2011] (in Japanese).

Sendai City, 2011b. *Purification center in Sendai.* [online] (4 January 2011) Available at: <http://www.city.sendai.jp/gesui/1193364_2478.html#gamou>, [Accessed 14 July 2011] (in Japanese).

TEPCO, 2010. *Complete the replacement work - fired our first commercial operation of Unit 4 for thermal power plant in Sendai*. [online] (29 July 2010) Available at: <http://www.Tōhoku-epco.co.jp/news/normal/1181641_1049.html> [Accessed 14 July 2011] (in Japanese).

TEPCO, 2011a. *Radiation dose measured in the Fukushima Daiichi Nuclear Power Station*. [online] Available at: <http://www.tepco.co.jp/en/nu/fukushima-np/f1/index-e.html#header)> [Accessed 14 July 2011].

TEPCO, 2011b. „Effects of the Earthquake and Tsunami on the Fukushima Daiichi and Daini Nuclear Power Stations". Tokyo Electric Power Company, 24 May 2011,

TEPCO, 2011c. [online] Available at: <http://www.Tōhoku-epco.co.jp/ICSFiles/afieldfile/2011/04/07/110407_np_b1.pdf>, [Accessed 14 July 2011] (in Japanese).

TEPCO, 2011d. April 25th 2011, „The Great East Japan Earthquake and current status of Nuclear power stations"

The Federation of Electric Power Companies, 2011. 17th May 2011, „Concerning the Fukushima Daiichi NPP Accident Caused by the Great East Japan Earthquake Disaster"

The Japan Atomic Power Company (JAPCO), 2011. [online] Available at: <http://www.japc.co.jp/news/bn/h23/230407.pdf> [Accessed 14 July 2011] (in Japanese).

USAID, 2011. *March 2011, Japan – Earthquake and Tsunami.* Fact Sheet #13, Fiscal Year (FY) 2011, [online] (24 March 2011) Available at: <http://reliefweb.int/sites/reliefweb.int/files/resources/3414B51FA19007C98525785D006BDBC5-Full_Report.pdf>, [Accessed 6th June 2011].

10. Tsunami preparedness, warning and evacuation

10.1. Tsunami preparedness in Japan

10.1.1. Brief summary of disaster management in Japan

Japan has a long history of disaster management activities, beginning with the Disaster Relief Act in 1947 during a decade where major disasters (5 earthquakes, 3 typhoons, 1 volcanic eruption) left 16,359 people dead or missing (Government of Japan Cabinet Office, 2007). Development of the disaster management system has continued in response to subsequent disasters, addressing prevention, mitigation and preparedness activities, emergency response, recovery and rehabilitation. For a full timeline of development, details on the numerous acts and roles of national, Prefectural and Municipal government see Government of Japan Cabinet Office (2007).

The Cabinet Office"s Central Disaster Management Council (CDMC) ensures that „comprehensive disaster countermeasures" are delivered through the Basic Disaster Management Plan, which includes tsunami under the Earthquake Disaster Countermeasures section. Municipal and Prefectural level government is responsible for formulating and implementing the Local Disaster Management Plan based on the national level Basic Disaster Management Plan. As part of CDMC activities to characterise regional earthquake hazard, a technical investigation "On countermeasures for the Trench-type Earthquakes in the Vicinity of the Japan and Chishima Trenches" was carried out between October 2003 and January 2006. The investigation aimed to define characteristics of expected earthquakes in that region, estimate the expected damage and develop necessary mitigation strategies. Eight earthquake scenarios were examined in this investigation including the Miyagi-ken-oki earthquake - the expected locally recurrent offshore event for the Tōhoku coastline, with an estimated 40-year return period. Estimates of seismic intensity and expected distribution of tsunami height were produced. The legislation "Countermeasures Basic Plan for Trench-type Earthquakes in the Vicinity of the Japan and Chishima Trenches" was drafted and 119 Municipalities in 5 Prefectures were identified as „countermeasure promotion areas" where the recommendations should be enacted (Government of Japan Cabinet Office, 2007).

Since 1984 the role of natural beaches in absorbing or reducing the impact of wave energy has been publicly and officially recognised by engineers, and coastal improvement works have been a core part of tsunami preparedness in Japan. The application of sea defences on the east coast of Japan is discussed in section 6. Since 2006, production of tsunami hazard maps and designation (by local governments) of tsunami evacuation buildings have also been carried out.

10.1.2. Hazard estimation and mapping

Two types of hazard maps are in use in Japan:

- Tsunami depth map showing a contour line of how long it will take for the scenario tsunami to reach 0.15 m depth (ankle depth)
- The common hazard map showing the maximum inundation extent and expected maximum depth of inundation.

As at April 2006, tsunami hazard maps had only been produced 12% of coastal Municipalities in Japan, and despite indicating schools or community centres as evacuation centres, few included evacuation routes (Suganuma, 2006). By 2011, 68% of coastal Municipalities had an inundation map – these are either created by the Municipality or adopted from the Prefectural level map or central government map (FDMA, 2011). Many of these maps are published online on Prefecture or Municipal government websites and accessible through a single web portal (Institute Ministry of Land, 2011). All but one coastal Municipality in Iwate, Miyagi and Fukushima has produced or adopted a tsunami inundation map although these are highly inconsistent in both content and format between Municipalities, in terms of historical events (1896, 1933 and 1960 tsunami) included and independent tsunami inundation modelling of the expected Miyagi-ken-oki source. The „expected" Miyagi-ken-oki scenario is an earthquake of approximate magnitude 7.5, which has a return period of around 30 years and last occurred in 1978. The expected source of this event is one of 3 areas between 10 and

>100 km offshore of Onagawa (Nakahara et al., 2006 and Figure 2.5) and had an expected probability of occurrence of 99% in the 30 years from 2005 to 2035, as assessed by the Earthquake Research Centre of HERP (Kanamori et al., 2006). Two examples of current tsunami hazard maps are shown in Figure 10.1 and Figure 10.2.

Following 11th March 2011, inundation maps using aerial photographs and satellite imagery are in circulation. It is unclear how the tsunami hazard mapping program will continue to develop and whether there will be increased consistency, but it is likely these sources of inundation extent will be incorporated in future maps. In most locations affected on 11th March 2011, recorded inundation extent and run-up height far exceed estimates from numerical modelling of the expected Miyagi-ken-oki source event and maximum inundation from previous events. While Municipalities warn residents that inundation depth / extent values on hazard maps are not absolute, the significant underestimation of modelled inundation is a flaw which must be addressed urgently, as these estimates form the basis of subsequent preparedness activities in many areas. Validation of the available maps in discussed in section 12.2.1.

Figure 10.1 (left) Extract of tsunami hazard and evacuation map for Kesennuma, Miyagi Prefecture. Coloured shading shows depth of expected inundation, arrows show evacuation routes, and 3 different types of evacuation shelters are illustrated, (City of Kesennuma, 2006).

Figure 10.2 (right) Extract of tsunami hazard and evacuation map for Natori, Miyagi Prefecture, (Miyagi Prefectural Government, 2005).

10.1.3. Evacuation planning and hazard awareness

The output of hazard estimation and mapping is combined with local knowledge and planning to establish the most appropriate evacuation routes to higher ground and / or evacuation structures. Community engagement and effective communication of the hazard and evacuation options is required to raise awareness among residents and visitors and encourage appropriate evacuation response in the event of a tsunami.

Relevant events in recent memory can help enhance and maintain the public"s hazard awareness. On 26th May 1983, a local tsunami in the Sea of Japan killed several people. Real-time videos recorded during the 1983 event were subsequently televised, and are cited as educational for the public understanding of evacuation to higher ground, and the need for technological enhancement in this field (Horikawa, 2000). A tsunami evacuation was initiated in Natori City following the Maule, Chile earthquake of 27th February 2010; the number of residents who participated in the evacuation was

considered by local officials to be inadequate, and this gave rise to enhanced public education in Natori during the year prior to 11th March 2011 (see section 10.3.5).

A longitudinal study on awareness of disaster preparedness in Japan (1991 to 2002) showed that public awareness decreased over time following the 1995 Kobe earthquake (Suganuma, 2006). In order to arrest this reduction and enhance awareness (alongside reviewing the effectiveness of current systems), regular disaster reduction drills are carried out across the country according to requirements set out in the CDMC Comprehensive Disaster Reduction Drills Plan. Japan holds "Disaster Reduction Day" on 1st September every year when each Prefecture carries out large-scale decision-making simulations (Government of Japan Cabinet Office, 2007) and Municipalities carry out evacuation drills according to their Local Disaster Management Plan (see example of Ōfunato in section 10.3.2).

Evidence of tsunami education and signage was apparent in many locations visited, including directional signs indicating evacuation routes (Figure 10.3), signs indicating entrance and exit from tsunami hazard zones (Figure 10.4), inundation markers (modern showing Chile 1960, see front cover, and historic stone inscription) and signs on vertical evacuation buildings (Figure 10.5).

Figure 10.3 (left) Tsunami evacuation route sign in Ōfunato stating "Tsunami emergency place of refuge".

Figure 10.4 (centre) A road sign on a main highway in Kamaishi stating "Start: Estimated Tsunami Inundation Area". Corresponding signs mark the end of this zone.

Figure 10.5 (right) Vertical evacuation signage in Kesennuma. This sign is present on visible areas of some designated vertical evacuation structures.

10.1.4. Hazard warning systems in Japan

Japan has one of the most advanced earthquake and tsunami warning systems in the world, which combines early detection and analysis of earthquake parameters with advanced communications systems to provide timely warnings.

Japanese Meteorological Association (JMA) maintains a network of seismometers and seismic intensity meters around Japan, facilitating rapid earthquake detection and analysis of hypocentral location, magnitude and distribution of shaking intensity. This network is used in the Earthquake Early Warning (EEW) system, which detects P-wave arrival time near the epicentre and uses this to estimate and announce the arrival time of more damaging S-wave. Depending on distance from the source this system can provide a few tens of seconds warning before the most severe ground shaking occurring. Its original use was to trigger automatic shutdown of bullet trains and industrial operations but since October 2007, this system also triggers automatic warnings to the public via media channels. The warning time can be sufficient for people to secure dangerous machinery or seek cover to limit injury from falling debris.

To provide effective communication of the warning, online and wireless systems link disaster management officials at all levels of government with media organisations, and dedicated radio communications systems connect national organisations and regional government with local disaster mitigation organisations and residents (Government of Japan Cabinet Office, 2007). The networks

provide wireless communication and real-time image transmission between organisations. A satellite communications network provides additional communication and warning transmission through a system called J-ALERT.

If analysis by JMA shows that a tsunami may have been generated from a detected earthquake, a tsunami advisory or warning is issued – this usually occurs within 2-3 minutes of the earthquake. Further announcements provide estimates of tsunami height and arrival times. Under the disaster management structure outlined in section 10.1.1, Municipality governments are responsible for issuing evacuation orders to the public on receipt of warnings from JMA or national government (Suganuma, 2006). These orders fall into the following four categories:

- Evacuation preparation order - issued when there is likely to be a natural hazard affecting the area. The main purpose of this order is to start moving the disabled/immobile people to evacuation facilities
- Evacuation recommendation - Issued by the head of the local district council when an event is likely to happen
- Evacuation order – As above
- No entry zone – assigned when it is decided that due to safety reasons, people are legally not allowed enter (e.g. the Fukushima NPP 30 km evacuation zone).

Notifications are transmitted to residents via media, emergency services and officials, loud speakers and local disaster mitigation organisations (Figure 10.6).

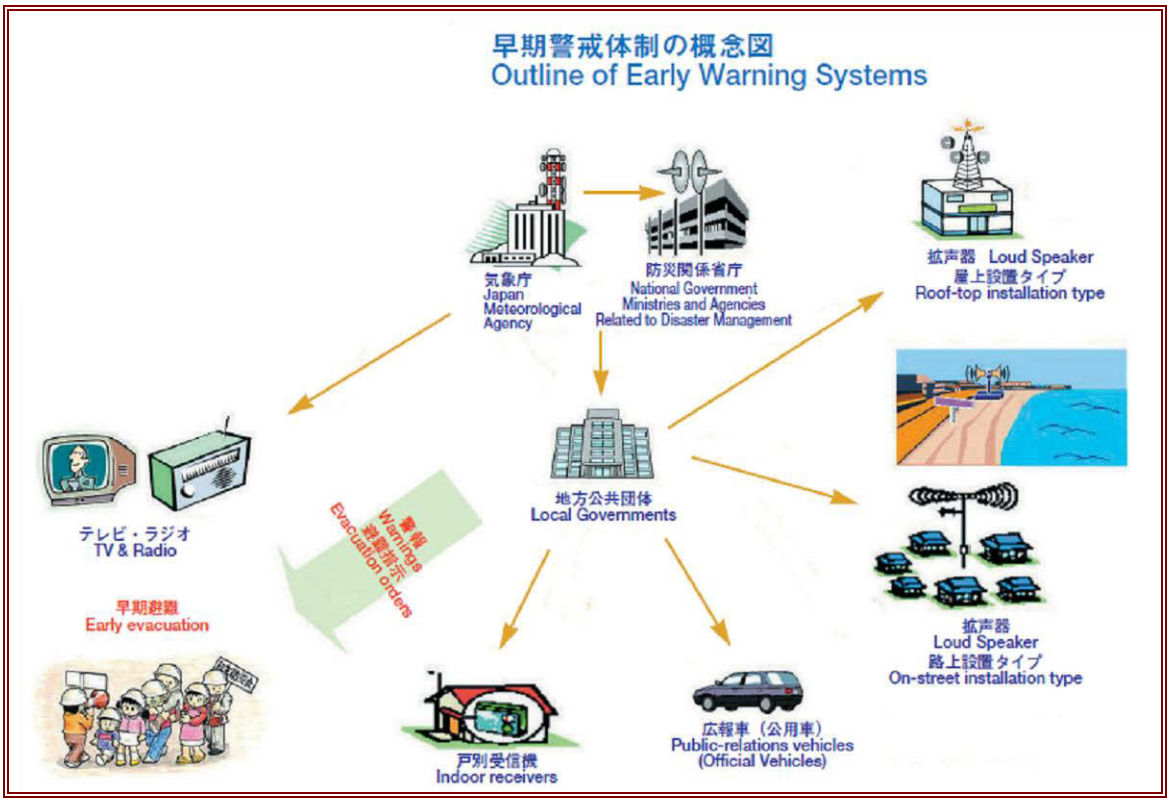

Figure 10.6 Early warning dissemination network in Japan (Government of Japan Cabinet Office, 2007).

10.1.5. Vertical evacuation structures

Japan has over 70,000 designated evacuation sites (Anon, 2011d) – some of which are buildings located on high ground or considered far enough inland to avoid inundation, others are designated vertical evacuation buildings. This event has shown the value of vertical evacuation structures but in some cases also highlighted inadequate design or designation where they have been inundated or overtopped.

While figures on the number of people evacuating into specific buildings are unavailable for some areas, published data shows that in 5 towns along the Iwate-Miyagi coastline, at least 9700 people survived the tsunami by evacuating to the upper floors of RC buildings. Table 10.1 and Figure 10.7 show the extremely high value of vertical evacuation: In Natori and Iwanuma the loss of life was significantly reduced by the use of vertical evacuation structures compared to areas such as Yamamoto-cho where there are a lack of suitable structures. As a result, in Yamamoto only 1% of residents living in the inundation zone were able to survive by entering such a building as opposed to 27% in Natori, 26% in Iwanuma, 15% in Watari and 7% in Sendai's coastal districts. A lack of vertical evacuation facilities was also apparent in parts of Sendai – for example, Wakabayashi-ku and Miyagino-ku.

Table 10.1 Impact of vertical evacuation structures in 5 Municipalities (Anon., 2011a).

District	Survivors on upper floors	Number of facilities
Sendai	2139	4
Natori	3285	5
Iwanuma	2095	5
Watari	2102	5
Yamamoto	91	1

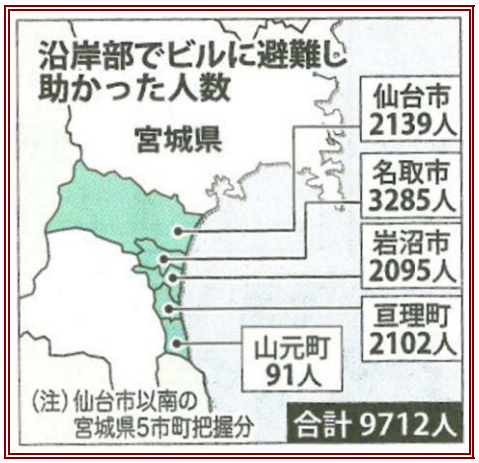

Figure 10.7 People saved by vertical evacuation in 5 Municipalities (Anon., 2011a).

EEFIT observations of vertical evacuation structures in the tsunami affected areas suggest inconsistencies between municipalities in the planning and designation of evacuation structures. While designated vertical evacuation structures performed well structurally (observed damage was generally limited to scour, debris strike, glazing and contents damage), the number of evacuation sites overtopped by tsunami waves shows that some designated sites were not appropriate for the extreme inundation depths experienced. Designation of suitable sites relies on adequate hazard estimation as well as structural assessment of the building. It is apparent that in this case, the estimation of hazard (using the expected Miyagi-ken-oki offshore event) was underestimated and led to poorly-informed decisions in designation of evacuation sites. Observations were made at several vertical evacuation structures during the mission, and key observations are described in section 10.3.

In addition to looking at the tsunami and earthquake impact on such structures, fire following the earthquake and tsunami is a significant hazard that must be considered. Consideration of the fire hazard is key for ensuring the safety of evacuees seeking refuge in designated structures – as seen in this event fire can affect large inundated areas, easily spreading to buildings that would otherwise survive the inundation (Figure 10.8).

Figure 10.8 Fire damaged school, Ishinomaki City. It is not known whether this building was used as an evacuation refuge during the tsunami.

10.2. Tsunami warnings on 11th March 2011

The first earthquake early warning was issued 8.6 seconds after detection on the first P-wave (JMA, 2011a), and the first tsunami warning issued at 14:49 (JST), only 3 minutes after the earthquake warning (JMA, 2011a; Table 10.2). Tsunami warnings and watches were issued for the Pacific region at 14:56 (JST) by the Pacific Tsunami Warning Center (ITIC, 2011). Figure 10.9 shows the warning as broadcast on Japanese NHK television at 15:03 JST, citing observations of tsunami up to 0.5 m in height.

Figure 10.9 Tsunami warning broadcast on NHK television. The caption states that observed tsunami was 50 cm height at Ayukawa, Ishinomaki City at 14:52 and 20 cm in height in Ōfunato City at 14:54. This information was also broadcasted on the radio (Sekine, 2011).

Dissemination of JMA warnings (based on modelled tsunami height) followed the timeline shown in Table 10.2. The Prefectures covered by a warning of waves >3 m in the first warning (14:49 JST) were Iwate, Miyagi and Fukushima; by 16:08 JST, this highest level of warning had been applied to 17 areas covering the whole northeast coastline. The coastal distribution of height-based JMA warnings for the first 4 warnings issued is shown in Figure 10.10. Section 5.4.2 discusses the evolution of tsunami height estimates from the initial estimates based on preliminary earthquake data, through to more refined estimates when tide gauge and buoy is available along with more constrained fault geometry data. Section 5.4.3 discusses the observed tsunami height at tide gauges and buoys.

Table 10.2 Timeline of official JMA tsunami bulletins from 11th March to 13th March 2011, (JMA, 2011a).

Date	Time (JST)	No. of Prefectures given warning of waves >= 3 m	No. of Prefectures given warning of waves up to 2 m	No. of Prefectures issued with advisory (0.5 m waves)	Action
11 March 2011	14:49	3	5	15	Warning Issued
11 March 2011	15:14	6	7	23	Warning Increased
11 March 2011	15:33	10	24	11	Warning Increased
11 March 2011	16:08	17	19	17	Warning Increased
11 March 2011	18:47	17	19	18	Warning Increased
11 March 2011	21:35	17	22	19	Warning Increased
11 March 2011	22:53	18	21	19	Warning Increased
12 March 2011	03:20	18	21	27	Warning Increased
12 March 2011	13:50	4	11	26	Warning Decreased
12 March 2011	20:20	0	4	21	Warning Decreased
13 March 2011	07:30	0	0	15	Warning Decreased
13 March 2011	17:58	0	0	0	Warning Cancelled

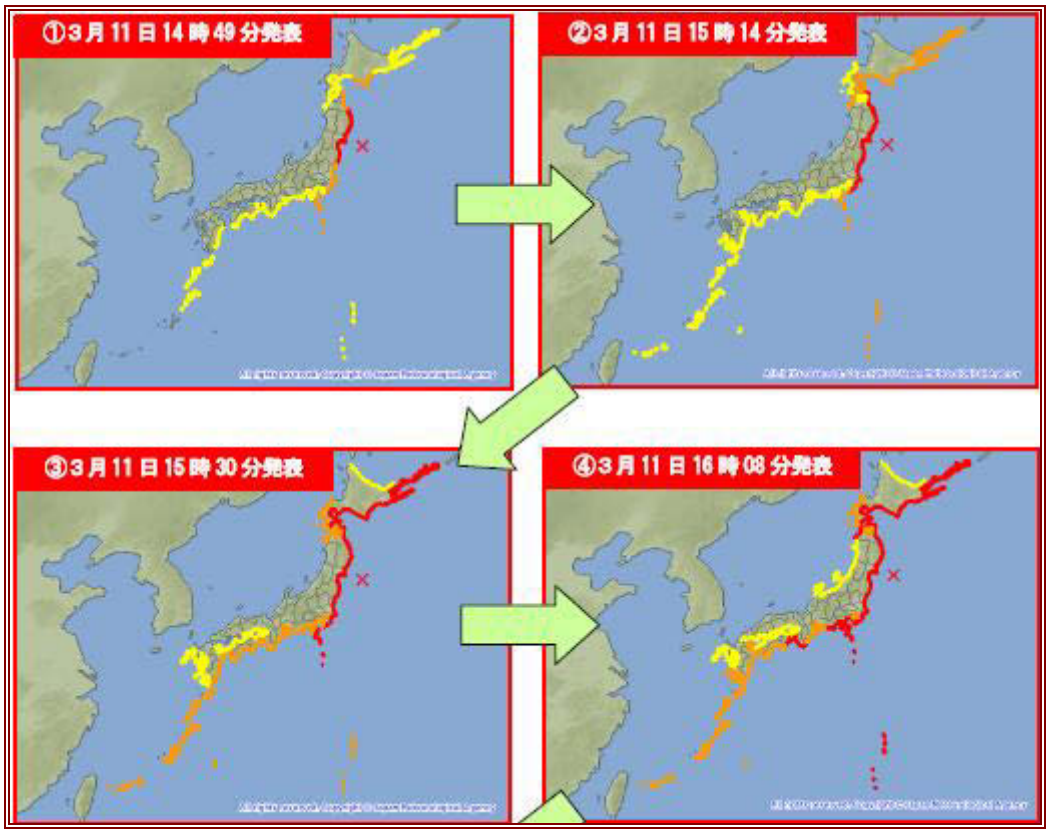

Figure 10.10 JMA tsunami warnings issued from 14:49 to 16:08 on 11th March 2011, showing the changing distribution of height-based advisory / warning levels (JMA, 2011b). Red: >3 m waves expected; Orange: up to 2 m; Yellow 0.5 m.

10.3. Local preparedness and evacuation on 11th March 2011

This section summarises tsunami preparedness in some locations visited by EEFIT. This information is not exhaustive and there may be further preparedness activities in place, which are not covered here.

Despite the communication networks set up for dissemination of warnings (section 10.1.4), the earthquake caused power outages which led to disruption of the warning system in some areas. A Fire and Disaster Management Agency (FDMA) survey shows that some areas did not have emergency power facilities in case of power outage. This was the case in Onagawa, Minamisanriku, Watari and Yamamoto-cho (FDMA, 2011). Videos recorded in Onagawa and Watari during tsunami inundation indicate no tsunami sirens were activated although loudspeaker announcements can be heard in the video.

10.3.1. Kamaishi City

Tsunami preparedness

Kamaishi City produces an information brochure for its visitors and residents outlining the services available in the city. Tsunami hazard information is published in this brochure, and includes advice on actions to take on feeling an earthquake or hearing a tsunami warning, a list of evacuation locations and a tsunami inundation / evacuation map. This map provides modelled inundation extent and inundation depth based on numerical simulation of the Miyagi-ken-oki earthquake, in addition to maximum inundation depth and arrival times in the 1896 and 1933 events. Kamaishi also has a network of loud speakers to disseminate warnings and designated evacuation sites (including one vertical evacuation building, an apartment building at the portside, discussed further in section 10.1.5).

Warnings and evacuation on 11th March 2011

On 11th March, there was a period of 28 minutes between the earthquake and first wave arrival at Kamaishi (Table 5.5). City officials confirmed that mains power supply was disrupted by the earthquake in this case, but that despite this, tsunami warnings were sounded.

According to the assumed evacuation walking speed discussed in section 10.3.2, the time to first wave arrival in Kamaishi (28 minutes) would be enough for elderly residents to walk to above 20 m elevation from any part of the port area (Figure 10.11). Despite this, 8.19% of people living in the inundated area were killed (as at 11th October 2011; FDMA, 2011). City officials reported that many people tried to evacuate by car, which caused congestion and may have contributed to this relatively high fatality rate. One resident of the apartment block designated as a vertical evacuation structure told EEFIT that he had tried to evacuate in his car, but on realising he could not drive it out of the car park he returned to the vertical evacuation structure and survived inundation on the third and fourth floors.

Vertical evacuation in Kamaishi

EEFIT investigated a designated vertical evacuation structure (8-storey RC frame construction) situated 70 m from the coastline (39° 16" 26.7" N, 14° 53" 17.6" E, Figure 7.5), with vertical evacuation signage at building entrances. The narrow side of this mixed-use office and apartment building faces seaward and a steel framed vertical structure is attached to the seaward face (Figure 10.12). Although it is unclear if this steel frame was deliberately designed as a sacrificial structure, but it has been damaged by debris impact with no damage to the main building behind. The ground floor towards the rear of the building is used as a car park and as such is open plan with RC infill panels which were damaged in the tsunami (Figure 10.13). This building was inundated to the 3rd floor, but occupants were able to evacuate to the designated evacuation area on the fourth floor and above.

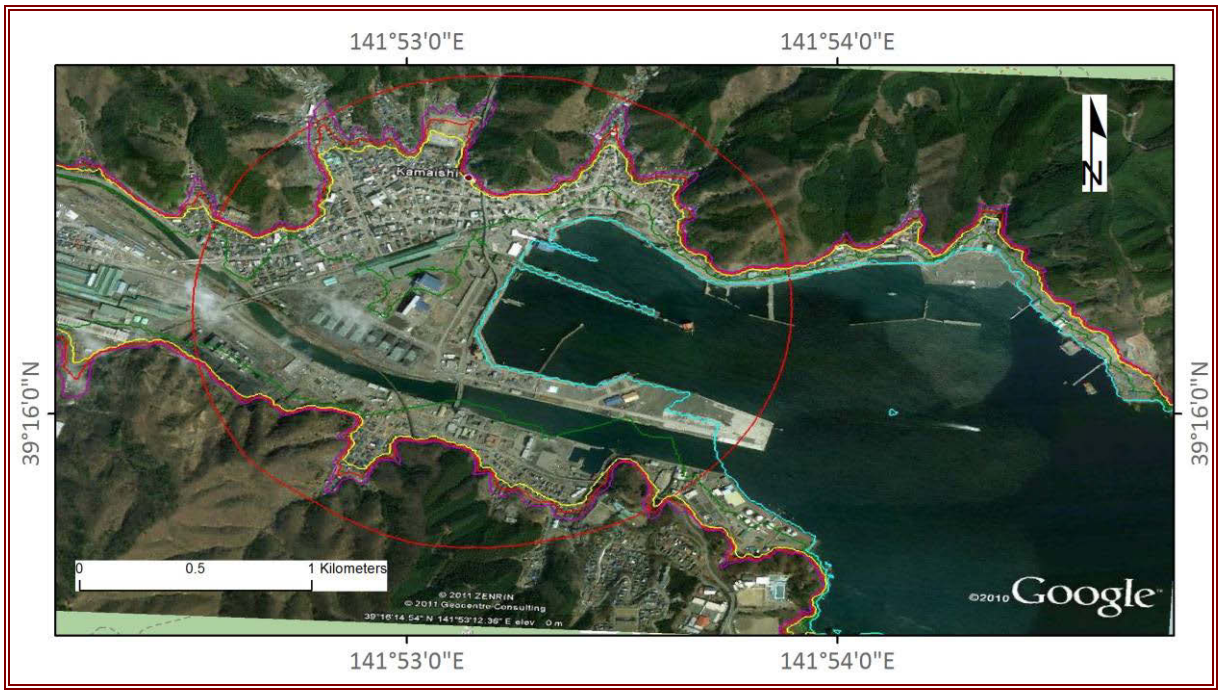

Figure 10.11 Port area of Kamaishi, Iwate Prefecture. Red circle indicates the 15 min (1 km) walking circle from the Nippon Steel Factory. Elevation contours are 0 m (cyan), 5 m (green), 10 m (yellow), 15 m (red) and 20 m (magenta), source: http://ktgis.net/.

Figure 10.12 (left) Eight-storey RC frame evacuation structure with steel frame structure on the seaward face. Two external staircases to the fourth floor exist on the other side of the building.

Figure 10.13 (right) RC in-fill panels damaged by tsunami flow or debris impact.

10.3.2. Ōfunato City

Tsunami preparedness

With a history of significant tsunami damage in 1896 (Meiji Sanriku), 1933 (Showa Sanriku) and 1960 (Chile), Ōfunato had various tsunami preparations in place at March 2011. These are outlined in the Ōfunato City Disaster Plan and Ōfunato City Disaster Mitigation section (no date) and summarised here:

- Tsunami breakwater constructed in 1967 extends 736 m across the mouth of the bay
- 23 coastal and river levees with flood gates (combined length of levees: 12 km)

- Disaster prevention broadcasting system comprising (at April 2010) 109 fixed broadcasting stations (4 are remote controlled) and 24 vehicle-mounted or portable stations in Ōfunato City
- Observations equipment comprising strong motion seismometer (from 1997), seismic intensity meter (from 1996) and Suzaki River water gate monitoring system (from 1993), 3 tide gauges linked to public website, Ōfunato fire station and disaster prevention control room
- Tsunami and High Tide Disaster Prevention Station – since 1997 this station has enabled remote monitoring and operation of flood gates
- 92 voluntary disaster prevention groups, established in response to the 1978 Miyagi-ken-oki earthquake, hold regular evacuation drills including the annual city drill on May 24th (anniversary of Chilean tsunami when 53 people died in Ōfunato). In 2010 20% of the city"s 40,000 population participated in the tsunami drill
- Disaster information material, tsunami hazard and evacuation maps (created in 2005) are distributed to residents. The map shows inundation from the 1896, 1933 and 1960 tsunami, and the expected Miyagi-ken-oki tsunami. It also includes the location of evacuation sites. Internet publication of the evacuation map is prevented because the base map is under copyright
- 36 inundation markers (indicating 1933 and 1960 inundation depths) and solar-powered evacuation guidance signs

These preparedness strategies appear to have resulted in a high level of hazard awareness and participation in previous evacuations following distant tsunami: Following the 27th February 2010 Maule, Chile earthquake and tsunami, 75% of Ōfunato"s population evacuated (22% to evacuation sites, the remainder went out of town due to the extended warning time).

Warnings and evacuation on 11th March 2011

On 11th March 2011, the tsunami evacuation order was given at 14:49 at the same time as the initial tsunami warning, and this was broadcast via 150 radio loudspeakers in the streets and a visual warning system at the port.

As of 11th October 2011, 466 people (2.34% of those living in the inundated area – MIAC, 2011) died or remain missing in Ōfunato due to the earthquake and tsunami (FDMA, 2011). The majority of casualties are attributed by city officials to people not evacuating when the warning was given or old people who may not have had necessary help to evacuate. Some houses in Ōfunato had been rebuilt after the 1960 event as 3 storey RC structures and some people may have thought they would be safe on the top floor. It is also believed that as this event occurred during the daytime, old people are likely to have been at home with fewer close neighbours than in an evening event, therefore had less help in the evacuation.

Adequate warning and timing of first wave arrival (25 minutes after the earthquake) allowed enough time to travel 1.3 km (based on the assumption of elderly residents" walking speed being 1 km (3281 feet) in 15 minutes. This assumption is based on a national preparedness document and is a higher walking speed assumption than that used by FEMA (2700 ft. / 15 mins). In Ōfunato, this evacuation time is enough for most residents to evacuate to high ground due to the layout of the urban area in a narrow valley.

There had been a community workshop in 2006 to study city evacuation strategies and although the workshop showed a need for vertical evacuation structures, no official designation of evacuation buildings was carried out. However, an agreement was reached with a 5 storey shopping centre, a 5 storey hotel and a bank, which in this event saved a total of 80 people who were close to these facilities at the time. Six of the total 58 evacuation sites in Ōfunato were inundated in this event (Anon, 2011d).

10.3.3. Minamisanriku

Tsunami preparedness

In Minamisanriku Town (Shizugawa Old Town) every neighbourhood association had made voluntary disaster plans in 2006 (Sekine, 2011), which were applied successfully during an evacuation in the 2010 Chilean tsunami when flow of 1.3 m inundated parts of the town but caused no casualties. This, in combination with the expectations of a local offshore event in the near future, shows that residents apparently have high awareness of the tsunami hazard.

Warnings and evacuation on 11th March 2011

As of 11th October 2011, 902 people are confirmed dead or still missing in Minamisanriku (FDMA, 2011), which represents 6.27% of the population living in the inundated area (GSI, 2011). Initial warnings disseminated for Minamisanriku cited an estimated tsunami height of 5 m, which resulted in instructions to evacuate to the 2nd floor of buildings. Flows of 11 m depth subsequently occurred, overtopping the Crisis Management Department building and inundating at least two designated vertical evacuation structures.

Vertical evacuation in Minamisanriku

Apartment block (38° 40' 25.10" N, 141° 26' 42.93" E)

A 4-storey RC apartment block at the harbour front (south-side), constructed between 2002 and 2010, and was designated for vertical evacuation in Minamisanriku. The structure is built with its long side parallel to the harbour front, which does not appear to have affected its structural performance (from external observations only). Signage indicating its vertical evacuation function is well positioned on the central columns and external staircases (Figure 10.14). Inundation occurred to at least the third storey and the structure has remained standing despite scouring of the piled foundations to at least 2 m below previous ground level (Figure 10.15). Detailed investigation of this building was not possible due to subsidence-induced flooding in the area, and it is not known how many people evacuated to this building.

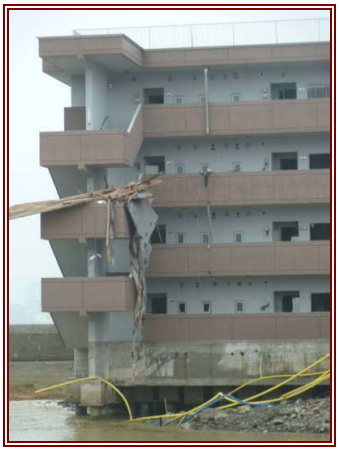

Figure 10.14 (left) Harbour-front designated evacuation structure. Vertical Evacuation signage (green) is visible on the landward (rear) side and at external staircases.

Figure 10.15 (right) Scour to over 2 metres deep exposing concrete piles at the north end of the building.

Shizugawa hospital (38° 40' 34.44" N, 141° 26' 44.99" E)

Three hundred metres inland from the apartment block above, Shizugawa hospital was inundated by an 11 m flow which inundated all floors but not the roof. The structure is a pre-2000 4 storey RC shear wall construction with steel bracing (Figure 10.16). The tsunami passed through the 4th floor of the hospital. Seventy four of 109 patients died, but around 200 people survived by taking refuge on the

roof, remaining there until the 12th March. This building showed significant non-structural damage from debris impact including parts of steel frame structures (Figure 10.17).

Figure 10.16 (left) View of the hospital (landward side) with steel bracing and damage to third storey visible.

Figure 10.17 (right) Seaward side of hospital building with rooftop railings and damage to every floor.

10.3.4. Sendai

Vertical evacuation in Sendai

Two key examples of vertical evacuation should be noted from Sendai – a non-designated raised park, and a designated structure that was unsuitable for this purpose in a tsunami.

Sendai port – raised park (38° 16' 17.78" N, 140° 59' 51.07" E)

This feature provides an example of an alternative method of vertical evacuation – onto a raised park or „berm", rather than to a building. Despite not being designated as a vertical evacuation area due to concerns over its stability in an earthquake (it is constructed from material dredged when making the port), this raised park was used for evacuation and people survived as it was not overtopped. The facility sustained some damage to the concrete defence at the seaward edge of the park, and suffered some subsidence.

This raised area has some characteristics of a designed vertical evacuation area, with three large, gently sloped access paths (one ramp but two with steps) and a shelter at its highest point. The seaward side is reinforced with concrete and brickwork.

Sendai port – gymnasium (38° 15' 39.30" N, 141° 00' 53.61" E)

This precast concrete gymnasium building has a damaged sign at the car park entrance designating it as a vertical evacuation site, despite design for its everyday function being unsuitable for evacuation requirements. This structure is situated immediately south of Sendai port and is 380 m from the open ocean with a small estuary (150 m wide) on the inland side of the beach. A series of dykes separates part of the estuary into individual ponds for unknown use – the dykes were breached by the tsunami and had been repaired with sandbags at the time of investigation. The building appears as tall as a three storey building, but due to its function as a sports court (single storey, high ceiling) it has no upper floor in the main hall, and very little second storey floor space in the adjoining building. There is no easy external access to the roof (only a small maintenance ladder). Only non-structural damage is apparent: glazing, damaged wall cladding, minor scour and lifting of the gymnasium floor.

Figure 10.18 (left) Shelter on the raised viewing area at Sendai port. This shelter was observed to accommodate at least 50 people.

Figure 10.19 (right) Access to the raised park from the north side (shopping centre and Sendai port).

Figure 10.20 (left) Seaward side of the gymnasium building. The maintenance ladder to the roof is visible in the upper left of photo.

Figure 10.21 (right) Evidence of damage to the sports hall, indicating the lack of upper-floor capacity here.

Arahama Elementary School (38° 13' 20.52" N, 140° 58' 49.88" E)

This structure provides an example of a vertical evacuation structure that performed its function well in this event. Inundation depth of 7.5 m occurred at this 4 storey pre-2001 RC shear wall structure. Debris observed on the second floor balconies indicating inundation of the lower 2 storeys.

The structure comprises shear walls on the narrow external seaward and landward faces, and in the central section with originally un-braced columns along the long faces. The building appears to have been retrofitted with steel bracing members incorporated to strengthen the un-braced column system resisting incoming tsunami forces. The bracing is situated only at the seaward side of the central shear walls and only at the lower three storeys (Figure 10.22) – it was concluded that this was installed specifically for additional resistance to tsunami loading. The subsequent retrofit may suggest that the building was either not originally built as an evacuation structure but was later identified as being the most suitable structure and retrofitted, or could have been designed as an evacuation structure before current thinking on evacuation structure design had been fully developed.

The building currently has rooftop railings, direct external roof access via a large brightly painted steel staircase to the rear and two sets of rooftop sirens. These sirens broadcast at different frequencies to reach different distances and one set of sirens is owned by the Municipality, one by JMA. No vertical evacuation signage was clearly displayed on the building.

Debris had entered the building in the longitudinal (vertical to the shoreline) direction, with timber and 3 cars inside the central ground floor corridor indicating significant flow velocity through the central corridor that runs the length of the building. The structure performed well and all other damage observed was non-structural: glazing and contents, and small debris strike at the seaward end.

Extensive collapse of timber buildings occurred in the area around this structure (Figure 10.23) and the adjacent steel frame school gymnasium suffered significant damage to its steel panel walls although the steel frame structure appeared to be only slightly damaged. A successful evacuation was carried out at this site: 380 people survived by evacuating to the roof (Anon., 2011a).

Figure 10.22 (left) The south face of Arahama Elementary School. Sirens and steel bracing are visible (2 instances, in the lower three storey windows), as is damage to the ground floor.

Figure 10.23 (right) Arahama Elementary School RC building 750 m from the coast (1) and steel framed gym building (2) partially sheltered on the landward side.

10.3.5. Natori City

Tsunami preparedness

Natori City officials reported that as recently as the 2010 Chilean tsunami, they had experienced a poor level of evacuation in response to tsunami warnings being issued. A much improved response was reported in this event, attributed to an increase in evacuation training since the Chilean event. Natori City has a published hazard and evacuation map (Figure 10.2), which shows the location of designated evacuation places including Arahama Elementary School, Sendai airport terminal and Yuriage Junior High School.

Warnings and evacuation on 11th March 2011

Despite improvements in evacuation response, there was a high level of casualties in Natori City: as at 11th October 2011, 981 people died or remain missing (FDMA, 2011). This represents 8.07% of the population residing in the inundated area (GSI, 2011). The majority of victims were elderly, and most casualties occurred in the residential area of Yuriage, rather than further south where agricultural land-use dominates the coastal area. City officials also reported that many police and fire personnel died in the tsunami as they were helping with the evacuation when the waves arrived. As Natori is a transit area between Sendai city and Sendai airport around 65 of the victims were not residents of Natori. Power failure reportedly prevented activation of the municipal digital radio tsunami warning network.

Vertical evacuation in Natori City

Five structures in Natori City saved over 3,200 lives in this event (Table 10.1). The buildings used were the local elementary and junior high schools, a 2-storey community centre, and the Sendai International Airport. Two of these are discussed in more detail here.

Yuriage Junior High School (38° 10 ' 38.70" N, 140° 56' 42.30" E)

Yuriage Junior high school suffered minor non-structural earthquake damage at seismically-designed separation joints (Figure 10.24), but remained effective as a vertical evacuation structure throughout tsunami inundation. The building is 1.5 km from the open ocean, 1 km from Yuriage harbour and only 320 m south of the Natori River. This building provided refuge to approximately 800 people and it was reported by Natori city officials that those who evacuated to this building remained there for 2 days following the tsunami.

This structure is constructed on a 1.8 m high embankment, raising the school above the level of surrounding rice fields. Inundation depth at the eastern (seaward) end of the school buildings was measured as 1.76 m; flow velocity appears to have been very low here with only flood damage observed to contents, and no debris impact or glazing damage (Figure 10.25), as had been observed at other locations. The total inundation depth around the school was therefore 3.56 m high – inundation of the school was reduced to 50% of this through its construction on the embankment.

Figure 10.24 (left) Minor earthquake damage at seismic detailing of Yuriage Junior High School: the staircase moved independently of the main building, and horizontal movement was accommodated in the separation joint shown by the vertical silver strip from ground to roof level.

Figure 10.25 (right) Seaward end of Yuriage Junior High School where watermarks indicate inundation depth.

Sendai airport terminal (38° 8' 17.15" N, 140° 55' 48.95" E)

On the tsunami warning being issued, police cars drove around the airport instructing people to shelter on the 3rd floor of the terminal. No casualties were recorded at the airport and 1,300 people sheltered in the airport terminal until 12th March. It is understood that some people died in this area while trying to flee in cars. Further information on damage to the airport terminal is presented in section 7.2.9.

10.4. Conclusions on tsunami preparedness, warnings and evacuation

The investment Japan has made in tsunami preparedness is wide-ranging and comprehensive, including seismic / tsunami detection and early warning systems, multi-channel systems for warning dissemination, hazard mapping, evacuation route planning and designation of evacuation refuges, regular public drills, and signage. These on-going activities have resulted in high public awareness of

tsunami hazard and the presence of such systems and facilities saved many lives in this event, as previously illustrated in this section.

As with all major disasters, there are lessons to be learned by all stakeholders in order to improve preparedness ahead of the next event – not only in the Tohoku region and Japan, but globally. Specifically for Tohoku there needs to be improved hazard assessment; any other preparedness initiatives rely on adequate depiction of the hazard in order to allocate resources effectively and to correctly plan evacuation strategies. As has already been discussed in this report, previous research in this region had underestimated the earthquake and tsunami hazard. Other areas at-risk from tsunami should now revisit their own hazard estimation to ensure this has been carried out with the most up to date seismic data and modelling techniques available.

Globally, there are lessons to learn on selecting and designating evacuation refuges. This event saw numerous evacuation refuges and critical infrastructure (such as hospitals, Crisis Management / Police headquarters) inundated. This not only resulted in tragic loss of life, but also removed from the towns many of the personnel trained to deal with such disasters. Further work must be carried out to ensure that refuges are properly designated in terms of location and in ensuring the structure is suitable for purpose – both of these follow on from adequate hazard estimation and mapping.

10.5. References

@disaster_i, 2011. 牛山素行, 9 May, [image online] Available at: <http://twitpic.com/4veg66> [Accessed 5 July 2011].

Anon., 2011a. 10,000 people survive after evacuating to a (designated evacuation) building. *Iwate Nichi Nichi Shinbun*, 30 May, 7b (in Japanese).

Anon., 2011b. More local governments designating evacuation structures – many surveys being carried out and calls for owners to put their buildings forward. *Iwate Nichi Nichi Shinbun*, 30 May, 7a (in Japanese).

Anon., 2011c. The tsunami warning limit? Meteorological blunder? Or ? : Earthquake East "Tsunami" is considered. [blog] Available at: <http://blog.goo.ne.jp/mimifuku_act08/e/a64e9d5bb98e1e6d1330effa4dfcc190> [Accessed 7 July 2011] (in Japanese).

Anon, 2011d. Tsunami hit more than 100 designated evacuation sites. *The Japan Times*, [online], 14 April 2011. Available at: <http://search.japantimes.co.jp/cgi-bin/nn20110414a4.html> [Accessed 7 July 2011].

City of Kesennuma, 2006. *Kesennuma Disaster Prevention Map (formerly Kesennuma Region) "Tsunami Advanced" version*. [image online] Available at: <http://www.city.kesennuma.lg.jp/www/contents/1253258421312/files/tunamishousai.pdf> [Accessed on 28 June 2011] (in Japanese).

FDMA, 2011. Fire and Disaster Management Agency of Japan, Report 140 on the effects of the March 11, 2011 Great Tōhoku earthquake, October 11, 2011. Available at: <http://www.fdma.go.jp/bn/2011/detail/691.html> [Accessed 10 November 2011].

Fujita T., 2011. *Tsunami impacting Eastern Japan and Preparedness for Extraordinary Disaster*. (Presentation, 25 May) Available at: <http://www.pari.go.jp/en/files/items/3733/File/2011052327IAPH.pdf> [Accessed 28 July 2011].

Government of Japan Cabinet Office, 2007, *Disaster Management in Japan* [online] Cabinet Office, Government of Japan. Available at: <http://www.cao.go.jp/en/doc/saigaipanf.pdf> [Accessed 29 May 2011].

Horikawa, K., 2000. History of Coastal Engineering In Japan. In P. Liu, ed. 2000. *Advances in Coastal and Ocean Engineering*, Volume 6, Singapore: World Scientific Publishing Co. Pte. Ltd, pp.1-56.

ITIC, 2011. *11 March 2011, M_W9.0, Near the East Coast of Honshu Japan Tsunami*. [online] Available at: <http://itic.ioc-unesco.org/index.php?option=com_content&view=article&id=1713&Itemid=2365&lang=en> [Accessed 7 July 2011].

JMA, 2011a. *The 2011 off the Pacific coast of Tōhoku earthquake Portal*. [online] Available at: <http://www.jma.go.jp/jma/en/2011_Earthquake.html> [Accessed 7 July 2011].

JMA, 2011b. *Monthly Report on Earthquakes and Volcanoes in Japan March 2011 - Overview,* Japanese Meteorological Agency. [online], Available at:

<http://www.seisvol.kishou.go.jp/eq/gaikyo/monthly201103/20110311_Tōhoku_1.pdf> [Accessed 7 July 2011].

Kanamori, H., Miyazawa, M., Mori, J., 2006. Investigation of the earthquake sequence off Miyagi prefecture with historical seismograms. *Earth Planets Space*, 58, pp.1533-1541.

MIAC (2011). Estimation of the population in the tsunami inundation zone, by municipality (analysis by the Geographical Information Authority of Japan). Ministry of Internal Affairs and Communications. Available at: <http://www.stat.go.jp/info/shinsai/zuhyou/sinsui.xls> [Accessed on 4 August 2011].

Miyagi Prefectural Government, 2005. Tsunami Hazard Map (Natori). [image online] (last updated 15 April 2005) Available at: <http://www.pref.miyagi.jp/sabomizusi/bousai/bou-ht2.html> [Accessed 29 June 2011] (in Japanese).

Nakahara, H., Sawazaki, K., Takagi, N., Nishimura, T., Sato. H., and Fujiwara, H., 2006. Strong ground motions recorded by a near-source seismographic array during the 16 August 2005 Miyagi-Ken-Oki, Japan, earthquake (M_W7.2). *Earth Planets Space*, 58, pp.1555-1559.

Ōfunato City Disaster Mitigation Section, no date. *Outline of Earthquake and Tsunami Disaster Countermeasures in Ōfunato City*, Disaster Mitigation Section, Ōfunato City, Iwate Prefecture.

Sekine, R., 2011. *Did the People Practice "Tsunami Tendenko"? The reality of the 3.11 tsunami which attacked Shizugawa Area, Minamisanriku Town, Miyagi Prefecture*, The 2011 East Japan Earthquake Bulletin of the Tōhoku Geographical Association. [online] (Published 13 June, 2011) Available at: <http://wwwsoc.nii.ac.jp/tga/disaster/articles/e-contents22.html> [Accessed 29 June 2011].

Suganuma K, 2006. Recent Trends in Earthquake Disaster Management in Japan, *Science and Technology Trends Quarterly Review*. 19, pp91-106.

The 2011 Tōhoku Earthquake Tsunami Joint Survey Group, 2011. *Survey Results – Uniform Survey Data* (data online] (ttjt_survey_15-Jul-2011_tidecorrected.csv). Available at: <http://www.coastal.jp/ttjt/index.php?%E7%8F%BE%E5%9C%B0%E8%AA%BF%E6%9F%BB%E7%B5%90%E6%9E%9C> [Accessed 28 June 2011] (in Japanese).

11. Observations on relief and recovery

11.1. Emergency response

Japan's buildings and infrastructure are designed and built to withstand the many natural disasters that affect the country, and the Government, emergency services and general population are generally well prepared and well-practiced in cases of emergency (see section 10.1 for an overview of disaster preparedness). None-the-less, the scale of the events that followed on from the 11th March M_W9.0 Tōhoku earthquake and tsunami are beyond those anticipated and have proved a major test of Japan"s emergency response strategies and resources.

Studying the aftermath of this event poses many lessons for the international emergency response community. The following section presents a brief summary of the factual information on relief and recovery events following the 11th March M_W9.0 Tōhoku earthquake and tsunami. The evacuation around the Fukushima Daiichi nuclear power station is discussed in section 9.

Whilst in Japan, EEFIT members were able to interview several high-ranking military and civilian staff of the Japan Self-Defence Forces (JSDF). Hence the role of the JSDF has been focused on here. For discussion on the role of the emergency services the reader is directed to the websites for Japan"s National Police Agency (National Police Agency, 2011), Fire Disaster Management Agency (Fire Disaster Management Agency, 2011) and Japan Coast Guard (Japan Coast Guard, 2011). EEFIT members were also able to interview the Director of Planning and Coordination for the Japanese Red Cross Society (JRCS), and as such a case study of the JRCS efforts is presented. For information on the other charities which have been active in Japan"s emergency response (such as, OXFAM, Save the Children and Care International) and recovery efforts (such as Architecture for Humanity-Japan), the reader is directed to their respective websites.

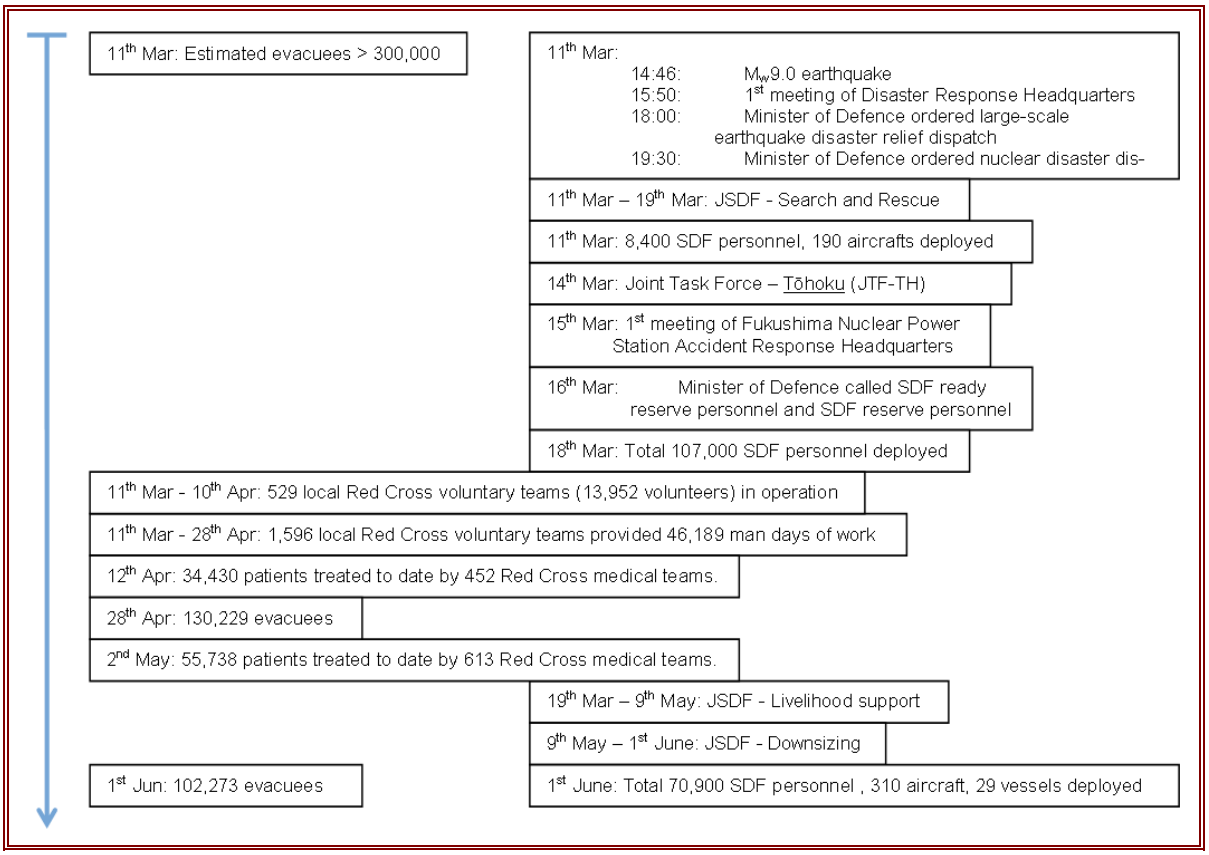

Figure 11.1 Timeline of key events in the emergency relief efforts of the Japanese Self-Defence Forces (JSDF) and the Japanese Red Cross Society (JRCS).

11.1.1. Timeline of the disaster response

The following is an overview of the chronology of the events from 1st March to 1st June, separated into the emergency relief efforts (Figure 11.1) and early recovery (Figure 11.2).

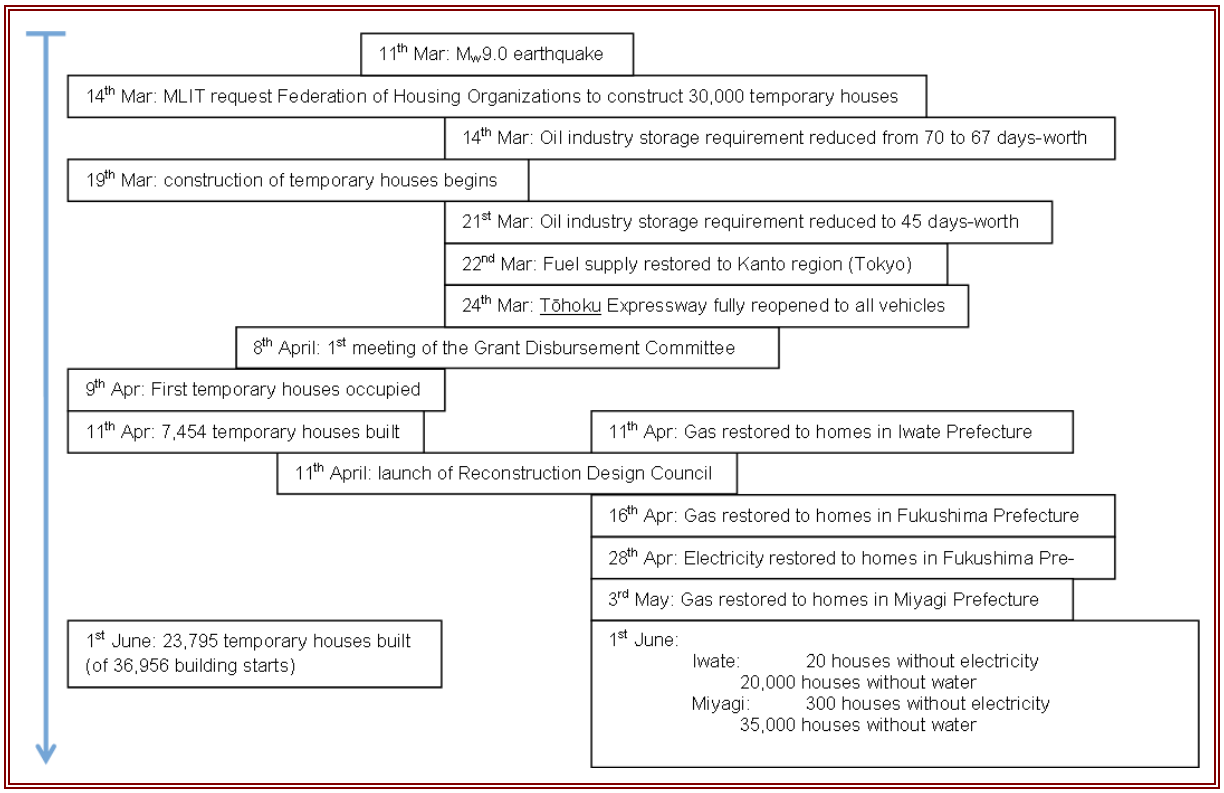

Figure 11.2 Timeline of key events in the early recovery.

11.1.2. Challenges faced in the immediate response

To understand the scale of the challenge faced in the emergency response, it must be considered that over 602,000 people lived within the area inundated by the tsunami on 11th March 2011. Table 11.1 shows data on fatalities (dead and missing), population in the inundation zones and proportion of the population that is 65 or more years old (from the 2005 Japan population census) in the locations investigated by EEFIT. The values presented in this table are as at 11th October 2011 (FDMA, 2011a; MIAC, 2011). This figure does not include those living outside of the inundation zone but who were affected by ground shaking, nor does it include those living within the Fukushima Daiichi nuclear power plant exclusion zone. It is shown that a large proportion of those affected were in Miyagi Prefecture. The percentage of the total population living within the inundated area in the cities and towns listed is above 30% in all but 3 cases shown. A very large proportion of residents became dependent on local authorities and emergency responders placing great strain on those services.

Tsunami debris

Another consideration is the large amount of debris created by the tsunami, including destroyed structures, building contents, washed away cars and boats and many other materials. The amount of debris in Miyagi Prefecture is estimated between 15-18 million tons – equivalent to 23 years of normal waste production (SEEDS Asia, 2011). A major concern is one of contamination of the debris. Sea water has saturated much of the debris; the salt contamination prevents much of it being incinerated. Many industrial facilities were also within the tsunami inundation zone, such as Sendai Kirin Beer factory (Figure 11.3) and Minami-Gamou sewage treatment plant (discussed in section 9.3.2), contaminating the tsunami debris with industrial chemicals and sewage. In addition a huge amount of debris was washed into the ocean and is now floating off the coast of Japan; some of this is being washed back onshore gradually and with the help of the Pacific Ocean currents (particularly the North

Pacific Gyre) some debris is expected to reach the Western coast of Canada and the USA within 12 to 24 months (easily floating debris such as boats and wood from the destroyed houses are expected to arrive first).

Municipalities of the affected areas have placed tenders for contractors to remove debris, emphasising employment of local people who have been affected by the tsunami. Debris removal was also conducted by the JSDF, homeowners (e.g. members of the EEFIT team observed several shop owners in Kamaishi clearing debris from their shop floors in preparation to reopen their businesses) and by communities (e.g. fishing communities clearing paths to the sea front). Debris is being moved to temporary storage areas, but there is a shortage of space as much of the suitable land (flat land away from the coast) is being used for temporary accommodation. Authorities aim to recycle as much of the debris as possible including the use of sediment from the sea being returned to the sea to form reclaimed land. It is estimated that it will take approximately one year to move all debris to the temporary storage areas before it can then be moved onto permanent sites (which have not yet been designated). Note that after the Great Hanshin Earthquake (1995), it took three years to process all of the debris and it is estimated that it will take longer in this case (Nikkei Business online, 2011).

Figure 11.3 (left) Kirin Beer Factory at Sendai port is one of many damaged industrial facilities within the tsunami zone, adding to industrial contaminants within tsunami debris (Blog, 2011).

Figure 11.4 (right) The railway line in Yamamoto-cho had been washed away and the railway station building was moderately damaged and abandoned.

Disruption to infrastructure

The ability to deal with these challenges was hampered in the first few days and weeks by the damage sustained to infrastructure (see section 5.5.2 for statistics on infrastructure damage). Travel restrictions were initially imposed to prioritise travel for authorities engaged in the relief efforts (e.g. fire services, police, military) and deliveries of supplies to the evacuees. These restrictions were gradually eased, with Tōhoku Expressway between Ichinoseki and Utsunomiya the last main route to be re-opened to all vehicles on 24th March (Japan Press Network 47 News, 2011).

There was a shortage of fuel in Tōhoku for several weeks after the tsunami due to damage to refineries (many of Japan"s refineries are located within Tōhoku and there was also damage outside of this region such as the fires at Cosmo Oil"s Chiba Refinery), over-buying in some areas and blocked access to some petrol stations. This petrol shortage also affected the Kantō region (including greater Tokyo) with fuel supply here not fully recovering until 22nd March (Sankei, 2011). The government response was to prioritise fuel allowance to those involved in the relief effort, arrange extra production in some refineries in the West of Japan (e.g. Sakai, Mie and Okayama) and reduce the requirement on the oil industry for storage of oil from 70 days-worth to 67 days-worth on 14th March and then to 45 days-worth on 21st March.

Many local government buildings as well as disaster management staff were also affected, further reducing the initial local capacity to coordinate a response. Towns which were required to relocate their disaster management headquarters include Minamisanriku (Figure 7.30), Onagawa, Ishinomaki, Iwanuma, Yamamoto and Watari (FDMA, 2011b). There was also a critical shortage of medical facilities as 9 hospitals and 68 clinics were reportedly destroyed, while 53 hospitals and 327 clinics were damaged (Japanese Red Cross Society, 2011a), including at Minamisanriku (Figure 7.34).

Table 11.1 Summary of casualty statistics (at 11th Ocotber 2011) and population statistics for municipalities that had >10 dead and missing in locations investigated by EEFIT. Locations are ordered north to south (FDMA, 2011a; MIAC, 2011).

City / Town (ordered North to South)	Dead + Missing	Population previously living in inundated area	% of total pop. previously living in inundated area	Fatality rate in inundated area	% of pop. ≥65 years of age (in 2005)
Miyako City	541	18,378	30.9%	2.94%	26.5%
Yamada Town	815	11,418	61.3%	7.14%	28.1%
Otsuchi Town	1,353	11,915	78.0%	11.36%	28.5%
Kamaishi City	1,078	13,164	33.3%	8.19%	31.2%
Ōfunato City	446	19,073	46.8%	2.34%	27.0%
Rikuzentakata	1,939	16,640	71.4%	11.65%	30.5%
Kesennuma City	1,404	40,331	54.9%	3.48%	26.2%
Minamisanriku Town	902	14,389	82.5%	6.27%	27.6%
Onagawa Town	980	8,048	80.1%	12.18%	30.0%
Ishinomaki City	3,892	112,276	69.0%	3.47%	24.2%
Higashimatsushima	1,138	34,014	79.3%	3.35%	20.5%
Shiogama	21	18,718	33.1%	0.11%	23.5%
Shichigahama	75	9,149	44.8%	0.82%	18.3%
Tagajo City	189	17,144	27.2%	1.10%	15.3%
Wakabayashi-ku	403	9386	7.1%	4.29%	16.1%
Miyagino-ku	286	17,375	9.1%	1.65%	14.6%
Natori City	981	12,155	16.6%	8.07%	17.3%
Watari	270	14,080	40.4%	1.92%	20.6%
Yamamoto-cho	690	8,990	53.8%	7.68%	27.8%

11.1.3. National disaster management

The Disaster Countermeasures Basic Act (originally enacted in 1961; also discussed in section 10.1.1) formulates a strategic disaster management system, which outlines the hierarchy for establishment of the national Disaster Management Operation Plan and translation to the individual Local Disaster Management Plans. The national plan is established by a panel consisting of the Prime Minister, 23 ministries and agencies and 63 public corporations including the Bank of Japan, Japanese Red Cross Society, NHK (broadcasting company), electric and gas companies and Nippon Telegraph and Telephone Corporation (NTT). This plan is then translated to a Prefectural level by the Prefectural Disaster Management Council and similarly at a Municipal level (Cabinet Office, 2011).

In the case of emergencies, the Major Disaster Management Headquarters are set up at the Cabinet Office, led by the Minister of State for Disaster Management. This has happened 18 times since 1977. On the 11th March, for the first time since the establishment of the Disaster Countermeasures Basic Act, the Extreme Disaster Management Headquarters were set up at the Prime Minister"s Office, led by the Prime Minister (Figure 11.5). There were 38 meetings of the Disaster Response Headquarters between 11th March and 1st June 2011 (Okuyama, 2011).

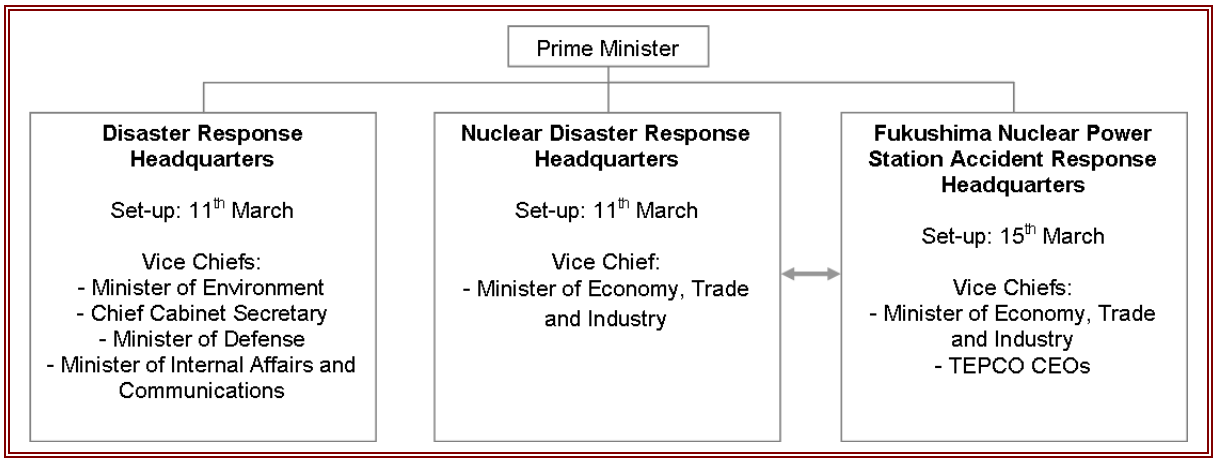

Figure 11.5 Branches of the Extreme Disaster Management Headquarters (Ministry of Economy, Trade and Industry, 2011).

11.1.4. Observations on search and rescue and rapid structural assessments

Approximately 26,700 people were assisted by search and rescue (SAR) teams (including those transported from difficult or inaccessible locations such as rooftops). Of this number, 19,286 were assisted by the Japanese Self-Defence Forces (JSDF), aided by teams from the US, Australia, UK, South Korea, India, Turkey, Russia, China, Singapore and Mexico (Ministry of Foreign Affairs of Japan, 2011). Several other SAR teams were either refused entry to Japan or refused permission to draw petrol (rationed initially) as many were unable to demonstrate that they could fully support themselves, particularly in terms of Japanese language skills, and some were not certified by the International SAR Advisory Group (INSARAG), both requirements that had been set by Japanese government for responding teams to enter the affected areas.

A rapid engineering assessment of buildings took place so that officials could issue damage certificates, which are required for building owners to receive compensation and support from the government. Although the assessments are linked, the compensation damage certificate is not the same as the labels put on buildings by inspecting engineers such as that shown in Figure 11.6 – this label relates to occupancy safety. Tsunami-damaged buildings are assessed on a four-grade system:

- T4: Complete Destruction – washed away
- T3: Extensive Half Destruction – inundation to ceiling level of ground floor
- T2: Half Destruction – inundation above the floor of ground floor level
- T1: Partial Destruction – inundation below the floor of ground floor level

Owners of houses categorised as T2 or above were eligible for financial assistance (see section 11.2.2). A similar grading system was used for damage due to earthquake ground shaking (Cabinet Office, 2011).

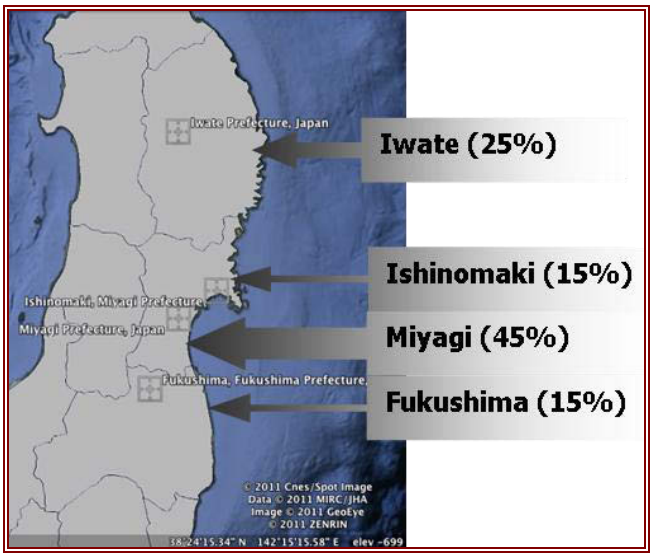

Figure 11.6 (left) Following engineering inspection unsafe buildings are labelled as shown, prohibiting entry. Similar green labels designate the building as „safe" and yellow labels as „limited entry", meaning for entry inspection purposes only.

Figure 11.7 (right) Allocation of JSDF resources among the 4 command centres.

Case study: Japan Self Defence Forces (JSDF)

The JSDF was vital to the relief effort in Tōhoku. See Figure 11.1 for a chronological overview of their main activities and the numbers of personnel deployed from 11th March to 1st June. On 11th March, JSDF personnel based in Tōhoku carried out reconnaissance of the affected areas, sending aerial photography and live videos back to the Disaster Response Headquarters for coordination of the response. Several JSDF bases were within the tsunami inundation zone (Tagajo Army Post and Matsushima Air Base, both in Miyagi Prefecture), sustaining variable levels of damage, but these bases contributed to the immediate reconnaissance mission where possible.

Four command centres were set up (Figure 11.7), one for each of the three affected Prefectures and a fourth specifically for Ishinomaki (the biggest city affected by the tsunami with the exception of Sendai"s two coastal districts). The additional base in Ishinomaki was required due to the loss of local government capacity and number of people affected (112,276 people living within the inundation zone, Figure 11.8). The army, navy and air forces operated under the Joint Task Force – Tōhoku (JTF-TH) from 14th March (headquarters in Sendai). At the peak of the JSDF response, a total of 107,000 personnel were deployed (Figure 11.1).

All values given hereafter in this section were current up to 1st June. The operations of the JSDF focused on Search and Rescue (SAR) from 11 to 19th March, assisting 19,286 of the total 26,700 people assisted. They have also been responsible for the recovery of bodies, recovering 9,450 of the total 15,270 bodies recovered, with the majority being recovered in March (Figure 11.9). Body retrieval from the Ocean started on 15th March and continued up to the time of our visit. Just over 400 bodies were recovered at sea by the end of May, beginning a few days after the tsunami (Figure 11.10).

From 19th March the JSDF focus moved from SAR towards livelihood support for the evacuees including: water and food supply to evacuees, provision of bathing and sanitation facilities (Figure 11.11 to Figure 11.13), transport of relief supplies (total 10,642 tons), debris and road clearance (320 km of road cleared), transporting fuel to isolated locations such as Miyakojima Island (total 1,396 kl), construction of destroyed bridges, and medical support (treating 22,950 persons). Relief supplies were transported from army posts across the country to major airbases where they were airlifted to airports within the affected Prefectures. From there they were taken to intermediate warehouses and finally transported to the evacuation centres by truck or helicopter. Some supplies were transported by sea, using troopships where ports were operational, and using LCAC (Landing Craft Air Cushion) class hovercraft where ports were inoperable (e.g. in Ishinomaki). The Ministry of Defence (MoD) of

Japan maintains three systems for reserve personnel: JSDF Ready Reserve Personnel, JSDF Reserve Personnel and Candidates for JSDF Reserve Personnel. On 16th March the MoD called the JSDF Ready Reserve Personnel and JSDF Reserve Personnel for the first time since the establishment of the JSDF. 2,400 personnel have been dispatched, involved primarily with interpretation (e.g. for Foreign SAR teams) and livelihood support.

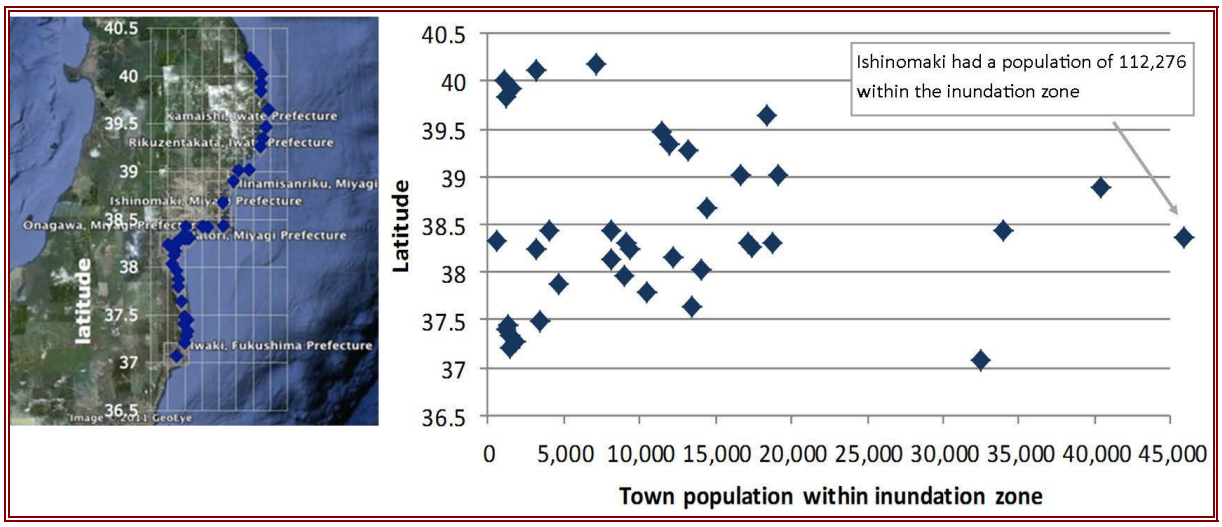

Figure 11.8 Populations of towns that sustained casualties in the tsunami. Ishinomaki is the only town with more than 40,331 people previously living in the area inundated on 11th March 2011.

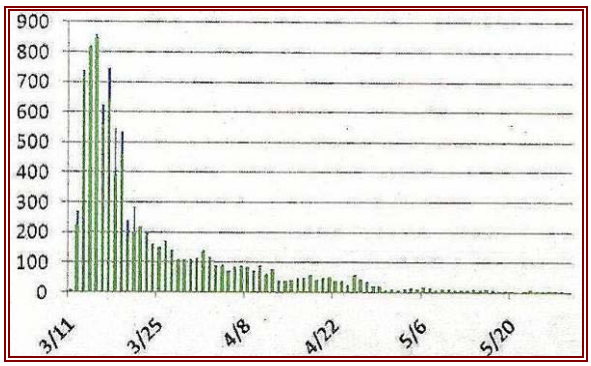

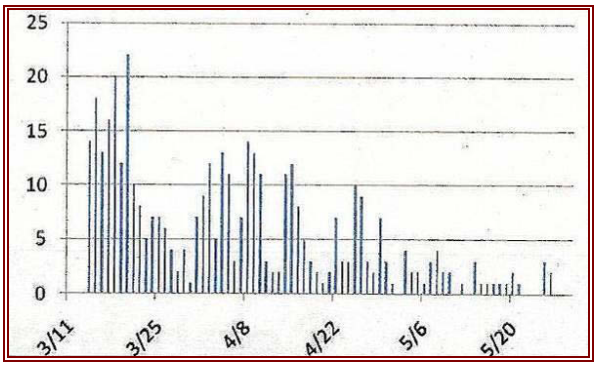

Figure 11.9 (left) Bodies recovered by the JSDF (land) (Okuyama, 2011).

Figure 11.10 (right) Bodies recovered by the JSDF (sea) (Okuyama, 2011).

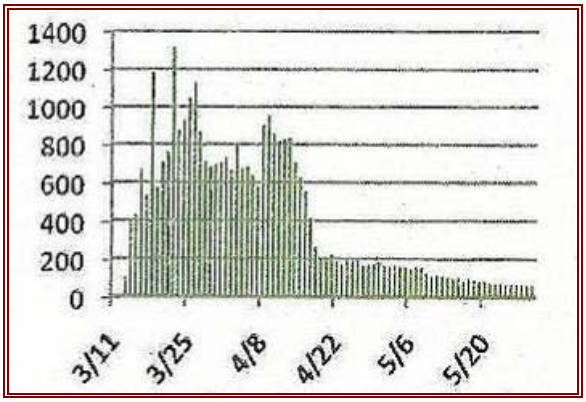

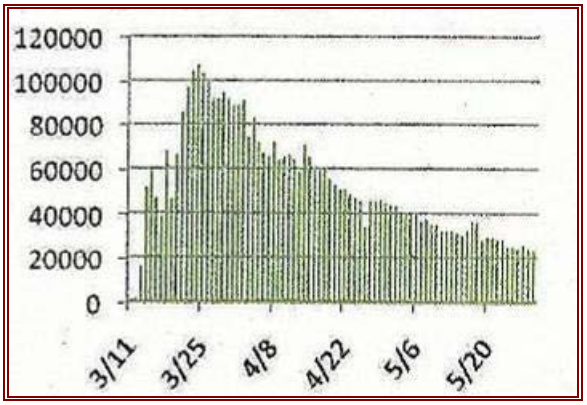

Figure 11.11 (left) Water supplied by JSDF (tons). Total = 32,259.7 tons (1st June) (Okuyama, 2011).

Figure 11.12 (right) Food supplied by JSDF (meals). Total = 4,266,266 meals (1st June) (Okuyama, 2011).

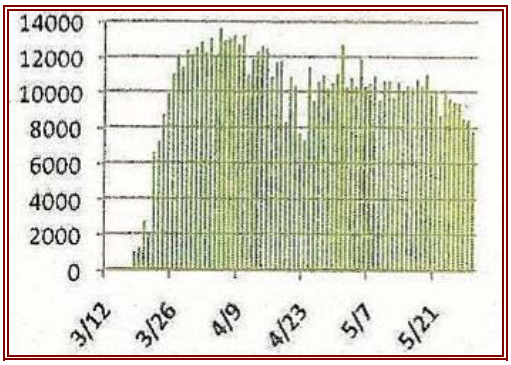

Figure 11.13 Bathing and sanitation support (persons). Total = 760,810 persons in 35 locations (1st June) (Okuyama, 2011).

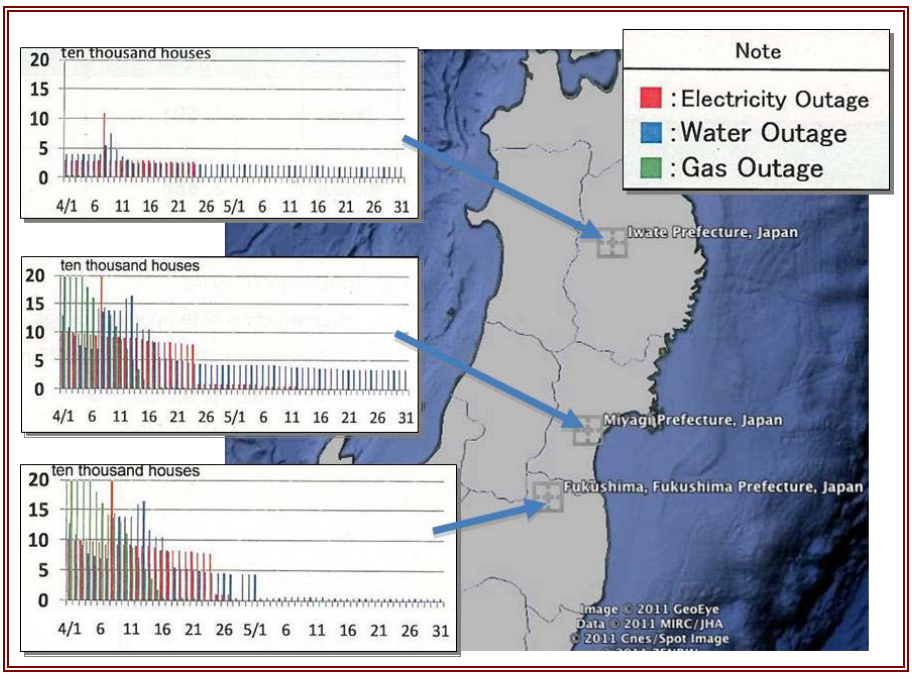

Figure 11.14 Restoration of utilities for the affected Prefectures (Okuyama, 2011).

11.1.5. Observations on evacuation centres

It is estimated that initially over 300,000 evacuees were displaced by the 11th March earthquake and tsunami (ADRC, 2011). See Figure 11.1 for a chronological overview of how evacuee numbers varied from 11th March to 1st June. Initial conditions in the evacuation centres were very cramped. There was a lack of bathing and sanitation facilities and concerns over physical and mental health. A major concern raised by the evacuees was the lack of privacy for activities such as breast feeding and certain medical activities. Another concern is the lack of communication in the initial stages. TV and radio were disconnected (including the emergency radio system in some areas) and both internet and mobile phones were initially disconnected. A breakdown of all relief items issued by the Japanese Red Cross Society (JRCS) can be found in their operational updates (Japanese Red Cross Society, 2011a). A high incidence of respiratory problems was noted attributed to the cold, wet and exposed conditions. 150 cases of pneumonia were registered at the Ishinomaki Red Cross Hospital between 11th March and 12th April, of which 11 have died, which is approximately 6 times the number of deaths during the same period in 2010(Japanese Red Cross Society, 2011a).

Figure 11.15 (left) Ōfunato Elementary School evacuation centre. Initially > 300 evacuees down to 70 by 30th May. In this centre cooking etc. is carried out by the evacuees themselves. People remove shoes when entering the centre, as is traditional in Japanese homes.

Figure 11.16 (right) Evacuation centres in Ōfunato, Miyagi Prefecture (IIS, 2011). Blue marker: occupied centre. White marker: now unoccupied. Blue line: tsunami inundation zone. Highlighted marker (A): Ōfunato Elementary School.

Initially, evacuees included: those whose homes had been washed away or were uninhabitable or unsafe, people who were unable to return home due to damaged or blocked roads and railways, those afraid of frequent aftershocks, people who had no means of sustaining themselves at home (no food, water, electricity etc.) and those evacuated from the Fukushima exclusion zone (around 80,000). Others were able to live at home and simply collect meals and relief items at the centres. Over time the number of evacuees is reducing as utilities are restored to people"s homes (Figure 11.14), people are finding accommodation with friends and family, and temporary accommodation is arranged (section 11.2). By 28th April, the number of evacuees had reduced to 130,230 in 2,560 shelters (SEEDS Asia, 2011) and by 1st June this had dropped further to 102,270 (Okuyama, 2011). Many shelters were located in public buildings such as school gymnasiums, town halls etc. (Figure 11.15) and in order to allow these buildings to resume their functions, shelters have been consolidated and rearranged as evacuee numbers have reduced (e.g. the white markers in Figure 11.16 show evacuation centres in Ōfunato that have now been vacated).

All evacuation centres are officially proposed to be closed by the end of August 2011 when the construction of all temporary accommodation is scheduled to be complete. However, there are many elderly who are reluctant to leave the centres as they feel that they may not receive adequate care once they move into temporary accommodation.

Case Study: Japanese Red Cross Society (JRCS)

The Japanese Red Cross Society (JRCS) have been central to the provision of emergency healthcare. The JRCS is mandated by Japan"s Disaster Relief Act and as such is required by law to act in an emergency. JRCS costs associated with internal disaster relief are partly funded by the government (Satoshi, 2011). The president of the JRCS sits on the Central Disaster Management Council responsible for formulating the Basic Disaster Management Plan (section 11.1.3). Note that this particular organisational form is unique to Japan as the role of each nation"s Red Cross Society varies.

Since 11th March the JRCS has mobilised between 600-700 medical teams, each consisting of 1 doctor, 3 nurses, 1 pharmacist and 1 administrator. The medical teams are made up of fully employed staff at the 92 JRCS privately run hospitals throughout Japan. There is one JRCS chapter for each of the 47 Prefectures of Japan, each with their own warehouse of emergency supplies. All pre-stocked supplies were used including 132,510 blankets, 30,150 "emergency sets" (including portable radio, light, info booklet on typical symptoms of illness etc. Issued 1 per family) and 13,500 "sleeping sets" (camping mattress, pillow, ear plugs etc.). Due in part to a shortage of fuel (section 11.1.2) the government restricted travel to the emergency services in the initial stages, meaning that it was difficult to move these supplies to the affected areas for the first 3 weeks, leading to a shortage of necessities for approximately the first month (Satoshi, 2011).

Although medical teams were dispatched from all over Japan, many could not reach the affected areas meaning that the local JRCS teams were initially required to work in isolation. The focus of activity for the first month was on emergency healthcare and emergency relief distributions. Healthcare was provided by mobile medical teams and field clinics. As of 2nd May, the JRCS Hospital was the only functioning hospital in Ishinomaki city (Miyagi Prefecture) and also served as the coordinating centre for non-JRCS medical teams working in the affected regions. Psychosocial support was provided to victims, volunteers and Municipal officers engaged in the emergency response with 15 specialised psychosocial programme (PSP) teams deployed in the affected areas of Miyagi and Iwate Prefecture. JRCS teams carried out rapid assessments to identify issues in environmental health (e.g. water supply) and as of 17th April, 12 water tanks and taps for washing hands were set up in 9 evacuation centres around Ishinomaki, benefiting the 2,204 evacuees at those centres at that time. Radiation medical specialists from Hiroshima & Nagasaki Red Cross Hospitals were stationed in Fukushima (Japanese Red Cross Society, 2011b).

In the absence of public services JRCS volunteers (see Figure 11.1) have been involved in running mobile kitchens, distribution of food and non-food items, fundraising, directing affected persons to evacuation centres, providing management and support to volunteer centres, and assisting home owners and communities clear debris from property. Four volunteer centres were setup (Tokyo HQ, Miyagi Chapter, Iwate Chapter and Fukushima Chapter) to coordinate the trained volunteer work/activities. As local medical facilities become re-established the JRCS focus is slowly moving to restoration of social welfare services and teams are beginning to return from the affected areas.

11.2. Japan"s Recovery

Previous disasters around the world have sometimes required that reconstruction be carried out by NGOs and relief organisations (such as several less economically developed countries affected by the 2004 Indian Ocean Earthquake and Tsunami). Japan, however, has the resources to carry out reconstruction largely via the government and private sector. Japan now faces many challenges such as the relocation and re-employment of displaced victims of the 11th March earthquake and tsunami, reestablishment of business activities disrupted by recent events, and strategies for minimizing the long-term impact on the economy. This section focuses primarily on the various forms of support being offered to victims of the 11th March earthquake and tsunami and ends by touching briefly on Japan"s longer-term plans for recovery.

11.2.1. Observations on the temporary housing strategy

See Figure 11.2 for a chronological overview of temporary housing construction. The first people started moving into temporary homes on 8th April, with priority given to families with children, the elderly and the disabled. Location of available land for the temporary houses has been a huge challenge and Table 11.2 gives the latest temporary housing statistics from the Ministry of Land, Infrastructure, Transport and Tourism (MLIT), showing that a further 1,078 units are yet to be scheduled for construction as of 15th July. As of 11 July, 28,100 available rooms have been identified in publicly owned accommodation, of which 5,910 have already been let to evacuees. A further 40,297 rooms have been identified in private accommodation and will potentially be rented by the government for use by the victims for 2 years 9 MLIT, 2011). All temporary housing is proposed to be completed by the end of August. Figure 11.17 to Figure 11.19 show examples of the units in Ōfunato. EEFIT observed the same type of units being constructed in Ishinomaki City. The Japanese Red Cross Society (JRCS) is equipping all new temporary houses with six home appliances: refrigerator,

washing machine, rice cooker, microwave, hot water dispenser and television (Figure 11.19). The assistance is worth an estimated US$160 mn and benefiting approximately 280,000 people (Japanese Red Cross Society, 2011b). However, due to logistical delays, as of mid-July one third of eligible households are yet to receive their appliances (Yomiuri Shimbun, 2011).

Table 11.2 Temporary housing statistics from the Ministry of Land, Infrastructure, Transport and Tourism (15th July) (MLIT, 2011b).

Prefecture	Required units	Scheduled but not yet started	Building starts	Completed houses	Total scheduled
Iwate	13,833	0	13,833	11,840	13,833
Miyagi	22,435	1,844	19,918	16,294	21,762
Fukushima	14,000	108	13,487	10,501	13,595
Total (including other affected Prefectures)	50,583	1,952	47,553	38,950	49,505

Figure 11.17 (left) Aerial photograph of Ōfunato Elementary School, showing the temporary housing foundations being laid (1st April).

Figure 11.18 (right) Temporary housing units at Ōfunato Elementary School.

Figure 11.19 Temporary housing interior (photo by Japanese Red Cross Society).

11.2.2. Livelihood support for evacuees

In an informal survey carried out in Miyagi Prefecture on 11 April 2011, which tried to find out what victims felt were their three greatest concerns, 53% cited money (for living expenses), 50% cited work and 40% cited housing (Japanese Red Cross Society, 2011a).

The government"s Grant Disbursement Committee first met on 8th April 2011 and have now decided to award the following compensations: victims who have lost immediate family members will receive ¥350,000 (US$4,200) per dead or missing member; households whose homes were destroyed (approximately 110,000), will receive ¥350,000 (US$4,200) each; households whose homes were severely damaged, (approximately 127,000) will get ¥180,000 (US$2,160) each; households located within 30 km of the Fukushima Daiichi nuclear plant that have had to evacuate (approximately 65,000) will receive ¥350,000 each. The committee is treating these 65,000 cases as if the house was destroyed – regardless of the level of damage actually sustained (Japanese Red Cross, 2011c).

Other forms of support available to the victims include donations, tax exemptions, student tuition waivers, debris removal and various kinds of loans. As of 29th June insurance claims amounted to ¥1.03 tn (US$12.7 bn) with 48% of claims from Miyagi Prefecture and 81.6% of claims already being settled (The General Insurance Association of Japan, 2011).

Although no international appeal has been initiated the Japanese Red Cross Society (JRCS) received donations from other Red Cross and Red Crescent Societies amounting to ¥10 bn by 12th April and ¥14.6 bn (approximately US$183 mn) by 2nd May (Japanese Red Cross Society, 2011b). Donations from other Japanese and international donor sources amounted to ¥166 bn by 28th April and ¥268.7 bn (approximately US$3.367 bn) (Japanese Red Cross, 2011d) by 15th July. Funding received from sister Red Cross and Red Crescent Societies is being used for immediate relief and recovery costs; all other donations are placed into the cash grants programme which is administered by the government"s Grant Disbursement Committee, of which the JRCS is a member. The Ministry of Health, Labour and Welfare has reported that as of 6th July only around 20% of the funds donated to four major charities (including the JRCS) had reached victims. The distribution of donations from overseas is described in Figure 11.20.

The Japanese Government is using targeted procurement and other measures to support jobs for those affected by the earthquake and tsunami of 11th March 2011, through the "„Japan as One" Work Project". New legislation has been formed to promote reconstruction projects and create jobs through those projects, subsidise companies that hire disaster victims, assist the reconstruction of small and medium enterprises, extend payments of employment insurance benefits, and match disaster victims and jobs through the "Japan as One" Job Council. The Japanese government has dedicated ¥4,296.6 bn (approximately US$54 bn) towards this project and is projecting to create employment for around 200,000 people and support employment for over 1.5 mn people (Employment Policy Division, 2011).

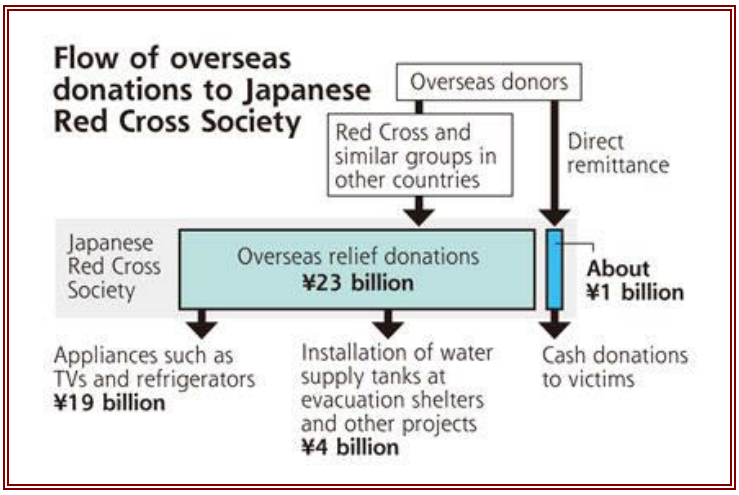

Figure 11.20 Distribution of overseas donations to the Japanese Red Cross Society (as at 20th July; Yomiuri Shimbun, 2011).

11.2.3. Longer-term plans for reconstruction

Four months after the 11th March earthquake and tsunami, the focus of efforts in Iwate and Miyagi Prefectures has largely moved away from emergency response and towards long-term reconstruction planning.

As reconstruction begins some Municipalities are too over-stretched for planning the reconstruction and there are several locations where the Ministry of Land, Infrastructure, Transport and Tourism (MLIT) has released tenders for private companies to carry out town planning. One topic of discussion is the relocation of coastal settlements to higher ground. The Government is discussing a budget to allocate to relocation of settlements however a study shows that of 30 settlements that moved inland following previous large tsunami, 21 were flooded following this event. This shows that hazard maps need to be revised in order to agree new settlement locations (NHK News, 2011).

Regarding Japan"s overall strategy for longer-term reconstruction, the Japanese Government launched its "Reconstruction Design Council" (RDC) on 11 April 2011. The RDC was set up to advise government on the prudent strategies for reconstruction, headed by the President of the National Defense Academy. The RDC published their report on the 25th June, making several recommendations to Government (Reconstruction Design Council, 2011). The report presented five types of reconstruction plan for areas of different topography (see Figure 11.21).

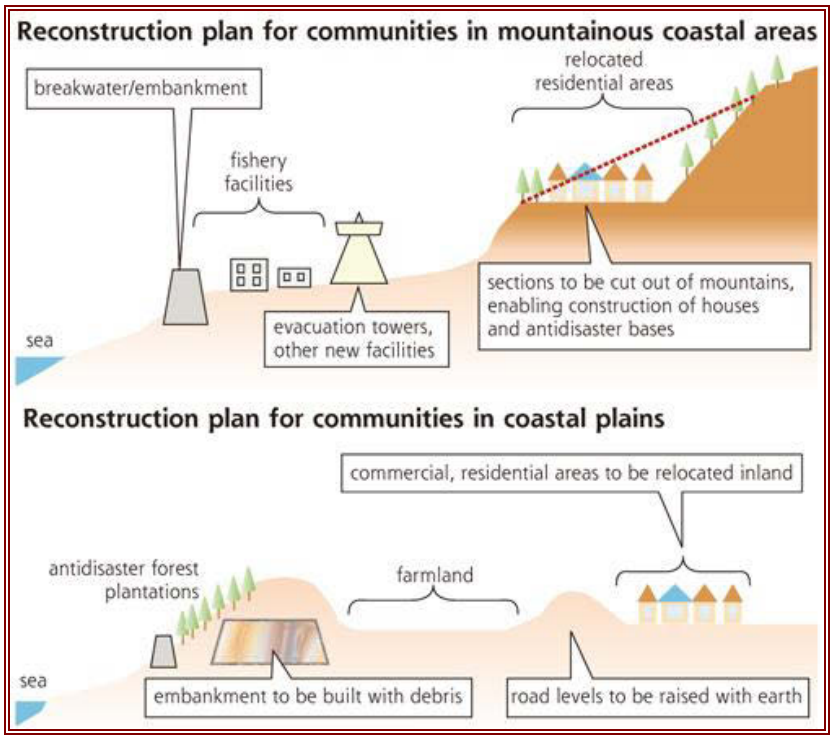

Figure 11.21 Examples of new proposed coastal town plans (Osamu Kawakami / Yomiuri Shimbun staff writer, 2011; adapted from Reconstruction Design Council).

It was recommended that town planning be improved to move residential areas away from the coast to incorporate several lines of sea defence and that sea defence design be improved so that sea walls remain intact even in the case of overtopping. Further recommendations include a move towards emphasizing preparation over complete prevention, including measures such as: increasing preparedness through better educating communities and extensive evacuation drills, improving hazard maps, improving tsunami predictions/warnings, establishing faster routes for evacuation and the provision of evacuation structures. It was also emphasised that local reconstruction must be led by local governments and that the role of the central Government is to indicate the reconstruction visions and provide support to enable local governments to act at full capacity. Advice on regeneration of the economy included a revision of the energy strategy to emphasise renewable energy, stressing that Japan should aim to become world leaders in environmental strategies.

Themes within the construction industry that are likely to emerge from the reconstruction visions include: reform of hospital networks in coastal and remote areas (telemedicine), eco-cities, renewable energy, smartgrids and compact town planning. As an indication of Japan"s intensions, Prime Minister Kan at the G8 summit stated that Japan would like to play a "bigger than ever role" in pushing for green energy and that Japan aims to bring down the cost of solar power generation to a third of its

present level by 2020 and install solar panels in 10 mn households. He also stated that Nuclear energy would remain one of several pillars of Japan"s energy policy (Terra Daily, 2011).

The latest meeting of the Reconstruction Design Council was on the 25th June, 1 day after the passing of the Tōhoku earthquake Reconstruction Basic Law. This law states the basic principles of the reconstruction and establishes the basic policies for the Tōhoku earthquake Response Headquarters and the newly formed Ministry of Reconstruction.

One criticism that has been voiced over the RDC"s recommendations is that they do not go into enough detail over how the reconstruction plans are to be funded. The RDC report does propose a tax increase but does not state which taxes will be raised or for how long. This omission is due to disagreement over the taxation issue within the RDC.

Further criticism that has been placed on the Government"s handling of Japan"s response and recovery are that Government actions have been delayed due to disputes between the two main political parties (Democratic Party of Japan, DPJ, and Liberal Democratic Party, LDP) and internally within the ruling party (DPJ). Prime Minister Naoto Kan survived a vote of no confidence (293-152 against) on 2nd June and has offered to resign once measures are put in place for Japan"s recovery (The Guardian, 2011).

The first of three supplementary budgets was passed on 2nd May, amounting to a ¥4 tn aid package. The second supplementary budget (¥2 tn or approximately US$25.46 bn) was passed on the 25th July and includes financial aid for individuals and small businesses, as well as assistance for the operator of the Fukushima Daiichi nuclear plant to pay compensation to residents of the affected areas. This second supplementary budget is small enough to be funded from last fiscal year"s surplus budget. A third supplementary budget is due for the end of September and expected to total ¥10 tn. The approval of this second supplementary budget satisfies one of three conditions that Prime Minister Kan has set out for his resignation. The two that remain are the passing of bills to: allow the government to issue bonds to fund 40% of the 2011-2012 main budget (which started in April), and to facilitate the sale of renewable energy to power companies (Sekiguchi, 2011).

11.3. Conclusions on the relief and recovery

The 11th March Tōhoku earthquake and tsunami has posed some of Japan"s greatest challenges in emergency response and recovery since the end of the Second World War. The tsunami alone inundated over 500 km^2 of land inhabited by 602,000 people, and the response to these events was hampered by extensive damage to infrastructure and lifelines as well as the tragic loss of many local personnel trained to deal with emergencies. Conditions were initially very difficult for the evacuees, surviving in cramped conditions, with few supplies and in cold weather. Despite the scale of these challenges, it can be concluded that the tragic loss of life was far lower than has been experienced in less-well prepared regions (consider the 228,000 life losses suffered due to the 2004 Indian Ocean tsunami, with the fatality rate in Sumatra"s coastal areas affected by the tsunami reaching 16.6% (EEFIT, 2005), as opposed to 3.4% in Japan). This relative success is due in part to the effectiveness of the emergency response and as-such it is important for the disaster relief community to identify the successful factors in Japan"s response.

Firstly, legislation was in place prior to the event on how emergencies should be managed at a national and local level. This allowed for rapid decision-making that enabled a large initial deployment of military and emergency services personnel. The stock-piling of emergency supplies aided the provision of essentials to evacuees, though this was initially slowed by the damaged infrastructure. The rapid restoration of infrastructure has since aided the movement of supplies and personnel to the affected areas. A strong sense of social responsibility has enabled evacuees to form make-shift, collaborative communities within the evacuation centres and has provided a large number of domestic volunteers from outside the affected areas. The restoration of lifelines has enabled many evacuees to return home and the rapid construction of temporary accommodation has further reduced burdens on evacuation centres.

Several criticisms have also been placed on the emergency response. The government was criticised in the initial stages for poor communication to evacuees and for not disclosing sufficient information on events at the Fukushima Daiichi Nuclear Power Station, highlighting the importance of transparency and public communication. Japan has also been criticised for poor coordination of

international organisations (e.g. with several search and rescue teams being turned away). Another major criticism has been on the weakness of the political situation, with arguments between (and within) political parties being accused of detracting from co-ordinated leadership on the response and recovery.

Japan now faces many long-term challenges. These include rehousing of evacuees as well as generating local economic activities and creating employment opportunities. The funding sources for Japan"s recovery are uncertain and further challenges include reassuring foreign investors and preventing the movement of effected businesses overseas. Efforts are being made to minimise the environmental impact of the reconstruction but stronger political leadership will be required to accelerate Japan"s recovery, realise ambitions to „build back better" and become world leaders in green energy.

11.4. References

Asian Disaster Reduction Centre (ADRC), 2011. Report on the Great East Japan Earthquake. *Asian Disaster Reduction Centre Monthly News*, Vol. 217, April 2011.

Cabinet Office, 2011. Japanese (Survey methods for approval of damaged houses by Tōhoku Earthquake), 12 April 2011. Available at: <http://www.bousai.go.jp/hou/pdf/h23jishin.pdf> [Accessed on 27 July 2011].

Daniels, MJ., 2011. Japan: Kirin Brewery spills beer in earthquake. *Mark J Daniels – my blog, my rules*, 13 March 2011. Available at: <http://markjdaniels.wordpress.com/2011/03/13/japan-kirin-brewery-spills-beer-in-earthquake/> [Accessed on 16 July 2011].

Director General of Disaster Management, 2011. Disaster Management in Japan. *Cabinet Office.*

EEFIT, 2005. The Indian Ocean Tsunami of 26 December 2004: Mission Findings in Sri Lanka and Thailand. Earthquake Engineering Field Investigation Team (EEFIT) Report. The Institution of Structural Engineers, London, UK. Available at: <http://www.istructe.org/knowledge/EEFIT/Documents/Indian_Ocean_Tsunami.pdf> [Accessed 1 June 2011].

Employment Policy Division, 2011. Japan as One Work Project- Countermeasures Phase 2 compiled at the Conference on promotion of employment support and job creation for the disaster victims. Press Release, 27 April 2011. Available at: <http://www.mhlw.go.jp/english/topics/2011eq/dl/emp02.pdf> [Accessed at 20 July 2011].

FDMA, 2011a. Fire and Disaster Management Agency of Japan, Report 140 on the effects of the March 11, 2011 Great Tōhoku earthquake, October 11, 2011. Available at: <http://www.fdma.go.jp/bn/2011/detail/691.html> [Accessed 10 November 2011].

FDMA, 2011b. Report 132 on the effects of the March 11, 2011 Great Tōhoku earthquake, 14 July 2011. Available at: <http://www.fdma.go.jp/bn/2011/detail/691.html> [Accessed on July 15 2011].

IIS, 2011. Tsunami line aerial photo map (1:10,000 scale), KMZ files for Google Earth converted from GSI Ortho aerial photos, and GIS datasets for the response for the 2011 off the pacific coast of Tōhoku earthquake. 12 May 2011. Available at: <http://stlab.iis.u-tokyo.ac.jp/eq_data/index_e.html> [Accessed on 12 July 2011].

Ishiwata, M., 2011, ガレキ処理はもっとスピードアップできる(The Debris Processing can be Sped Up). *Nikkei Business online*, 15 July 2011. Available at: <http://business.nikkeibp.co.jp/article/money/20110712/221457/?P=1> [Accessed on 17 July 2011].

Japan Coast Guard, 2011. Website: <http://www.kaiho.mlit.go.jp/> [Accessed on 23 July 2011].

Japanese Red Cross Society, 2011a. Japan Earthquake and Tsunami: Operations Update no 1, April 13 2011. Available at <http://www.jrc.or.jp/english/relief/l4/Vcms4_00002144.html>.

Japanese Red Cross Society, 2011b. Japan Earthquake and Tsunami: Operations Update no 2, 2 May 2011. Available at <http://www.jrc.or.jp/english/relief/l4/Vcms4_00002144.html>.

Japanese Red Cross, 2011c. Status of Donations Received and Redistributed, 11 July 2011. <http://www.jrc.or.jp/contribution/l3/Vcms3_00002096.html> [Accessed on 20 July 2011].

Japanese Red Cross, 2011d. Status of Donations Received and Redistributed, 11 July 2011. <http://www.jrc.or.jp/contribution/l3/Vcms3_00002096.html> [Accessed on 20 July 2011].

JR East, 2011. 津波を受けた７線区の主な被害と点検状況 (Damage survey of the 7 railway lines that were affected by the tsunami as of 4 April), 5 April 2011.

Kawakami, O., 2011. Funding key to achieving quake recovery. *The Daily Yomiuri*, 27 June 2011. Available at: <http://www.yomiuri.co.jp/dy/national/T110626002371.htm> [Accessed on 27 July 2011].

Kyodo Tsushin, 2011. 東北道全線が開通　一般車両通行規制を解除 (Reopening of the Tōhoku Motorway). *Japan Press Network 47 News,* 24 March 2011. Available at: <http://www.47news.jp/CN/201103/CN2011032401000087.html> [Accessed at 16 July 2011].

McCurry, J., 2011. Japan's Naoto Kan survives no-confidence vote. *The Guardian*, 2 June 2011. Available at: <http://www.guardian.co.uk/world/2011/jun/02/japan-naoto-kan-no-confidence-vote> [Accessed on 27 July 2011].

MIAC, 2011. Estimation of the population in the tsunami inundation zone, by municipality (analysis by the Geographical Information Authority of Japan). Ministry of Internal Affairs and Communications. Available at: <http://www.stat.go.jp/info/shinsai/zuhyou/sinsui.xls> [Accessed on 4 August 2011].

Ministry of Economy, Trade and Industry, 2011. Tōhoku earthquake Response Headquarters, 25 April 2011 Available at: <http://www.sato-nobuaki.jp/activity/a_20110425-002.pdf> [Accessed on 16 July 2011].

Ministry of Foreign Affairs of Japan, 2011. Press Releases, March 2011. Available at: <http://www.mofa.go.jp/mofaj/press/release/23/3/index.html> [Accessed on 16 July 2011].

Ministry of Foreign Affairs of Japan, 2011. Press Releases, March 2011. Available at: <http://www.mofa.go.jp/mofaj/press/release/23/3/index.html> [Accessed on 16 July 2011].

MLIT, 2011a. Tōhoku earthquake - Update from Housing Department, 11 July 2011. Available at: <http://www.mlit.go.jp/common/000142179.pdf> [Accessed on 18 July 2011].

MLIT, 2011b. Building starts and completion of temporary houses, 15 July 2011. Available at: <http://www.mlit.go.jp/common/000140307.pdf> [Accessed on 18 July 2011].

National Police Agency, 2011. Website: <http://www.npa.go.jp/> [Accessed on 23 July 2011].

Okuyama. H., 2011. Deputy Director Defence Operations Division at MoD, Tokyo. [meeting] (Personal communication, 3 June 2011).

Reconstruction Design Council, 2011. Towards Reconstruction “Hope Beyond the Disaster”, 25 June 2011. Available at: <http://www.cas.go.jp/jp/fukkou/pdf/fukkouhenoteigen.pdf> [Accessed on 22 July 2011].

Satoshi. S., 2011. Director of Planning & Coordination for the Japanese Red Cross Society at the JRCS headquarters, Tokyo. [meeting] (Personal communication, 3 June 2011).

SEEDS Asia, 2011. The Great Eastern Japan Earthquake: In depth damage report by affected cities, GLIDE: EQ-2011-000028-JPN, 28 April 2011.

Sekiguchi, T., 2011. Japan Passes Budget, Taking Kan Closer to His Resignation. *The Wall Street Journal*, 25 July 2011. Available at: <http://online.wsj.com/article/SB10001424053111903999904576467371004861018.html> [Accessed on 27 July 2011].

Staff Writers, 2011. 70% of homes get Red Cross appliances / Overseas donors pay for disaster aid. *The Daily Yomiuri*, 20 July 2011. Available at: <http://www.yomiuri.co.jp/dy/national/T110719005794.htm> [Accessed on 27 July 2011].

Staff Writers, 2011. Kan reassures G8 partners of Japan recovery. *Terra Daily*, 27 May 2011. Available at: <http://www.terradaily.com/reports/Kan_reassures_G8_partners_of_Japan_recovery_999.html> [Accessed on 23 July 2011].

Staff Writers, 2011. 首都圏ガソリン不足、週内にも解消へ　製油所操業再開 (Restart of oil refineries: Fuel shortage in capital region to be resolved by the end of the week). *Sankei News*, 22 March 2011. Available at: <http://sankei.jp.msn.com/economy/news/110322/biz11032220570030-n1.htm> [Accessed on 16 July 2011].

Staff Writers, 2011. 高台移転地でも津波の被害 (High altitude relocation zones still damaged by the tsunami). *NHK News*, 10 July 2011. Available at: <http://kamou.blog.so-net.ne.jp/2011-07-11-3> [Accessed on 27 July 2011].

The General Insurance Association of Japan, 2011. The Value and Number of Earthquake Insurance Claims Following the Tōhoku Earthquake, 29 June 2011. Available at:

<http://www.sonpo.or.jp/news/release/2011/1106_12.html> [Accessed on 20 July 2011].

12. The use of geospatial data for damage mapping and disaster management

12.1. Introduction

In recent years, remotely sensed data is increasingly being used globally in an operational environment to rapidly map the damage resulting from a natural hazard event. In terms of operational use of remotely sensed data, the 2010 Haiti earthquake was a turning point, where many types of remotely sensed data were made available for free to organisations dealing with the disaster. The rise of crowd sourced damage assessment methodologies, an example being GEO-CAN, was another notable development. GEO-CAN results subsequently became part of the joint JRC/UNOSAT/GFDRR-World Bank damage mapping effort another development that arose from the mapping efforts in Haiti. Details of these efforts are due to be published in academic journals in autumn 2011 (Booth et al., 2011 and Corbane et al., 2011). Through these efforts, the accuracy achievable through damage assessments using remotely sensed data are investigated for the first time.

Japan has a well-established track record in disaster mapping. As early as 1995 following the Hanshin-Awaji (Kobe) earthquake, remotely sensed data was used in an attempt to map the damage. Examples include a study that used still photos extracted from high-resolution NHK video footage to map the damage using semi-automated methods, among many others. A summary of these studies carried out following the Kobe earthquake can be found in Saito (2008). The results of the rapid building damage assessment carried out on the ground were also recorded digitally at the building by building level in a GIS database (e.g. Usui et al., 1998; Maki et al., 2001). Building footprints for the entire country, which are updated regularly, have been available commercially for many years. Examples include the commercial datasets available from NTT data and ZENRIN (NTT Data, 2011; ZENRIN, 2011). Some of these footprints have been provided for free for organisations and local governments involved in relief and recovery following the Tōhoku event. This service was terminated as of 31st May 2011. The building footprints in Japan can now be seen in Google Earth. It has become standard practice for the air survey companies to deploy their fleet of aircrafts immediately after natural disasters to capture the change caused by the disaster.

In Japan, hazard maps are prepared and used as part of the disaster preparedness plans by local governments to raise awareness of the risk from the various hazards to the local residents. Hazard maps have also been referred to in section 10.1.2 of this report in the context of tsunami preparedness. All districts along the Tōhoku coastline had a tsunami hazard map prepared and published prior to the event (FDMA, 2011), although it is emerging that the maximum inundation extent experienced in some areas in March far exceeded the predicted extents in these maps. Figure 12.1 shows an example of a hazard map for Minamisanriku in Miyagi Prefecture, overlaid with the extent of the inundation following the M_w9.0 Tōhoku earthquake. The hazard map portal site developed by Ministry of Land, Infrastructure, Transport and Tourism (MLIT), provides a link to all the hazard maps produced in Japan (MLIT, 2011).

In the following sections, the various geospatial tools in use in Japan following this event to collect data and map the damage, as well as assist in the relief activities, will be summarised.

12.2. The use of geospatial data for damage assessment

For damage mapping, two components are required, i.e. information on the *hazard* and of the *built environment* that has been exposed to the hazard. JAXA (Japan Aerospace Exploration Agency) has been using ALOS (PALSAR – L band RADAR) data to create interferograms of the Tōhoku area to measure the permanent crustal deformation in the earthquake affected area (Figure 2.7).

The tsunami affected a long stretch coastline (approximately 500 km long) making remotely sensed data ideal as a tool to assess the extent of the inundation. The maximum inundation extent from the tsunami has been mapped by several organisations using various remotely sensed data. Some organisations have attempted to map the presence of stagnant water by carrying out time series analysis. Figure 12.2 shows the change in the size of stagnant water seen in the aerial photographs taken by GSI (Sawada et al., 2011). Table 12.1 lists the known inundation extent maps (vectors) created following the tsunami in Tōhoku. The maps published during the first few days, which are not

included in this table, were mostly estimates of the inundation extent based on the low-lying elevation. An example is the map produced by Pacific Disaster Center (PDC), currently available through ArcGIS online published on the 15th of March, 2011 (ESRI, 2011).

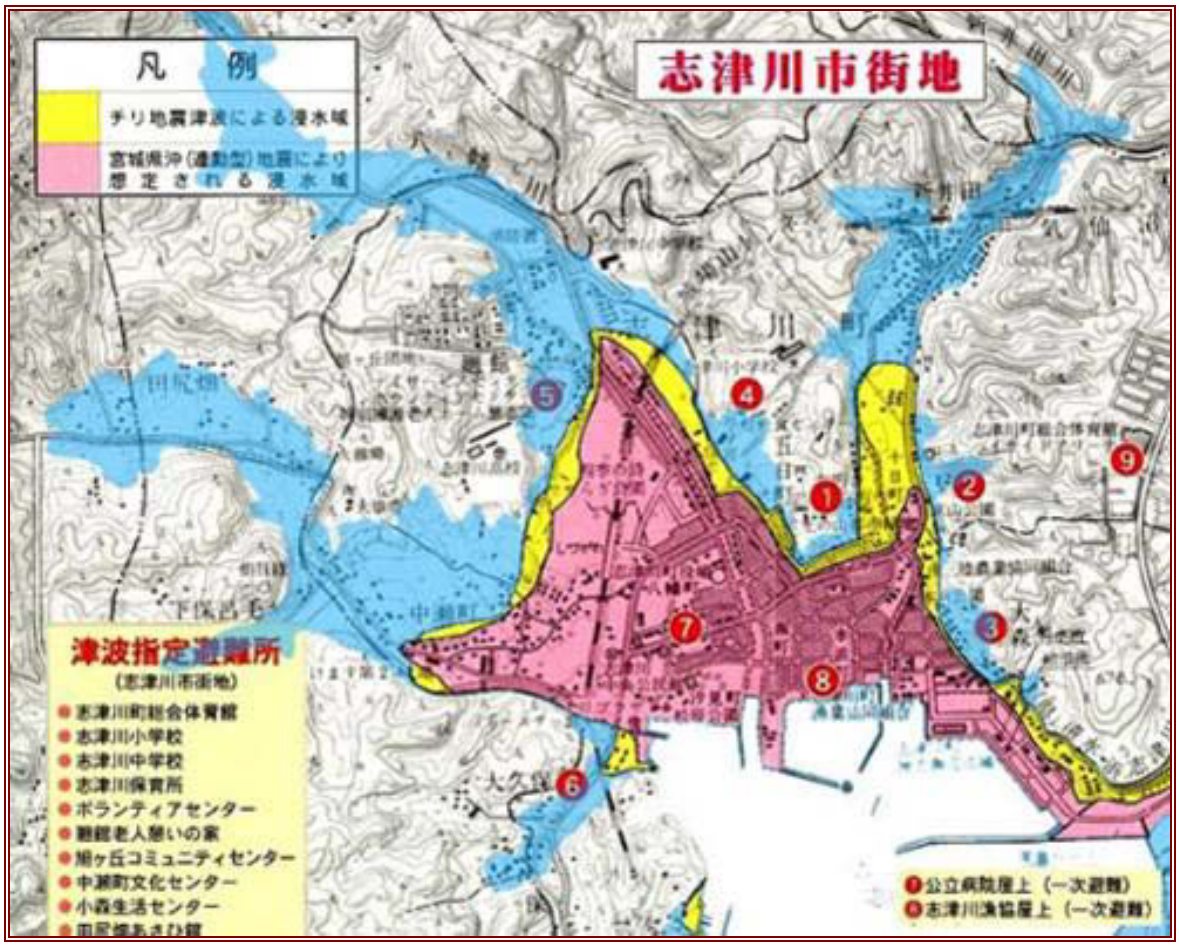

Figure 12.1 Tsunami hazard map of Minamisanriku-machi overlaid with the inundation extent of the Tōhoku earthquake tsunami. Yellow: inundation extent following the Chile earthquake tsunami in 1960. Pink: modelled inundation extent expected due to the expected, recurrent „Miyagi-ken oki" (offshore Miyagi Prefecture) earthquake. Source: http://abcpicture.exblog.jp/16181458/.

Immediately following the earthquake and tsunami, various satellites were tasked to produce images of the affected areas in Tōhoku. JAXA, the Japanese Space Agency, owns and manages ALOS (Advanced Land Observation Satellite), a suite of earth observation satellite sensors. Sadly, the satellite has halted operations on 22nd April 2011 due to power failure on board the satellite. The sensors on board ALOS are AVNIR-2 (multispectral and near infrared bands), PRISM (stereo) and PALSAR (L band RADAR) all of which have been acquiring data of the earthquake and tsunami affected areas.

The International Charter was activated upon the request of the Cabinet Office of Japan on 11th March, 2011. Through the International Charter, the affected country can receive satellite images of the affected area free of charge, which are to assist in the relief process. Asian Institute of Technology (AIT) was appointed as the project manager, and many organisations participated in the mapping efforts. JAXA has published a summary of the data produced as well as conducted a survey on how the end users utilised the data delivered, both from the domestic, as well as the international organisations (Table 12.2) (JAXA, 2011a, b).

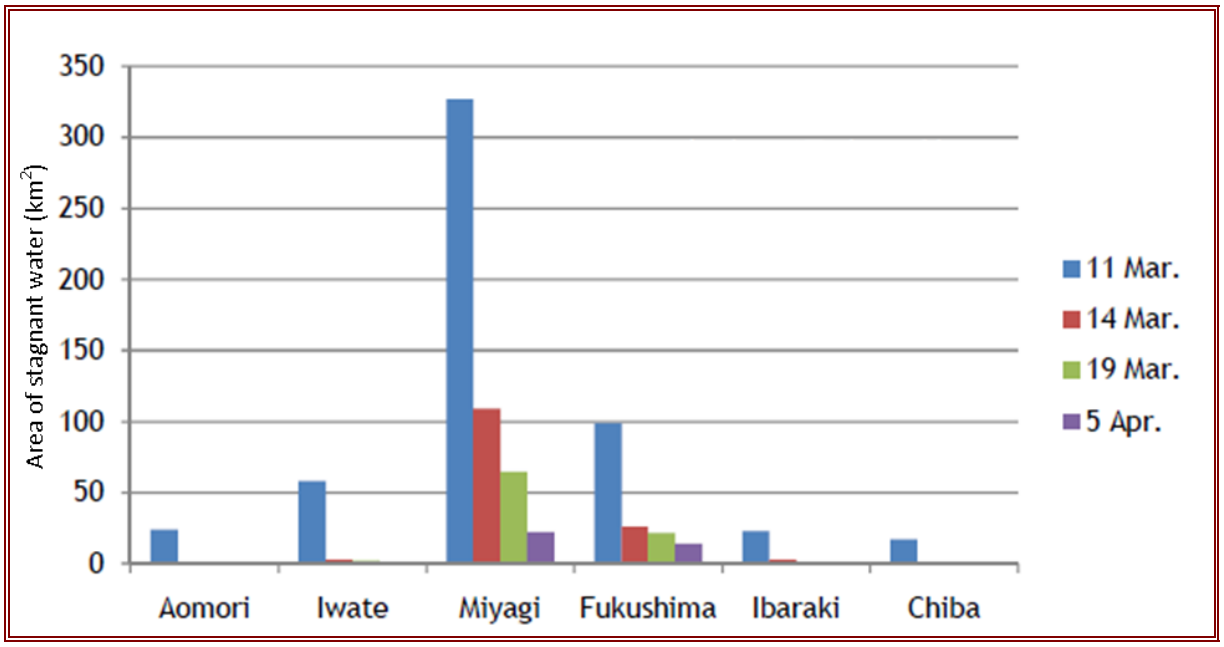

Figure 12.2 Changes in area of stagnant water by prefecture, measured using ALOS PULSAR data (Sawada, 2011).

The Geospatial Information Authority of Japan (GSI), as well as the other private surveying companies started flying aircrafts to take aerial photographs of the affected areas immediately after the earthquake. The seven private air surveying companies in Japan have an agreement with GSI to collaboratively acquire aerial photographs of the affected region in case of a major natural disaster. GSI commissioned these companies to fly and take aerial photographs of the affected areas following the Tōhoku earthquake and tsunami. Some of their aircrafts were damaged, and local governments who needed aerial photographs urgently commissioned some private companies directly to take aerial photographs of their locality. This type of direct contact between the local governments and the air surveying companies is becoming more common in the recent years (Hamamoto, 2011). Using these aerial photographs, maximum inundation extents were mapped by various Japanese organisations which are listed in Table 12.1. At the time this report is being written, the inundation map produced by GSI published on the 18th April 2011 has been adopted by the government as the official inundation extent.

On the 16th of March, 5 days after the tsunami, GSI issued an early estimate of the total area inundated by the tsunami as approximately just over 400 km^2, roughly 4.6 times the area inside the Yamanote line in Tokyo (GSI, 2011a). This estimate was revised after more complete sets of aerial photographs were acquired over the affected areas. The final estimate published on the 18th April 2011 was 561 km^2 (GSI, 2011b) which includes the inundation extents from Chiba and Ibaragi Prefectures that were not included in previous versions.

12.2.1. Comparison of the various inundation extent maps

As with the earthquake damage assessment, it is important for the accuracy of these inundation extent maps to be assessed for these methodologies to gain credibility in an operational setting. Sawada et al. (2011) has started this validation process by comparing their interpretation results (600 km^2 in total) against the GSI results. They have also compared the JAXA estimated inundation extents against the GSI extents in seven towns along the coastline, which show that GSI has mapped almost twice as much inundated areas compared to the JAXA (satellite based) assessment. The Statistics Bureau has compared the inundation extent by PASCO which was until 20 April being used as the official extent, as the GSI extent published on the 18th of April. The comparison shows a rather large discrepancy in some locations – Figure 12.3 shows inundation extents mapped using MODIS Terra and GSI aerial photographs for the Sendai area.

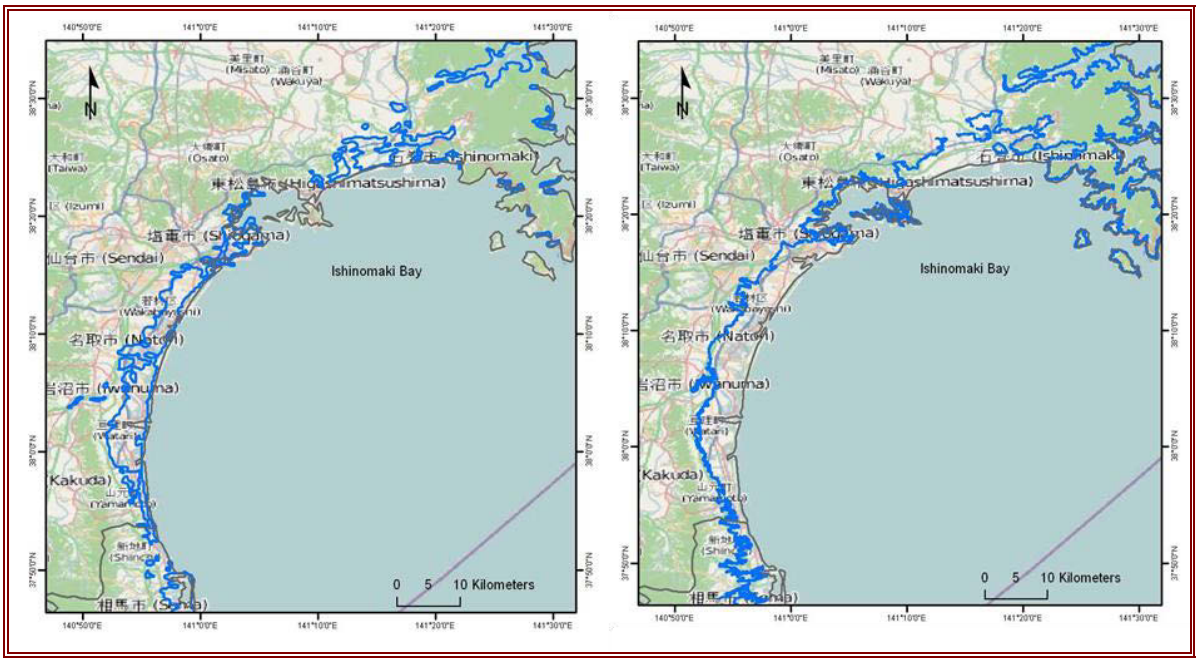

Figure 12.3 Inundation extents mapped using MODIS Terra (left: Asia Air Survey KK, 2011) and GSI aerial photographs (right: Sawada et al., 2011). Basemap taken from OpenStreetMap Japan. For sources, see **Table 12.1**.

Table 12.1 Inundation extent mapping using remotely sensed data carried out both inside and outside Japan. GSD= Ground Sampling Distance, ESRI-J= Environmental Systems Research Institute, Japan

Inundation mapping org	Data source	Source data characteristics	Data extraction method	Date first released / area covered	Vector data downloadable?
GSI	GSI Aerial photos and satellite images	80 cm GSD Images taken on 12-13 March.	Visual interpretation	18 Mar/ Entire Tōhoku coastline	As PDF maps http://www.gsi.go.jp/kikaku/kikaku60003.html
ESRI-J	ALOS (AVNIR-2)	10 m GSD, visible/NIR bands,	Visual interpretation	31 Mar/ Entire Tōhoku coastline	Yes, as kml from EMT website http://175.41.251.35/arcgis/rest/services/3_Damage/PhotoInterpretedFloodAreasEJ/MapServer
Association of Japanese Geographers	GSI Aerial photographs	80 cm GSD	Visual interpretation	30 Mar/ Entire Tōhoku coastline	No. View in *Digital Japan Web system* or *e-Community platform http://danso.env.nagoya-u.ac.jp/20110311/map/index_e.html*
Sawada-Takeuchi Lab, Tokyo University	GSI Aerial photographs	80 cm GSD	Visual interpretation	30 Mar/ Entire Tōhoku coastline	Yes, as kml and shp. http://stlab.iis.u-tokyo.ac.jp/eq_data/#sendaiwan

Asia Air Survey KK + others	IKONOS and GSI inundation extent maps based on aerial photographs	1 m GSD and 80 cm GSD respectively	Semi-automated extraction validated using visual interpretation	29 Mar (updated on 22 Apr)/ Entire Tōhoku Coastline	Yes, as kml from GDMS http://113.37.94.100/gdms/downloads/index.php?id=file_4db17403eb93a
Kokusai Kogyo KK	RADARSAT-2	C band, 5.6 cm wavelength, taken on 13 Mar	Semi-automated extraction (post-event image only)	Not known/ Entire Tōhoku coastline	Contact info-saigai@kkc.co.jp http://www.kk-grp.jp/csr/disaster/201103_touhoku-taiheiyo/index.html
Kokusai Kogyou KK	MODIS Terra	14 Mar 10:30am	Semi-automatic extraction, augmented with tsunami models and visual interpretation	16 Mar/ Entire Tōhoku coastline	Contact info-saigai@kkc.co.jp http://www.kk-grp.jp/csr/disaster/201103_touhoku-taiheiyo/index.html
International Charter	Various	Mapping at various scale provided by more than 20 organisations	Mostly visual interpretation	Various/ Most areas along the Tōhoku coast are covered, at various scales	As PDF maps. http://www.disasterscharter.org/web/charter/activation_details?p_r_p_1415474252_assetId=ACT-359
Asia Air Survey KK	IKONOS	1 m GSD, Multispectral, taken on 12th March.	Semi-Automated extraction of stagnant water and maximum inundation extent	14 Mar(v1)/ Souma City and Minami Souma City	Yes (kml) from GDMS website http://113.37.94.100/gdms/downloads/index.php?id=file_4d8e808010ac6
Asia Air Survey KK	Airborne SAR	March 2011	Stagnant water mapping, semi-automated extraction (experimental)	8 Apr / Higashi Matsushima city and Ishinomaki city	As PDF map http://www.ajiko.co.jp/bousai/touhoku2011/sar-ishinomaki-v3.pdf
Pasco	Terra-SAR X	13,14 Mar, 4 Apr	Semi-automatic extraction of stagnant water inundation extent	Not Known / Ibaragi to Ishinomaki	As PDF maps. All of Pasco"s data can be accessed at http://www.pasco.co.jp/disaster_info/110311/

Table 12.2 Examples from the end user survey results on the use of satellite based remotely sensed data carried out by JAXA (2011b).

End user	Use of data
Cabinet Secretariat	Spot checks of areas of interest, e.g. Sendai airport, Fukushima NPP. Pre- and post-event comparison images. Maximum inundation maps.
Cabinet Office	Overview map using ALOS post-earthquake images. International Charter products. Fukushima NPP related imagery.
Ministry of Land, Infrastructure, Transport and Tourism	Maximum inundation extent maps. Provided data based on interpretation of PALSAR and AVNIR-2 taken on 21, 25 and 30 March. Information on areas with stagnant water also being continuously provided. Request to monitor the 40,000 designated high risk from landslide areas. Wild fire monitoring.
Ministry of Agriculture, Forestry and Fishery (MAFF)	Request for information on the inundation and presence of stagnant water in agricultural areas. MAF F estimates inundated agricultural area to be 24,000 Ha in 6 Prefectures. Information on the inundation in the north part of Chiba and Ibaragi Prefectures also requested. This data to be used by MAFF to validate the ground surveys as well as for recovery planning.
Fisheries Agency	Collaboration sought to assist in the off shore search for lost ships.
Ministry of Environment	Request to assist in mapping the floating debris off the coast of Sanriku coastline. 560,000 m^2 of debris already identified just in the vicinity of Rikuzentakata. This is close to the assessment by the Ministry of Environment
Ministry of Education, Culture, Sports, Science and Technology	Images of the Fukushima NPP
Geospatial Information Authority of Japan	Providing all available imagery. Using the electronic control points provided by GSI and InSAR data analysed by JAXA, crustal deformation of 3.5 m identified in Oshika peninsula.
Miyagi Prefecture	Sighting of an SOS sign in a park in Miyagi Prefecture was reported by the International Charter.
Iwate Prefecture/University	Monitoring of the road accessibility
Kanto Regional Development Bureau	Mapping of the liquefaction areas provided through the international charter.

Table 12.3 Differences between the estimated population within the tsunami inundation zones in Miyagi Prefecture, mapped by GSI and PASCO. Statistics Bureau (2011) contains the full list for the other Prefectures.

Municipality	GSI inundation extent		PASCO inundation extent		GSI - PASCO	
	Pop.	Households	Pop.	Households	Pop.	Households
Miyagino-ku	17,375	6,551	11,858	4,192	5,517	2,359
Wakabayashi-ku	9,386	2,698	8,700	2,470	686	228
Taihaku-ku	3,201	1,136	2,519	818	682	318
Ishinomaki	112,276	42,157	102,670	39,091	9,606	3,066
Shiogama	18,718	6,973	173	80	18,545	6,893

To assess the damage from the tsunami, the inundation extent can be overlaid on maps that contain information on the built environment. In Japan, as mentioned earlier, detailed statistics on the built

environment is available at varying spatial resolutions. The so-called mesh (grid) data is published for population, as well as number of businesses and employees and other indicators such as agriculture. Population census is produced every 10 years. In Japan the last population census was carried out in 2010, thus early results were available to be used as a layer for damage assessment by various organisations. However, this data is only provided in Japanese, hence the international organisations attempting to map the damage employed other global datasets such as Landscan and GRUMP (RMS, 2011) for population data. To get a feel for the difference in the two datasets Landscan data from 2005 for an area near Sendai city is compared with the Japanese mesh population data from 2004 (Figure 12.4). Some early loss estimates were based on Landscan data.

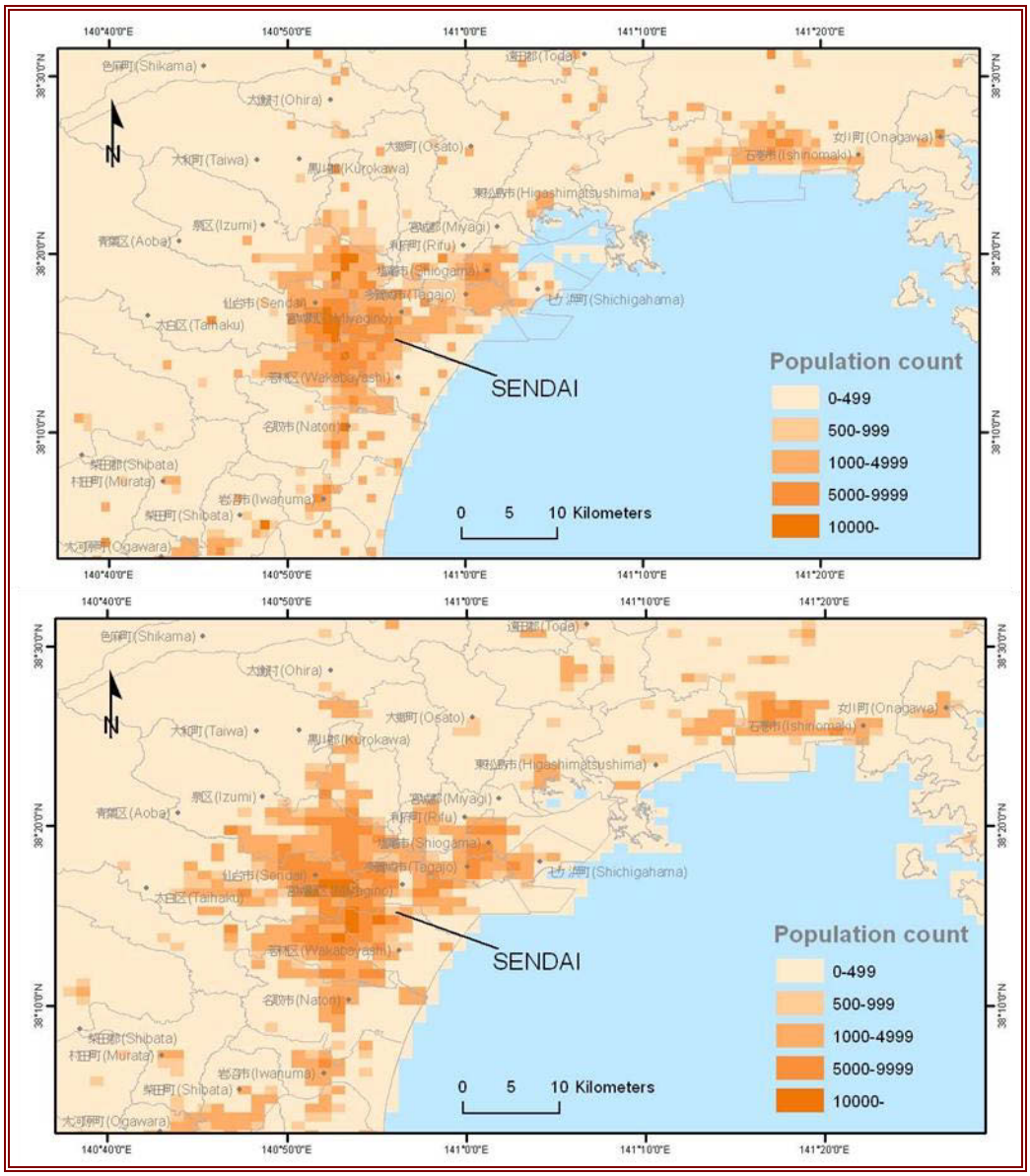

Figure 12.4 Landscan data (above) and 500 m mesh population count data from 2005 Japanese census (below).

Figure 12.5 shows an example of a tsunami damage mapping system developed following the earthquake. GSI aerial photographs are overlaid with ZENRIN building footprint data. The footprints even show the name of the owner/company occupying the building. This system has been used by the General Insurance Association of Japan to designate the areas where 100% of the structures have been washed away, thus automatically granting full payment without sending an inspector to the property on the ground. A list of addresses that have been approved as 100% washed away is available through the SONPO website (SONPO, 2011).

Similar systems are being tested to assess the accuracy of crowd sourced tsunami wash away/damage assessments. Several universities are participating in this project which will assess the accuracy of the interpreters according to their background/experience of image interpretation (Hamamoto, 2011).

Figure 12.5 Post-tsunami aerial photograph taken by GSI (top left). The same aerial photograph with the ZENRIN footprint dataset overlaid (middle). List of addresses where 100% of the structures are recognised by SONPO to have been washed away by the tsunami using aerial photographs (top right). Taken from ZENRIN website (ZENRIN, 2011).

12.3. Data collection, management and distribution over the internet

Information management is a crucial aspect of disaster relief. The needs of the people on the ground must reach the appropriate relief or governmental organisation that can provide help. Previously information was only provided one way i.e. top down. However, new tools that allow individuals in the affected areas to generate and publish information about their own needs have emerged. Some of these examples include Ushahidi and Sahana. These online tools are developed as open source software and are maintained by volunteers. A terminology called VTC (volunteer technology communities) has been coined to describe these communities (GFDRR, 2011). Following the 11th March earthquake and tsunami, these tools were deployed by VTCs to assist in the relief and recovery efforts.

OpenStreetMap is a volunteer community that provides open and free, editable basemaps in areas where there are none. Google Mapmaker has a similar mandate; however, the licensing of the resulting map differs. Basemaps of the Tōhoku region were created by OpenStreetMap (OSM) Japan following the event which had place names in both alphabetic and in Japanese characters. The maps started to be updated and released to the general public few hours after the earthquake, and can be downloaded and edited for free (Furuhashi, 2011). Using this as a basemap, the OSM-J team developed an information portal called sinsai.info, which is based on the open source Ushahidi platform (Ushahidi, 2011). Similar platforms where various datasets are available, such as: Emergency Mapping Team (EMT), Geospatial Disaster-management Mashup Service Study (GDMS), sinsai.info, All311 and e-com (Figure 12.6 to Figure 12.10). These portals function as a means for the local people to request help to the volunteer community, exchange information and also as a data archive/distribution system. Some of the inundation maps mentioned earlier, as well as the

vulnerability data are available to download from these sites. Most of these platforms have a map interface where the data contained inside the system is visualised spatially.

Figure 12.6 (left) All311 front page (All311, 2011).

Figure 12.7 (right) Inundation footprints by the Association of Japanese Geographers can be visualised through the e-com platform. In Japanese only.

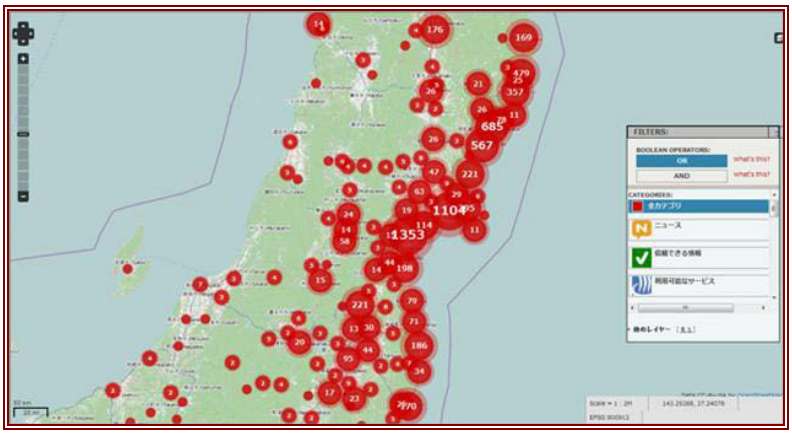

Figure 12.8 Map interface of sinsai.info. The circles show the number of requests registered in that location from people asking for help.

Figure 12.9 Front page of Emergency Mapping Team website.

Figure 12.10 Front page of Geospatial Disaster-management Mash-up Service Study (GDMS).

12.4. Conclusions on the use of geospatial data

Satellite images and aerial photographs were acquired immediately after the event. They were used to map the inundation extents. The earliest total inundation area estimate result was published on the 16th March 2011, 5 days after the event. The first inundation extent map based on analysis of remotely sensed data was produced for the whole of the Tōhoku coastline on the 18th March 2011.

Different data sources and methodologies caused discrepancies in the inundation extent estimates and the resulting estimates on the population affected as well as the building stock. Investigation into the causes for these discrepancies should be carried out through validation activities.

12.5. References

ALL311, 2011, <http://all311.ecom-plat.jp/> (In Japanese). [Accessed on 22 July 2011].

Booth, E., Spence, R. J., Saito, K., Madabushi, S.P.G., Eguchi, R., and Gill, S. P. D, Validating assessments of seismic damage made from remote sensing, Earthquake Spectra, to be published in autumn 2011.

Corbane, C., Saito, K., E. Bjorgo, L. Dell"Oro, R. Eguchi, G. Evans, S. Ghosh, Adams, B.,R. Gartley, F. Ghesquiere, S. Gill, T. Kemper, R.S.G. Krishnan, G. Lemoine, B. Piard, O. Senegas, R. Spence, W. Svekla, and J. Toro, A Comprehensive Analysis of Building Damage in the January 12, 2010 M7 Haiti Earthquake using High-Resolution Satellite and Aerial Imagery, Special issue on the 2010 Haiti Earthquake, Photogrammetric Engineering and Remote Sensing, to be published September 2011

ESRI, 2011, <http://www.arcgis.com/home/item.html?id=1d7647de29f44039997e63394e8ad907>.

Fire and Disaster Management Authority (FDMA), 2011, 地方公共団体の防災対策及び東日本大震災における災害対応等 (slide 2), 第1回 地域防災計画における地震・津波対策の充実・強化に関する検討会, available from <http://www.fdma.go.jp/disaster/chiikibousai_kento/01/shiryo_05.pdf> [Accessed on 7th July, 2011] (In Japanese).

Furuhashi, D., 2011, Personal communication on 22 July, 2011.

Geographical Information Authority of Japan (GSI), 2011a, Estimate of the inundation area (version 1). <http://www.gsi.go.jp/kikaku/kikaku60001.html> (in Japanese). [Accessed on 22 July, 2011].

Geographical Information Authority of Japan (GSI), 2011b, Estimate of the inundation area (version 5, final). <http://www.gsi.go.jp/common/000059939.pdf> (In Japanese). [Accessed on 22 July, 2011].

Global Facility for Disaster Reduction and Recovery (GFDRR), 2011, Volunteer Technology Communities Open Development, downloadable from <http://www.gfdrr.org/gfdrr/sites/gfdrr.org/files/documents/Volunteer%20Technology%20Communities%20-%20Open%20Development.pdf>. Last accessed: 22 July 2011

Google Mapmaker, 2011, Terms of use.
<http://www.google.com/mapmaker/intl/en_ALL/mapfiles/s/terms_mapmaker.html>.

Hamamoto, R., 2011, Personal communication with Mr. Ryota Hamamoto, ESRI-J, on 13 June, 2011.

JAXA, 2011a, <http://www.eorc.jaxa.jp/ALOS/gallery/lib_data/j3disaster.htm> (in Japanese).

JAXA, 2011b, Use of satellite based data for the Great East Japan earthquake and tsunami,
<www.jaxa.jp/press/2011/04/20110406_sac_earthquakes.pdf> Accessed on 22 July, 2011 (In Japanese).

Maki, N., Horie, K., Hayashi, H., and Tanaka, S., 2001, Physical damage level comparison of the damage assessments results in the Hanshin-Awaji Earthquake Disaster, Journal of the Institute of Social Safety Science, vol. 3, November 2011.

MLIT, 2011, <http://disapotal.gsi.go.jp/> Last accessed: July 2011. (In Japanese)

NTT Data, 2011, Madore building inventory data for Japan (in Japanese).
http://madore.glbs.jp/contents/contents_map_info.html. LAst accessed: 8 October, 2011

Risk Management Solutions (RMS), 2011,
<http://www.rms.com/Reports/RMS_Japan_EQ_Client_Advisory_March_2011.pdf>

Saito, K., 2008, Use of High-Resolution Optical Satellite Images for Post-earthquake Damage Assessment, PhD thesis, Department of Architecture, University of Cambridge.

Sawada, H., 2011, Remote Sensing for Emergency Mapping, Powerpoint presentation. Downloaded from <stlab.iis.u-tokyo.ac.jp/~sawada/files/GreatEarthquakePresentatio0425.pdf> [Accessed on 22 July 2011] (In Japanese)

SONPO. 2011, <http://www.sonpo.or.jp/news/2011quake/area.html> last accessed: 7th July, 2011 (In Japanese)

Statistics Bureau, 2011, <www.stat.go.jp/info/shinsai/zuhyou/sai.xls> (In Japanese).

Ushahidi, 2011, <http://www.ushahidi.com/>.

Usui, T., 2002, GIS analysis of the relationship between disaster damage and landform in Nishinomiya city. Memoirs of Nara University, vol. 31, pp.79-96. Available at: <repo.nara-u.ac.jp/modules/xoonips/download.php?file_id=80>

ZENRIN, 2011, <http://www.zenrin.co.jp/news/110415.html> Accessed on 7 July 2011 (In Japanese).